arXiv:hep-ph/0604226v1 26 Apr 2006

VRIJE UNIVERSITEIT

Single spin asymmetries and gauge invariance in hard scattering processes

ACADEMISCH PROEFSCHRIFT

ter verkrijging van de graad Doctor aan
de Vrije Universiteit Amsterdam,
op gezag van de rector magnificus
prof.dr. T. Sminia,
in het openbaar te verdedigen
ten overstaan van de promotiecommissie
van de faculteit der Exacte Wetenschappen
op donderdag 12 januari 2006 om 13.45 uur
in de aula van de universiteit,
De Boelelaan 1105

door

Fetze Pijlman

geboren te Leiden

promotor: prof.dr. P.J.G. Mulders

This thesis is partly based on the following publications:

B. L. G. Bakker, M. van Iersel, and F. Pijlman,
Comparison of relativistic bound-state calculations in front-form and instant-form dynamics, Few Body Syst. **33**, 27 (2003).

D. Boer, P. J. Mulders, and F. Pijlman,
Universality of T-odd effects in single spin and azimuthal asymmetries,
Nucl. Phys. B **667**, 201 (2003).

A. Bacchetta, P. J. Mulders, and F. Pijlman,
New observables in longitudinal single-spin asymmetries in semi-inclusive DIS,
Phys. Lett. B **595**, 309 (2004).

C. J. Bomhof, P. J. Mulders, and F. Pijlman,
Gauge link structure in quark-quark correlators in hard processes,
Phys. Lett. B **596**, 277 (2004).

F. Pijlman,
Color gauge invariance in hard processes,
Few Body Syst. **36**, 209 (2005).

F. Pijlman,
Factorization and universality in azimuthal asymmetries,
Proceedings of the 16th international spin physics symposium 2004, hep-ph/0411307.

A. Bacchetta, C. J. Bomhof, P. J. Mulders, and F. Pijlman,
Single spin asymmetries in hadron-hadron collisions,
Phys. Rev. D **72**, 034030 (2005).

Printed by Universal Press - Veenendaal, The Netherlands.

Contents

1 Introduction **7**

1.1 Particle physics, it is amazing! 7
1.2 QCD and single spin asymmetries 8
1.3 Outline of the thesis 12

2 High energy scattering and quark-quark correlators **13**

2.1 Kinematics of electromagnetic scattering processes 14
  2.1.1 Semi-inclusive deep-inelastic lepton-hadron scattering 14
  2.1.2 The Drell-Yan process 17
  2.1.3 Semi-inclusive electron-positron annihilation 18
2.2 Cross sections 19
2.3 Operator product expansion 21
2.4 The diagrammatic expansion and the parton model 23
2.5 Quark distribution functions for spin-$\frac{1}{2}$ hadrons 29
  2.5.1 Integrated distribution functions 31
  2.5.2 Transverse momentum dependent distribution functions 33
2.6 Quark fragmentation functions into spin-$\frac{1}{2}$ hadrons 38
  2.6.1 Integrated fragmentation functions 38
  2.6.2 Transverse momentum dependent fragmentation functions 40
2.7 Summary and conclusions 42
2.A Outline of proof of Eq. 2.18 43
2.B The diagrammatic expansion 45

3 Electromagnetic scattering processes at leading order in α_S **49**

3.1 Leading order in α_S 50
3.2 Semi-inclusive deep-inelastic scattering 51
  3.2.1 Leading order in M/Q 54

- 3.2.2 Next-to-leading order in M/Q . . . 63
- 3.2.3 Some explicit cross sections and asymmetries . . . 67
- 3.3 The Drell-Yan process . . . 74
- 3.4 Semi-inclusive electron-positron annihilation . . . 78
- 3.5 Fragmentation and universality . . . 80
- 3.6 Deeply virtual Compton scattering . . . 82
- 3.7 Summary and conclusions . . . 86
- 3.A Hadronic tensors . . . 87

4 Color gauge invariance in hard scattering processes 89
- 4.1 Gauge links in tree-level diagrams . . . 90
  - 4.1.1 Gauge links in quark-quark scattering . . . 90
  - 4.1.2 Gauge links in semi-inclusive DIS and Drell-Yan with an additional gluon in the final state 95
  - 4.1.3 Prescription for deducing gauge links in tree-level diagrams . . . 101
- 4.2 Relating correlators with different gauge links . . . 105
- 4.3 Unitarity in two-gluon production . . . 108
- 4.4 Gauge links in gluon-gluon correlators . . . 112
- 4.5 Factorization and universality . . . 115
  - 4.5.1 Virtual corrections . . . 117
  - 4.5.2 Evolution, factorization, and universality . . . 120
- 4.6 Summary and conclusions . . . 125

5 Results for single spin asymmetries in hadronic scattering 127
- 5.1 Introduction . . . 128
- 5.2 Calculating cross sections for hadronic scattering . . . 129
- 5.3 Results for cross sections and asymmetries . . . 135
- 5.4 Summary and conclusions . . . 139
- 5.A Partonic cross sections . . . 140

6 Summary and conclusions 143

Acknowledgements 147

Bibliography 149

Samenvatting 157

1

Introduction

1.1 Particle physics, it is amazing!

Progress in the understanding of elementary particles is amazing. For more than a century the smallest building blocks of nature have been studied, and discoveries are still being made today. While studying the ingredients of nature, fundamental and inspiring theories have been developed making this field of increasing interest.

At the beginning of the last century, Einstein studied the concept of time in order to explain the discrepancy between the theories of Newton and Maxwell. This led to the publication of his theory of special relativity in 1905 [1]. Combining this theory and the quantum theory, Dirac predicted the existence of the antiparticle of both the electron and proton [2]. The antiparticle of the electron, the positron, was discovered in 1933 by Anderson [3] and the antiproton was found in 1955 by Chamberlain et al.[4]

Around the 1930's, explanations were sought for β-decay, which is one particular form of nucleus-disintegration. Experimental studies of this phenomenon seemed to show that the energy before and after the decay were not the same: some energy was missing. To circumvent the potential violation of energy conservation (Newton's law), Pauli suggested between 1930 and 1933 at several conferences a new kind of particle[1], which would be produced during radioactive decay without notice. This new particle, called neutrino by Fermi, was observed in 1956 by Reines and Cowan [5].

---

[1] Pauli publicized this new particle at several conferences among which the Solvay Congresses in 1930 and 1933.

Around 1960 particle accelerators discovered new kinds of hadronic matter. In order to classify the observed hadrons Gell-Mann in Ref. [6] and Zweig in Ref. [7] introduced, independently, a substructure with three types of quarks. Since then several other quark-types have been discovered and just a decade ago the last quark with a mass of almost 200 times the proton mass, the top quark, was discovered at Fermilab [8, 9]. Since this quark and its mass were already predicted on the basis of data taken by the large electron-positron collider at CERN, this was once again a stunning success for particle physics.

In the last century particles have been found which were predicted by theory and theories have been developed on the basis of experimental observations. It is expected that during this century some of the predicted particles, such as the ones responsible for spontaneous symmetry breaking (the Higgs-sector), will be observed. The interplay between experiment and theory in this field is a guaranteed success to explore what nature will offer us next.

1.2 QCD and single spin asymmetries

Quantum chromodynamics (QCD) describes the interactions between quarks and gluons and is constructed from powerful theories and concepts. The main ingredients are: the theory of relativity, the quantum theory, and the concept of gauge invariance. The first gauge theory was developed more than a century ago. Around 1865 Maxwell wrote down his equations describing the interactions between electromagnetic fields and matter. The equations are a set of differential equations which also raised some questions, one of which was that the potentials obeying the equations are not unique. This point became clarified towards the end of the nineteenth century; it was considered as a mathematical symmetry which was apparently left in the equations. This mathematical symmetry allowed for a set of transformations of the potentials which would not affect physical observables. Nowadays this symmetry is named *gauge invariance* and the potentials are often called the gauge fields.

In the beginning of the twentieth century gauge invariance was considered more seriously. While incorporating the symmetry in quantum mechanics, Fock discovered that, besides the gauge fields, the wave function of the electron should transform as well to maintain consistency with the theory of relativity. In order to preserve invariance of observables under gauge transformations, the wave function of the electron must obtain a space-time-dependent phase. However, the question remained whether the gauge fields were to be considered as fundamental fields or whether they just alleviated complex calculations. For a review on the historical roots of gauge invariance the reader is referred to Jackson, Okun [10].

In the second half of the twentieth century the question on whether potentials are more fundamental than electric and magnetic fields was finally addressed. Aharonov

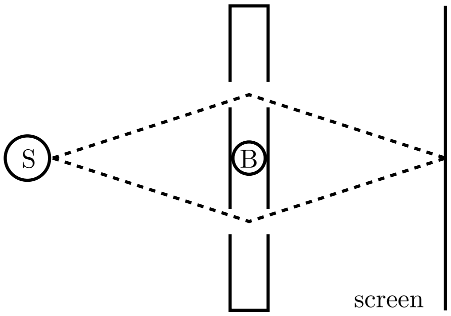

Figure 1.1: The schematic setup of an Aharonov-Bohm like experiment. S represents a source of electrons producing an interference pattern on the screen owing to the two slits. The interference pattern shifts in a particular direction if the solenoid in B, pointing out of the plane, is given a current. If the screen is far away from the two slits then the shift is proportional to $\oint \mathrm{d}\mathbf{x} \cdot \mathbf{A}(\mathbf{x})$. The path of the integral is the closed path formed by the two dashed lines and $\mathbf{A}(\mathbf{x})$ is the potential field. One can call this shift of interference pattern an asymmetry because the direction of the shift depends on the direction of the magnetic field.

and Bohm apparently[2] rediscovered that an electron can obtain a phase shift from its interaction with the potential even if it only travels in regions in which there is no electric or magnetic field [13]. The experiment carried out by Chambers showed that instead of the electric and magnetic fields, the non-uniquely defined potentials should be considered as the fundamental fields in quantum electrodynamics [14]. A schematic setup of the experiment is given in Fig. 1.1.

As compared to electrons and photons, the situation of quarks and gluons is much more involved. In contrast to electrons and photons, free quarks and gluons have for instance never been observed. They only seem to exist in a hadron (confinement) which indicates a strong interaction. On the other hand, perturbation theory turns out to provide a satisfactory description for collisions involving hadrons at high energies, showing that the interaction at high energies must be weak. This particular scale dependence of the interaction strength confronted physicists with a big challenge.

The solution came from a quantum field theory. In quantum field theories infinities often appear. In the 1940's Dyson, Feynman, Schwinger, and Tomonaga showed that in quantum electrodynamics such infinities can be handled by renormalizing the observables. In contrast to the general expectation, 't Hooft and Veltman showed in 1972 that this was also possible for non-Abelian gauge theories [16, 17]. Using the machinery of

---

[2] It seems that Ehrenberg and Siday already pointed out that enclosed magnetic fluxes could cause phase shifts. Their work [11] has been cited in the subsequent paper of Aharonov and Bohm [12].

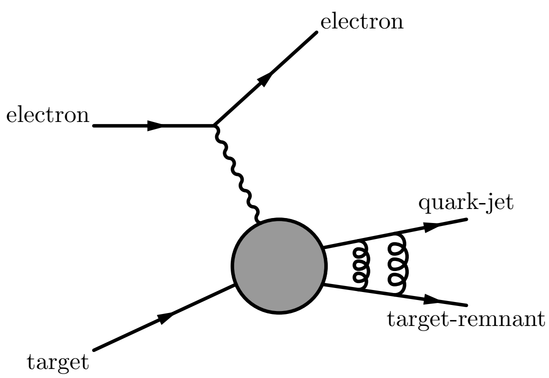

Figure 1.2: An illustration of the interactions between the quark-jet and the target-remnant (Sivers effect). These interactions, which are on the amplitude level and lead to phases as we will see in chapter 3, give rise to interference contributions in the cross section and could produce single spin asymmetries in the idealized jet-production in semi-inclusive deep-inelastic scattering.

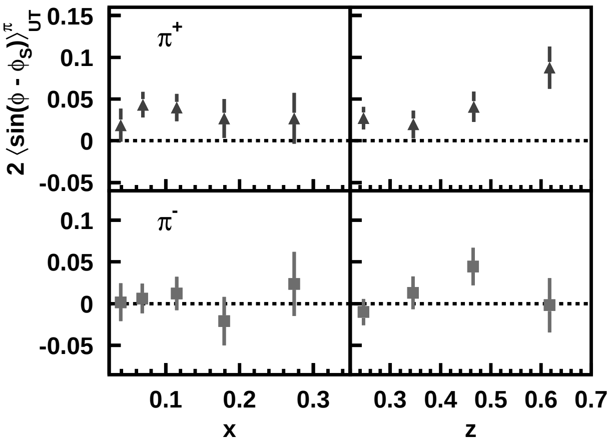

Figure 1.3: A nonzero transverse single target-spin asymmetry for π^+ and π^- in electron-proton scattering measured by the HERMES collaboration. As will be explained in chapter 3, the asymmetry is in the scaling limit proportional to the phase picked up by the outgoing quark and is also called the Sivers effect. The plot was taken from Ref. [15].

’t Hooft and Veltman, Gross, Politzer, and Wilczek derived in Ref. [18, 19] that a scale-dependent interaction strength appears when quarks and gluons are characterized with a color. The constructed non-Abelian gauge theory, called quantum chromodynamics, has a vanishing interaction strength at large momentum transfers - as those occurring in high energy collision experiments - which is called asymptotic freedom.

Not being able to apply perturbation theory, most of the low energy regime of quantum chromodynamics is at present not calculable from first principles. Bjorken and Feynman introduced the idea of absorbing the nonperturbative part in parton probability functions which could be measured in several experiments. These functions describe how quarks are distributed in hadrons (distribution functions) or how they “decay” into a hadron and accompanying jet (fragmentation functions). The functions introduced by Feynman depend only on the longitudinal momentum fraction because at high energies the transverse momenta of quarks in hadrons can often be neglected. This somewhat ad hoc procedure of absorbing the nonperturbative part in functions, called the parton model, can be translated into more rigorous QCD and is very successful in describing various kinds of data.

One observation, studied in this thesis, cannot be explained by the parton model, namely the observation of single spin asymmetries. In single spin asymmetries, one of the participating particles in a scattering process carries or acquires a certain polarization. If the scattering cross section depends on the direction of this polarization, one has a single spin asymmetry. Large single spin asymmetries in inelastic collisions were discovered in hyperon-production in hadron-hadron scattering at Fermilab [20]. Since then, single spin asymmetries have been observed in various processes.

Several explanations for single spin asymmetries at large scales were developed over the last two decades. One of the most important ideas, proposed by Sivers in Ref. [21, 22], was to allow for a nontrivial correlation between the transverse momentum of the quark and its polarization. After incorporating the transverse momenta of quarks in an extended version of the parton model, it is at present understood that there are two sources for single spin asymmetries. The first is the presence of interactions within a fragmentation process (see Collins [23]). The other source, appearing in the idealized single jet-production in semi-inclusive deep-inelastic scattering, see Fig. 1.2, turns out to be the phase which the struck quark picks up due to its interaction with the target-remnant (also exists for fragmentation). This particular phase shows up as a gauge link, which is a mathematical operator, in the definition of transverse momentum dependent distribution functions. Since these functions are defined in terms of nonlocal operators inside matrix elements, the presence of this gauge link is also needed for invariance under local gauge transformations. Note that the obtained phase of the outgoing quark has similarities with the phases of the electrons in the Aharonov-Bohm experiment. Having the same origin of the effect for both asymmetries is surprising. The first nonzero experimental data which directly measures this phase was obtained by the HERMES collaboration in 2004 and is given in Fig. 1.3.

1.3 Outline of the thesis

The appearance and treatment of phases in several hard scattering processes will be studied in this thesis. In 2002 this particular topic became popular after Brodsky, Hwang, and Schmidt showed that such phases, leading to single spin asymmetries, could be generated within a model calculation [24]. The obtained phases were attributed by Collins [25], Belitsky, Ji, and Yuan [26] to the presence of a fully closed gauge link in the definition of parton distribution functions. In this thesis these ideas are implemented in a diagrammatic expansion which is a field theoretical description of hard scattering processes. The effect of the gauge link is studied in several hard processes like hadron-hadron and lepton-hadron scattering. Although only QCD is studied in this thesis, gauge links also appear in other gauge theories like quantum electrodynamics. It is therefore to be expected that gauge links could provide a description of single spin asymmetries in pure electromagnetic scattering as well.

For a full appreciation of the contents of this thesis familiarity with particle physics and quantum field theory is needed. Some excellent textbooks or reviews have been written by Anselmino, Efremov, Leader [27], Barone, Ratcliffe [28], Halzen, Martin [29], Leader [30], Peskin, Schroeder [31], Ryder [32], Weinberg [33, 34].

Chapter 2 will begin with an introduction of the kinematics of some processes in which the hard scale is set by an electromagnetic interaction. A discussion of the diagrammatic approach will be given together with the definitions of distribution and fragmentation functions. This chapter contains some new results from Ref. [35, 36].

In chapter 3, the diagrammatic approach will be applied to obtain cross sections of some electromagnetic processes assuming factorization. The gauge link inside the definition of parton distribution and fragmentation functions will be derived, showing the consistency of the applied approach at leading order in α_S (tree-level). The presence of the gauge link will lead to the interesting prediction of Collins [25] that T-odd distribution functions in the Drell-Yan process appear with a different sign compared to semi-inclusive deep-inelastic scattering. This chapter is based on Ref. [35, 36].

Chapter 4 will begin by considering gauge links in more complicated processes (and beyond tree-level). Besides the gauge links which are found in the electromagnetic processes new gauge links will be encountered which is quite a surprise. We will also see that the appearance of these new structures is an essential ingredient in the discussion of factorization. A set of tools will be developed which allows for a quick determination of the gauge link for arbitrary scattering processes. This chapter contains unpublished material of which some results were given in Ref. [37, 38, 39].

In chapter 5 the physical effect of the new gauge links will be illustrated in almost back-to-back hadron-production in hadron-hadron scattering. A new observable is constructed which is directly sensitive to the intrinsic transverse momenta of partons. In the same way as T-odd distribution functions change sign in the electromagnetic processes, the T-odd distribution functions receive a gauge link dependent factor in the studied asymmetries of hadron-hadron scattering. This chapter is based on Ref. [40].

2

High energy scattering and quark-quark correlators

The formalism will be introduced which was initiated by Collins, Ralston, and Soper in Ref. [41, 42, 43, 44]. The formalism carefully considers the role of intrinsic transverse momenta of partons in hard scattering processes. Although the first part of the chapter is already present in the literature (and partly based on Ref. [45]), it remains worthwhile to look at some parts in more detail to elaborate upon the approximations and the philosophy behind certain approaches. Since this part is meant as an introduction for the non-experts, the reader can skip those sections which are familiar to him or her.

Starting from section 2.5, the second part contains new elements which have been developed over the last few years. These new elements, which are one of the highlights in QCD-phenomenology, originate from the presence of Wilson lines or gauge links in parton distribution and fragmentation functions. These functions will be defined and they turn out to provide valuable information of partons inside hadrons and parton decay into hadrons. As we will see in the following chapters, the presence of these Wilson lines in the definitions of these functions lead to interesting predictions. A summary will be given at the end of this chapter.

2.1 Kinematics of electromagnetic scattering processes

Physicists use often the Lorentz-invariance of the theory to choose the most convenient frame for their purposes. This has produced several frame definitions and frame-dependent interpretations. In principle the definitions and results can be compared by making the appropriate coordinate transformations but in practice this has often led to confusion. In this section several scattering processes will be introduced and their kinematics will be set up such that theoretical predictions and experimental results can be compared frame-independently.

As was advocated at the Transversity workshop in Trento 2004 (see also Ref. [46]), one can, in order to clarify this situation, express all results in easy-to-compare frame-independent observables which is possible owing to the Lorentz-invariance of the theory. For example, the variables in the invariant cross section are usually the momentum and spin vectors which have specific transformation properties. A much better choice would be to express the cross section in terms of the possible invariants. The invariants are frame-independent and can therefore be directly calculated in any frame!

A drawback of this approach is that equations become rather lengthy and that we are not used to think in a frame-independent manner. To aid our intuition and to support the frames which are already in use, a Cartesian basis will be employed which will serve as an interface. Such bases were already introduced before, see for instance Lam, Tung [47] and Meng, Olness, Soper [48]. This will result in short expressions while maintaining manifest frame-independence.

In this thesis the metric tensor of Bjorken and Drell [49] will be employed, reading

$$g^{00} = -g^{11} = -g^{22} = -g^{33} = 1, \qquad g^{ij} = 0 \ \text{ for } i \neq j, \tag{2.1}$$

and the antisymmetric tensor is normalized such that $\epsilon^{0123} = 1$. The Einstein summation convention will also be used, meaning that if a certain index appears twice in a product it is automatically summed over all its values unless stated otherwise. Furthermore, natural units with $\hbar = c = 1$ will be used.

2.1.1 Semi-inclusive deep-inelastic lepton-hadron scattering

In the deep-inelastic scattering (DIS) process, a lepton with momentum l and mass m_e, strikes with a large momentum difference ($l \cdot P \gg M^2$) a hadron (sometimes called target), with momentum P and mass M. The interaction, mediated through the exchange of a highly virtual photon with momentum q (and $-M^2 \gg q^2$), causes the hadron to break up into all kinds of particles being most often other hadrons. The measurement is called: *inclusive* if only the scattered electron is measured, *semi-inclusive* if an additional particle (or more) with momentum P_h and mass M_h is measured, and *exclusive* if all (but one) final-state particles are detected. The semi-inclusive process is illustrated in Fig. 2.1a.

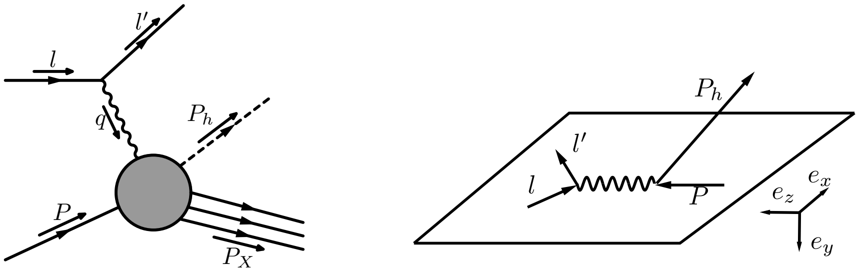

(a) (b)

Figure 2.1: Semi-inclusive DIS. Figure (a) illustrates the process in leading order in $\alpha_{\text{e.m.}}$. Figure (b) presents the definition of the Cartesian basis, except for the vectors e_y and P_h all vectors lie in the plane shown.

Traditionally the following Lorentz-invariants have been introduced to characterize experimental events

$$Q^2 \equiv -q^2, \qquad W^2 \equiv (P+q)^2, \qquad s \equiv (P+l)^2, \qquad x_B \equiv \frac{Q^2}{2P\cdot q},$$
$$y \equiv \frac{P\cdot q}{P\cdot l}, \qquad z_h \equiv \frac{-2P_h\cdot q}{Q^2}, \qquad z \equiv \frac{P\cdot P_h}{P\cdot q}, \tag{2.2}$$

several Lorentz-invariants in semi-inclusive DIS

where $z = z_h(1+\mathcal{O}(M^2/Q^2))$ and $y = Q^2(1+\mathcal{O}(M^2/Q^2))/(x_B s)$.

The Cartesian basis is defined through an orthogonal set of basis vectors e_i (see Fig. 2.1b). The space-like vector e_z is chosen such that it is pointing in the opposite direction of q. The time-like vector e_t is constructed from P subtracting its projection along q, and the transverse directions are fixed by choosing e_x along the components of the sum of the lepton momenta which are perpendicular to e_z and e_t. The definition of e_y follows from demanding a right-handed coordinate system. This Cartesian basis is by construction frame independent and is mathematically defined as

$$e_z^\mu \equiv \frac{-q^\mu}{Q}, \qquad e_t^\mu \equiv \frac{q^\mu + 2x_B P^\mu}{Q\sqrt{1+\frac{4x_B^2M^2}{Q^2}}},$$
$$g_\perp^{\mu\nu} \equiv g^{\mu\nu} - e_t^\mu e_t^\nu + e_z^\mu e_z^\nu, \quad A_\perp^\mu \equiv g_\perp^{\mu\nu}A_\nu \text{ (for any } A\text{)}, \quad \epsilon_\perp^{\rho\nu} \equiv \epsilon^{\sigma\mu\rho\nu} e_{z\sigma} e_{t\mu},$$
$$e_x^\nu \equiv \frac{l_\perp^\nu + l_\perp'{}^\nu}{\left|\mathbf{l}_\perp + \mathbf{l}'_\perp\right|}, \qquad e_y^\rho \equiv \epsilon_\perp^{\rho\nu} e_{x\nu}, \qquad -1 = \epsilon_{\mu\nu\rho\sigma} e_t^\mu e_x^\nu e_y^\rho e_z^\sigma. \tag{2.3}$$

Cartesian basis for semi-inclusive DIS

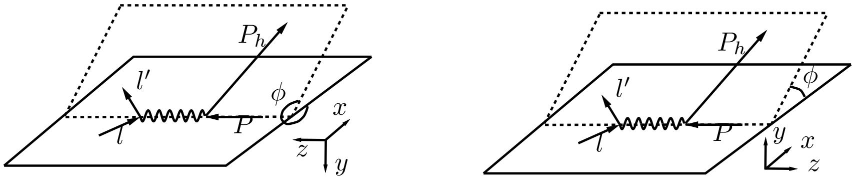

(a) (b)

Figure 2.2: Two examples of fixed frames. Only the momentum P_h has a nonzero y-component and lies in the dashed planes.

Note that the antisymmetric tensor, $\epsilon_{\perp}^{\rho\nu}$, has been defined.

In a Cartesian basis a general vector can be easily decomposed into a linear combination of the basis vectors having frame-independent coefficients, for example

$$P_h = (P_h \cdot e_t)\, e_t - (P_h \cdot e_x)\, e_x - (P_h \cdot e_y)\, e_y - (P_h \cdot e_z)\, e_z. \tag{2.4}$$

By using such decompositions *head-on* cross sections[1] can be written in terms of invariants only. Those cross sections can be indicated with the following notation: $\sigma(\text{Inv: } p_1, p_2, \ldots) = \sigma(\text{all possible invariants of } p_1, p_2, \ldots)$.

The advantage of this approach becomes clear by the following example. Suppose we are interested in azimuthal asymmetries in semi-inclusive DIS and we would like to predict or measure the quantity

$$A = \int \mathrm{d}^2\mathbf{P}_{h\perp}\;\; \mathbf{P}_{h\perp} \cdot \mathbf{e}_y\, \frac{\mathrm{d}^2\sigma(\text{Inv: } l, l', P, S, P_h)}{\mathrm{d}^2\mathbf{P}_{h\perp}}. \tag{2.5}$$

If our frame would be defined such that our proton is moving along the $+z$-axis and our $+x$-axis is proportional to $l^{\perp} + l'^{\perp}$ (see Fig. 2.2a), then A would read in that frame

$$\text{frame a: } A = \int \mathrm{d}^2\mathbf{P}_{h\perp}\;\; |\mathbf{P}_{h\perp}| \sin\phi_{\mathbf{P}_{h\perp}}\, \frac{\mathrm{d}^2\sigma(\text{Inv:} l, l', P, S, P_h)}{\mathrm{d}^2\mathbf{P}_{h\perp}}, \tag{2.6}$$

while if our z-axis would lie in the opposite direction and keeping the same x-axis (see Fig. 2.2b), A would read

$$\text{frame b: } A = -\int \mathrm{d}^2\mathbf{P}_{h\perp}\;\; |\mathbf{P}_{h\perp}| \sin\phi_{\mathbf{P}_{h\perp}}\, \frac{\mathrm{d}^2\sigma(\text{Inv:} l, l', P, S, P_h)}{\mathrm{d}^2\mathbf{P}_{h\perp}}. \tag{2.7}$$

Although the appearance of the expressions differs by a sign (due to a different definition of the azimuthal angle $\phi_{\mathbf{P}_{h\perp}}$), the quantity A is the same in the two different coordinate systems.

---

[1] Cross sections are generally not invariant under Lorentz transformations in contrast to head-on cross sections (see for instance Ref. [31]). In the latter the initial particles are aligned.

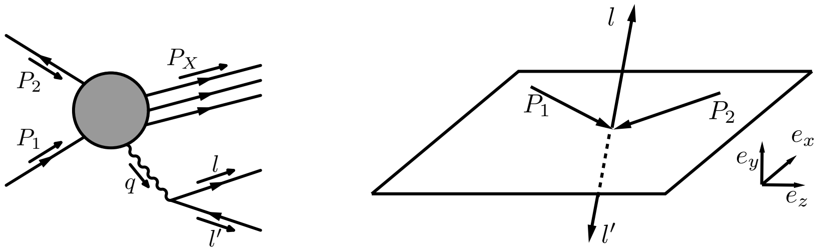

(a) (b)

Figure 2.3: The Drell-Yan process. Figure (a) illustrates the process in leading order in $\alpha_{\text{e.m.}}$. Figure (b) presents the Cartesian basis in which only l, l', and e_y are out of the drawn plane.

2.1.2 The Drell-Yan process

In the Drell-Yan process two hadrons with momentum P_1 and P_2 collide and produce a virtual photon with a large invariant momentum squared $q^2 \gg M^2$. This virtual photon decays into an antilepton and lepton which are measured in the final state. The process has been illustrated in Fig. 2.3a.

Characterizing invariants for this process are

$$Q^2 \equiv q^2, \quad s \equiv (P_1 + P_2)^2, \quad x_1 \equiv \frac{Q^2}{2P_1 \cdot q}, \quad x_2 \equiv \frac{Q^2}{2P_2 \cdot q}, \quad y \equiv \frac{l \cdot P_1}{q \cdot P_1}, \tag{2.8}$$

several Lorentz-invariants in Drell-Yan

and the Cartesian basis is chosen to be (see also Fig. 2.3b)

$$e_t^\mu \equiv \frac{q^\mu}{Q}, \qquad e_z^\mu \equiv \frac{\sqrt{\frac{x_1}{x_2}}P_1 - \sqrt{\frac{x_2}{x_1}}P_2}{\sqrt{s - M_1^2\left(1-\frac{x_1}{x_2}\right) - M_2^2\left(1-\frac{x_2}{x_1}\right)}}, \tag{2.9}$$
$$g_\perp^{\mu\nu} \equiv g^{\mu\nu} - e_t^\mu e_t^\nu + e_z^\mu e_z^\nu, \quad A_\perp^\mu \equiv g_\perp^{\mu\nu} A_\nu \text{ (for any } A), \quad \epsilon_\perp^{\rho\nu} \equiv \epsilon^{\sigma\mu\rho\nu} e_{z\sigma} e_{t\mu},$$
$$e_x^\mu \equiv \frac{-(P_1 + P_2)_\perp^\mu}{\sqrt{-(P_1 + P_2)_\perp^2}}, \qquad e_y^\rho \equiv \epsilon_\perp^{\rho\nu} e_{x\nu}, \qquad -1 = \epsilon_{\mu\nu\rho\sigma} e_t^\mu e_x^\nu e_y^\rho e_z^\sigma.$$

Cartesian basis for Drell-Yan

Since q is now time-like, e_t is chosen along q. The vector e_z is chosen perpendicular to q and such that P_1 has a large positive component. The sum of the incoming hadron momenta perpendicular to e_t and e_z sets the direction of e_x, and e_y follows from e_x.

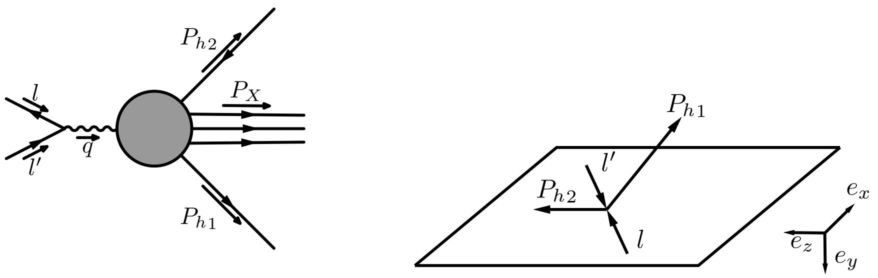

(a) (b)

Figure 2.4: The electron-positron annihilation process. Figure (a) illustrates the process in leading order in $\alpha_{\text{e.m.}}$. Figure (b) presents the Cartesian basis in which only P_{h_1} and e_y are out of the plane.

2.1.3 Semi-inclusive electron-positron annihilation

In electron-positron annihilation an electron and positron collide with a large momentum difference, producing at leading order in α_S two jets (see Fig. 2.4a). We will assume here that in both jets one hadron is detected and that $Q^2 > M^2$.

The variables which characterize this process are (see Fig. 2.4b)

$$Q^2 \equiv q^2, \qquad s \equiv (l_1 + l_2)^2, \qquad z_{h1} \equiv \frac{2P_{h1} \cdot q}{Q^2}, \qquad z_{h2} \equiv \frac{2P_{h2} \cdot q}{Q^2}. \tag{2.10}$$

several Lorentz-invariants in electron-positron annihilation

The Cartesian basis is defined through

$$\begin{aligned}
&e_t^\mu \equiv \frac{q^\mu}{Q}, && e_z^\mu \equiv \frac{\frac{2}{z_{h2}}P^\mu_{h2} - q^\mu}{Q\sqrt{1 - \frac{4M^2_{h2}}{z^2_{h2}Q^2}}}, && \\
&g_\perp^{\mu\nu} \equiv g^{\mu\nu} - e_t^\mu e_t^\nu + e_z^\mu e_z^\nu, && A_\perp^\mu \equiv g_\perp^{\mu\nu} A_\nu \text{ (for any } A\text{)}, && \epsilon_\perp^{\rho\nu} \equiv \epsilon^{\sigma\mu\rho\nu} e_{z\sigma} e_{t\mu}, \\
&e_x^\mu \equiv \frac{l_\perp^\mu}{\sqrt{-l_\perp{}^2}}, && e_y^\rho \equiv \epsilon_\perp^{\rho\nu} e_{x\nu}, && -1 = \epsilon_{\mu\nu\rho\sigma} e_t^\mu e_x^\nu e_y^\rho e_z^\sigma.
\end{aligned} \tag{2.11}$$

Cartesian basis for electron-positron annihilation

2.2 Cross sections

In this section the cross section formula for semi-inclusive DIS will be derived and results for Drell-Yan and electron-positron annihilation will be stated. First, some conventions will be given.

The helicity of a parton with momentum p and spin s is defined here to be

$$\lambda \equiv \frac{\mathbf{s}\cdot\mathbf{p}}{|\mathbf{s}\cdot\mathbf{p}|}. \tag{2.12}$$

Dirac spinors and particle states are normalized such that

$$\bar{u}(k,\lambda)\,u(k,\lambda') = 2m\,\delta_{\lambda\lambda'}, \tag{2.13}$$

$$\langle \mathbf{P},\lambda\,|\,\mathbf{P}',\lambda'\rangle = 2E_{\mathbf{P}}\,(2\pi)^3\,\delta^3(\mathbf{P}'-\mathbf{P})\,\delta_{\lambda\lambda'}. \tag{2.14}$$

The standard cross section for semi-inclusive DIS is (see for example Ref. [31])

$$\begin{aligned} d\sigma = {} & \frac{1}{F}\frac{d^3\mathbf{P}_h}{(2\pi)^3 2E_{\mathbf{P}_h}}\,\frac{d^3\mathbf{l}'}{(2\pi)^3 2E_{\mathbf{l}'}} \\ & \times \sum_X \int \frac{d^3\mathbf{P}_X}{(2\pi)^3 2E_{\mathbf{P}_X}} |\mathcal{M}|^2\,(2\pi)^4\delta^4\left(l+P-P_X-P_h-l'\right). \end{aligned} \tag{2.15}$$

As we can see from this equation, the cross section is built up out of: several phase-space factors, a sum over all possible final states, an invariant amplitude, a delta-function which expresses momentum conservation, and a flux factor F which is given by

$$F \equiv 4\,E_{\mathbf{l}}E_{\mathbf{P}}\,|v_l - v_P|, \tag{2.16}$$

where v_l and v_P are the velocities. The phase-space factors together with the delta-function are Lorentz invariant. Since the invariant amplitude is also Lorentz invariant the transformation properties of the cross section are set by the flux. In this thesis only *head-on* collisions will be considered, meaning that the motion of the initial particles is aligned. In that case the flux takes the form

$$F = 2s\left(1+\mathcal{O}\left(M^2/Q^2\right)\right). \tag{2.17}$$

For nucleons, consisting of strongly interacting quarks and gluons, the interaction between the electrons and the hadrons is at lowest order in $\alpha \equiv e^2/(4\pi)$ mediated through the exchange of a virtual photon. Owing to the presence of charged quarks, the virtual photon feels the electromagnetic current between the incoming and outgoing hadrons. The process is illustrated in Fig. 2.5 and leads for the invariant amplitude to

$$i\mathcal{M} = (-ie)\,\bar{u}(l',\lambda')\gamma_\rho u(l,\lambda)\,\frac{-i}{q^2}\;{}_{\text{out}}\langle P_h, P_X|(-ie)J^\rho(0)|P,S\,\rangle_{\text{in,c}} + \mathcal{O}(e^3), \tag{2.18}$$

where the subscript c indicates that only connected matrix elements should be considered. The blob in Fig. 2.5 expresses that all kinds of interactions are present. Mathematically this means that the currents in Eq. 2.18 are in the Heisenberg picture. A derivation of this equation is often omitted in textbooks but gives considerable insight into the approximations made. Therefore, a schematic derivation for the interested reader is provided in appendix 2.A.

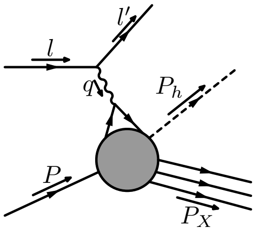

Figure 2.5: The virtual photon coupling to the quark current in semi-inclusive DIS.

The square of the amplitude, needed for the cross section, can be written as a contraction between the leptonic tensor and a hadronic part in leading order of α, giving (neglecting lepton masses)

$$|\mathcal{M}|^2 = \frac{e^4}{Q^4}\, L^{(lH)}_{\mu\nu} H^{\mu\nu}_{(lH)} \left(1 + \mathcal{O}(e^2)\right), \tag{2.19}$$

$$L^{(lH)}_{\mu\nu} = \delta_{\lambda\lambda'} \left(2l_\mu l'_\nu + 2l_\nu l'_\mu - Q^2 g_{\mu\nu} + 2i\lambda\, \epsilon_{\mu\nu\rho\sigma} q^\rho l^\sigma\right), \tag{2.20}$$

$$\begin{aligned} H^{\mu\nu}_{(lH)} = {}& {}_{\text{in}}\langle P, S\,|J^\mu(0)|P_X; P_h, S_h\rangle_{\text{out,c}} \\ & \times {}_{\text{out}}\langle P_X; P_h, S_h|J^\nu(0)|P, S\,\rangle_{\text{in,c}}, \end{aligned} \tag{2.21}$$

where the λ is the helicity of the incoming electron and λ' is the helicity of the outgoing electron. Defining now the hadronic tensor W to be

$$2M\, W^{\mu\nu}_{(lH)} = \frac{1}{(2\pi)^4} \sum_X \int \frac{d^3\mathbf{P}_X}{(2\pi)^3 2E_{\mathbf{P}_X}} (2\pi)^4 \delta^4(l' + P_h + P_X - P - l)\, H^{\mu\nu}_{(lH)}, \tag{2.22}$$

enables us to write the cross section as

$$E_{\mathbf{P}_h} E_{\mathbf{l}'}\, \frac{d^6\sigma}{d^3\mathbf{l}'\, d^3\mathbf{P}_h} = \frac{M}{s}\, \frac{\alpha^2}{Q^4}\, L^{(lH)}_{\mu\nu}\, W^{\mu\nu}_{(lH)}\, (1 + \mathcal{O}(\alpha))\,. \tag{2.23}$$

cross section for semi-inclusive DIS

The interesting information on the distribution and fragmentation of quarks is captured in the hadronic tensor $W^{\mu\nu}_{(lH)}$.

The inclusive cross section can be obtained by summing over all observed final-state hadrons and integrating over their phase space. This leads for the hadronic tensor to

$$\begin{aligned} 2M\, W^{\mu\nu}_{(DIS)} = {}& \frac{1}{2\pi} \sum_X \int \frac{d^3\mathbf{P}_X}{(2\pi)^3 2E_{\mathbf{P}_X}} (2\pi)^4 \delta^4(l' + P_X - P - l) \\ & \times {}_{\text{in}}\langle P, S\,|J^\mu(0)|P_X\rangle_{\text{out,c}}\; {}_{\text{out}}\langle P_X|J^\nu(0)|P, S\,\rangle_{\text{in,c}}, \end{aligned} \tag{2.24}$$

and gives for the cross section

$$E_{\mathbf{l}'}\,\frac{\mathrm{d}^3\sigma}{\mathrm{d}^3\mathbf{l}'} = \frac{2M}{s}\,\frac{\alpha^2}{Q^4} L^{(lH)}_{\mu\nu} W^{\mu\nu}_{(DIS)}\,(1+\mathcal{O}(\alpha))\,. \tag{2.25}$$

cross section for inclusive DIS

The cross sections for Drell-Yan and electron-positron annihilation can be derived similarly. One obtains for Drell-Yan in terms of

$$L^{(DY)}_{\mu\nu} = \delta_{\lambda\lambda'}\left(2l_\mu l'_\nu + 2l_\nu l'_\mu - Q^2 g_{\mu\nu} + 2i\lambda\epsilon_{\mu\nu\rho\sigma}q^\rho l^\sigma\right), \tag{2.26}$$

$$H^{\mu\nu}_{(DY)} = {}_{\mathrm{in}}\langle P_A, S_A; P_B, S_B|J^\mu(0)|P_X\rangle_{\mathrm{out,c}}\ {}_{\mathrm{out}}\langle P_X|J^\nu(0)|P_A, S_A; P_B, S_B\rangle_{\mathrm{in,c}}, \tag{2.27}$$

$$W^{\mu\nu}_{(DY)} = \frac{1}{(2\pi)^4}\sum_X\int\frac{\mathrm{d}^3\mathbf{P}_X}{(2\pi)^3 2E_{\mathbf{P}_X}}(2\pi)^4\delta^4(P_1+P_2-l-l'-P_X)H^{\mu\nu}_{(DY)}, \tag{2.28}$$

the following cross section (a factor 2 was included for summing over lepton polarizations)

$$E_{\mathbf{l}}E_{\mathbf{l}'}\,\frac{\mathrm{d}^6\sigma}{\mathrm{d}^3\mathbf{l}\,\mathrm{d}^3\mathbf{l}'} = \frac{\alpha^2}{sQ^4} L^{(DY)}_{\mu\nu} W^{\mu\nu}_{(DY)}\,(1+\mathcal{O}(\alpha))\,. \tag{2.29}$$

cross section for Drell-Yan

For electron-positron annihilation the cross section for producing two almost back-to-back hadrons reads (a factor $\frac{1}{2}$ was included for averaging over lepton polarizations)

$$E_{\mathbf{P}_{h1}}E_{\mathbf{P}_{h2}}\,\frac{\mathrm{d}^6\sigma}{\mathrm{d}^3\mathbf{P}_{h1}\,\mathrm{d}^3\mathbf{P}_{h2}} = \frac{\alpha^2}{4Q^6} L^{(e^+e^-)}_{\mu\nu} W^{\mu\nu}_{(e^+e^-)}\,(1+\mathcal{O}(\alpha))\,, \tag{2.30}$$

cross section for electron-positron annihilation

where (with $|\Omega\rangle$ representing the physical vacuum)

$$L^{(e^+e^-)}_{\mu\nu} = \delta_{\lambda\lambda'}\ \left(2l_\mu l'_\nu + 2l_\nu l'_\mu - Q^2 g_{\mu\nu} + 2i\lambda\ \epsilon_{\mu\nu\rho\sigma}l^\rho l'^\sigma\right), \tag{2.31}$$

$$\begin{aligned} H^{\mu\nu}_{(e^+e^-)} &= \langle\Omega|J^\mu(0)|P_X; P_{h1}, S_{h1}; P_{h2}, S_{h2}\rangle_{\mathrm{out,c}} \\ &\qquad\times {}_{\mathrm{out}}\langle P_X; P_{h1}, S_{h1}; P_{h2}, S_{h2}|J^\nu(0)|\Omega\rangle_{\mathrm{c}}, \end{aligned} \tag{2.32}$$

$$W^{\mu\nu}_{(e^+e^-)} = \frac{1}{(2\pi)^4}\int\frac{\mathrm{d}^3\mathbf{P}_X}{(2\pi)^3 2E_{\mathbf{P}_X}}\ (2\pi)^4\delta^4(q-P_X-P_{h1}-P_{h2})\ H^{\mu\nu}_{(e^+e^-)}. \tag{2.33}$$

2.3 Operator product expansion

There are two methods to gain more information from the hadronic tensor. In 1968 the first method was proposed by Wilson in Ref. [50] and is called the *operator product* *expansion*. The second method, *the diagrammatic expansion*, was proposed by Politzer in Ref. [51] in 1980 and will be introduced in the next section.

The operator product expansion is useful for inclusive measurements. As an illustration let us consider the inclusive DIS process. Having no hadrons observed in the final state, the sum over all final QCD-states is complete. Together with the fact that the proton is a stable particle one can rewrite the hadronic tensor in Eq. 2.24 into[2]

$$2MW^{\mu\nu}_{(DIS)} = \frac{1}{2\pi}\int \mathrm{d}^4x\; e^{iqx}\langle P,S\,|\,[J^\mu(x),J^\nu(0)]\,|P,S\,\rangle_{\mathrm{c}}. \tag{2.34}$$

According to the Einstein causality principle the commutator of two physical operators should vanish for space-like separations. In our case this means that only the area $x^2 > 0$ gives a contribution. Under the assumption that the hadronic tensor is well behaving for $x^2 > 0$ one can show that the main contribution comes from $x^2 \approx 0$ in the Bjorken limit (fixed x_B and $Q \to \infty$), implying light-cone dominance.

The idea of Wilson, which was later proven in perturbation theory in 1970 by Zimmerman[3], is that for small separations one can make a Taylor expansion for operators. This expansion is called the operator product expansion and reads

$$O_A(x)O_B(0) \underset{x\approx 0}{\approx} \sum_n C^n_{AB}O_n(0). \tag{2.35}$$

This above relation also holds for commutators and by using dispersion relations the short distance expansion can be applied for inclusive DIS.

In Drell-Yan the sum over final QCD-states is complete which enables one to obtain a product of current operators. One can gain insight in the various structure functions in which the cross section can be decomposed but since these structure functions will depend on the two hadrons they are inconvenient for the study of the structure of a single nucleon. In addition, the process is not light-cone dominated which complicates the application of the operator product expansion.

Another situation is encountered in electron-positron annihilation. When summing over all final states the commutator can be obtained, but if we are interested in how quarks decay into hadrons we would not be able to sum over such a complete set. The use of the operator product expansion is therefore limited here as well.

Summarizing, the operator product expansion is a useful approach that finds applications in inclusive DIS and electron-positron annihilation. At the same time, it is also limited to those processes. Parton distribution functions which are measured in DIS cannot be compared to more complex or less inclusive processes and quark decay cannot be studied within this approach. We will proceed by applying an extended form of

---

[2] A necessary condition to have a stable particle is that the sum over energies of its possible decay products is larger than the energy of the considered particle. Together with the fact that the zeroth momentum component of the virtual photon in DIS is positive, it can be shown that the hadronic tensor vanishes if q is replaced by $-q$. This enables one to obtain the commutator.

[3] For reference, please consider chapter 20 of Ref. [34].

Feynman's parton model. In the original parton model it is assumed that the underlying process is a partonic scattering process multiplied by distribution and fragmentation functions. These functions describe the probability of finding on shell constituents in a hadron or how a quark decays into a particular hadron. In the next section the diagrammatic approach as an extension of this model will be discussed.

2.4 The diagrammatic expansion and the parton model

Background of the diagrammatic expansion

The operator product expansion is of limited use for the study of the nucleon's structure. In the case of Drell-Yan we were not able to study the structure of a single nucleon although one could imagine that the chance of producing a virtual photon should just be proportional to the chances of finding a quark in the nucleon and an antiquark in the other nucleon. This idea of expressing the cross section in terms of probability functions which are then convoluted with some parton scattering cross section was suggested by Feynman and is nowadays called the *parton model*.

The parton model had already lots of successes. It gave for instance an intuitive explanation for the approximate Bjorken scaling which was observed at SLAC. In an QCD-improved version of the parton model one could even predict the scaling violation with a set of equations called *evolution equations* (for example see Altarelli, Parisi [52]). Another success of the parton model is the observation of jets. A jet is a set of particles of which their momentum differences can be characterized with a hadronic size. By assuming that these jets are produced by partons which "decay" into these jets one is able to predict the number of jets appearing in scattering processes. However, the appearance of jets also creates a problem with color. Since partons carry color charges, they should somehow loose this color when decaying into a set of colorless hadrons. It appears that this issue does not influence the scattering cross sections at large momentum transfers.

The success of the parton model relies on the asymptotic freedom property of QCD [18, 19]. This property allows one to apply perturbation theory for elementary particle scattering in strong interaction physics in the presence of large scales. Strictly speaking, it remains, however, to be proven whether one can apply perturbation theory in hadronic scattering processes as well. The present idea is that suitable hadronic scattering processes can be described in terms of short-distance physics, the hard scattering part, and the long-distance nonperturbative physics which is captured in probability and decay functions. Since the latter are nonperturbative in nature, the approach should at least be self-consistent to all orders in perturbation theory. This description in separated terms is called *factorization*.

The diagrammatic approach is an extended form of Feynman's parton model. Originating from field theory, the approach includes the possibility that several parton-fields from a hadron can participate in a scattering process (involving multi-parton correlators), whereas the parton model only considers the possibility of hitting a single parton. The approach agrees with the operator product expansion when applicable. In 1980 it was suggested by Politzer in Ref. [51] in order to describe the subleading orders in M/Q, involving “higher twist” operators in matrix elements (to be discussed in chapter 3). Subsequently, it was applied by Ellis, Furmanski, and Petronzio in Ref. [53, 54]. Although similar assumptions as in the parton model are made, the starting point is more general because it allows for more possible interactions. As we will see later, some of these interactions will provide an explanation for single spin asymmetries (see the work of Qiu and Sterman [55, 56, 57]). The diagrammatic approach was further developed and used in several applications, some of which to be discussed later in this thesis.

The assumption in the diagrammatic approach is that interactions between the incoming hadrons and outgoing jets can be described in perturbation theory and hence can be diagrammatically expanded with in the hard part a sufficiently small coupling constant. With respect to asymptotic freedom this requires the incoming hadrons and outgoing jets to be well separated in momentum space. We will therefore impose that the products of external momenta are large ($P_i \cdot P_j \gg M^2$ for $i \neq j$) and assume that interactions between outgoing jets can be neglected. Non-perturbative physics inside the jets and hadrons is maintained. Together with the assumption of adiabatically switching on and off the interactions, the applied assumptions are sufficient to describe general QCD-scattering processes.

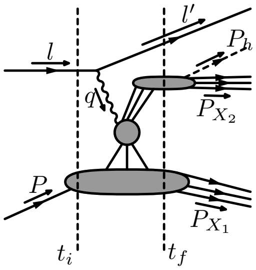

Figure 2.6: The diagrammatic approach illustrated for two jet-production and an observed hadron in semi-inclusive DIS.

As an example, in the case of semi-inclusive DIS a hadron is detected which is well separated from the incoming nucleon in momentum space. Hence, there must have been a partonic scattering. The virtual photon has struck a quark which after interacting with the photon decays in a separate jet including the observed hadron. This process is illustrated in Fig. 2.6. There is also the chance that more jets are being produced which may not be observed. However, that possibility is expected to be subleading in α_s. In section 2.2 an expression for the invariant amplitude was obtained in Eq. 2.18. Making the assumption of adiabatically switching on and off the interactions more explicit (see also Fig. 2.6), this result can be rewritten into (see also appendix 2.A)

$$
\begin{aligned}
&\langle e', P_X, P_h | iT | P, e\rangle \\
&\quad = \bar{u}(k_e', \lambda')(-ie)\gamma_\mu u(k_e, \lambda)\, \frac{-i}{q^2} \\
&\qquad \times \lim_{\substack{t_i \to -\infty \\ t_f \to \infty}} \int \mathrm{d}^4 z\, e^{-iqz}\, {}_{\text{out}}\langle P_h, P_X | U(t_0, t_f) \Big[U(t_f, t_i)(-ie) J_I^\mu(z) \Big] U(t_i, t_0) | P, S\rangle_{\text{in,c}}, \qquad (2.36)
\end{aligned}
$$

where the subscript I denotes the interaction picture and t_0 defines the quantization plane.

The assumption of the diagrammatic expansion can now be used to expand the bracketed term in the above equation. In general a complete expansion will connect an arbitrary number of lines to the several jets. Such a complete expansion, however, is not necessary. The interactions between lines which are connected to one jet as illustrated in Fig. 2.7 can be absorbed in the matrix elements. Therefore, only those parts will be expanded which cannot be absorbed in one of the participating jets. In general this leads to matrix elements in which the interaction picture fields become Heisenberg fields.

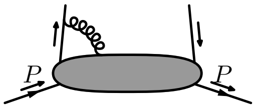

Figure 2.7: An interactions which can be absorbed in the jet definition

Applying the diagrammatic expansion

Using the diagrammatic approach the cross section for a general scattering process can be calculated in a number of steps. An outline of its derivation for two examples is given in appendix 2.B.

1. Write down all squared Feynman diagrams with an arbitrary amount of external parton-lines and connect them in all possible ways to the external jets and particles. Each external parton-line carries an independent momentum variable (for example p_i or k_i). Any interaction which can be absorbed in one of the participating jets should not be included.

2. Replace the external spinors or polarization vectors of step 1 by an appropriate correlator as will be defined below. For instance, $u\overline{u} \rightarrow \Phi$, $u\epsilon^{\mu}\overline{u} \rightarrow \Phi_A^{\alpha}$, etc.

3. Integrate over all parton momenta and impose total momentum conservation by adding $(2\pi)^4\delta^4$(incoming $-$ outgoing parton momenta).

4. If there is any QED part in the diagram, calculate that part with ordinary Feynman rules.

5. Divide by the flux factor and multiply by the phase-space factors of the produced particles, $\mathrm{d}^3\mathbf{k}_i\ /((2\pi)^3 2E_{\mathbf{k}_i})$.

Some of the correlators which appear in cross sections are (see also Fig. 2.8 and Fig. 2.9)

$$\Phi_{ij,ab}(p) = \int \frac{\mathrm{d}^4\xi}{(2\pi)^4}\; e^{ip\xi}\langle P,S\,|\overline{\psi}_{j,b}(0)\;\psi_{i,a}(\xi)|P,S\,\rangle_{\mathrm{c}}, \tag{2.37}$$

$$\Phi^{\alpha}_{A_l\,ij,ab}(p,p_1) = \int \frac{\mathrm{d}^4\xi\;\mathrm{d}^4\eta}{(2\pi)^8}\; e^{ip\xi}e^{ip_1(\eta-\xi)}\langle P,S\,|\overline{\psi}_{j,b}(0)\;A^{\alpha}_{l}(\eta)\;\psi_{i,a}(\xi)|P,S\,\rangle_{\mathrm{c}}, \tag{2.38}$$

$$\begin{aligned}&\Phi^{\alpha_1\ldots\alpha_n}_{A_{l_1}\ldots A_{l_n}\,ij,ab}(p,p_1,\ldots,p_n)\\ &\qquad= \int \frac{\mathrm{d}^4\xi\;\mathrm{d}^4\eta_1\;\ldots\mathrm{d}^4\eta_n}{(2\pi)^{4(n+1)}}\; e^{ip\xi}e^{ip_1(\eta_1-\xi)}\ldots e^{ip_n(\eta_n-\xi)}\\ &\qquad\qquad\times\langle P,S\,|\overline{\psi}_{j,b}(0)\;A^{\alpha_1}_{l_1}(\eta_1)\ldots A^{\alpha_n}_{l_n}(\eta_n)\;\psi_{i,a}(\xi)|P,S\,\rangle_{\mathrm{c}},\end{aligned} \tag{2.39}$$

some parton distribution correlators containing two quark-fields

$$\begin{aligned}\Delta_{ij,ab}(k) = &\sum_X\int\frac{\mathrm{d}^3\mathbf{P}_X}{(2\pi)^3 2E_{\mathbf{P}_X}}\int\frac{\mathrm{d}^4\xi}{(2\pi)^4}e^{ik\xi}\langle\Omega|\psi_{i,a}(\xi)|P_h,S_h;P_X\rangle_{\mathrm{out,c}}\\ &\times{}_{\mathrm{out}}\langle P_h,S_h;P_X|\overline{\psi}_{j,b}(0)|\Omega\rangle_{\mathrm{c}},\end{aligned} \tag{2.40}$$

$$\begin{aligned}\Delta^{\alpha}_{A_l\,ij,ab}(k,k_1) = &\sum_X\int\frac{\mathrm{d}^3\mathbf{P}_X}{(2\pi)^3 2E_{\mathbf{P}_X}}\int\frac{\mathrm{d}^4\xi\;\mathrm{d}^4\eta}{(2\pi)^8}e^{ik\xi}e^{-ik_1\eta}\langle\Omega|\psi_{i,a}(\xi)|P_h,S_h;P_X\rangle_{\mathrm{out,c}}\\ &\times{}_{\mathrm{out}}\langle P_h,S_h;P_X|\overline{\psi}_{j,b}(0)A^{\alpha}_{l}(\eta)|\Omega\rangle_{\mathrm{c}},\end{aligned} \tag{2.41}$$

$$\begin{aligned}&\Delta^{\alpha_1\ldots\alpha_n}_{A_{l_1}\ldots A_{l_n}\,ij,ab}(k,k_1,\ldots,k_n)\\ &\qquad=\sum_X\int\frac{\mathrm{d}^3\mathbf{P}_X}{(2\pi)^3 2E_{\mathbf{P}_X}}\int\frac{\mathrm{d}^4\xi\mathrm{d}^4\eta_1\ldots\mathrm{d}^4\eta_n}{(2\pi)^{4(n+1)}}e^{ik\xi}e^{-ik_1\eta_1}\ldots e^{-ik_n\eta_n}\\ &\qquad\qquad\times\langle\Omega|\psi_{i,a}(\xi)|P_h,S_h;P_X\rangle_{\mathrm{out,c}}\\ &\qquad\qquad\times{}_{\mathrm{out}}\langle P_h,S_h;P_X|\overline{\psi}_{j,b}(0)A^{\alpha_1}_{l_1}(\eta_1)\ldots A^{\alpha_n}_{l_n}(\eta_n)|\Omega\rangle_{\mathrm{c}}.\end{aligned} \tag{2.42}$$

some parton fragmentation correlators containing two quark-fields

All fields, so ψ and A, carry a color index ($a,b\in 1,2,3,\ l_i\in 1,\ldots,8$) over which it is summed in the cross section (no averaging for initial states), and the indices $\{i,\,j\}$ denote Dirac indices. Time-ordering is not present because the matrix elements are connected and the correlators will be integrated over the small parton's momentum component, putting the fields on the light-front (see Jaffe [58, 59], Diehl, Gousset [60]).

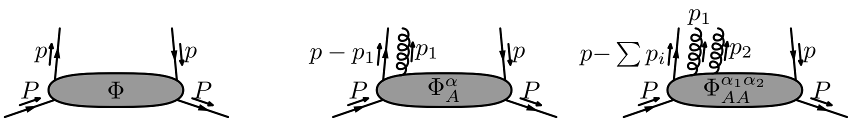

Figure 2.8: Some of the distribution correlators containing two quark-fields

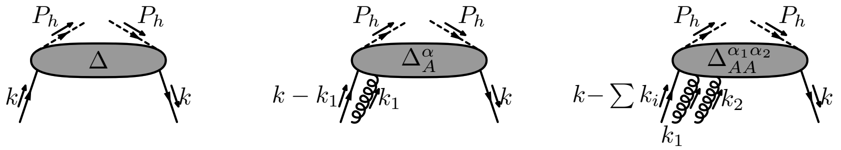

Figure 2.9: Some of the fragmentation correlators containing two quark-fields

To illustrate these rules we return to our example in which there are only two jets produced (see the amplitude diagram in Fig. 2.6). In step 1 we have to write down for the cross section *all* squared Feynman diagrams which contribute to this process. Let us consider one of the contributing diagrams as given in Fig. 2.10a. Expressing the colors very explicitly by giving the spinors and polarization vector a color charge (superscript) and a color index (subscript), one finds for the diagram (note also that $\overline{u}_a^{q_1} \sim \delta_{q_1 a}$)

$$\begin{aligned}\sum_{\substack{q_1,q_2,\\ q_3,q_4,g_1}} &\overline{u}_a^{(q_1)}(k) i\gamma_\alpha t^l_{ab} i \frac{\not{k} - \not{p}_1 + m}{(k-p_1)^2 - m^2 + i\epsilon} \gamma^\nu u_b^{(q_2)}(p-p_1) g \epsilon_l^{(g_1)\alpha}(p_1) \times \left[\overline{u}_c^{(q_3)}(k)\gamma^\mu \delta_{cd} u_d^{(q_4)}(p)\right]^\dagger \\ &= \mathrm{Tr}^{D,C}\Big([u_c(k)\overline{u}_a(k)] i\gamma_\alpha t^l_{ab} i \frac{\not{k} - \not{p}_1 + m}{(k-p_1)^2 - m^2 + i\epsilon}\gamma^\nu [u_b(p-p_1) g \epsilon_l^\alpha(p_1) \overline{u}_c(p)]\gamma^\mu\Big), \qquad (2.43)\end{aligned}$$

where $\mathrm{Tr}^{D,C}$ stands for a trace in color and Dirac space, and $u_c(k) \equiv \sum_q u_c^{(q)}$ and similarly for ϵ_l. According to step 2 we replace the bracketed terms by Δ and $\Phi_{A_l}^\alpha$ and in step 3 we integrate over p, k, and p_1, and multiply this by $(2\pi)^4\delta(p+q-k)$. In step 4 we multiply the result of step 3 with the leptonic tensor and the photon propagator. Applying step 5 this diagram contributes to the cross section as

$$\begin{aligned}d\sigma = &\frac{1}{2s} \frac{d^3\mathbf{P}_h}{(2\pi)^3 2E_{\mathbf{P}_h}} \frac{d^3\mathbf{l}'}{(2\pi)^3 2E_{\mathbf{l}'}} L_{\mu\nu}^{(lH)} \frac{e^4}{Q^4} \int d^4p\, d^4k\, d^4p_1\, (2\pi)^4 \delta^4(p+q-k) \\ &\times \mathrm{Tr}^{D,C}\left([\Delta(k)]\, i\gamma_\alpha t_l i \frac{\not{k} - \not{p}_1 + m}{(k-p_1)^2 - m^2 + i\epsilon} \gamma^\nu [\Phi_{A_l}^\alpha(p,p_1)]\gamma^\mu\right) + \ldots, \qquad (2.44)\end{aligned}$$

where the dots denote contributions from other diagrams.

The previous example illustrates that the diagrammatic approach enables one to express any cross section in a set of correlators. The result is in general an *infinite*

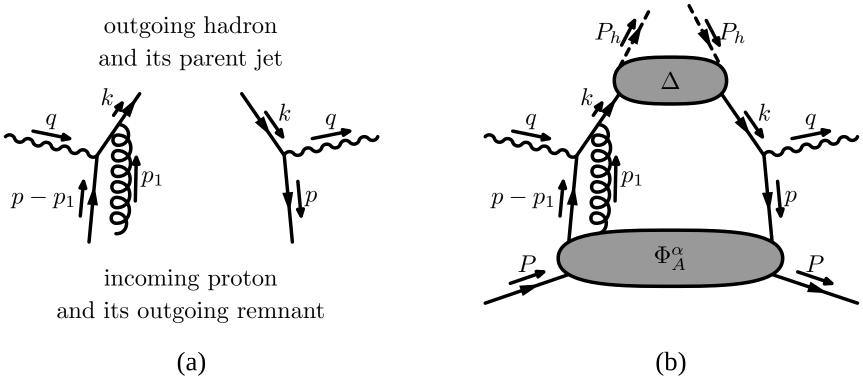

Figure 2.10: Application of the diagrammatic approach in semi-inclusive DIS. Figure (a) represents the two jets and the interactions between them, and in figure (b) the correlators describing the jets are included.

sum of partonic scattering diagrams connected to *all kinds* of correlators. That result is fairly exact; it relies on the possibility of applying perturbation theory between the external jets and the possibility of defining the jets. However, the cross section is not yet a product of probability functions as it is in the parton model. In order to obtain this product similar assumptions as in the parton model will be made here.

These assumptions are that the parton-lines connecting the soft blobs are approximately on their mass-shell and collinear with their *parent hadron*, the hadron which is connected to the blob of the parton. This assumption is less strict than the assumptions of the successful parton model in which partons were treated as in essence free, collinear, and on the mass-shell. Since the assumptions made here are similar to those made in the parton model, we will refer to them as the parton model assumptions.

To exploit these assumptions a set of light-like vectors will be chosen such that $P \sim Q\, n_+ + \mathcal{O}(M^2/Q)\, n_-$ and $P_h \sim Q\, n_- + \mathcal{O}(M^2/Q)\, n_+$ and

$$n_- \cdot n_+ = 1, \qquad \text{and} \qquad \bar{n}_- \sim n_+, \tag{2.45}$$

where the bar on a vector denotes reversal of the spatial vector components. This introduction of vectors, called a *Sudakov-decomposition*, has the advantage that it seems that our target-hadron is now moving very fast in a particular direction without actually having boosted the target. The frame in which the proton is moving very fast is also called the *infinite momentum frame* and if its momentum is opposite to the momentum of the photon one also refers to it as the *Breit frame*. Using the parton model assumptions for the integration over $p \cdot n_-$ and $k \cdot n_+$ and applying the relation $\Delta_{ab}(k) = \delta_{ab}\, \mathrm{Tr}^C\, \Delta(k)/3$, one obtains for Eq. 2.44 ($p^{\pm} \equiv p \cdot n_{\mp}$, etc.)

$$\begin{aligned}
d\sigma = & \frac{1}{2s} \frac{d^3\mathbf{P}_h}{(2\pi)^3 2E_{\mathbf{P}_h}} \frac{d^3\mathbf{l}'}{(2\pi)^3 2E_{\mathbf{l}'}} L^{(lH)}_{\mu\nu} \frac{e^4}{Q^4} \int d^2p_T\, d^2k_T\, d^2p_{1T}\, dp_1^+\, (2\pi)^4 \delta^2(p_T + q_T - k_T) \\
& \times \mathrm{Tr}^D \left[\frac{1}{3} \mathrm{Tr}^C \left(\int dk^+\, \Delta(k) \right) \mathrm{Tr}^C \left(i\gamma_\alpha t_l i \frac{\not{k} - \not{p}_1 + m}{(k-p_1)^2 - m^2 + i\epsilon} \Big|_{\substack{p_1^- = 0 \\ k^+ = 0}} \gamma^\nu \right. \right. \\
& \left. \left. \times \int dp^-\, dp_1^-\, \Phi^\alpha_{A_l}(p, p_1)) \gamma^\nu \right) \right] \Big|_{\substack{p^+ = -q^+ \\ k^- = q^-}} \left(1 + O\left(M^2/Q^2\right)\right) + \ldots, \qquad (2.46)
\end{aligned}$$

where the subscript T denotes transverse components with respect to n_- and n_+.

The applied Sudakov-decomposition can be used for general scattering processes as long as the scalar product of the observed momenta is large. For each observed hadron one can introduce a light-like vector along which the hadron is moving. Since the parton-lines are approximately collinear and on shell, one of the components of the parton momenta, $p \cdot n$, must appear to be very small. In general one should be able to neglect these components in the hard scattering part such that one can integrate the considered correlator over this variable. In the next section we will see that correlators which are integrated over the small momentum components are probabilities in leading order in M/Q.

2.5 Quark distribution functions for spin-$\frac{1}{2}$ hadrons

The various functions for spin-$\frac{1}{2}$ hadrons will be introduced and their relevance will be pointed out. For spin-1 targets the reader is referred to Bacchetta, Mulders [61]. To define the parton distributions a set of light-like vectors is constructed such that

$$\begin{aligned}
1 &= n_- \cdot n_+, & n_- &\sim \overline{n}_+, \\
P &= \frac{M^2}{2P^+} n_- + P^+ n_+, & \epsilon_T^{\mu\nu} &\equiv \epsilon^{\rho\sigma\mu\nu} n_{+\rho} n_{-\sigma}, \\
g_T^{\mu\nu} &= g^{\mu\nu} - n_+^\mu n_-^\nu - n_+^\nu n_-^\mu, & A_T^\mu &= g_T^{\mu\nu} A_\nu, \text{ for any } A. \qquad (2.47)
\end{aligned}$$

the basis in which parton distribution functions are defined

For any vector A we also define $A^{\pm} \equiv A \cdot n_{\mp}$, which means that P^+ is defined to be a Lorentz-invariant. To describe the spin of the hadron one usually introduces

$$S = -S_L \frac{M}{2P^+} n_- + S_L \frac{P^+}{M} n_+ + S_T, \qquad \text{with } S_L^2 + \mathbf{S}_T^2 = 1, \qquad (2.48)$$

which satisfies the necessary constraints: $P \cdot S = 0$, $S^0 = 0$ if $\mathbf{P} = 0$, and $S^2 = -1$.

In the next subsections we will parametrize an expansion in M/P^+ of quark-quark correlators, but M/P^+ does not have to be small. However, in order to make use of the truncated expansion, calculations in the next chapters will be performed such that $P^+ \gg M$. Since the light-like vectors n_- and n_+ are defined up to a rescaling ($n_+ \to \alpha n_+$, $n_- \to \alpha^{-1} n_-$), this does not put any constraint on P or the frame. In fact, for a target at rest one has for instance $n_+ = (M/2P^+)\,(1,0,0,1)$ and $n_- = (P^+/M)\,(1,0,0,-1)$ where $P^+ \gg M$ can still be chosen.

As discussed in the previous section, one encounters in the diagrammatic expansion an infinite set of correlators which can all be integrated over the small momentum components. As we will see in the next chapter, this infinite set can be rewritten into a single new correlator containing the gauge link (to be defined below). In the discussed electromagnetic processes basically two kinds of correlators appear in the final result.

The first kind appears in cross sections which are not sensitive to the transverse momenta of the constituents and is the so-called *integrated* correlator. Including a *Wilson line operator* $\mathcal{L}$, it reads

$$\Phi_{ij}(x,P,S) = \int \frac{\mathrm{d}\xi^-}{2\pi}\, e^{ixP^+\xi^-} \langle P,S\,|\bar{\psi}_j(0)\mathcal{L}^{0_T,\,\xi^+}(0^-,\xi^-)\psi_i(\xi)|P,S\,\rangle_{\mathrm{c}}\Big|_{\substack{\xi^+=0,\\ \xi_T=0}} \qquad (2.49)$$

where over the color indices was summed and where x is the longitudinal momentum fraction of the quark with respect to its parent hadron, $x \equiv p^+/P^+$. The Wilson line operator, or also called *gauge link*, is a 3×3 color-matrix-operator and makes the bilocal operator $\bar{\psi}_{j,b}(0)\,\psi_{i,a}(\xi)$ invariant under color gauge transformations. A Wilson line along a path $\Xi^\mu(\lambda)$ with $\Xi^\mu(0) = a^\mu$ and $\Xi^\mu(1) = b^\mu$ is defined as

$$\mathcal{L}(a,b) \equiv 1 - ig\int_0^1 \mathrm{d}\lambda\, \frac{\mathrm{d}\Xi^\mu}{\mathrm{d}\lambda} A_\mu(\Xi(\lambda))$$
$$+ (-ig)^2 \int_0^1 \mathrm{d}\lambda_1\, \frac{\mathrm{d}\Xi^\mu}{\mathrm{d}\lambda_1} A_\mu(\Xi(\lambda_1)) \int_{\lambda_1}^1 \mathrm{d}\lambda_2\, \frac{\mathrm{d}\Xi^\mu}{\mathrm{d}\lambda_2} A_\mu(\Xi(\lambda_2)) + \ldots, \qquad (2.50)$$

where $A^\mu = A^\mu_l t^l$. In Eq. 2.49 an abbreviation was introduced for links along straight paths. In the abbreviation it is indicated which variables are constant along the path (0_T and ξ^+) and which coordinates are running (the minus components). The path for this case is illustrated in Fig. 2.11a. The integrated correlator will be parametrized in the next subsection.

The second kind of correlator is encountered in cross sections which are sensitive to the transverse momenta of the quarks. Calling it the *unintegrated correlator*, it also contains a Wilson line operator and reads

$$\Phi^{[\pm]}_{ij}(x,p_T,P,S) = \int \frac{\mathrm{d}\xi^-\,\mathrm{d}^2\xi_T}{(2\pi)^3}\, e^{ip\xi} \langle P,S\,|\bar{\psi}_j(0)\,\mathcal{L}^{[\pm]}(0,\xi^-)\,\psi_i(\xi)|P,S\,\rangle_{\mathrm{c}}\Big|_{\substack{\xi^+=0\\ p^+=xP^+}}, \qquad (2.51)$$

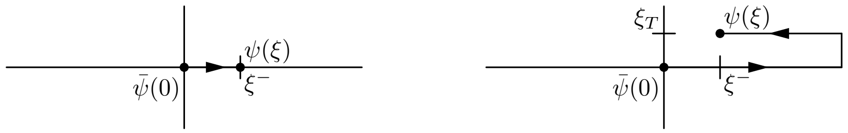

a: $\mathcal{L}^{0_T,\,\xi^+}(0^-,\xi^-)$ b: $\mathcal{L}^{[+]}(0,\xi^-)$

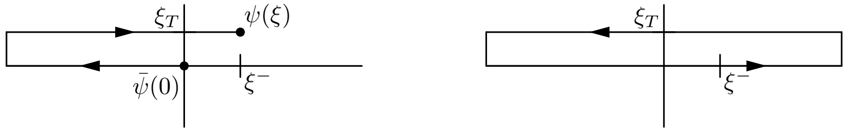

c: $\mathcal{L}^{[-]}(0,\xi^-)$ d: $\mathcal{L}^{[\Box]}(0,\xi^-)$

Figure 2.11: The paths of the various gauge links which connect the two quark-fields in the correlator.

where

$$\mathcal{L}^{[\pm]}(0,\xi^-) \equiv \mathcal{L}^{0_T,\,\xi^+}(0^-,\pm\infty^-)\mathcal{L}^{\pm\infty^-,\,\xi^+}(0_T,\xi_T)\mathcal{L}^{\xi_T,\,\xi^+}(\pm\infty^-,\xi^-), \tag{2.52}$$

and similarly for $\{\xi^+,\xi^-,\infty^-\} \leftrightarrow \{\xi^-,\xi^+,\ \infty^+\}$. In these correlators the link runs via a nontrivial path like the ones drawn in Fig. 2.11b and Fig. 2.11c. After an integration over p_T the unintegrated correlator reduces to the integrated correlator. The nontrivial paths in the unintegrated correlator are a source for interesting phenomena like single spin asymmetries. These correlators will be parametrized in the second subsection.

As a last remark, in chapter 4 and 5 we will also encounter a gauge link of which its path is closed, see Fig. 2.11d. This “closed” gauge link or Wilson loop is defined as

$$\mathcal{L}^{[\Box]}(0,\xi^\pm) \equiv \left[\mathcal{L}^{[+]}(0,\xi^\pm)\right]\left[\mathcal{L}^{[-]}(0,\xi^\pm)\right]^\dagger. \tag{2.53}$$

2.5.1 Integrated distribution functions

The specific form of the integrated distribution correlator (Eq. 2.49) has the following analytical properties

$$\Phi^\dagger(x,P,S) = \gamma^0\ \Phi(x,P,S)\,\gamma^0 \qquad \text{(hermiticity)}, \tag{2.54}$$

$$\Phi(x,P,S) = \gamma^0\ \Phi(x,\bar{P},-\bar{S})\,\gamma^0 \qquad \text{(parity)}, \tag{2.55}$$

$$\Phi^*(x,P,S) = i\gamma_5 C\ \Phi(x,\bar{P},\bar{S})\ i\gamma_5 C \qquad \text{(time-reversal)}, \tag{2.56}$$

where C denotes charge conjugation and $\gamma_5 \equiv i\gamma^0\gamma^1\gamma^2\gamma^3$. Note that $P \to \bar{P}$ implies that $n_- \leftrightarrow n_+$. Using these constraints the correlator has been decomposed on a basis of Dirac structures [44, 62, 63]. In the notation of Ref. [63] this gives[4] (for conventions on names see for instance Ref. [64])

$$
\begin{aligned}
\Phi(x,P,S) \; &= \frac{1}{2}\Big(f_1\, \not{n}_+ + S_L\, g_1\, \gamma_5 \not{n}_+ + h_1\, \gamma_5 \not{S}_T \not{n}_+ \Big) && \text{(twist 2)}\\
&+ \frac{M}{2P^+}\Big(e + g_T\, \gamma_5 \not{S}_T + S_L\, h_L\, \gamma_5 \frac{[\not{n}_+, \not{n}_-]}{2} \Big) && \text{(twist 3)}\\
&+ \text{higher twist.} && (2.57)
\end{aligned}
$$

parametrization of the integrated correlator

where all functions depend on x and on a renormalization scale. The scale dependence can be calculated by applying evolution equations (for example see Ref. [65, 66]). The above expansion in M/P^+ is not to all orders. Calculations of cross sections should therefore be constructed such that M/P^+ is small in order to employ the above parametrization.

In the parametrization we have indicated the twist of the distribution functions. The twist of a distribution function defines at which order in M/P^+ the function appears in the parametrization. This definition of "operational twist" for nonlocal operators was introduced by Jaffe in Ref. [67]. The standard definition of twist, which counts the dimensions of local operators, agrees with this definition for local operators appearing in the Taylor expansion of the nonlocal matrix element.

As will be shown in the next subsection, the leading twist functions allow for a probability interpretation. In order to obtain a parton interpretation for the functions, the Heisenberg field operators, which are present in the correlators, can be expanded in creation and annihilation operators at particular point in time. Therefore, the functions which are integrated over x and are local in time allow for a parton interpretation. Moreover, in those matrix elements the gauge link has vanished, simplifying the interpretation. The function f_1 describes the chance of hitting an unpolarized quark (red, green, or blue) in an unpolarized nucleon, the function g_1 describes longitudinally polarized quarks - or actually chirally left or right handed quarks - in a longitudinally polarized nucleon, and h_1 or *transversity* describes it for transverse polarizations. This last function is at present the only leading twist integrated function which has not yet been measured. Recently, it has been suggested in Ref. [68] by Bakker, Leader, and Trueman that this function appears together with orbital angular momentum of the partons in a simple sum-rule. This would provide for the first time in semi-inclusive DIS access to the orbital angular momentum of partons inside a nucleon, making the transversity function of increasing interest. For more information on the interpretation of these functions the reader is referred to Ref. [28, 69].

---

[4] T-odd integrated distribution functions are in this approach zero and have therefore been discarded.

2.5.2 Transverse momentum dependent distribution functions

Gauge Invariant correlators and T-odd behavior

In electromagnetic processes one encounters at first sight two kinds of unintegrated correlators in the final result of the diagrammatic expansion. They are defined as

$$\Phi_{ij}^{[\pm]}(x, p_T, P, S) = \int \frac{\mathrm{d}\xi^- \, \mathrm{d}^2\xi_T}{(2\pi)^3} e^{ip\xi} \langle P, S | \overline{\psi}_j(0) \, \mathcal{L}^{[\pm]}(0, \xi^-) \, \psi_i(\xi) | P, S \rangle_c \Big|_{\substack{\xi^+=0 \\ p^+=xP^+}} , \tag{2.58}$$

where the two different paths of the gauge links $\mathcal{L}^{[\pm]}$ are indicated in Fig. 2.11b,c. In general also other paths will appear in link operators, but those will be discussed in chapter 4 and 5. The analytical structure of the correlator has the following properties

$$\Phi^{[\pm]\dagger}(x, p_T, P, S) = \gamma^0 \, \Phi^{[\pm]}(x, p_T, P, S) \, \gamma^0 \qquad \text{(hermiticity)}, \tag{2.59}$$

$$\Phi^{[\pm]}(x, p_T, P, S) = \gamma^0 \, \Phi^{[\pm]}(x, -p_T, \bar{P}, -\bar{S}) \, \gamma^0 \qquad \text{(parity)}, \tag{2.60}$$

$$\Phi^{[\pm]*}(x, p_T, P, S) = i\gamma_5 C \, \Phi^{[\mp]}(x, -p_T, \bar{P}, \bar{S}) \, i\gamma_5 C \qquad \text{(time-reversal)}. \tag{2.61}$$

The last equation shows that the time-reversal operation relates the two different paths of the gauge links. This enables us to decompose Φ in two classes, one which is the average and is called T-even, and one which is the difference and is called T-odd (T-odd does not mean breaking of time-reversal in QCD, the name is similar to P-odd)

$$\Phi^{[\text{T-even}]}(x, p_T, P, S) = \frac{1}{2}\Big(\Phi^{[+]}(x, p_T, P, S) + \Phi^{[-]}(x, p_T, P, S)\Big), \tag{2.62}$$

$$\Phi^{[\text{T-odd}]}(x, p_T, P, S) = \frac{1}{2}\Big(\Phi^{[+]}(x, p_T, P, S) - \Phi^{[-]}(x, p_T, P, S)\Big). \tag{2.63}$$

Although the phenomenology of T-odd distribution functions was studied, see for instance Anselmino, D'Alesio, Boglione, Murgia [70, 71, 72] and Boer, Mulders [73], T-odd distribution functions were not really believed to exist as separate distributions (for example see Collins in Ref. [23]). After Brodsky, Hwang, and Schmidt showed in Ref. [24] that unsuppressed T-odd effects could be generated in a particular model, the existence of T-odd distribution functions was taken as a serious possibility (see also Collins [25] and Belitsky, Ji, Yuan [26]). At present the data of HERMES as shown in chapter 1, Fig. 1.3, indicate that T-odd functions might really exist.

Another mechanism for T-odd functions has also been suggested by Anselmino, Barone, Drago, and Murgia in Ref. [74] based on nonstandard time-reversal. This mechanism is not taken into account here but could be included at a later stage. If this mechanism is realized in nature it would lead to universality problems for the distribution functions similar to those already appearing for fragmentation functions. The latter problem will be discussed in the next section.

The T-even and T-odd parts of $\Phi^{[\pm]}$ have identical parity and hermiticity properties and they can be parametrized in a set of functions. Before going to the explicit parametrizations it is interesting to note that a distribution correlator can now be given by a T-even and a sign dependent T-odd part

$$\Phi^{[\pm]}(x, p_T, P, S) = \Phi^{[\text{T-even}]}(x, p_T, P, S) \pm \Phi^{[\text{T-odd}]}(x, p_T, P, S). \tag{2.64}$$

This means that T-odd distribution functions enter with a sign [25, 75] depending on the path of the gauge link. In the next chapters we will see that this path is set by the process or subprocess.

The introduction of the distribution functions

The correlator can be parametrized as follows [36, 63, 76, 77, 78, 79]

$$\begin{aligned}
&\Phi^{[\text{T-even}]}(x, p_T, P, S) \\
&\quad = \frac{1}{2}\left(f_1\, \not{n}_+ + \left(S_L\, g_{1L} - \tfrac{p_T\cdot S_T}{M}\, g_{1T}\right)\gamma_5 \not{n}_+\right) && \text{(twist 2)} \\
&\quad\quad + \frac{1}{2}\left(h_{1T}\, \gamma_5 \not{S}_T \not{n}_+ + \left(S_L\, h_{1L}^{\perp} - \tfrac{p_T\cdot S_T}{M}\, h_{1T}^{\perp}\right)\frac{\gamma_5 \not{p}_T \not{n}_+}{M}\right) && \text{(twist 2)} \\
&\quad\quad + \left(\frac{M}{2P^+}\right)\left(e + f^{\perp}\, \frac{\not{p}_T}{M}\right) && \text{(twist 3, unpolarized)} \\
&\quad\quad + \left(\frac{M}{2P^+}\right)\left(\left(S_L\, g_L^{\perp} - \tfrac{p_T\cdot S_T}{M}\, g_T^{\perp}\right)\frac{\gamma_5 \not{p}_T}{M} + g_T'\, \gamma_5 \not{S}_T\right) && \text{(twist 3, polarized)} \\
&\quad\quad + \left(\frac{M}{2P^+}\right)\left(h_T^{\perp}\, \frac{\gamma_5[\not{S}_T, \not{p}_T]}{2M}\right) && \text{(twist 3, polarized)} \\
&\quad\quad + \left(\frac{M}{2P^+}\right)\left(\left(S_L\, h_L - \tfrac{p_T\cdot S_T}{M}\, h_T\right)\frac{\gamma_5[\not{n}_+, \not{n}_-]}{2}\right) && \text{(twist 3, polarized)} \\
&\quad\quad + \text{higher twist,} \\
&\Phi^{[\text{T-odd}]}(x, p_T, P, S) \\
&\quad = \frac{1}{2}\left(f_{1T}^{\perp}\, \frac{\epsilon_T^{\mu\nu} S_{T\mu} p_{T\nu} \not{n}_+}{M} + h_1^{\perp}\, \frac{i \not{p}_T \not{n}_+}{M}\right) && \text{(twist 2)} \\
&\quad\quad + \left(\frac{M}{2P^+}\right)\left(h\, \frac{i[\not{n}_+, \not{n}_-]}{2} + g^{\perp}\, \frac{\epsilon_T^{\mu\nu}\, p_{T\mu} \gamma_\nu \gamma_5}{M}\right) && \text{(twist 3, unpolarized)} \\
&\quad\quad + \left(\frac{M}{2P^+}\right)\left(\frac{\epsilon_T^{\mu\nu} S_{T\mu} p_{T\nu}}{M} e_T^{\perp} - f_T\, \epsilon_T^{\mu\nu} \gamma_\mu S_{T\nu}\right) && \text{(twist 3, polarized)} \\
&\quad\quad - \left(\frac{M}{2P^+}\right)\left((S_L\, f_L^{\perp} - \tfrac{p_T\cdot S_T}{M}\, f_T^{\perp})\frac{\epsilon_T^{\mu\nu} \gamma_\mu p_{T\nu}}{M}\right) && \text{(twist 3, polarized)} \\
&\quad\quad - \left(\frac{M}{2P^+}\right)\left(\left(S_L\, e_L - \tfrac{p_T\cdot S_T}{M}\, e_T\right) i\gamma_5\right) && \text{(twist 3, polarized)} \\
&\quad\quad + \text{higher twist.}
\end{aligned} \tag{2.65}$$

parametrization of the distribution quark-quark correlator

All functions have the arguments x and p_T^2 and also depend on a renormalization scale.

In contrast to the integrated distribution functions the scale dependence is not known for transverse momentum dependent functions (see for instance Henneman [66]).

In the T-odd correlator the new functions $g^{\perp}$, $e_T^{\perp}$, and $f_T^{\perp}$ are included. The function $g^{\perp}$ (as defined in Ref. [36]) and the existence of the others were discovered in Ref. [36]. Subsequently, a complete parametrization was given by Goeke, Metz, and Schlegel in Ref. [79]. The fact that $\int \mathrm{d}^2 p_T \;\; \Phi^{[\text{T-odd}]}(x, p_T) = 0$ leads to constraints for the T-odd functions h, f_T, e_L, and $f_T^{\perp}$ (see for example Ref. [35, 79]).

The first transverse moment of the correlator Φ and some function f_i is defined as

$$\Phi_{\partial}^{\alpha}(x, P, S) \equiv \int \mathrm{d}^2 p_T \; p_T^{\alpha} \; \Phi(x, p_T, P, S). \tag{2.66}$$

$$f_i^{(1)}(x) \equiv \int \mathrm{d}^2 p_T \; \frac{\mathbf{p}_T^2}{2M^2} \; f_i(x, p_T^2). \tag{2.67}$$

The introduced functions describe how the quarks are distributed in the nucleon. The leading twist functions (twist 2) are again probability functions and therefore contain valuable information. For instance, the functions $f_1(x, p_T^2)$ and $g_{1L}(x, p_T^2)$ are generalizations of $f_1(x)$ and $g_1(x)$. For more information on the interpretation of T-even functions the reader is referred to Ref. [64, 80].

For the interested reader the proof for the probability interpretation of f_1 is given here (see for instance Ref. [59, 81], and Ref. [82] for related work)

$$\begin{aligned}
f_1 &= \frac{1}{2} \,\mathrm{Tr}\, \not{n}_{-} \Phi^{[\text{T-even}]} \\
&= \sum_X \int \frac{\mathrm{d}^3 \mathbf{P}_X}{(2\pi)^3 2E_{\mathbf{P}_X}} \int \frac{\mathrm{d}^2 \xi_T \, \mathrm{d}\xi^-}{(2\pi)^3} e^{ip\xi} \langle P, S | \Big(\tfrac{\gamma^- \gamma^+}{2} \psi(0) \Big)^{\dagger} \mathcal{L}^{0_T,\, \xi^+}(0^-, \infty^-) \mathcal{L}^{\infty^-,\, \xi^+}(0_T, \infty_T) | P_X \rangle_{\mathrm{c}} \\
&\quad \times \frac{1}{\sqrt{2}} \langle P_X | \mathcal{L}^{\infty^-,\, \xi^+}(\infty_T, \xi_T) \mathcal{L}^{\xi_T,\, \xi^+}(\infty^-, \xi^-) \tfrac{\gamma^- \gamma^+}{2} \psi(\xi) | P, S \rangle_{\mathrm{c}} \Big|_{\xi^+=0} \\
&= \frac{1}{\sqrt{2}} \sum_X \int \frac{\mathrm{d}^3 \mathbf{P}_X}{(2\pi)^3 2E_{\mathbf{P}_X}} \; \delta(p^+ + P_X^+ - P^+) \; \delta^2(p_T - P_{XT}) \\
&\quad \times \left| \langle P, S | \Big(\tfrac{\gamma^- \gamma^+}{2} \psi(0) \Big)^{\dagger} \mathcal{L}^{0_T,\, \xi^+}(0^-, \infty^-) \mathcal{L}^{\infty^-,\, \xi^+}(0_T, \infty_T) | P_X \rangle_{\mathrm{c}} \right|^2 \Big|_{\xi^+=0} > 0.
\end{aligned} \tag{2.68}$$

For the other leading twist functions (T-even and T-odd) the proof is analogous. The fact that the leading twist functions are probabilities leads to several positivity bounds, see for instance Soffer [83], and Bacchetta et al. [81].

The leading twist T-odd functions (such as the *Sivers function* $f_{1T}^{\perp}$) do not have a parton interpretation in terms of quarks although they are probabilities as well. To obtain an interpretation we consider the transverse moment of a T-odd correlator (see also Eq. 2.66) and rewrite the quark transverse momentum as a derivative acting on the gauge links alone

$$\begin{aligned}\Phi_{\partial}^{[\text{T-odd}]\alpha}(x,P,S) = \frac{1}{2}\int \mathrm{d}^2 p_T \int \frac{\mathrm{d}\xi^-\,\mathrm{d}^2\xi_T}{(2\pi)^3} e^{ip\xi} \langle P,S|\overline{\psi}_j(0) \\ \times \left(i\partial_{\xi_T}^{\alpha} \left[\mathcal{L}^{[+]}(0,\xi^-) - \mathcal{L}^{[-]}(0,\xi^-) \right] \right) \psi_i(\xi)|P,S\rangle_{\text{c}}\Big|_{\substack{\xi^+=0 \\ p^+=xP^+}} . \qquad (2.69)\end{aligned}$$

Using identities of Ref. [35] (the second identity can be proven by using that $G^{+\alpha} \sim [iD^+, iD^\alpha]$, $i\partial_{\xi}^{+}\mathcal{L}^{\xi^+,\xi_T}(\eta^-,\xi^-) = \mathcal{L}^{\xi^+,\xi_T}(\eta^-,\xi^-)iD^+(\xi)$, and shifting iD^+ to the side)

$$\begin{aligned} & i\partial_{\xi_T}^{\alpha}\mathcal{L}^{\pm\infty^-,\,a^+}(0_T,\xi_T) \\ & \qquad = \mathcal{L}^{\pm\infty^-,\,a^+}(0_T,\xi_T) iD_T^{\alpha}(\pm\infty, a^+, \xi_T), \\ & \\ & iD_T^{\alpha}(\zeta^-, a^+, \xi_T)\mathcal{L}^{\xi_T,\,a^+}(\zeta^-,\xi^-) \\ & \qquad = \mathcal{L}^{\xi_T,\,a^+}(\zeta^-,\xi^-) iD_T^{\alpha}(\xi^-, a^+, \xi_T) \\ & \qquad\qquad - g\int_{\zeta^-}^{\xi^-} \mathrm{d}\eta^-\; \mathcal{L}^{\xi_T,\,a^+}(\zeta^-,\eta^-) G_T^{+\alpha}(\eta^-, a^+, \xi_T) \mathcal{L}^{\xi_T,\,a^+}(\eta^-,\xi^-), \qquad (2.70)\end{aligned}$$

identities concerning gauge links

where a^+ is some constant and $iD_T^{\alpha}(\xi^-, a^+, \xi_T) \equiv i\partial_{\xi_T}^{\alpha} + gA_T^{\alpha}(\xi^-, a^+, \xi_T)$, the derivative on the difference of the links can be written as

$$\begin{aligned}\Phi_{\partial}^{[\text{T-odd}]\alpha}(x,P,S) = \frac{g}{2}\int \frac{\mathrm{d}\xi^-\,\mathrm{d}\eta^-}{2\pi} e^{ixP^+\xi^-} \langle P,S|\overline{\psi}_j(0) \\ \times \mathcal{L}^{0_T,\,\xi^+}(0^-,\eta^-) G_T^{+\alpha}(\eta) \mathcal{L}^{0_T,\,\xi^+}(\eta^-,\xi^-)\psi_i(\xi)|P,S\rangle_{\text{c}}\Big|_{\substack{\eta^+=\xi^+=0 \\ \eta_T=\xi_T=0}} . \qquad (2.71)\end{aligned}$$

This matrix element is also called a *gluonic pole matrix element*. In 1991 such a matrix element was suggested by Qiu and Sterman in Ref. [84, 85] as an explanation for single spin asymmetries in photon-production in hadron-hadron scattering and it has been subsequently studied in several other articles [57, 86, 87, 88, 89, 90]. We see here that the same matrix element appears in the two separately suggested mechanisms for T-odd effects [35] (the soft gluon effects of Qiu and Sterman and the gauge link).

At first sight it seems strange that the nontrivial path is the origin of T-odd functions. One might think that such functions should vanish, since in the light-cone gauge, $A^+ = 0$, the T-odd distribution functions become proportional to transverse gauge links at infinity (see Eq. 2.69 and Fig. 2.11c, d) and shouldn't those matrix elements vanish? Since we are at present not able to calculate those matrix elements in QCD we do not really know the answer, but we do know that nonzero A-fields can give effects in areas where the physical fields, like $G^{\alpha\beta}$, are required to vanish. An example of such an effect is the Aharanov-Bohm experiment which was discussed in chapter 1.

The Lorentz invariance relations and $g^\perp$

Before the paper of Brodsky, Hwang, and Schmidt [24] appeared, physical effects from the gauge link were assumed to be absent which led to several interesting observations. Not only did T-odd effects disappear, but relations between the various functions in the correlator were also obtained. By arguing that the correlator $\Phi(x, p_T, P, S)$ could be written in terms of only fermion fields, the starting point then was another object $\Phi(p, P, S)$ which is defined by

$$\Phi_{ij}(p, P, S) = \int \frac{\mathrm{d}^4\xi}{(2\pi)^4}\, e^{ip\xi}\, \langle P, S\,|\, \bar{\psi}_j(0)\, \psi_i(\xi)\, |P, S\,\rangle_{\mathrm{c}}. \tag{2.72}$$

This quantity $\Phi(p, P, S)$ is the fully unintegrated correlator, from which $\Phi(x, p_T, P, S)$ (without gauge link) is obtained via

$$\Phi(x, p_T, P, S) = \int \mathrm{d}p^-\, \Phi(p, P, S). \tag{2.73}$$

Without the gauge link the parametrization of the object $\Phi(p, P, S)$ contains less functions than $\Phi(x, p_T, P, S)$. This led to the so-called *Lorentz-invariance relations*[5] (see Boer, Jakob, Henneman, Mulders, Tangerman [63, 78, 94, 95])

$$\begin{aligned} &g_T(x) = g_1(x) + \frac{\mathrm{d}}{\mathrm{d}x} g_{1T}^{\perp(1)}(x), \qquad g_L^\perp(x) = -\frac{\mathrm{d}}{\mathrm{d}x} g_T^{\perp(1)}(x), \quad h_T(x) = -\frac{\mathrm{d}}{\mathrm{d}x} h_{1T}^{\perp(1)}(x), \\ &h_L(x) = h_1(x) - \frac{\mathrm{d}}{\mathrm{d}x} h_{1L}^{\perp(1)}(x), \quad h_{1L}^\perp(p^+, \mathbf{p}_T^2) = h_T(p^+, \mathbf{p}_T^2) - h_T^\perp(p^+, \mathbf{p}_T^2). \end{aligned} \tag{2.74}$$

Similar relations for T-odd distribution functions were obtained as well.

Taking the gauge link into account affects these relations. Since the gauge link runs in the n_--direction via infinity (see Fig. 2.11), it is not clear how to construct an n_--independent $\Phi(p, P, S)$ which after an integration over p^- leads to $\Phi(x, p_T, P, S)$ containing the gauge link. In 2003, this was made explicit by Goeke, Metz, Pobylitsa, and Polyakov in Ref. [96]. Taking the n_--dependence into account, they showed that the former proof of the Lorentz-invariance relations failed.

It seems to be impossible to maintain the Lorentz-invariance relations for T-odd functions since the involved matrix elements are intrinsically nonlocal (see for instance Eq. 2.71). This is in contrast to the first transverse moment of a T-even function which is local in the light-cone gauge. This could imply that the Lorentz-invariance relations might still hold for the T-even functions.

The n_--dependence of the gauge link implies not only the need to revisit the Lorentz-invariance relations [96], but also leads to new functions in the parametrizations as discovered in Ref. [36] and confirmed in Ref. [79]. Since the origin of $g^\perp$ is connected to the non-validity of the Lorentz-invariance relations, a measurement of $g^\perp$ or checking the Lorentz-invariance relations (Eq. 2.74) would be interesting. In the next chapter it will be pointed out how $g^\perp$ can be accessed.

---

[5] Based on Lorentz invariance, relations were also derived by Bukhvostov, Kuraev, and Lipatov in Ref. [91, 92, 93]. It is at present unclear why their relations are different from the relations given here.

2.6 Quark fragmentation functions into spin-$\frac{1}{2}$ hadrons

The introduction of the fragmentation functions proceeds analogously to the introduction of the distribution functions. A set of light-like vectors is introduced such that

$$\boxed{\begin{aligned}
1 &= n_- \cdot n_+, & n_- &\sim \overline{n}_+, \\
P_h &= P_h^-\, n_- + \frac{M_h^2}{2P_h^-}\, n_+, & \epsilon_T^{\mu\nu} &\equiv \epsilon^{\rho\sigma\mu\nu} n_{+\rho} n_{-\sigma}, \\
g_T^{\mu\nu} &= g^{\mu\nu} - n_+^\mu n_-^\nu - n_+^\nu n_-^\mu, & A_T^\mu &= g_T^{\mu\nu} A_\nu,\ \text{for any } A. \qquad (2.75) \\
&& &\textit{the basis in which parton fragmentation functions are defined}
\end{aligned}}$$

Also here we define for every vector A the Lorentz-invariants $A^\pm \equiv A \cdot n_\mp$. The spin of the observed hadron is decomposed as

$$S_h = S_{hL} \frac{P_h^-}{M_h}\, n_- - S_{hL} \frac{M_h}{2P_h^-}\, n_+ + S_{hT} \qquad \text{with } S_{hL}^2 + \mathbf{S}_{hT}^2 = 1. \tag{2.76}$$

Similarly as for distribution functions, M_h/P_h^- does not have to be small. However, calculations of cross sections will be constructed in such a way that $P_h^- \gg M_h$.

In general one encounters integrated and unintegrated fragmentation functions. The integrated fragmentation functions will be discussed in the next subsection. For the unintegrated functions we will see that the two different link structures (as for the distribution functions) produce problems with universality [35]. In the second subsection, these functions will be parametrized.

2.6.1 Integrated fragmentation functions

The integrated correlator which appears in cross sections is expressed as[6]

$$\begin{aligned}
\Delta_{ij}(z^{-1}, P_h, S_h) \equiv \frac{1}{3} \sum_X \int \frac{d^3\mathbf{P}_X}{(2\pi)^3 2E_{\mathbf{P}_X}} \int \frac{d\eta^+}{2\pi} e^{iz^{-1}P_h^-\eta^+} {}_{\text{out}}\langle P_h, S_h; P_X | \overline{\psi}_j(0) | \Omega \rangle_{\text{c}} \\
\times \langle \Omega | \mathcal{L}^{0_T,\,\eta^-}(0^+, \eta^+) \psi_i(\eta) | P_h, S_h; P_X \rangle_{\text{out,c}} \Big|_{\substack{\eta^-=0,\\ \eta_T=0}}, \qquad (2.77)
\end{aligned}$$

---

[6] In order to write the gauge link in one of the matrix elements the light-cone gauge was chosen in an intermediate step.

where a factor 1/3 is introduced in the definition to average over the initial quark's color, and where the color indices are contracted. Its analytical structure satisfies the following constraints

$$\Delta^{\dagger}(z^{-1}, P_h, S_h) = \gamma^0\, \Delta(z^{-1}, P_h, S_h)\, \gamma^0 \qquad \text{(hermiticity)}, \tag{2.78}$$

$$\Delta(z^{-1}, P_h, S_h) = \gamma^0\, \Delta(z^{-1}, \bar{P}_h, -\bar{S}_h)\, \gamma^0 \qquad \text{(parity)}. \tag{2.79}$$

For fragmentation functions there is no constraint from time-reversal. In the case of distribution functions we have that $\mathcal{T}|P\rangle_{\text{in}} = |P\rangle_{\text{out}} = |P\rangle_{\text{in}}$, but for fragmentation functions there are several particles in the out-state which might interact with each other. Therefore, such an identity does not hold and integrated T-odd fragmentation functions appear (in contrast to the integrated distribution functions). This mechanism to generate T-odd functions was introduced by Collins in Ref. [23] and was shown to exist in model calculations by Bacchetta, Kundu, Metz, and Mulders in Ref. [97, 98].

We continue by defining T-odd and T-even for fragmentation and write

$$\Delta(z^{-1}, P_h, S_h) \equiv \Delta^{[\text{T-even}]}(z^{-1}, P_h, S_h) + \Delta^{[\text{T-odd}]}(z^{-1}, P_h, S_h), \tag{2.80}$$

where $\Delta^{[\text{T-even}]}(z^{-1}, P_h, S_h)$ and $\Delta^{[\text{T-odd}]}(z^{-1}, P_h, S_h)$ obey

$$\Delta^{[\text{T-even}]*}(z^{-1}, P_h, S_h) = \quad (i\gamma_5 C)\, \Delta^{[\text{T-even}]}(z^{-1}, P_h, S_h)\, (i\gamma_5 C), \tag{2.81}$$

$$\Delta^{[\text{T-odd}]*}(z^{-1}, P_h, S_h) = (-)(i\gamma_5 C)\, \Delta^{[\text{T-odd}]}(z^{-1}, P_h, S_h)\, (i\gamma_5 C). \tag{2.82}$$

This gives the following parametrization of fragmentation into a spin-$\frac{1}{2}$ hadron

$$\boxed{\begin{aligned} \Delta(z^{-1}, P_h, S_h) = {} & \frac{1}{z}\Big(D_1\, \not{n}_- - S_{hL}\, G_1\, \not{n}_-\gamma_5 + H_1\, \not{S}_{hT}\not{n}_-\gamma_5\Big) && \text{(twist 2, T-even)} \\ & + \frac{M_h}{zP_h^-}\Big(-G_T\, \not{S}_{hT}\gamma_5 + S_{hL}\, H_L\, \frac{[\not{n}_-, \not{n}_+]}{2}\gamma_5 + E\Big) && \text{(twist3, T-even)} \\ & + \frac{M_h}{zP_h^-}\Big(D_T\, \epsilon_T^{\rho\sigma}\gamma_\rho S_{hT\sigma} - S_{hL}\, E_L\, i\gamma_5 + i\, H\, \frac{[\not{n}_-, \not{n}_+]}{2}\Big) && \text{(twist3, T-odd)} \\ & + \text{higher twist.} && (2.83) \\ & && \textit{parametrization of the integrated fragmentation correlator} \end{aligned}}$$

where all functions depend on z and a renormalization scale.

The functions D_1, G_1, and H_1 have similar interpretations as the analogous distribution functions. The function D_1 describes for instance how an unpolarized quark (being either red, green, or blue) decays into a hadron plus jet (over final state colors is summed). T-odd effects appear at subleading twist for fragmentation into spin-$\frac{1}{2}$ hadrons, in contrast to fragmentation into spin-1 hadrons where T-odd effects already appear at leading twist (see for example Bacchetta, Mulders [99]).

2.6.2 Transverse momentum dependent fragmentation functions

Gauge invariant correlators and T-odd behavior

Similarly as for the unintegrated distribution correlators one encounters fragmentation correlators with two different links, defined through

$$\begin{aligned}
&\Delta_{ij}^{[\pm]}(z^{-1}, k_T, P_h, S_h) \\
&\quad \equiv \frac{1}{3}\sum_X \int \frac{d^3\mathbf{P}_X}{(2\pi)^3 2E_{\mathbf{P}_X}} \int \frac{d\eta^+\, d^2\eta_T}{(2\pi)^3} e^{ik\eta} \\
&\qquad \times {}_{\text{out}}\langle P_h, S_h; P_X|\overline{\psi}_j(0)\mathcal{L}^{0_T,\,\eta^-}(0,\pm\infty^+)\mathcal{L}^{\pm\infty^+,\,\eta^-}(0_T,\infty_T)|\Omega\rangle_{\text{c}} \\
&\qquad \times \langle\Omega|\mathcal{L}^{\pm\infty^+,\,\eta^-}(\infty_T,\eta_T)\mathcal{L}^{0_T,\,\eta^-}(\pm\infty^+,\eta^+)\psi_i(\eta)|P_h, S_h; P_X\rangle_{\text{out,c}}\Big|_{\substack{\eta^-=0 \\ k^-=z^{-1}P_h^-}} .
\end{aligned} \tag{2.84}$$

When studying the analytical structure of this correlator one finds

$$\Delta^{[\pm]\dagger}(z^{-1}, k_T, P_h, S_h) = \gamma^0\, \Delta^{[\pm]}(z^{-1}, k_T, P_h, S_h)\, \gamma^0 \qquad \text{(hermiticity)}, \tag{2.85}$$

$$\Delta^{[\pm]}(z^{-1}, k_T, P_h, S_h) = \gamma^0\, \Delta^{[\pm]}(z^{-1}, -k_T, \bar{P}_h, -\bar{S}_h)\, \gamma^0 \qquad \text{(parity)}. \tag{2.86}$$

As for the integrated correlators, the time-reversal operation does not lead to additional constraints. This means that the functions appearing in the two different fragmentation correlators, $\Delta^{[\pm]}$, cannot be related. That holds for the T-odd functions as well as for the T-even functions. Since the functions become universal after an integration over k_T, there could be a universality relation for the unintegrated functions but at present such a QCD-relation is unknown. This forms a problem for the by Collins [23] suggested method of accessing transversity via the *Collins function* $H_1^\perp$ (*Collins effect*).

The problem with universality comes from the interplay of two effects, the final-state interactions (in and out-states) and the gauge link. If one of the two mechanisms would be suppressed the situation is simplified. For instance, if final-state interactions in the out-states are suppressed, then T-odd functions will enter with a sign depending on the gauge link or process similar to the situation for the distribution functions. On the other hand, if gauge links do not influence the expectation value of matrix elements, then fragmentation functions will be the same in all processes (no gauge link means no process-dependence from that source). The latter scenario has been observed by Metz in a model calculation [100] and has subsequently been advocated by Metz and Collins in Ref. [101]. In the next chapter the discussion on universality will be continued.

The parametrizations

Transverse moments of fragmentation functions are often encountered. For a function $D_i(z, z^2k_T^2)$, it is defined as

$$D_i^{(1)}(z) \equiv z^2 \int d^2k_T\, \frac{\mathbf{k}_T^2}{2M_h^2}\, D_i(z, z^2k_T^2). \tag{2.87}$$

The correlator is decomposed as (see also Ref. [36, 79, 102, 103])

$$
\begin{aligned}
&\Delta^{[\pm]}(z^{-1}, k_T, P_h, S_h) = \Delta^{[\pm,\text{T-even}]}(z^{-1}, k_T, P_h, S_h) + \Delta^{[\pm,\text{T-odd}]}(z^{-1}, k_T, P_h, S_h) \\
&\Delta^{[\pm,\text{T-even}]}(z^{-1}, k_T, P_h, S_h) \\
&\quad = z\left(D_1^{[\pm]}\,\not{n}_- + \left(S_{hL}\,G_{1L}^{[\pm]} - \tfrac{k_T\cdot S_{hT}}{M_h}\,G_{1T}^{[\pm]}\right)\gamma_5\not{n}_-\right) && \text{(twist 2)} \\
&\qquad + z\left(H_{1T}^{[\pm]}\,\gamma_5\not{S}_{hT}\not{n}_- + \left(S_{hL}\,H_{1L}^{\perp[\pm]} - \tfrac{k_T\cdot S_{hT}}{M_h}\,H_{1T}^{\perp[\pm]}\right)\frac{\gamma_5\not{k}_T\not{n}_-}{M_h}\right) && \text{(twist 2)} \\
&\qquad + \left(\frac{zM_h}{P_h^-}\right)\left(E^{[\pm]} + D^{\perp[\pm]}\,\frac{\not{k}_T}{M_h}\right) && \text{(twist 3, unpolarized)} \\
&\qquad + \left(\frac{zM_h}{P_h^-}\right)\left(\left(S_{hL}G_L^{\perp[\pm]} - \tfrac{k_T\cdot S_{hT}}{M_h}\,G_T^{\perp[\pm]}\right)\frac{\gamma_5\not{k}_T}{M_h} + G_T^{\prime[\pm]}\,\gamma_5\not{S}_{hT}\right) && \text{(twist 3, polarized)} \\
&\qquad + \left(\frac{zM_h}{P_h^+}\right)\left(H_T^{\perp[\pm]}\,\frac{\gamma_5[\not{S}_{hT}, \not{k}_T]}{2M_h}\right) && \text{(twist 3, polarized)} \\
&\qquad + \left(\frac{zM_h}{P_h^-}\right)\left(S_{hL}\,H_L^{[\pm]} - \tfrac{k_T\cdot S_{hT}}{M_h}\,H_T^{[\pm]}\right)\frac{\gamma_5[\not{n}_-, \not{n}_+]}{2} && \text{(twist 3, polarized)} \\
&\qquad + \text{higher twist,} \\
&\Delta^{[\pm,\text{T-odd}]}(z^{-1}, k_T, P_h, S_h) \\
&\quad = z\left(D_{1T}^{\perp[\pm]}\,\frac{\epsilon_T^{\mu\nu}k_{T\mu}S_{hT\nu}\not{n}_-}{M_h} + H_1^{\perp[\pm]}\,\frac{i\not{k}_T\not{n}_-}{M_h}\right) && \text{(twist 2)} \\
&\qquad + \left(\frac{zM_h}{P_h^-}\right)\left(H^{[\pm]}\,\frac{i[\not{n}_-, \not{n}_+]}{2} + G^{\perp[\pm]}\,\frac{\epsilon_T^{\mu\nu}k_{T\mu}\gamma_\nu\gamma_5}{M_h}\right) && \text{(twist 3, unpolarized)} \\
&\qquad + \left(\frac{zM_h}{P_h^-}\right)\left(\frac{\epsilon_T^{\mu\nu}k_{T\mu}S_{hT\nu}}{M_h}E_T^{\perp[\pm]} + D_T^{[\pm]}\,\epsilon_T^{\mu\nu}\gamma_\mu S_{h\nu}\right) && \text{(twist 3, polarized)} \\
&\qquad + \left(\frac{zM_h}{P_h^-}\right)\left((S_{hL}\,D_L^{\perp[\pm]} - \tfrac{k_T\cdot S_{hT}}{M_h}\,D_T^{\perp[\pm]})\frac{\epsilon_T^{\mu\nu}\gamma_\mu k_{T\nu}}{M_h}\right) && \text{(twist 3, polarized)} \\
&\qquad - \left(\frac{zM_h}{P_h^-}\right)\left(S_{hL}\,E_L^{[\pm]} - \tfrac{k_T\cdot S_{hT}}{M_h}\,E_T^{[\pm]}\right)i\gamma_5 && \text{(twist3, polarized)} \\
&\qquad + \text{higher twist.} && (2.88)
\end{aligned}
$$

parametrization of the fragmentation quark-quark correlator

where all functions depend on z and $z^2k_T^2$. Also here a renormalization scale is involved. In order to address the universality issue, it is important to measure T-even and T-odd fragmentation functions in different processes. For fragmentation functions a set of Lorentz invariance relations has also been put forward. For the validity of these relations, the same issues as discussed in the previous section play a role.

2.7 Summary and conclusions

We introduced several Cartesian bases and expressed head-on cross sections in terms of Lorentz-invariants. It was shown how frame-independent observables can be defined, simplifying comparisons between theoretical predictions, experimental observations, and fixed frame definitions which are already in use in the literature.

Two approaches were discussed to access the parton distribution functions. The first approach is the operator product expansion. Although this method has a firm theoretical basis its applicability turns out to be limited. The other approach, the diagrammatic expansion, is a field theoretical extension of the parton model. Although slightly less rigorous than the operator product expansion, it can be applied to most hadronic scattering processes and agrees with the operator product expansion when applicable. The diagrammatic approach will be used in the rest of the thesis.

It was indicated that an infinite set of diagrams, appearing in the diagrammatic expansion, can be rewritten such that transverse momentum dependent correlators including a gauge link appear. These correlators underlie the definition of parton distributions, and provide important information on the partonic structure of hadrons. The definition of these correlators contains a bilocal operator and a gauge link which ensures invariance under local color gauge transformations. Since the path of the gauge link introduces a directional dependence, new parton distribution and fragmentation functions were discovered at twist three (for related work, see Goeke, Metz, Schlegel [79]). A measurement of these new functions would contribute to the understanding of the theoretical description.

Using time-reversal, the functions can be divided in two classes, called T-even and T-odd. It was shown that the first transverse moment of T-odd distribution functions corresponds to the gluonic pole matrix element, which Qiu and Sterman suggested to explain T-odd effects [84, 85]. As discovered by Collins [25], it was also found that T-odd distribution functions appear with opposite signs in the parametrization of correlators which have a gauge link via plus or minus infinity. In chapter 4 we will see that other link structures in correlators can appear, giving more complex factors.

For fragmentation functions a universality problem was encountered due to the two possible mechanisms to produce T-odd effects, the final-state interactions and the presence of a gauge link. This means that the value of unintegrated fragmentation functions and their transverse moments can be different for different experiments, forming a potential problem for extracting transversity via the Collins effect. It is therefore important to compare fragmentation functions which are measured in different processes (for example their z-dependences). If for instance one of the two effects is suppressed, a simple sign relation (plus or minus) should appear between functions which have gauge links via plus or minus infinity. The discussion on the universality of fragmentation functions will be continued in the next chapter.

2.A Outline of proof of Eq. 2.18

For the interested reader a derivation of Eq. 2.18 will be presented here. The derivation is based on section 4.2 and 7.2 of Peskin and Schroeder [31].

The invariant amplitude can be obtained via the S-matrix

$$S \equiv \mathbf{1} + iT, \tag{2.89}$$

$$_{\text{free}}\langle P_X, P_h, l'|iT|P, l\rangle_{\text{free}} \equiv (2\pi)^4 \delta^4 \left(l + P - l' - P_h - P_X\right) i\mathcal{M}, \tag{2.90}$$

and the *LSZ reduction formula*

$$\begin{aligned}
&_{\text{free}}\langle P_X, P_h, l'|S|P, l\rangle_{\text{free}} \\
&\times \frac{iZ_e}{l^2 - m_e^2 + i\epsilon} \frac{iZ_P}{P^2 - M^2 + i\epsilon} \frac{iZ_e}{l'^2 - m_e^2 + i\epsilon} \frac{iZ_h}{P_h^2 - M_h^2 + i\epsilon} \frac{iZ_X}{P_X^2 - M_X^2 + i\epsilon} \\
&\quad \sim \int \mathrm{d}^4x_1\, \mathrm{d}^4x_2\, \mathrm{d}^4y_1\, \mathrm{d}^4y_2\, \mathrm{d}^4y_3\; e^{i(l'y_1 + P_h y_2 + P_X y_3 - P x_1 - l x_2)} \\
&\qquad \times \langle\Omega|\mathcal{T}\left[\tfrac{\overline{u}(l',\lambda')\psi_e(y_1)}{2m_e}\right] \Phi_h(y_2)\Phi_X(y_3) \left[\tfrac{\bar{\psi}_P(x_1)U(P,S)}{2M}\right]\left[\tfrac{\bar{\psi}_e(x_2)u(l,\lambda)}{2m_e}\right]|\Omega\rangle,
\end{aligned} \tag{2.91}$$

where the Z_i's represent the field-strength renormalizations, $|\Omega\rangle$ represents the physical vacuum, $\mathcal{T}$ is the time-ordering operator, and $\sim$ means that the two expressions agree in the vicinity of the poles. These poles are generated by the unbounded interval of the integrals and correspond to the asymptotic incoming and outgoing states. The task is now to work out the right-hand-side and to identify these poles.

The time-ordered product can be calculated in the interaction picture. In the interaction picture the Heisenberg fields are decomposed in creation and annihilation operators at some point in time, t_0, which also defines the *quantization plane*. Evolving these operators in time by the Hamiltonian defines the *interaction picture fields*. Since the creation and annihilation operators can be interpreted as asymptotic states it is a priory not clear whether this expansion is valid for quarks and gluons in QCD. Since our final result in this section does not depend on the explicit expansion of these creation and annihilation operators, we will skip here this technical point. Assuming the vacuum structure of QCD to be simple and indicating the fields in the interaction picture with a superscript I, we obtain

$$\begin{aligned}
\text{Eq. (2.91)} \sim \lim_{T\to\infty(1-i\epsilon)} &\int \mathrm{d}^4x_1\, \mathrm{d}^4x_2\, \mathrm{d}^4y_1\, \mathrm{d}^4y_2\, \mathrm{d}^4y_3\; e^{i(l'y_1 + P_h y_2 + P_X y_3 - P x_1 - l x_2)} \\
&\times \langle 0|\mathcal{T}\left[\tfrac{\overline{u}(l',\lambda')\psi_e^I(y_1)}{2m_e}\right] \Phi_h^I(y_2)\Phi_X^I(y_3)U(T,-T) \left[\tfrac{\bar{\psi}_P^I(x_1)U(P,S)}{2M}\right]\left[\tfrac{\bar{\psi}_e^I(x_2)u(l,\lambda)}{2m_e}\right]|0\rangle \\
&\times \left[\langle 0|U(T,-T)|0\rangle\right]^{-1},
\end{aligned} \tag{2.92}$$

where

$$\Phi_i^I(x) \equiv U(x^0, t_0)\ \Phi(x)\ U^\dagger(x^0, t_0), \tag{2.93}$$

$$U(t_b, t_a) \equiv \mathcal{T} \exp\left[-i \int_{t_a}^{t_b} \mathrm{d}t'\ H_I(t')\right], \tag{2.94}$$

and where H_I is the interacting part of the Hamiltonian in the interaction picture, and $|0\rangle$ is the bare vacuum. The interaction Hamiltonian contains the electromagnetic and QCD interactions. The electromagnetic interactions can be treated in perturbation theory while the QCD interactions in general cannot.

To produce nonforward matrix elements there should be at least two electromagnetic interactions, once between the incoming and outgoing electron and once between the incoming and outgoing hadrons, giving

$$\begin{aligned}
&{}_{\text{free}}\langle P_X, P_h, l'|iT|P, l\rangle_{\text{free}} \\
&\quad\times \frac{iZ_e}{l^2 - m_e^2 + i\epsilon}\frac{iZ_P}{P^2 - M^2 + i\epsilon}\frac{iZ_e}{l'^2 - m_e^2 + i\epsilon}\frac{iZ_h}{P_h^2 - M_h^2 + i\epsilon}\frac{iZ_X}{P_X^2 - M_X^2 + i\epsilon} \\
&\sim \int \mathrm{d}^4x_1\ \mathrm{d}^4x_2\ \mathrm{d}^4y_1\ \mathrm{d}^4y_2\ \mathrm{d}^4y_3\ e^{i(l'y_1 + P_h y_2 + P_X y_3 - P x_1 - l x_2)} (-i)^2 \lim_{T\to\infty(1-i\epsilon)} \int \mathrm{d}^4z_1\ \mathrm{d}^4z_2 \\
&\quad\times \langle 0|\mathcal{T}\left[\tfrac{\overline{u}(l',\lambda')\psi_e^I(y_1)}{2m_e}\right] \Phi_h^I(y_2)\Phi_X^I(y_3)U(T, z_1)A_\rho^I(z_1)eJ_{e,I}^\rho(z_1)U(z_1, z_2)A_\sigma^I(z_2) \\
&\quad\times eJ_{q,I}^\sigma(z_2)U(z_2, -T)\left[\tfrac{\overline{\psi}_P^I(x_1)U(P,S)}{2M}\right]\left[\tfrac{\overline{\psi}_e^I(x_2)u(l,\lambda)}{2m_e}\right]|0\rangle\ [\langle 0|U(T, -T)|0\rangle]^{-1}\,,
\end{aligned} \tag{2.95}$$

where $J_{e/q,I}^\rho(z) = Q_{e/q}\ \overline{\psi}_{e/q}^I(z)\gamma^\rho\psi_{e/q}^I(z)$. Using Wick's theorem the lowest nontrivial order in e can be worked out, giving explicitly

$$\begin{aligned}
&\text{Eq. (2.95)} \\
&= \int \mathrm{d}^4x_1\ \mathrm{d}^4x_2\ \mathrm{d}^4y_1\ \mathrm{d}^4y_2\ \mathrm{d}^4y_3\ e^{i(l'y_1 + P_h y_2 + P_X y_3 - P x_1 - l x_2)} (-i)^2 \lim_{T\to\infty(1-i\epsilon)} \int \mathrm{d}^4z_1\ \mathrm{d}^4z_2 \\
&\quad\times \langle 0|\mathcal{T}\left[\tfrac{\overline{u}(l',\lambda')\psi_e^I(y_1)}{2m_e}\right] eJ_{e,I}^\rho(z_1)\left[\tfrac{\overline{\psi}_e^I(x_2)u(l,\lambda)}{2m_e}\right]|0\rangle\langle 0|\mathcal{T}A_\rho^I(z_1)A_\sigma^I(z_2)|0\rangle \\
&\quad\times \langle 0|\mathcal{T}\Phi_h^I(y_2)\Phi_X^I(y_3)U(T, z_1)U(z_1, z_2)eJ_{q,I}^\sigma(z_2)U(z_2, -T)\left[\tfrac{\overline{\psi}_P^I(x_1)U(P,S)}{2M}\right]|0\rangle \\
&\quad\times [\langle 0|U(T, -T)|0\rangle]^{-1} + \mathcal{O}(e^3) \\
&= \frac{i}{l^2 - m_2^2 + i\epsilon}\frac{i}{l'^2 - m_2^2 + i\epsilon}(-ie)\overline{u}(l', \lambda')\gamma_\rho u(l, \lambda) \int \mathrm{d}^4x_1\ \mathrm{d}^4y_2\ \mathrm{d}^4y_3\ e^{i(P_h y_2 + P_X y_3 - P x_1)} \\
&\qquad\times (-i) \lim_{T\to\infty(1-i\epsilon)} \int \mathrm{d}^4z_2\ e^{-iqz_2}\frac{-i}{q^2}\langle 0|\mathcal{T}\Phi_h^I(y_2)\Phi_X^I(y_3)U(T, z_1)U(z_1, z_2)eJ_I^\sigma(z_2) \\
&\qquad\times U(z_2, -T)\left[\tfrac{\overline{\psi}_P^I(x_1)U(P,S)}{2M}\right]|0\rangle\ [\langle 0|U(T, -T)|0\rangle]^{-1} + \mathcal{O}(e^3).
\end{aligned} \tag{2.96}$$

In order to obtain the singularities in the hadron energies it is assumed that the incoming hadron only starts interacting after some point in time, t_i, and that the outgoing hadrons are well-separated wave-packets after some point in time called t_f. These assumptions, known as *adiabatically switching on and off the interactions*, restricts z_2^0 to be $t_i < z_2^0 < t_f$. By doing so, the poles of the incoming nucleon and outgoing hadrons can be identified after which the limits $t_i \to -\infty$ and $t_f \to \infty$ can be taken. One obtains

$$
\begin{aligned}
\text{Eq. (2.96)} = {} & \frac{i}{l^2 - m_2^2 + i\epsilon} \frac{i}{l'^2 - m_2^2 + i\epsilon} (-ie)\overline{u}(l', \lambda')\gamma_\rho u(l, \lambda) \frac{-i}{q^2} \\
& \times \int d^4x_1\, d^4y_2\, d^4y_3\, e^{i(P_h y_2 + P_X y_3 - P x_1)} (-i) \lim_{\substack{t_i \to -\infty \\ t_f \to \infty}} \lim_{T \to (\infty - i\epsilon)} \int d^4 z_2\, e^{-iqz_2} \\
& \times \langle 0 | \mathcal{T} \Phi_h^I(y_2) \Phi_X^I(y_3) U(T, t_f) \Big[U(t_f, t_i) e J_I^\sigma(z_2) \Big] U(t_i, -T) \left[\tfrac{\bar{\psi}_P^I(x_1) U(P,S)}{2M} \right] | 0 \rangle \\
& \times [\langle 0 | U(T, -T) | 0 \rangle]^{-1} + \mathcal{O}(e^3) \\
= {} & \frac{i}{l^2 - m_2^2 + i\epsilon} \frac{i}{l'^2 - m_2^2 + i\epsilon} \frac{iZ_P}{P^2 - M^2 + i\epsilon} \frac{iZ_X}{P_X^2 - M_X^2 + i\epsilon} \frac{iZ_h}{P_h^2 - M_h^2 + i\epsilon} \\
& \times (-ie)\overline{u}(l', \lambda')\gamma_\rho u(l, \lambda)(-i) \lim_{\substack{t_i \to -\infty \\ t_f \to \infty}} \int d^4 z_2\, e^{-iqz_2} \frac{-i}{q^2} \\
& \times {}_{\text{out}}\langle P_h, P_X | \mathcal{T} U(t_0, t_f) \Big[U(t_f, t_i) e J_I^\sigma(z_2) \Big] U(t_i, t_0) | P, S \rangle_{\text{in,c}} + \mathcal{O}(e^3). \qquad (2.97)
\end{aligned}
$$

Note that all the necessary poles including the field-strength renormalizations at order e^2 (for nonforward matrix elements $Z_e = 1$ at this order) have been produced. After shifting the current, $J^\sigma(z_2)$, yielding the delta-function which expresses momentum conservation, we can read off the invariant amplitude $\mathcal{M}$ from Eq. 2.90, giving

$$
\begin{aligned}
i\mathcal{M} = {} & (-ie)\overline{u}(l', \lambda')\gamma_\rho u(l, \lambda) \\
& \times \lim_{\substack{t_i \to -\infty \\ t_f \to \infty}} \frac{-i}{q^2} {}_{\text{out}}\langle P_h, P_X | U(t_0, t_f) \Big[U(t_f, t_i)(-ie) J_I^\rho(0) \Big] U(t_i, t_0) | P, S \rangle_{\text{in,c}} + \mathcal{O}(e^3) \\
= {} & (-ie)\, \overline{u}(l', \lambda')\gamma_\rho u(l, \lambda)\, \frac{-i}{q^2}\, {}_{\text{out}}\langle P_h, P_X | (-ie) J^\rho(0) | P, S \rangle_{\text{in,c}} + \mathcal{O}(e^3). \qquad (2.98)
\end{aligned}
$$

Note that the current, J^ρ, is here in the Heisenberg picture.

2.B The diagrammatic expansion

For the interested reader a short outline of the derivation of two diagrams in the diagrammatic approach will be given here. It will be pointed out how the results can be generalized.

Following the same procedure as applied for semi-inclusive DIS in the previous appendix, one can derive that the invariant amplitude for general processes reads

$$\langle\text{free states } P|iT|\text{free states } Q\rangle = \lim_{\substack{t_i\to-\infty \\ t_f\to\infty}} {}_{\text{out}}\langle P|U(t_0,t_f)\Big[U(t_f,t_i)\Big]U(t_i,t_0)|Q\rangle_{\text{in,c}}, \tag{2.99}$$

where the U's are defined in Eq. 2.94. When applying the diagrammatic expansion one expands the bracketed term.

At tree-level the result is expressed in terms of fields inside matrix elements. These fields can always be transported to the origin, yielding momentum conservation for the incoming and outgoing particles. The lowest order result is the tree-level squared Feynman diagram with spinors or polarization vectors replaced by Heisenberg fields in matrix elements, multiplied by a delta-function expressing momentum conservation.

For example, consider hadron-hadron scattering with momenta P_1 and P_2 producing two hadrons with momenta K_1 and K_2 approximately back-to-back in the azimuthal plane. It is assumed that the outgoing hadrons are well separated from the incoming hadrons. If this is not the case then fracture functions are needed to describe the combined process of distribution and fragmentation. Although the incoming and outgoing partons can be quarks or gluons, we will restrict ourselves to (anti)quarks as external partons, the gluons can be included later on. In that case the incoming quarks or antiquarks interact via a gluon giving quarks and antiquarks in the final state. Expanding the bracketed term of Eq. 2.99 to lowest order this contribution is

$$\begin{aligned}&\langle K_1,K_2,X|iT|P_1,P_2\rangle\\ &= (ig)^2\int d^4x\, d^4y\ {}_{\text{out}}\langle K_1,K_2,X|\mathcal{T}\,\overline{\psi}(x)\not{A}(x)\psi(x)\overline{\psi}(y)\not{A}(y)\psi(y)|P_1,P_2\rangle_{\text{in,c}} + \mathcal{O}(g^3).\end{aligned} \tag{2.100}$$

Overall momentum conservation can be simply obtained by making an overall shift of x and subsequently redefining y. One finds

$$\begin{aligned}\langle K_1,K_2,X|iT|P_1,P_2\rangle = \int d^4y\ &{}_{\text{out}}\langle K_1,K_2,X|\mathcal{T}\,\overline{\psi}(0)\not{A}(0)\psi(0)\overline{\psi}(y)\not{A}(y)\psi(y)|P_1,P_2\rangle_{\text{in,c}}\\ &\times(2\pi)^4\delta^4(P_1+P_2-K_1-K_2-\sum_i P_{X_i}) + \mathcal{O}(g^3).\end{aligned} \tag{2.101}$$

Since no gluons appear in the initial or final state, those fields need to be contracted with each other yielding the gluon propagator (Wick's theorem). Each of the quark-fields can be connected to one of the incoming or outgoing jets. All possibilities should be included. Picking one of the contributions as displayed in Fig. 2.12a and working out the contractions gives ($k_1 \equiv P_{X_3}+K_1$, $k_2 \equiv P_{X_4}+K_2$, $p_i \equiv P_i-P_{x_i}$)

$$\begin{aligned}\text{Eq. (2.101)} = &(2\pi)^4\delta^4(P_1+P_2-K_1-K_2-\sum_i P_{X_i})\frac{-ig^2}{(p_2-k_2)^2+i\epsilon}\\ &\times {}_{\text{out}}\langle K_1,P_{X3}|\overline{\psi}(0)|\Omega\rangle_{\text{c}}\ (it_b\gamma^\mu)\ {}_{\text{out}}\langle P_{X1}|\psi(0)|P_1\rangle_{\text{in,c}}\\ &\times {}_{\text{out}}\langle K_2,P_{X4}|\overline{\psi}(0)|\Omega\rangle_{\text{c}}\ (it_b\gamma_\mu)\ {}_{\text{out}}\langle P_{X2}|\psi(0)|P_2\rangle_{\text{in,c}}.\end{aligned} \tag{2.102}$$

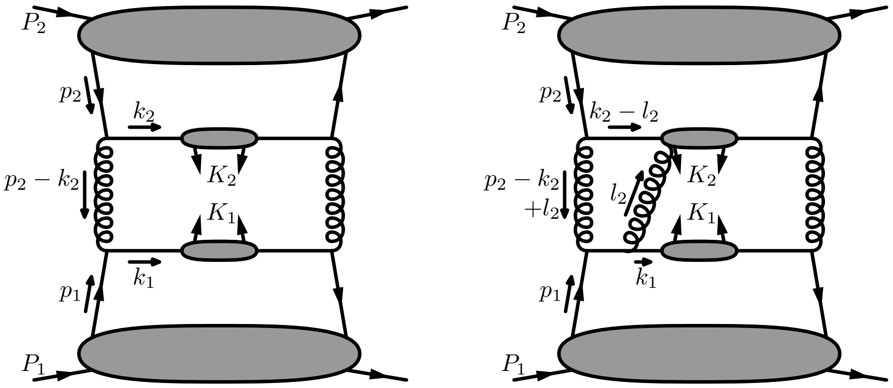

(a) (b)

Figure 2.12: Two contributions which appear in the diagrammatic approach.

If more interactions are included these steps can be performed in the same manner. Each interaction in U consists of fields which are fully integrated over their independent coordinate variables. As an example we will consider one higher order contribution which will yield Fig. 2.12b. The interaction can be expressed as

$$\begin{aligned}
&\langle K_1, K_2, X|iT|P_1, P_2\rangle \\
&= (ig)^3 \int \mathrm{d}^4z\, \mathrm{d}^4y\ {}_{\mathrm{out}}\langle K_1, K_2, X|\mathcal{T}\,\bar{\psi}(z)\not{A}(z)\psi(z)\bar{\psi}(0)\not{A}(0)\psi(0)\bar{\psi}(y)\not{A}(y)\psi(y)|P_1, P_2\rangle_{\mathrm{in,c}} \\
&\qquad \times (2\pi)^4\delta^4(P_1{+}P_2{-}K_1{-}K_2{-}\sum P_{X_i}) + \ldots, \qquad (2.103)
\end{aligned}$$

where the dots denote contributions from other interactions. We need to include all possible contractions but we will consider now one of the possibilities. Contracting $\psi(z)$ with $\bar{\psi}(0)$ and $A(0)$ with $A(y)$ and considering the remaining fields to be connected to the jets in a certain way, we find

$$\begin{aligned}
&\text{One contribution of Eq. (2.103)} \\
&= (2\pi)^4\delta^4(P_1{+}P_2{-}K_1{-}K_2{-}\sum P_{X_i})g^3 \int \mathrm{d}^4z\, \mathrm{d}^4y\, \frac{\mathrm{d}^4l_1\, \mathrm{d}^4l_2}{(2\pi)^8} e^{il_1y}e^{-il_2z}\frac{-i}{l_1^2} \\
&\times {}_{\mathrm{out}}\langle K_1, P_{X_3}|\bar{\psi}(z)|\Omega\rangle_{\mathrm{c}}\, i\gamma_\alpha t_a \frac{i(\not{l}_2 + m)}{l_2^2 - m^2 + i\epsilon} i\gamma^\mu t_b\, {}_{\mathrm{out}}\langle P_{X_1}|\psi(0)|P_1\rangle_{\mathrm{in,c}} \\
&\times {}_{\mathrm{out}}\langle K_2, P_{X_4}|\bar{\psi}(y)A_a^\alpha(z)|\Omega\rangle_{\mathrm{c}}\, i\gamma_\mu t_b\, {}_{\mathrm{out}}\langle P_{X_2}|\psi(0)|P_2\rangle_{\mathrm{in,c}} \qquad (2.104)
\end{aligned}$$

We would like the fields which already appeared at “tree-level” to be at the origin.

Shifting those fields and redefining the other integration variables, one finds

$$\begin{aligned}\text{Eq. (2.104)} =&(2\pi)^4\delta^4(P_1{+}P_2{-}K_1{-}K_2{-}\sum_i P_{X_i})g^3\int \mathrm{d}^4z\,\frac{\mathrm{d}^4 l_2}{(2\pi)^4}e^{-il_2z}\frac{1}{(l_2{+}p_2{-}k_2)^2}\\ &\times {}_{\mathrm{out}}\langle K_1,P_{X_3}|\overline{\psi}(0)|\Omega\rangle_{\mathrm{c}}i\gamma_\alpha t_a\frac{i(\not{l}_2+\not{k}_1+m)}{(l_2{+}k_1)^2{-}m^2+i\epsilon}i\gamma^\mu t_{b\mathrm{out}}\langle P_{X_1}|\psi(0)|P_1\rangle_{\mathrm{in,c}}\\ &\times {}_{\mathrm{out}}\langle K_2,P_{X_4}|\overline{\psi}(0)A_a^\alpha(z)|\Omega\rangle_{\mathrm{c}}i\gamma_\mu t_{b\mathrm{out}}\langle P_{X_2}|\psi(0)|P_2\rangle_{\mathrm{in,c}}\end{aligned} \tag{2.105}$$

The result is the original expression plus an additional interaction which contains integrals over z and l_2. We are actually deriving the Feyman rules. If we would have considered a virtual correction there would have been an additional contraction and one would remain with one integral over l_2.

In general one should have the following situation: the tree-level result consists of momentum conservation and matrix elements containing fields at the origin; if more external partons[7] are present then the corresponding fields are integrated over their coordinates and momenta, and their interactions are described by the Feynman rules. Virtual corrections are similar except that the integral over the coordinates can be carried out.

The cross section is obtained by removing the delta-function related to momentum conservation, taking the square, and multiplying with the removed delta-function (see Eq. 2.15, 2.89, 2.90). Except for the phase-space and flux factors this is the cross section. In general the total momentum conservation can be rewritten by giving each matrix element a number (i) and naming the sum of the outgoing momenta (also P_{Xi} here) $K_{i\mathrm{out}}$ and incoming momentum $P_{i\mathrm{in}}$. The total momentum conservation can then be written as

$$\begin{aligned}(2\pi)^4\delta^4\left(\sum_{i=1}K_{i\mathrm{out}}-\sum_{j=1}P_{j\mathrm{int}}\right)=\prod_n\left[\int \mathrm{d}^4t_n\;\delta^4(t_n\pm P_{n\mathrm{in}}\mp K_{n\mathrm{out}})\right]&\\ \times(2\pi)^4\delta^4(\text{external parton momenta}),&\end{aligned} \tag{2.106}$$

where t_i are the momenta of the external partons and where the last delta-function expresses the momentum conservation of the external partons. The first n delta-functions are used to shift the fields of the matrix elements by introducing another integral over the coordinates

$$\delta^4(t_n\pm P_{n\mathrm{in}}\mp K_{n\mathrm{out}})=\int\frac{\mathrm{d}^4\xi_n}{(2\pi)^4}e^{i(t_n\pm P_{n\mathrm{in}}\mp K_{n\mathrm{out}})\xi_n}. \tag{2.107}$$

After an integration over the unobserved momenta one obtains the correlators as introduced in section 2.4.

---

[7] External partons are incoming or outgoing partons connected to correlators or decaying as a jet.

3

Electromagnetic scattering processes at leading order in α_S

The diagrammatic approach, introduced in the previous chapter, will be employed to describe at leading order in α_S cross sections in which the hard scale is set by an electromagnetic interaction. In the discussion on the meaning of α_S it will be argued that even at leading order there is an infinite amount of interactions that should be considered. Including next-to-leading order corrections in inverse powers of the hard scale, these leading-order-α_S-interactions will be evaluated in order to obtain the cross sections for semi-inclusive DIS, electron-positron annihilation, and Drell-Yan in terms of distribution and fragmentation correlators. These correlators contain gauge links of which their paths are different for different processes. Using the parametrizations of these correlators some explicit asymmetries for semi-inclusive DIS will be given.

In the second part of this chapter, the universality of fragmentation functions will be discussed and the link structures appearing in deeply-virtual Compton scattering will be studied. The calculation of the latter illustrates the wide-ranging applicability of the diagrammatic approach. A summary is provided at the end of this chapter.

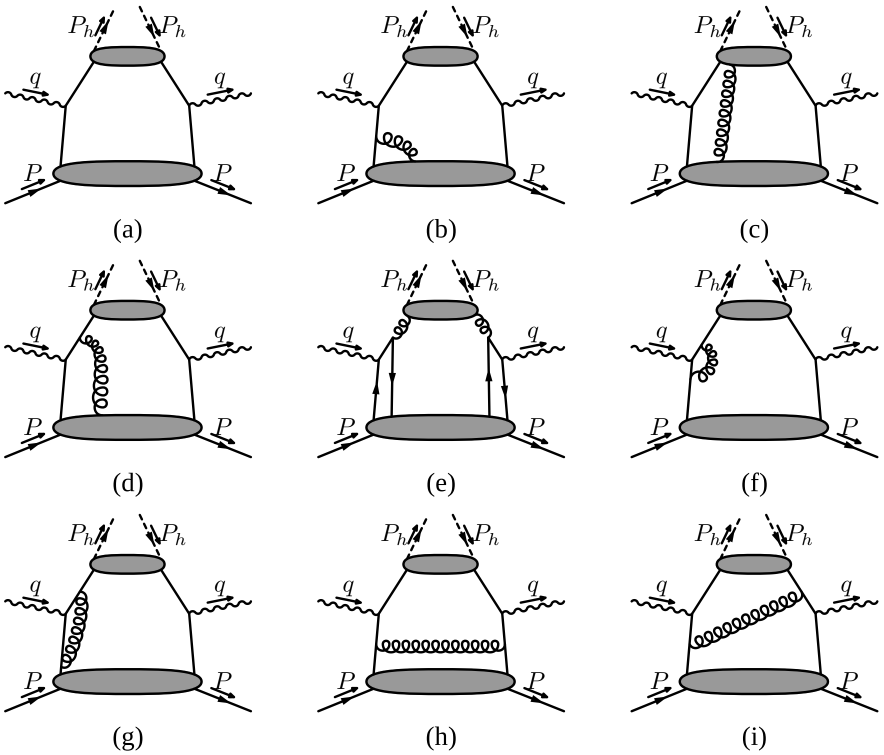

Figure 3.1: Various interactions between the two jets and the elementary scattering part in semi-inclusive DIS.

3.1 Leading order in α_S

In the previous chapter the diagrammatic expansion was developed to handle scattering processes. In order to apply this expansion, the various jets need to be well separated. This can be further translated into the demand to have large momentum transfers, implying that the inner products of momenta connected to different jets are large. Besides an expansion in α_s, this presence of large energy-scales allows for a possible expansion of physical observables in the inverse powers of that energy-scale (M/Q). Both expansions will be made throughout the chapter.

Applying the diagrammatic expansion, all leading α_S diagrams which can contribute to the processes need to be included. For semi-inclusive DIS, the lowest order (in g) diagram is given in Fig. 3.1a. Interactions which can be absorbed, like the one in Fig. 3.1b, are already present in the correlator definition and should not be included separately. Diagrams which have several jets are α_s suppressed compared to diagrams which contain less jets. The restriction to leading order in α_s leads to only two outgoing jets for semi-inclusive DIS, electron-positron annihilation, and Drell-Yan. Further, the interactions between the jets as illustrated in Fig. 3.1c are considered to be weak and will be neglected. This assumption is directly related to the question on whether factorization holds for the correlators. This will be discussed in the next chapter.

Another possible contribution is that a gluon-line will connect a jet with the elementary scattering diagram. Since there can be interferences, such as depicted in Fig. 3.1d, such an interaction is proportional to the coupling constant, g, and is not α_s suppressed. We shall see in the next section that one can resum all collinear gluon-lines connecting the correlator and the scattering diagram to all orders in g. The other possibility of additional collinear quarks, such as in Fig. 3.1e, is not taken into account here. Ellis, Furmanski, and Petronzio [53, 54], found that such contributions are suppressed with M^2/Q^2 and are therefore beyond the aimed accuracy of this chapter.

Besides additional parton-lines from the correlator one might wonder whether there are other corrections in the scattering diagram itself which need to be included at leading order α_s. Such corrections consist of loops and gluon radiation and can partly be absorbed in the correlator definitions. For instance, if the loop diagram in Fig. 3.1f contains a far off shell gluon, then it cannot be absorbed. However, if the gluon is approximately on shell and collinear to one of the jets, as illustrated in Fig. 3.1g, then it is absorbed in the correlator definition up to some scale. For gluon radiation a similar situation applies. If the gluon in Fig. 3.1h has a small transverse momentum with respect to the parent hadron (P), then it is already present in the correlator definition. The gluon in Fig. 3.1i cannot be absorbed and represents an α_S correction.

Absorbing interactions in the correlator introduces a particular scale. There were a few attempts to calculate this scale dependence (evolution equations), but including effects from intrinsic transverse momentum this has not been achieved so far. For a discussion on the scale dependence and various other difficulties the reader is referred to Ellis, Furmanski, Petronzio [54], Collins, Soper, Sterman [104, 105], Hagiwara, Hikasa, Kai [106], Ahmed, Gehrmann [107], Boer [108], and Henneman [66].

The conclusion of this section is that, restricted to leading order in α_s, one must resum over all possible gluons which connect the correlators and the scattering diagram to obtain the cross section (generalizations of Fig. 3.1.d). Such resummations will be performed for several processes in this chapter.

3.2 Semi-inclusive deep-inelastic scattering

In the first two subsections the expressions for the hadronic tensor including M/Q corrections will be derived. In the third subsection the results for the hadronic tensor will be used to express some asymmetries in terms of distribution and fragmentation functions. We will begin here by introducing the calculation of the hadronic tensor.

Applying the general rules of the diagrammatic expansion, the hadronic tensor is found to be a sum over various diagrams. Considering only leading order in α_s, all those diagrams (to all orders in g) will be considered that are not already absorbed in the correlators. In order to structure the calculation we shall treat here the lowest and one higher order contribution in g. Those contributions in combination with a number of other diagrams will be studied in detail in the next subsections. The final result, Eq. 3.46, will consist of correlators containing gauge links for which parametrizations have been given in the previous chapter (see Eq. 2.57, 2.65, 2.83, 2.88).

At lowest order in g (see also Fig. 3.1a), the contribution to the hadronic tensor is a convolution between the scattering diagram, the fragmentation correlator, and the distribution correlator. In this section arguments connected to the parent hadron will be often omitted for notational convenience, so $\Phi(p, P, S) \to \Phi(p)$. The result for the hadronic tensor reads

$$2MW^{\mu\nu} = \int \mathrm{d}^4p\, \mathrm{d}^4k\, \delta^4(p+q-k)\, \mathrm{Tr}^{D,C}\left[\Phi(p)\gamma^\mu\Delta(k)\gamma^\nu\right] + \mathcal{O}(g), \tag{3.1}$$

where Φ and Δ were defined in the previous chapter (Eq. 2.37, 2.40). Note that the Heisenberg fields in the correlator contain interactions to all orders in g, see for example the interaction in Fig. 3.1b.

In order to evaluate the result, a Sudakov-decomposition is made. A set of light-like vectors ($\{n_-, n_+\}$ with $n_- \cdot n_+ = 1$ and $\bar{n}_- \sim n_+$, where the bar denotes reversal of spatial components) is introduced such that

$$\begin{aligned}
P &= \frac{x_B M^2}{\tilde{Q}\sqrt{2}}\, n_- + \frac{\tilde{Q}}{x_B\sqrt{2}}\, n_+,\\
P_h &= \frac{z_h\tilde{Q}}{\sqrt{2}}\, n_- + \frac{M_h^2}{z_h\tilde{Q}\sqrt{2}}\, n_+,\\
q &= \frac{\tilde{Q} + \mathcal{O}(M^2/\tilde{Q})}{\sqrt{2}}\, n_- - \frac{\tilde{Q} + \mathcal{O}(M^2/\tilde{Q})}{\sqrt{2}}\, n_+ + q_T,
\end{aligned} \tag{3.2}$$

Sudakov-decomposition for semi-inclusive DIS

where $\tilde{Q}^2 \equiv Q^2 + q_T^2 = Q^2 + \mathcal{O}(M^2)$. Using the parton model assumptions the correlators in Eq. 3.1 can be integrated over the small momentum components

$$\begin{aligned}
2MW^{\mu\nu} = \int & \mathrm{d}^2p_T\, \mathrm{d}^2k_T\, \delta^2(p_T + q_T - k_T)\\
& \times \frac{1}{3}\,\mathrm{Tr}^D\left[\mathrm{Tr}^C\left(\int \mathrm{d}p^-\, \Phi(p)\right)_{p^+=-q^+} \gamma^\mu\, \mathrm{Tr}^C\left(\int \mathrm{d}k^+\, \Delta(k)\right)_{k^-=q^-} \gamma^\nu\right]\\
& \times \left(1 + \mathcal{O}\left(M^2/Q^2\right)\right) + \mathcal{O}(g) + \mathcal{O}(\alpha_S),
\end{aligned} \tag{3.3}$$

where the relation $\Phi_{ab} = \delta_{ab}\,\mathrm{Tr}^C\,\Phi/3$ was applied.

At higher orders in g one needs to include gluonic diagrams in which gluon-lines are connected to the correlators. If there is more than one soft correlator present, as is studied here, the inclusion of such interactions becomes more complex. A simplification can be obtained by assuming the expressions for the cross section to be color gauge invariant, allowing for a suitable gauge choice. A convenient gauge turns out to be the light-cone gauge with retarded boundary conditions. In such gauges, see for example Ref. [26], one of the light-cone components is set to zero together with the transverse polarizations at light-cone minus infinity, or $A^-(\eta) = A_T^\alpha(\eta^-, -\infty, \eta_T) = 0$.

In the calculation of the hadronic tensor, we shall employ the equations of motion. It has been put forward by Politzer [51] and subsequently by Boer [64] that the classical equations of motion, $(i\not{D} - m)\psi(x) = 0$, hold within physical matrix elements. They lead to the following identity for the correlators Δ and Δ_A^α (see also Eq. 2.40 and Eq. 2.41 and where $\Delta_A^\alpha \equiv \Delta_{A_l}^\alpha t_l$)

$$\Delta(k)(\not{k} - m) = -g \int \mathrm{d}^4k_1\, \Delta_A^\alpha(k, k_1)\gamma_\alpha. \tag{3.4}$$

We will briefly come back to the validity of these equations in the next chapter (subsection 4.5.2, Drell-Yan).

When including gluons from the fragmentation and distribution correlator, the standard treatment shows that gluons which are backwardly polarized ($S^\mu \sim \bar{p}^\mu$) lead to $\mathcal{O}\left(M^2/Q^2\right)$ suppressed matrix elements and can therefore be safely neglected. This means that the A^+-gluons from the fragmentation correlator and the A^--gluons from the distribution correlator can be discarded. Together with the chosen light-cone gauge this means that only the transversely polarized gluons of the fragmentation correlator and the longitudinally and transversely polarized gluons from the distribution correlator need to be considered.

We shall continue the calculation by considering a simple higher order interaction. Taking a gluon from the distribution correlator as displayed in Fig. 3.1d gives the following contribution to the hadronic tensor

$$2MW^{\mu\nu} = 2MW^{\mu\nu}_{\text{Fig. (3.1)}d} + \text{other diagrams}, \tag{3.5}$$

$$\begin{aligned} 2MW^{\mu\nu}_{\text{Fig. (3.1)}d} = & \int \mathrm{d}^4p\, \mathrm{d}^4k\, \mathrm{d}^4p_1\, \delta^4(p + q - k) \\ & \times \mathrm{Tr}^{D,C}\left[\Phi_{A_l}^\alpha(p, p_1)\gamma^\mu\Delta(k)\,(ig\gamma_\alpha t_l)\, i\frac{\not{k} - \not{p}_1 + m}{(k - p_1)^2 - m^2 + i\epsilon}\gamma^\nu\right], \end{aligned} \tag{3.6}$$

where Φ_A is now the quark-gluon-quark correlator as defined in Eq. 2.38. In the next equation the above expression is rewritten to indicate how the various parts of the quark-propagator in combination with the gluon polarization contribute to the cross section

$$\begin{aligned} 2MW^{\mu\nu}_{\text{Fig (3.1)}d} &= \int \mathrm{d}^4p\, \mathrm{d}^4k\, \delta^4(p+q-k) \\ &\qquad \times \Big(2Mw^{\mu\nu}_{L,\not{k}+m} + 2Mw^{\mu\nu}_{L,-\not{p}_{1T}} + 2Mw^{\mu\nu}_{T,\not{k}-\not{p}_{1T}+m} + 2Mw^{\mu\nu}_{T,-p_1^+\gamma^-} \Big), \qquad (3.7) \\ 2Mw^{\mu\nu}_{L,\not{k}+m} &= \int \frac{\mathrm{d}^4p_1\,(-g)}{(k-p_1)^2-m^2+i\epsilon}\, \mathrm{Tr}^{D,C}\Big[\Phi^{+}_{A_l}(p,p_1)\gamma^\mu\Delta(k)\gamma^- t_l\,(\not{k}+m)\,\gamma^\nu\Big], \qquad (3.8) \\ 2Mw^{\mu\nu}_{L,-\not{p}_{1T}} &= \int \frac{\mathrm{d}^4p_1\,(-g)}{(k-p_1)^2-m^2+i\epsilon}\, \mathrm{Tr}^{D,C}\Big[\Phi^{+}_{A_l}(p,p_1)\gamma^\mu\Delta(k)\gamma^- t_l\,(-\not{p}_{1T})\,\gamma^\nu\Big], \qquad (3.9) \\ 2Mw^{\mu\nu}_{T,\not{k}-\not{p}_{1T}+m} &= \int \frac{\mathrm{d}^4p_1\,(-g)}{(k-p_1)^2-m^2+i\epsilon}\, \mathrm{Tr}^{D,C}\Big[\Phi_{A_l}{}^{\alpha}_{T}(p,p_1)\gamma^\mu\Delta(k)\gamma_\alpha t_l\,(\not{k}-\not{p}_{1T}+m)\,\gamma^\nu\Big], \qquad (3.10) \\ 2Mw^{\mu\nu}_{T,-p_1^+\gamma^-} &= \int \frac{\mathrm{d}^4p_1\,(-g)}{(k-p_1)^2-m^2+i\epsilon}\, \mathrm{Tr}^{D,C}\Big[\Phi_{A_l}{}^{\alpha}_{T}(p,p_1)\gamma^\mu\Delta(k)\gamma_\alpha t_l\,(-p_1^+\gamma^-)\,\gamma^\nu\Big]. \qquad (3.11) \end{aligned}$$

As we will see later in this section, the various terms contribute to the following orders in M/Q: $2Mw^{\mu\nu}_{L,\not{k}+m}$ contributes at leading order to the longitudinal gauge link, $2Mw^{\mu\nu}_{L,-\not{p}_{1T}}$ contributes at subleading order, $2Mw^{\mu\nu}_{T,\not{k}-\not{p}_{1T}+m}$ contributes at leading order to the transverse gauge link, and $2Mw^{\mu\nu}_{T,-p_1^+\gamma^-}$ contributes at subleading order.

In the following subsections we will evaluate these terms and include higher order gluon insertions from the distribution correlator. We will begin by analyzing the leading order in detail which leads to the gauge link; the next-to-leading order in M/Q will be discussed in the second subsection in which transversely polarized gluons from the fragmentation correlator contribute as well.

3.2.1 Leading order in M/Q

Longitudinal gauge link

We will study here in detail the contribution of a longitudinally polarized gluon inserted in the diagram. This follows the leading order in M/Q calculations of Bjorken, Kogut, Soper [109]; Efremov, Radyushkin [110]; and Collins, Soper, Sterman [111, 112, 113]. In Boer, Mulders [114] those calculations were extended by including M/Q corrections in the diagrammatic approach. In that paper explicit calculations were given to order g^2 which were generalized by using arguments based on Ward identities.

When studying this problem Ward identities should be handled with care [39]. The considered gluon (with momentum p_1) is approximately longitudinally polarized and is inserted at various places in an amplitude, seducing one to use $p_1^\mu \mathcal{M}_\mu(p_1) = 0$. However, in the limit of $p_1 \to 0$ the Ward identity does not contain any information ($0 = 0$). Since this issue especially becomes relevant in more complicated diagrams (chapter 4) explicit calculations will be performed in this chapter.

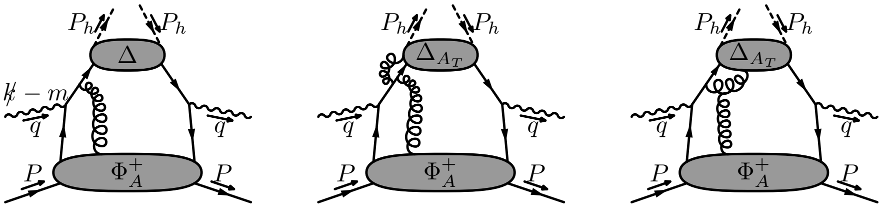

(a) (b) (c)

Figure 3.2: Various contributions to the hadronic tensor. The interactions in the figures cannot be absorbed in a single jet and therefore need to be considered. Figure (c) is not of the type of figure 3.1.d because the interaction is connected with the hard part. In figure (a) only the indicated part of the numerator of the quark propagator is considered. The part which is not indicated will be treated in the next subsection.

Inserting the gluon on the left-hand-side of the cut, see also Fig. 3.2a, we need to evaluate Eq. 3.8 and Eq. 3.9. The contribution from Eq. 3.9 will be calculated in the next subsection and turns out to appear at subleading order. To perform the integral over p_1, the denominator $((k{-}p_1)^2{-}m^2{+}i\epsilon)^{-1}$ in Eq. 3.8 is simplified into $(-2p_1^+k^- + i\epsilon)^{-1}$. This simplification, called the *eikonal approximation*, is justified when making the parton model assumptions which were discussed in section 2.4. The integral over p_1^+ in $2Mw^{\mu\nu}_{L,\not{k}+m}$ (Eq. 3.8) takes now the following form

$$\int \mathrm{d}p_1^+ \, \frac{e^{ip_1^+(\eta-\xi)^-}}{-2p_1^+k^- + i\epsilon} A_l^+(\eta). \tag{3.12}$$

Assuming k^- to be positive, the integral can be performed by calculating the residue. This leads to a Heaviside function (θ)

$$\text{Eq. (3.12)} = \frac{2\pi i}{-2k^-}\, \theta(\eta^- - \xi^-)\, A_l^+(\eta). \tag{3.13}$$

The Heaviside function expresses that there will be only contributions to the hadronic tensor when $\eta^-{>}\xi^-$, meaning that $A^+(\eta^-{\to}\infty)$ contributes, but $A^+(\eta^-{\to}{-}\infty)$ does not.

Using the equations of motion one finds for $2Mw^{\mu\nu}_{L,\not{k}+m}$ $(\gamma^-(\not{k}{+}m){=}2k^-{-}(\not{k}{-}m)\gamma^-)$

$$\begin{aligned} 2Mw^{\mu\nu}_{L,\not{k}+m} = &\int \frac{\mathrm{d}^4\xi}{(2\pi)^4} e^{ip\xi} \langle P,S\,|\overline{\psi}(0)\gamma^\mu\, \mathrm{Tr}^C\!\left[\frac{\Delta(k)}{3}\right]\gamma^\nu(-ig)\int_\infty^{\xi^-} \mathrm{d}\eta^-\, A^+(\eta^-,\xi^+,\xi_T)\psi(\xi)|P,S\,\rangle_\mathrm{c} \\ &\times\Big(1+\mathcal{O}\Big(M^2/Q^2\Big)\Big) \\ &-g\int \mathrm{d}^4p_1\,\mathrm{Tr}^{D,C}\left[\Phi^+_{A_l}(p,p_1)\gamma^\mu \int \mathrm{d}^4k_1\, \Delta_A^\beta(k,k_1)\gamma_\beta t_l \frac{\gamma^-}{-2k^-p_1^+ + i\epsilon}\gamma^\nu\right], \end{aligned} \tag{3.14}$$

where the relation $\Delta_{ab} = \delta_{ab}\,\mathrm{Tr}^C\,\Delta(k)/3$ was used. The first term above contributes at leading twist and is exactly the first order gauge link expansion running via infinity. The second term in Eq. 3.14, coming from applying the equations of motion, is canceled when the other diagrams of Fig. 3.2 are included. Although this cancellation[1] occurs in the chosen light-cone gauge, where the gluon propagator has the numerator (see for example Ref. [26])

$$d^{\mu\nu}(l) = g^{\mu\nu} - \frac{l^\mu n_+^\nu}{l^- - i\epsilon} - \frac{n_+^\mu l^\nu}{l^- + i\epsilon}, \tag{3.15}$$

one does obtain another term proportional to Δ_{AA}. We see that by considering the other diagrams the Δ_A term got replaced by a Δ_{AA} term. This cancellation was observed in Boer, Mulders [114]. Since this issue only plays a role when considering fragmentation correlators (a free outgoing quark does not produce Δ_A terms), this kind of cancellation is expected to hold to all orders. One should find by including higher order diagrams that the Δ_{AA} term gets replaced by a Δ_{AAA} term and so on. This cancellation, which is expected to hold at each order in g, has not been proven to all orders and deserves further investigation.

Before continuing it should be pointed out that the cancellation also occurs when the Feynman gluon propagator is taken in the hard part. This suggests the hard part and the correlators to be separately gauge invariant, which is a minimal requirement for a factorized description.

In order to generalize the above result, Eq. 3.14, we consider n longitudinally polarized gluon insertions on the left-hand-side of the cut which contribute to the hadronic tensor as

$$2MW^{\mu\nu} = \int \mathrm{d}^4p\,\mathrm{d}^4k\,\delta^4(p+q-k)\,2Mw^{\mu\nu}_{nA^+} + \text{other diagrams}, \tag{3.16}$$

$$\begin{aligned} 2Mw^{\mu\nu}_{nA^+} = \int \mathrm{d}^4p_1\,\ldots\mathrm{d}^4p_n\;\mathrm{Tr}^{D,C}\Big[&\Phi^{+\ldots+}_{A_{l_1}\ldots A_{l_n}}(p, p_1{-}p_2, \ldots, p_{n-1}{-}p_n, p_n)\gamma^\mu\Delta(k)\\ &\times(-g)^n(t_{l_n}\gamma^-)\frac{\not{k}-\not{p}_n+m}{(k{-}p_n)^2{-}m^2{+}i\epsilon}\ldots(t_{l_1}\gamma^-)\frac{\not{k}-\not{p}_1+m}{(k{-}p_1)^2{-}m^2{+}i\epsilon}\gamma^\nu\Big]. \end{aligned} \tag{3.17}$$

Performing all the p_i-integrals one straightforwardly obtains an ordered product

$$\begin{aligned} 2Mw^{\mu\nu}_{nA^+} = \int \frac{\mathrm{d}^4\xi}{(2\pi)^4}e^{ip\xi}\langle P,S\,|\bar{\psi}(0)\gamma^\mu\,\mathrm{Tr}^C\left[\frac{\Delta(k)}{3}\right]\gamma^\nu(-ig)^n\int_\infty^{\xi^-}\mathrm{d}\eta_1^-\int_{\eta_1^-}^{\xi^-}\mathrm{d}\eta_2^-\ldots\int_{\eta_{n-1}}^{\xi^-}\mathrm{d}\eta_n^-\\ \times A^+(\eta_1^-,\xi^+,\xi_T)\ldots A^+(\eta_n^-,\xi^+,\xi_T)\psi(\xi)|P,S\,\rangle_c\,(1+\mathcal{O}(M/Q)), \end{aligned} \tag{3.18}$$

which is the n^{th}-order longitudinal gauge link expansion.

---

[1] In order to achieve this cancellation it was assumed that the gluon connecting the fragmentation correlator is outgoing and approximately on its mass-shell ($k_1^- > 0$).

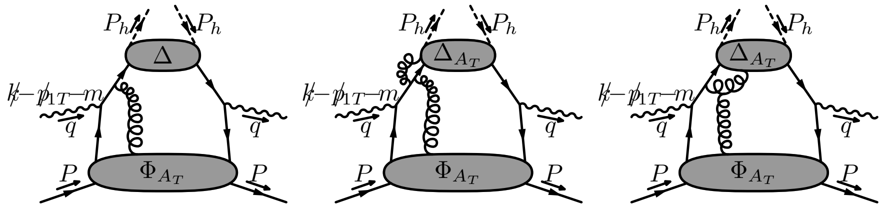

(a) (b) (c)

Figure 3.3: Various contributions to the hadronic tensor. In each of the diagrams it is indicated which part of the numerator of the quark propagator is considered.

To summarize, by including longitudinally polarized gluons from a distribution correlator which interact with an outgoing quark, one obtains the longitudinal gauge link $\mathcal{L}^{\xi_T,\,\xi^+}(\infty^-,\xi^-)$ (for definition see section 2.5). Inserting longitudinally polarized gluons from the distribution correlator on the right-hand-side of the cut also produces a longitudinal gauge link. Its result can be obtained by taking the complex conjugate of the result we just obtained (Eq. 3.18) and interchanging μ with ν. For those insertions one finds the gauge link $\mathcal{L}^{0_T,\,\xi^+}(0^-,\infty^-)$.

Transverse gauge link

We continue by studying the leading contributions from transversely polarized gluons. For a long time transversely polarized gluons were thought to appear always suppressed in cross sections (see for instance Mulders, Tangerman [115]). In 2002 Belitsky, Ji, and Yuan showed in Ref. [26] that this idea is wrong and that transversely polarized gluons at leading order give rise to a transverse gauge link. Although their calculation showed how the transverse gauge link could be derived, it also contained a few points which deserved further clarification. Some of these points were given attention in Ref. [35] but other points were unintentionally left open. All issues will be discussed here in considerable detail.

We start with $2Mw^{\mu\nu}_{T,\not{k}-\not{p}_{1T}+m}$ as given in Eq. 3.10 (represented in Fig. 3.3a)

$$2Mw^{\mu\nu}_{T,\not{k}-\not{p}_{1T}+m}=\int\frac{\mathrm{d}^4p_1\,(-g)}{(k-p_1)^2-m^2+i\epsilon}\mathrm{Tr}^{D,C}\Big[\Phi_{A_l}{}^{\alpha}_{T}(p,p_1)\gamma^\mu\Delta(k)g\gamma_\alpha t_l\,(\not{k}-\not{p}_{1T}+m)\gamma^\nu\Big]. \quad (3.19)$$

Performing the integral over p_1^+ would lead to $\int_{\xi^-}^{\infty}\mathrm{d}\eta^-\;A_T^\alpha(\eta)$ as was also encountered when calculating the longitudinal link. In gauges where the gluon fields vanish at infinity this would form a perfect matrix element, but in those gauges where the fields do not vanish the matrix element is divergent and needs subtractions[2].

---

[2] A similar problem occurs also with the longitudinally polarized gluons. In order to keep the matrix

In order to consider the transverse fields at infinity more precisely one expresses the A-fields as

$$A_T^\alpha(\eta) = A_T^\alpha(\infty, \eta^+, \eta_T) + [A_T^\alpha(\eta) - A_T^\alpha(\infty, \eta^+, \eta_T)]\,. \qquad (3.20)$$

In this decomposition the η^--dependence has vanished in the first term. When performing the η^--integral over the first term of Eq. 3.20 in Eq. 3.19 (which is proportional to $\exp[ip_1(\eta - \xi)]$) a delta-function in p_1^+ emerges[3]. This delta-function eliminates the large momenta in the denominator in Eq. 3.19, making the contribution leading in M/Q. When performing the p_1^+-integral one finds that the second term in Eq. 3.20 contributes at order M^2/Q^2 and can be neglected. The choice for taking the subtracting point in Eq. 3.20 at infinity might seem arbitrary but actually it is not. Choosing the subtraction point at $\eta^- = -\infty$ would produce, after an integration over p_1^+, the divergent term $\int_\infty^{\xi^-} \mathrm{d}\eta^- [A_T^\alpha(\eta) - A_T^\alpha(-\infty^-, \eta^+, \eta_T)]$. Hence it is the $i\epsilon$ prescription in Eq. 3.19 (or process) which forces us to take the subtraction point at infinity in order to keep the contributions from both terms in Eq. 3.20 finite.

We continue with the first term and find [35]

$$\begin{aligned} 2Mw^{\mu\nu}_{T,\not{k}-\not{p}_{1T}+m} = &\int \mathrm{d}^2p_{1T}\ \mathrm{d}p_1^- \int \frac{\mathrm{d}^4\xi\ \mathrm{d}\eta^+\ \mathrm{d}^2\eta_T}{(2\pi)^7} e^{ip\xi + ip_{1T}(\eta-\xi)_T + ip_1^-(\eta-\xi)^+} \\ &\times \lim_{p_1^+\to 0} \langle P,S\,|\overline{\psi}(0)\gamma^\mu \Delta(k) i\gamma_\alpha i \frac{\not{k} - \not{p}_{1T} + m}{(k-p_1)^2 - m^2 + i\epsilon}\gamma^\nu \\ &\times g\partial_\eta^\alpha \int_C^{\eta_T} \mathrm{d}\zeta_T\ \cdot A_T(\infty, \eta^+, \zeta_T)\psi(\xi)|P,S\,\rangle_{\mathrm{c}} \Big(1 + \mathcal{O}\Big(M^2/Q^2\Big)\Big), \qquad (3.21) \end{aligned}$$

where C is some constant. To arrive at an equivalent expression the existence of a pure gauge at infinity was assumed in Eq. (38) of Belitsky, Ji, Yuan [26]. This assumption makes the treatment for QCD less general and is avoided here.

Having the gluon collinear means that the delta-function in p_1^+ also pushes the transverse momentum down. In order to proceed we needed to interchange those limits. Therefore, when taking the limit $p_1^+ \to 0$ we keep p_{1T} finite. This exchange of limits, which is also present in Ref. [26] and seems to be unavoidable, might lead to problems at higher orders in α_S.

---

elements containing the longitudinal gauge link convergent one should require the longitudinally polarized fields to vanish at infinity. This requirement is supported in those gauges where the gluon-fields at infinity can be described with a scalar potential (see also Ref. [26])

$$\phi(\eta) = \int_C^{\eta} \mathrm{d}\zeta\ \cdot A(\zeta).$$

In order to have the potential finite at $\eta^- = \infty$ which seems to be physically reasonable, the A^+-fields need to vanish at that point. This argument does not hold for transversely polarized gluons.

[3] The boundary terms were also studied by Boer, Mulders, and Teryaev in Ref. [87].

Doing now a partial integration and applying the equations of motion one finds by performing first the η^--integral, the p_1^+-integral, and then the rest of the integrals $(\Delta(k)[-\not{p}_{1T}][\not{k}-\not{p}_{1T}+m] = [\Delta(k)[\not{k}-\not{p}_{1T}-m] + g\int \mathrm{d}^4k_1\ \Delta_A^\alpha(k,k_1)\gamma_\alpha][\not{k}-\not{p}_{1T}+m])$

$$
\begin{aligned}
&2Mw^{\mu\nu}_{T,\not{k}-\not{p}_{1T}+m} \\
&\quad = \int \frac{\mathrm{d}^4\xi}{(2\pi)^4} e^{ip\xi} \langle P,S|\bar{\psi}(0)\gamma^\mu\Delta(k)\gamma^\nu(-ig)\int_C^{\xi_T} \mathrm{d}\zeta_T\ \cdot A_T(\infty,\xi^+,\zeta_T)\psi(\xi)|P,S\rangle_\mathrm{c} \\
&\qquad \times \left(1+\mathcal{O}\left(M^2/Q^2\right)\right) \\
&\qquad + g\int \frac{\mathrm{d}^4\xi\ \mathrm{d}\eta^+\ \mathrm{d}^2\eta_T}{(2\pi)^7} \lim_{p_1^+\to 0} e^{ip\xi}e^{ip_1(\eta-\xi)}\langle P,S|\bar{\psi}(0)\gamma^\mu \int \mathrm{d}^4k_1\ \Delta_A^\alpha(k,k_1)\gamma_\alpha \\
&\qquad \times \frac{\not{k}-\not{p}_{1T}+m}{(k-p_1)^2-m^2+i\epsilon}\gamma^\nu(-ig)\int_C^{\eta_T} \mathrm{d}\zeta_T\ \cdot A_T(\infty,\eta^+,\zeta_T)\psi(\xi)|P,S\rangle_\mathrm{c},
\end{aligned} \tag{3.22}
$$

where the first term is exactly the first order expansion of the transverse gauge link. The second term was not considered in Ref. [26], while in Ref. [35] it was thought to be suppressed in M/Q. In the case of jet-production in DIS the second term does not appear (the outgoing quark is assumed to be free), but when considering the fragmentation of a quark into a hadron neither observations of Ref. [26, 35] are in general valid. The second term is as leading as the first term and will be considered here.

Similar terms were also encountered when deriving the longitudinal gauge link. Also here one finds that when including the diagrams in Fig. 3.3b and Fig. 3.3c that the second term is exchanged with a term proportional to Δ_{AA}. Similarly as for the longitudinal gauge link, it will be assumed that this behavior can be generalized to all orders. When taking the Feynman gauge for the hard part, one finds that the diagram in Fig. 3.3c has an additional contribution at next-to-leading order in M/Q. In the next subsection where we will discuss the subleading order in M/Q, it will be pointed out where this term gets canceled.

Generalizing the result above to all orders by inserting n transversely polarized gluons, one obtains for the hadronic tensor

$$
2MW^{\mu\nu} = \int \mathrm{d}^4p\ \mathrm{d}^4k\ \delta^4(p+q-k)\ 2Mw^{\mu\nu}_{nA_T} + \text{other diagrams}, \tag{3.23}
$$

$$
\begin{aligned}
2Mw^{\mu\nu}_{nA_T} = &\int \mathrm{d}^4p_1\ \ldots \mathrm{d}^4p_n\ \frac{\mathrm{d}^4\xi\ \mathrm{d}^4\eta_1\ \ldots \mathrm{d}^4\eta_n}{(2\pi)^{4(n+1)}} e^{i(p-p_1)\xi}e^{i(p_1-p_2)\eta_1}\ldots e^{i(p_{n-1}-p_n)\eta_{n-1}}e^{ip_n\eta_n} \\
&\times(-g)^n\langle P,S|\bar{\psi}(0)\gamma^\mu\Delta(k)\gamma_{\alpha_n}t_{l_n}\frac{\not{k}-\not{p}_{nT}+m}{(k-p_n)^2-m^2+i\epsilon}\ldots\gamma_{\alpha_1}t_{l_1}\frac{\not{k}-\not{p}_{1T}+m}{(k-p_1)^2-m^2+i\epsilon} \\
&\times\gamma^\nu A^{\alpha_n}_{l_n,T}(\eta_n)\ldots A^{\alpha_1}_{l_1,T}(\eta_1)\psi(\xi)|P,S\rangle_\mathrm{c}\left(1+\mathcal{O}(M/Q)\right).
\end{aligned} \tag{3.24}
$$

Following exactly the same steps as done for the single transversely polarized gluon one obtains

$$\begin{aligned}2Mw^{\mu\nu}_{nA_T} = \int & \mathrm{d}^4 p_1 \dots \mathrm{d}^4 p_{n-1} \frac{\mathrm{d}^4\xi\, \mathrm{d}^4\eta_1 \dots \mathrm{d}^4\eta_{n-1}}{(2\pi)^{4n}} e^{i(p-p_1)\xi} e^{i(p_1-p_2)\eta_1} \dots e^{i(p_{n-2}-p_{n-1})\eta_{n-2}} e^{ip_{n-1}\eta_{n-1}} \\ & \times \langle P,S\,|\bar{\psi}(0)\gamma^\mu \Delta(k) \gamma_{\alpha_{n-1}} \frac{\not{k} - \not{p}_{n-1T} + m}{(k-p_{n-1})^2 - m^2 + i\epsilon} \dots \gamma_{\alpha_1} \frac{\not{k} - \not{p}_{1T} + m}{(k-p_1)^2 - m^2 + i\epsilon} \gamma^\nu \\ & \times (-ig) \int_C^{\eta_{n-1T}} \mathrm{d}\zeta_n \;\cdot A(\infty, \xi^+, \zeta_{nT}) (-g)^{n-1} A^{\alpha_{n-1}}(\eta_{n-1}) \dots A^{\alpha_1}(\eta_1) \psi(\xi) |P,S\,\rangle_{\mathrm{c}} \\ & \times (1 + \mathcal{O}(M/Q))\,. \end{aligned} \tag{3.25}$$

Using now an identity which holds for non-Abelian fields[4] [35]

$$\boxed{\begin{aligned} & \int_C^{\eta_T} \mathrm{d}\zeta_{1T} \;\cdot A(\zeta_1) \int_{\zeta_{1T}}^{\eta_T} \mathrm{d}\zeta_{2T} \;\cdot A(\zeta_2) \dots \int_{\zeta_{n-1,T}}^{\eta_T} \mathrm{d}\zeta_{nT} \;\cdot A(\zeta_n)\, A^\alpha(\eta) \\ & \qquad = \partial^\alpha_\eta \int_C^{\eta_T} \mathrm{d}\zeta_{1T} \;\cdot A(\zeta_1) \int_{\zeta_{1T}}^{\eta_T} \mathrm{d}\zeta_{2T} \;\cdot A(\zeta_2) \dots \int_{\zeta_{nT}}^{\eta_T} \mathrm{d}\zeta_{n+1,T} \;\cdot A(\zeta_{n+1}), \qquad (3.26) \\ & \qquad\qquad\qquad\qquad\qquad\qquad\qquad\qquad \textit{identity for non-Abelian fields} \end{aligned}}$$

one can subsequently perform all the integrals and obtain

$$\begin{aligned} 2Mw^{\mu\nu}_{nA_T} = \int \frac{\mathrm{d}^4\xi}{(2\pi)^4} e^{ip\xi} \langle P,S\,|\bar{\psi}(0)\gamma^\mu\, \mathrm{Tr}^C\left[\frac{\Delta}{3}\right] \gamma^\nu (-ig)^n \int_C^{\xi_T} \mathrm{d}\zeta_{1_{\alpha_1}} \int_{\zeta_1}^{\xi_T} \mathrm{d}\zeta_{2_{\alpha_2}} \dots \int_{\zeta_{n-1}}^{\xi_T} \mathrm{d}\zeta_{n_{\alpha_n}} \\ \times A^{\alpha_1}(\infty, \xi^+, \zeta_{1T}) \dots A^{\alpha_n}(\infty, \xi^+, \zeta_{nT}) \psi(\xi) |P,S\,\rangle_{\mathrm{c}} (1 + \mathcal{O}(M/Q))\,. \end{aligned} \tag{3.27}$$

This is the n^{th}-order expansion of the transverse gauge link $\mathcal{L}^{\infty^-,\,\xi^+}(C,\xi_T)$.

The gluon insertions in the conjugate part of the diagram can be evaluated as we did for the longitudinal gauge link. Taking the complex conjugate and interchanging μ and ν one obtains $\mathcal{L}^{\infty^-,\,\xi^+}(0,C)$.

The complete leading order result

In the previous paragraphs we resummed gluons from the distribution correlator on one side of the cut being either longitudinally or transversely polarized. When taking the combination of longitudinally and transversely polarized gluons on one side of the cut, one finds in leading order only contributions from those diagrams in which the gluons couple in a specific order. This can be seen as follows.

---

[4] In contrast, Eq. (47) of Ref. [26] does not hold in QCD.

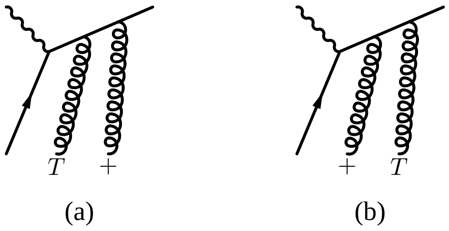

Figure 3.4: Two contributions in the diagrammatic approach. The parton-lines entering from the bottom of the graphs belong to the distribution correlator.

Consider a diagram containing a single A_T-insertion. The sum over all possible longitudinally polarized gluon insertions between the inserted vertex of the transversely polarized gluon and the fragmentation correlator (see for instance Fig. 3.4.a) yields a longitudinal gauge link between infinity and the A_T-field which is at some coordinate η. The leading contribution of this diagram comes when this A_T-field is at infinity and therefore this longitudinal gauge link vanishes. Only the longitudinally polarized gluons, which couple between the vertex of the A_T-gluon and the virtual photon (for instance Fig. 3.4.b), contribute at leading order and provide the longitudinal gauge link. It is exactly this order which also appears in the full gauge link.

Taking combinations on the left-hand-side and on the right-hand-side of the cut is relatively easy. The contributions on each side can be evaluated without using information from the other side of the cut. One simply obtains a product of both insertions, so $\mathcal{L}^{0_T,\,\xi^+}(0^-,\infty^-)\mathcal{L}^{\infty^-,\,\xi^+}(0_T,\infty_T)\mathcal{L}^{\infty^-,\,\xi^+}(\infty_T,\xi_T)\mathcal{L}^{\xi_T,\,\xi^+}(\infty^-,\xi^-) = \mathcal{L}^{[+]}(0,\xi^-)$.

Up to now we inserted gluons from a distribution correlator to an amplitude and looked at their final contribution in the cross sections. It turned out that the transversely polarized gluons at infinity contribute at leading order and yield the transverse gauge link. The same calculation can be done for transversely polarized gluons from the fragmentation correlator. The only leading contribution comes when those fields are at minus infinity, but those fields do not contribute in the chosen gauge ($A^-(\eta) = A_T^\alpha(\eta^-,-\infty,\eta_T) = 0$). This means that the transversely polarized gluons from the fragmentation correlator always appear at subleading order in this gauge. In order to find the gauge invariant fragmentation correlator we assume that the expression for the cross section is gauge invariant. In that case, there is only one link operator possible for the fragmentation correlator which vanishes in this particular gauge. That is a gauge link running via minus infinity. This gauge link is also found when one would have chosen to work in $A^+ = A_T(\infty,0,\xi_T) = 0$ gauge.

In this process we have found that inserting gluons on an outgoing quark yields a gauge link via infinity, while coupling gluons to an incoming quark gives a gauge link via minus infinity. In other processes we will encounter the same behavior. Coupling to outgoing parton-lines leads to gauge links via plus infinity, while coupling to incoming

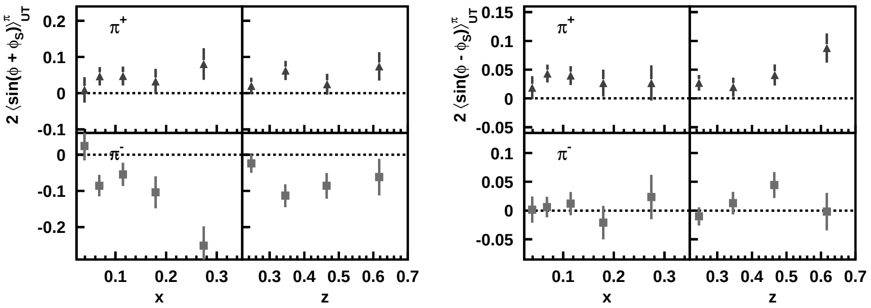

(a) (b)

Figure 3.5: Two projected single transverse target-spin asymmetries measured by HERMES [15]. The following cuts were applied: $Q^2 > 1$ GeV^2, $W^2 > 10$ GeV^2, and $0.1 < y < 0.85$. According to Boer, Mulders [73] the asymmetry in figure (a) is proportional to $h_1 H_1^{\perp(1)}$ while the asymmetry in figure (b) is proportional $f_{1T}^{\perp(1)} D_1$ (in the scaling limit).

parton-lines leads to gauge links via minus infinity.

The hadronic tensor at leading order in M/Q can now be expressed as (the color factor $1/3$ has been absorbed in the fragmentation correlator)

$$
\begin{aligned}
2MW^{\mu\nu} = \int \mathrm{d}^2 p_T\, \mathrm{d}^2 k_T\, \delta^2(p_T + q_T - k_T)\, \mathrm{Tr}^D \Big[\Phi^{[+]}(x_B, p_T)\gamma^\mu \Delta^{[-]}(z^{-1}, k_T)\gamma^\nu\Big] \\
\times (1 + \mathcal{O}(M/Q)) + \mathcal{O}(\alpha_S). \quad (3.28)
\end{aligned}
$$

This result includes an infinite amount of diagrams at leading order in M/Q and is almost equivalent to the result of Boer, Mulders [78]. The only difference is that the correlators above are fully gauge invariant (without assuming A_T-fields at ∞^- to vanish inside matrix elements), forming a natural explanation for transverse momentum dependent T-odd distribution functions. By integrating the hadronic tensor over q_T, these T-odd distribution functions disappear, because the resulting p_T-integrated distribution correlator contains a gauge link of which its path is just a straight-line on the light-cone and does not produce T-odd effects. The integrated distribution functions $e_L(x)$, $f_T(x)$, and $h(x)$, as introduced in Ref. [78], are therefore zero within this approach.

From the hadronic tensor, like the above expression, several asymmetries were calculated in Ref. [78]. Two of these asymmetries were recently measured by HERMES. In the scaling limit ($Q^2 \to \infty$) the asymmetries given in Fig. 3.5a and Fig. 3.5b become proportional to the Sivers function, $f_{1T}^{\perp(1)}$, and the Collins function $H_1^{\perp(1)}$.

3.2.2 Next-to-leading order in M/Q

In the previous subsection we restricted ourselves to leading order in M/Q. Here the calculation will be continued to next-to-leading order. We will start by analyzing in detail the contributions from a single gluon insertion at order in M/Q (Eq. 3.9 and Eq. 3.11) and include the other contributing diagrams later on.

Evaluating Eq. 3.9 (see also Fig. 3.6a) one finds

$$
\begin{aligned}
2Mw^{\mu\nu}_{L,-\not{p}_{1T}} = {} & \int \frac{\mathrm{d}^4\xi}{(2\pi)^4} e^{ip\xi} \langle P,S\,|\overline{\psi}(0)\gamma^\mu\,\mathrm{Tr}^C\left[\frac{\Delta(k)}{3}\right]\frac{\gamma^-\gamma_\alpha}{2k^-}\gamma^\nu \\
& \times g\int_{\xi^-}^{\infty}\mathrm{d}\eta^-\ \left[\partial_T^\alpha A^+(\eta^-,\xi^+,\xi_T)\right]\psi(\xi)|P,S\,\rangle_{\mathrm{c}}\,(1+\mathcal{O}(M/Q))\,. \qquad (3.29)
\end{aligned}
$$

This contribution was discovered in Boer, Mulders [114]. Another contribution at subleading order comes from a transversely polarized gluon, see Eq. 3.11 and Fig. 3.6b. Using the relation $p_1^+/(-p_1^+{+}c{+}i\epsilon) = -1+(c{+}i\epsilon)/(-p_1^+{+}c{+}i\epsilon)$ and a decomposition like Eq. 3.20, that term gives

$$
\begin{aligned}
2Mw^{\mu\nu}_{T,-p_1^+\gamma^-} = {} & \int \frac{\mathrm{d}^4\xi}{(2\pi)^4} e^{ip\xi} \langle P,S\,|\overline{\psi}(0)\gamma^\mu\,\mathrm{Tr}^C\left[\frac{\Delta(k)}{3}\right]\frac{-\gamma_\alpha\gamma^-}{2k^-}\gamma^\nu \\
& \times\left(gA_T^\alpha(\xi)-gA_T^\alpha(\infty,\xi^+,\xi_T)\right)\psi(\xi)|P,S\,\rangle_{\mathrm{c}}\,(1+\mathcal{O}(M/Q))\,. \qquad (3.30)
\end{aligned}
$$

The contributions from Eq. 3.29 and Eq. 3.30 can be combined into

$$
\begin{aligned}
& 2Mw^{\mu\nu}_{L,-\not{p}_{1T}} + 2Mw^{\mu\nu}_{T,-p_1^+\gamma^-} \\
& \quad = \int \frac{\mathrm{d}^4\xi}{(2\pi)^4} e^{ip\xi} \langle P,S\,|\overline{\psi}(0)\gamma^\mu\,\mathrm{Tr}^C\left[\frac{\Delta(k)}{3}\right]\frac{-\gamma_{\alpha T}\gamma^-}{2k^-}\gamma^\nu \\
& \qquad \times g\int_{\infty}^{\xi^-}\mathrm{d}\eta^-\ G_T^{+\alpha}(\eta^-,\xi^+,\xi_T)\psi(\xi)|P,S\,\rangle_{\mathrm{c}}\,(1+\mathcal{O}(M/Q))+\mathcal{O}(g^2). \qquad (3.31)
\end{aligned}
$$

The above result will be generalized to all orders in g in the following paragraphs.

The sum over all possible insertions on both sides of the cut yields in leading order the full gauge link. Some of the insertions, like $2Mw^{\mu\nu}_{L,-\not{p}_{1T}}$ encountered in Eq. 3.9 and $2Mw^{\mu\nu}_{T,-p_1^+\gamma^-}$ in Eq. 3.11, give a suppression in M/Q. In the sum over all insertions and considering the next-to-leading order in M/Q such terms appear only once, either on the left or on the right-hand-side of the cut.

Consider the case that this term is on the left-hand-side and that the gluon from the distribution correlator, which is related to the suppression, is longitudinally polarized

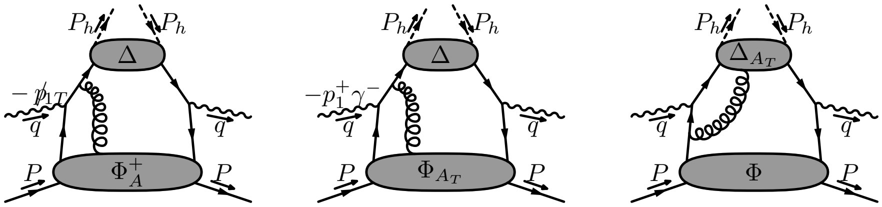

(a) (b) (c)

Figure 3.6: Various diagrams contributing at next-to-leading order in M/Q.

(similar to $2Mw^{\mu\nu}_{L,-\not{p}_{1T}}$ as in Eq. 3.9). In that case the other gluon insertions in the diagram will contribute to the gauge link. Those gluons cannot have their vertices between the vertex of the A^+-gluon giving the suppression and the vertex of the virtual photon. The reason is that the suppressed term is proportional to γ^- which prevents a longitudinal link between it, and that the suppressed term vanishes when fields at light-cone infinity couple between the suppressed term and the virtual photon. The conclusion is that the suppressed term always couples directly next to the photon vertex and the other leading insertions are adjacent to the fragmentation correlator. This contributes to the hadronic tensor as

$$
\begin{aligned}
&2Mw^{\mu\nu}_{L,-\not{p}_{1T}}\ \text{(generalized)}\\
&\quad = \int \mathrm{d}^4 p_1 \int \frac{\mathrm{d}^4\xi\ \mathrm{d}^4\eta}{(2\pi)^8} e^{ip\xi + ip_1(\eta-\xi)}\\
&\qquad \times \langle P,S\,|\overline{\psi}(0)\gamma^\mu \Delta(k)\mathcal{L}^{[+]}(0,\eta^-) i\gamma^- i\frac{-\not{p}_{1T}}{-2k^- p_1^+ + i\epsilon}\gamma^\nu g A^+(\eta)\psi(\xi)|P,S\,\rangle_{\mathrm{c}}.
\end{aligned}
\tag{3.32}
$$

By performing the integral over p_1^+, using the relation $\int_\infty^{\xi^-}\mathrm{d}\eta^-\ i\partial^\alpha_{\eta_T}\mathcal{L}^{[+]}(0,\eta^-)A^+(\eta) = \int_\infty^{\xi^-}\mathrm{d}\eta^-\ i\partial^+_\eta i\partial^\alpha_{\eta_T}\mathcal{L}^{[+]}(0,\eta^-)$, and applying the identities of the previous chapter (Eq. 2.70) to work out the transverse derivative (note that $\langle G^{+\alpha}(\infty,\eta^+,\eta_T)\rangle = 0$), one finds

$$
\begin{aligned}
&2Mw^{\mu\nu}_{L,-\not{p}_{1T}}\ \text{(generalized)}\\
&= \int \frac{\mathrm{d}^4\xi}{(2\pi)^4} e^{ip\xi}\langle P,S\,|\overline{\psi}(0)\gamma^\mu\Delta(k)\frac{\gamma_\alpha\gamma^-}{2k^-}\Big[-\mathcal{L}^{0_T,\,\xi^+}(0^-,\infty^-)\mathcal{L}^{\infty^-,\,\xi^+}(0_T,\xi_T) g A_T^\alpha(\infty,\xi^+,\xi_T)\\
&\quad + \mathcal{L}^{[+]}(0,\xi^-) g A_T^\alpha(\xi) - g\int_\infty^{\xi^-}\mathrm{d}\eta^-\ \mathcal{L}^{[+]}(0,\eta^-) G_T^{+\alpha}(\eta)\mathcal{L}^{\xi_T,\xi^+}(\eta^-,\xi^-)\Big]\gamma^\nu\psi(\xi)|P,S\,\rangle_{\mathrm{c}}\Big|_{\substack{\eta^+=\xi^+\\ \eta_T=\xi_T}}\\
&\quad \times (1+\mathcal{O}(M/Q))\,.
\end{aligned}
\tag{3.33}
$$

If the suppression term comes from a transversely polarized gluon like $2Mw^{\mu\nu}_{T,-p_1^+\gamma^-}$

in Eq. 3.11, then one generally has (following the same arguments)

$$\begin{aligned}
&2Mw^{\mu\nu}_{T,-p_1^+\gamma^-}\ \text{(generalized)}\\
&\quad = \int \mathrm{d}^4p_1 \int \frac{\mathrm{d}^4\xi\ \mathrm{d}^4\eta}{(2\pi)^8}\, e^{ip\xi+ip_1(\eta-\xi)}\\
&\qquad \times \langle P,S\,|\overline{\psi}(0)\gamma^\mu \Delta(k)\mathcal{L}^{[+]}(0,\eta^-)i\gamma_\alpha i\frac{-p_1^+\gamma^-}{-2k^-p_1^+ + i\epsilon}\gamma^\nu g A_T^\alpha(\eta)\psi(\xi)|P,S\,\rangle_{\mathrm{c}}, \qquad (3.34)
\end{aligned}$$

which can be rewritten into

$$\begin{aligned}
&2Mw^{\mu\nu}_{T,-p_1^+\gamma^-}\ \text{(generalized)}\\
&\quad = \int \frac{\mathrm{d}^4\xi}{(2\pi)^4} e^{ip\xi}\langle P,S\,|\overline{\psi}(0)\gamma^\mu\,\mathrm{Tr}^C\left[\frac{\Delta(k)}{3}\right]\frac{-\gamma_\alpha\gamma^-}{2k^-}\gamma^\nu\\
&\qquad \times g\Big[\mathcal{L}^{[+]}(0,\xi^-)A_T^\alpha(\xi) - \mathcal{L}^{0_T,\ \xi^+}(0^-,\infty^-)\mathcal{L}^{\infty^-,\ \xi^+}(0_T,\xi_T)A_T^\alpha(\infty,\xi^+,\xi_T)\Big]\psi(\xi)|P,S\,\rangle_{\mathrm{c}}\\
&\qquad \times (1+\mathcal{O}(M/Q))\,. \qquad (3.35)
\end{aligned}$$

The sum of Eq. 3.33 and Eq. 3.35 gives

$$\begin{aligned}
&2Mw^{\mu\nu}_{L,-\not{p}_{1T}} + 2Mw^{\mu\nu}_{T,-p_1^+\gamma^-}\ \text{(generalized)}\\
&\quad = \int \frac{\mathrm{d}^4\xi}{(2\pi)^4} e^{ip\xi}\langle P,S\,|\overline{\psi}(0)\gamma^\mu\,\mathrm{Tr}^C\left[\frac{\Delta(k)}{3}\right]\frac{-\gamma_{\alpha T}\gamma^-}{2k^-}\gamma^\nu\\
&\qquad \times g\int_\infty^{\xi^-} \mathrm{d}\eta^-\ \mathcal{L}(0,\eta^-)G^{+\alpha}(\eta)\mathcal{L}^{\xi_T,\ \xi^+}(\eta^-,\xi^-)\psi(\xi)|P,S\,\rangle_{\mathrm{c}}\Big|_{\substack{\eta^+=\xi^+\\ \eta_T=\xi_T}} (1+\mathcal{O}(M/Q))\,. \qquad (3.36)
\end{aligned}$$

If the suppression is on the right-hand-side of the cut, one obtains the complex conjugate of this expression with μ and ν interchanged.

Integrated over p^-, the matrix elements as above appear often in cross sections, leading to the following abbreviation for it

$$\begin{aligned}
&\left(\Phi^{[\pm]}_{\partial^{-1}G}\right)^\alpha_{ij}(x,p_T,P,S)\\
&\equiv \int \frac{\mathrm{d}^2\xi_T\ \mathrm{d}\xi^-}{(2\pi)^3} e^{ip\xi}\\
&\quad \times \langle P,S\,|\overline{\psi}_j(0)g\int_{\pm\infty}^{\xi^-} \mathrm{d}\eta^-\mathcal{L}^{[\pm]}(0,\eta^-)G_T^{+\alpha}(\eta)\mathcal{L}^{\xi_T,\ \xi^+}(\eta^-,\xi^-)\psi_i(\xi)|P,S\,\rangle_{\mathrm{c}}\Big|_{\substack{\eta^+=\xi^+=0\\ \eta_T=\xi_T\\ p^+=xP^+}}. \qquad (3.37)
\end{aligned}$$

Note that $\Phi^{[\pm]\ \ \alpha}_{\partial^{-1}G\,ij}$ has only nonzero transverse components. Using the identities of the previous chapter, Eq. 2.70, one can show that

$$\Phi^{[\pm]\ \ \alpha}_{\partial^{-1}G}(x,p_T,P,S) = \Phi^{[\pm]\alpha}_{D\ \ T}(x,p_T,P,S) - p_T^\alpha\ \Phi^{[\pm]}(x,p_T,P,S), \qquad (3.38)$$

where

$$\Phi_{D\ \ ij}^{[\pm]\alpha}(x,p_T,P,S)\equiv\int\frac{\mathrm{d}^2\xi_T\mathrm{d}\xi^-}{(2\pi)^3}e^{ip\xi}\langle P,S|\bar{\psi}_i(0)\mathcal{L}^{[\pm]}(0,\xi^-)iD_\xi^\alpha\psi_j(\xi)|P,S\rangle_{\mathrm{c}}\Big|_{\substack{\xi^+=0\\ p^+=xP^+}}. \tag{3.39}$$

At subleading order in M/Q one also encounters a contribution from the interaction of a transversely polarized gluon from the fragmentation correlator with the hard part (see Fig. 3.6c). Such a contribution gives

$$2MW^{\mu\nu}=\int\mathrm{d}^4p\ \mathrm{d}^4k\ \delta^4(p+q-k)\ 2Mw_{T,frag}^{\mu\nu}+\text{other diagrams,} \tag{3.40}$$

$$\begin{aligned}2Mw_{T,frag}^{\mu\nu}&=-g\int\mathrm{d}^4k_1\ \ \mathrm{Tr}^{D,C}\left[\Phi\gamma^\mu\Delta_{A_T}^\alpha(k,k_1)\gamma^\nu\frac{\not{p}+\not{k}_1+m}{(p+k_1)^2-m^2+i\epsilon}\gamma_\alpha t_l\right]\\&=-g\int\mathrm{d}^4k_1\ \ \mathrm{Tr}^{D,C}\left[\mathrm{Tr}^C\left[\frac{\Phi}{3}\right]\gamma^\mu\Delta_{A_T}^\alpha(k,k_1)\gamma^\nu\frac{\gamma^+}{2p^+}\gamma_\alpha\right].\end{aligned} \tag{3.41}$$

This result can be generalized by considering gluons from the distribution correlator as well, yielding the gauge link in the distribution correlator. When applying the Feynman gauge for the elementary part, the gluon from the distribution correlator which couples to the gluon going to the fragmentation correlator contains an additional term. This term cancels exactly the term which arises when calculating the leading order transverse gauge link with the Feynman gauge for the hard part (see the previous subsection). The result in the applied light-cone gauge reads

$$2Mw_{T,frag}^{\mu\nu}\ (\text{generalized})=\frac{-g}{3}\int\mathrm{d}^4k_1\ \ \mathrm{Tr}^D\left[\Phi^{[+]}\gamma^\mu\ \mathrm{Tr}^C\left(\Delta_{A_T}^\alpha(k,k_1)\right)\gamma^\nu\frac{\gamma^+}{2p^+}\gamma_\alpha\right] \tag{3.42}$$

Because this result is obtained in the light-cone gauge with retarded boundary conditions, the fragmentation correlator appears to be non-gauge-invariant. Assuming gauge invariance of the expression for the cross section one finds that the correlator $\int\mathrm{d}k^+\ \mathrm{d}^4k_1\ \Delta_{A_T}^\alpha(k,k_1)$ corresponds to the correlator $\gamma^0\left[\Delta_{\partial^{-1}G}^{[-]\ \ \alpha}(z^{-1},k_T,P_h,S_h)\right]^\dagger\gamma^0$, which is gauge invariant and defined as

$$\begin{aligned}&\Delta_{\partial^{-1}G}^{[\pm]\ \ \alpha}(z^{-1},k_T,P_h,S_h)\\&\equiv\frac{1}{3}\sum_X\int\frac{\mathrm{d}^3\mathbf{P}_X}{(2\pi)^3 2E_{\mathbf{P}_X}}\int\frac{\mathrm{d}^2\eta_T\ \mathrm{d}\eta^+}{(2\pi)^3}e^{ik\eta}{}_{\mathrm{out}}\langle P_h;P_X|\bar{\psi}(0)\mathcal{L}^{0_T,\,\eta^-}(0,\pm\infty^+)\mathcal{L}^{\pm\infty^+,\,\eta^-}(0,\eta_T)|\Omega\rangle_{\mathrm{c}}\\&\times\langle\Omega|g\int_{\pm\infty}^{\eta^+}\mathrm{d}\zeta^+\mathcal{L}^{\eta_T,\,\eta^-}(\pm\infty^+,\zeta^+)G_T^{-\alpha}(0,\zeta^+,\eta_T)\mathcal{L}^{\eta_T,\,\eta^-}(\zeta^+,\eta^+)\psi(\eta)|P_h;P_X\rangle_{\mathrm{out,c}}\Big|_{\substack{\eta^-=0\\ k^-=z^{-1}P_h^-}}\end{aligned} \tag{3.43}$$

Also here one has the relation

$$\Delta_{\partial^{-1}G}^{[\pm]\ \ \alpha}(z^{-1},k_T,P_h,S_h)=\Delta_{D\ \ T}^{[\pm]\alpha}(z^{-1},k_T,P_h,S_h)-k_T^\alpha\ \Delta^{[\pm]}(z^{-1},k_T,P_h,S_h), \tag{3.44}$$

where

$$\begin{aligned}
&\Delta_{D\ \ ij}^{[\pm]\alpha}(z^{-1}, k_T, P_h, S_h) \\
&\quad \equiv \frac{1}{3}\sum_X \int \frac{\mathrm{d}^3\mathbf{P}_X}{(2\pi)^3 2E_{\mathbf{P}_X}} \int \frac{\mathrm{d}^2\xi_T\ \mathrm{d}\xi^+}{(2\pi)^3} e^{ik\xi}\,{}_{\mathrm{out}}\langle P_h; P_X|\overline{\psi}_j(0)\mathcal{L}^{0_T,\ \xi^-}(0, \pm\infty^+)|\Omega\rangle_{\mathrm{c}} \\
&\qquad \times \langle\Omega|\mathcal{L}^{\pm\infty^+,\ \xi^-}(0_T, \xi_T)\mathcal{L}^{\xi_T,\ \xi^-}(\pm\infty^+, \xi^+) iD_\xi^\alpha \psi_i(\xi)|P_h; P_X\rangle_{\mathrm{out,c}}\Big|_{\substack{\xi^-=0 \\ k^-=z^{-1}P_h^-}} .
\end{aligned} \tag{3.45}$$

Considering now all insertions on both sides of the cut one finds that the hadronic tensor including M/Q corrections now (finally) reads [35] (for notational reasons the contribution from $\gamma^0[\Delta_{\partial^{-1}G}^{-\alpha}(z^{-1}, k_T, P_h, S_h)]^\dagger\gamma^0$ was put in $(\mu \to \nu)^*$)

$$\boxed{\begin{aligned}
2MW^{\mu\nu} = &\int \mathrm{d}^2p_T\ \mathrm{d}^2k_T\ \delta^2(p_T + q_T - k_T)\bigg[\mathrm{Tr}^D\Big[\Phi^{[+]}(x_B, p_T)\gamma^\mu\Delta^{[-]}(z^{-1}, k_T)\gamma^\nu\Big] \\
&+ \mathrm{Tr}^D\Big[-\gamma_\alpha\frac{\not{n}_+}{Q\sqrt{2}}\gamma^\nu\Phi_{\partial^{-1}G}^{[+]\ \ \alpha}(x_B, p_T)\gamma^\mu\Delta^{[-]}(z^{-1}, k_T) \\
&\qquad - \Delta_{\partial^{-1}G}^{[-]\ \ \alpha}(z^{-1}, k_T)\gamma^\nu\Phi^{[+]}(x_B, p_T)\gamma_\alpha\frac{\not{n}_-}{Q\sqrt{2}}\gamma^\mu + (\mu \leftrightarrow \nu)^*\Big]\bigg] \\
&\times \Big(1 + \mathcal{O}\big(M^2/Q^2\big) + \mathcal{O}(\alpha_S)\Big) .
\end{aligned}} \tag{3.46}$$

hadronic tensor for semi-inclusive DIS includingM/Q corrections

This expression completes the descriptions of Mulders, Tangerman [115] and Boer, Mulders [114] by including the transverse gauge link. Apart from diagrams which are connected to the equations of motion, all possible gluon-interactions between the correlators and the elementary part have been included. Although an infinite set of diagrams was calculated including M/Q corrections, the final result still looks remarkably simple. It is basically expressed in two types of correlators, Φ and $\Phi_{\partial^{-1}G}$, and similar ones for fragmentation. For Φ one can simply plug in the parametrizations of the previous chapter. We could in principle parametrize $\Phi_{\partial^{-1}G}$ as well but it will turn out that this correlator only appears in certain kind of traces. Using the equations of motion those traces can be rewritten in terms of the already defined functions of Φ.

3.2.3 Some explicit cross sections and asymmetries

In the previous subsection the hadronic tensor was derived including next-to-leading order corrections in M/Q. This tensor was expressed in correlators which have been parametrized in terms of distribution and fragmentation functions. Inserting these parametrizations, the expressions for the longitudinal target-spin and beam-spin asymmetries, as published in Ref. [36], will be given. Three other papers considered recently beam-spin asymmetries as well and motivated the publication of Ref. [36]. Using a model calculation, Afanasev and Carlson estimated in Ref. [116] the beam-spin asymmetry and compared their results to CLAS data. Yuan obtained in Ref. [117] an expression for the asymmetry and made an estimation by using a chiral quark model and a bag model. Metz and Schlegel claimed in Ref. [118], which also considers longitudinal target-spin asymmetries, that the calculation of Ref. [116] is incomplete. They completed the model by including other diagrams which, as the authors point out themselves, are not compatible with the parton model at order M/Q. In Ref. [36] the analysis of Yuan [117] is completed by including quark-mass effects and the new function $g^{\perp}$.

Explicit leading order cross sections can easily be obtained by replacing the correlators $\Phi^{[+]}$ and $\Delta^{[-]}$ in Eq. 3.46 with the explicit parametrizations of the previous chapter (see Eq. 2.57, 2.65, 2.83, 2.88). Note that our choice of light-like vectors, Eq. 3.2, is easily related to the frame in which the correlators were defined, Eq. 2.47, 2.75. At order M/Q the other correlators ${\Phi^{[+]}_{\partial^{-1}G}}^{\alpha}$ and ${\Delta^{[-]}_{\partial^{-1}G}}^{\alpha}$ need to be included. They will be handled here by making a *Fierz-decomposition* which relies on the identity

$$\begin{aligned}
&\mathrm{Tr}^D[AB] = a_1 b_1 + a_2 b_2 + a_3^{\alpha} b_{3\alpha} + a_4^{\alpha} b_{4\alpha} + a_5^{\alpha\beta} b_{5\alpha\beta},\\
&\text{where}\quad a_1 = \frac{1}{2}\,\mathrm{Tr}^D[A], \qquad a_2 = \frac{1}{2}\,\mathrm{Tr}^D[A\gamma_5], \qquad a_3^{\alpha} = \frac{1}{2}\,\mathrm{Tr}^D[A\gamma^{\alpha}],\\
&\qquad a_4^{\alpha} = \frac{1}{2}\,\mathrm{Tr}^D[Ai\gamma^{\alpha}\gamma_5], \quad a_5^{\alpha\beta} = \frac{1}{2\sqrt{2}}\,\mathrm{Tr}^D[A\sigma^{\alpha\beta}\gamma_5] \qquad \text{and similarly for } b_i.
\end{aligned}$$

Using the Fierz-decomposition one encounters $\Phi_{\partial^{-1}G}$ and $\Delta_{\partial^{-1}G}$ only in particular combinations of traces which allow for a simplification by the use of the equations of motion. Showing only the argument connected to the polarization of the parent hadron, the correlators $\Phi_{\partial^{-1}G}$ and $\Delta_{\partial^{-1}G}$ are decomposed into

$$ {\Phi^{[+]}_{\partial^{-1}G}}^{\alpha}(S) = {\Phi^{[+]}_{\partial^{-1}G}}^{\alpha}(0) + {\Phi^{[+]}_{\partial^{-1}G}}^{\alpha}(S_L) + {\Phi^{[+]}_{\partial^{-1}G}}^{\alpha}(S_T), \tag{3.47}$$

$$ {\Delta^{[-]}_{\partial^{-1}G}}^{\alpha}(S_h) = {\Delta^{[-]}_{\partial^{-1}G}}^{\alpha}(0) + {\Delta^{[-]}_{\partial^{-1}G}}^{\alpha}(S_{hL}) + {\Delta^{[-]}_{\partial^{-1}G}}^{\alpha}(S_{hT}). \tag{3.48}$$

Using the relation $[i\not{D}-m]\psi = 0$, which straightforwardly gives $[iD^{\mu}+\sigma^{\mu\nu}D_{\nu}-m\gamma^{\mu}]\psi = [i\gamma^{\mu}D^{\nu}-i\gamma^{\nu}D^{\mu}+im\sigma^{\mu\nu}+i\epsilon^{\mu\nu\rho\sigma}\gamma_{\sigma}\gamma_5 iD_{\rho}]\psi = 0$, one finds for an unpolarized target (the functions depend on x and p_T^2)

$$\frac{1}{2}\mathrm{Tr}[{\Phi^{[+]}_{\partial^{-1}G}}^{\alpha}(0){\sigma_{\alpha}}^{+}] = iMx\,e - im\,f_1 + Mx\,h - \frac{p_T^2}{M}\,h_1^{\perp}, \tag{3.49}$$

$$\frac{1}{2}\mathrm{Tr}[{\Phi^{[+]}_{\partial^{-1}G}}^{\alpha}(0)\,i{\sigma_{\alpha}}^{+}\gamma_5] = 0, \tag{3.50}$$

$$\frac{1}{2}\mathrm{Tr}[{\Phi^{[+]}_{\partial^{-1}G}}^{\alpha}(0)\,\gamma^{+}]-\frac{1}{2}\,\epsilon_T^{\alpha\beta}\mathrm{Tr}[\Phi^{[+]}_{\partial^{-1}G\beta}(0)\,i\gamma^{+}\gamma_5] = p_T^{\alpha}(x\,f^{\perp}+i\frac{m}{M}\,h_1^{\perp}+ix\,g^{\perp}-f_1), \tag{3.51}$$

and for unpolarized observed hadrons (where the functions depend on z and $z^2k_T^2$)

$$\frac{1}{4}\,\mathrm{Tr}[{\Delta^{[-]}_{\partial^{-1}G}}^{\alpha}(0){\sigma_{\alpha}}^{-}] = iM_hE^{[-]} - imzD_1^{[-]} + M_hH^{[-]} - \frac{zk_T^2}{M_h}H_1^{\perp[-]}, \tag{3.52}$$

$$\frac{1}{4}\,\mathrm{Tr}[\Delta_{\partial^{-1}G}^{[-]}{}^{\alpha}(0)i\sigma_{\alpha}{}^{+}\gamma_5] = 0, \tag{3.53}$$

$$\frac{1}{4}\,\mathrm{Tr}[\Delta_{\partial^{-1}G}^{[-]}{}^{\alpha}(0)\gamma^{-}] + \frac{1}{4}\epsilon_{T\beta}^{\alpha}\,\mathrm{Tr}[\Delta_{\partial^{-1}G}^{[-]}{}^{\beta}(0)i\gamma^{-}\gamma_5]$$
$$= k_T^{\alpha}(D^{\perp[-]} + iz\frac{m}{M_h}H_1^{\perp[-]} - iG^{\perp[-]} - zD_1^{[-]}). \tag{3.54}$$

For longitudinal target-spin asymmetries one has the relations

$$\frac{1}{2}\mathrm{Tr}[\Phi_{\partial^{-1}G}^{[+]}{}^{\alpha}(S_L)\sigma_{\alpha}{}^{+}] = 0 \tag{3.55}$$

$$\frac{1}{2}\mathrm{Tr}[\Phi_{\partial^{-1}G}^{[+]}{}^{\alpha}(S_L)\,i\sigma_{\alpha}{}^{+}\gamma_5] = -mS_L\,g_{1L} + iMxS_L e_L + MxS_L\,h_L - \frac{p_T^2}{M}S_L\,h_{1L}^{\perp}, \tag{3.56}$$

$$\frac{1}{2}\mathrm{Tr}[\Phi_{\partial^{-1}G}^{[+]}{}^{\alpha}(S_L)\,\gamma^{+}] - \frac{1}{2}\,\epsilon_T^{\alpha\beta}\mathrm{Tr}[\Phi_{\partial^{-1}G\beta}^{[+]}(S_L)\,i\gamma^{+}\gamma_5]$$
$$= -\epsilon_T^{\alpha\beta}p_{T\beta}(xS_L\,f_L^{\perp} - i\frac{m}{M}S_L\,h_{1L}^{\perp} + ixS_L\,g_L^{\perp} - iS_L\,g_{1L}). \tag{3.57}$$

It turns out[5] that these relations are sufficient to rewrite the appearing correlators $\Phi_{\partial^{-1}G}$ and $\Delta_{\partial^{-1}G}$ in terms of the distribution and fragmentation functions.

The vectors in which the cross section is expressed need to be related to the vectors of the Cartesian basis as introduced in the previous chapter. The following relations can be found for the vectors P, q, and P_h ($e_{\pm} \equiv (e_t \pm e_z)/\sqrt{2}$)

$$q = \frac{Q}{\sqrt{2}}\,e_{-} - \frac{Q}{\sqrt{2}}\,e_{+}, \tag{3.58}$$

$$P = \frac{x_B M^2 + \mathcal{O}(M^4/Q^2)}{Q\sqrt{2}}\,e_{-} + \frac{Q + \mathcal{O}(M^2/Q)}{x_B\sqrt{2}}\,e_{+}, \tag{3.59}$$

$$P_h = \frac{z_h Q + \mathcal{O}(M_h^2/Q)}{\sqrt{2}}\,e_{-} + \frac{M_h^2 - P_{h\perp}^2 + \mathcal{O}(M_h^4/Q^2)}{z_h\sqrt{2}Q}\,e_{+} + P_{h\perp}. \tag{3.60}$$

Comparing these relations with Eq. 3.2 (and neglecting M^2/Q^2 corrections) one finds

$$n_{+} = e_{+}, \qquad n_{-} = e_{-} + \frac{\sqrt{2}}{z_h\tilde{Q}}P_{h\perp}, \qquad q_{T\perp} = -P_{h\perp}/z. \tag{3.61}$$

This gives the following relations for any two transverse vectors m_T and n_T

$$m_T = m_{T\perp} + m_T{\cdot}e_{-}\,e_{+} + m_T{\cdot}e_{+}\,e_{-} = m_{T\perp} + \frac{\sqrt{2}}{Q}q_T{\cdot}m_T\,e_{+}, \tag{3.62}$$

$$m_T{\cdot}n_T = m_{T\perp}{\cdot}n_{T\perp}. \tag{3.63}$$

---

[5] In the way the calculation is presented here, it is remarkable that the equations of motion contain sufficient information to rewrite the appearing correlators $\Phi^{\alpha}_{\partial^{-1}G}$ and $\Delta^{\alpha}_{\partial^{-1}G}$ in terms of Φ, Φ^{α}_{∂}, Δ, and $\Delta^{\alpha}_{\partial}$. It has been pointed out by Qiu in Ref. [119] that one can avoid the quark-gluon-quark correlators by using the equations of motion at an earlier stage in the calculation. That could make the result less surprising.

So, by applying the Fierz-decomposition, using the equations of motion, expressing the result in the Cartesian basis, and using FORM [120], the hadronic tensor can be obtained. The tensor, also given in appendix 3.A, reads explicitly [36]

$$
\begin{aligned}
2MW^{\mu\nu} &= \Big[2MW_A^{\mu\nu} + 2MW_S^{\mu\nu}\Big]\Big(1 + \mathcal{O}\big(M^2/Q^2\big) + \mathcal{O}(\alpha_S)\Big), \qquad (3.64)\\
2MW_A^{\mu\nu} &\approx 2z\int \mathrm{d}^2p_T\,\mathrm{d}^2k_T\;\delta^2\Big(p_{T\perp} - \frac{P_{h\perp}}{z} - k_{T\perp}\Big)\\
&\quad\times\Bigg\{\; i\frac{2e_t^{[\mu}k_{T\perp}^{\;\nu]}}{Q}\left[-\frac{M}{M_h}x_B\,eH_1^{\perp[-]} + \frac{m}{M_h}f_1H_1^{\perp[-]} - \frac{1}{z}f_1G^{\perp[-]}\right]\\
&\qquad +i\frac{2e_t^{[\mu}p_{T\perp}^{\;\nu]}}{Q}\left[-\frac{m}{M}h_1^{\perp}D_1^{[-]} + \frac{M_h}{zM}h_1^{\perp}E^{[-]} - x_Bg^{\perp}D_1^{[-]}\right]\\
&\qquad +i\epsilon_{\perp}^{\mu\nu}\left[S_L\,g_{1L}D_1^{[-]} - \frac{p_{T\perp}\cdot S_{T\perp}}{M}g_{1T}D_1^{[-]}\right]\\
&\qquad +iS_L\frac{2e_t^{[\mu}\epsilon_{\perp}^{\nu]\rho}k_{T\perp\rho}}{Q}\left[g_{1L}\frac{D^{\perp[-]}}{z} - g_{1L}D_1^{[-]} - \frac{m}{M}h_{1L}^{\perp}D_1^{[-]} - x_B\frac{M}{M_h}e_LH_1^{\perp[-]}\right]\\
&\qquad +iS_L\frac{2e_t^{[\mu}\epsilon_{\perp}^{\nu]\rho}p_{T\perp\rho}}{Q}\left[x_Bg_L^{\perp}D_1^{[-]} + \frac{M_h}{M}h_{1L}^{\perp}\frac{E^{[-]}}{z} - \frac{m}{M}h_{1L}^{\perp}D_1^{[-]}\right]\Bigg\}\\
2MW_S^{\mu\nu} &\approx 2z\int \mathrm{d}^2p_T\,\mathrm{d}^2k_T\;\delta^2\Big(p_{T\perp} - \frac{P_{h\perp}}{z} - k_{T\perp}\Big)\\
&\quad\times\Bigg\{ - g_{\perp}^{\mu\nu}f_1D_1^{[-]} + \frac{g_{\perp}^{\mu\nu}k_{T\perp}\cdot p_{T\perp} - k_{T\perp}^{\{\mu}p_{T\perp}^{\;\nu\}}}{MM_h}h_1^{\perp}H_1^{\perp[-]}\\
&\qquad +\frac{2e_t^{\{\mu}k_{T\perp}^{\;\nu\}}}{Q}\left[-f_1D_1^{[-]} + f_1\frac{D^{\perp[-]}}{z} + x_B\frac{M}{M_h}h\frac{H_1^{\perp[-]}}{z}\right]\\
&\qquad +\frac{2e_t^{\{\mu}p_{T\perp}^{\;\nu\}}}{Q}\left[x_Bf^{\perp}D_1^{[-]} + \frac{M_h}{M}h_1^{\perp}\frac{H^{[-]}}{z} + \frac{\mathbf{k}_T^2}{MM_h}h_1^{\perp}H_1^{\perp[-]}\right]\\
&\qquad -\frac{k_{T\perp}^{\{\mu}\epsilon_{\perp}^{\nu\}\rho}p_{T\perp\rho} + p_{T\perp}^{\{\mu}\epsilon_{\perp}^{\nu\}\rho}k_{T\perp\rho}}{2MM_h}\left[S_Lh_{1L}^{\perp}H_1^{\perp[-]} - \frac{k_{T\perp}\cdot S_{T\perp}}{M}h_{1T}^{\perp}H_1^{\perp[-]}\right]\\
&\qquad -\frac{k_{T\perp}^{\{\mu}\epsilon_{\perp}^{\nu\}\rho}S_{T\perp\rho} + S_{T\perp}^{\{\mu}\epsilon_{\perp}^{\nu\}\rho}k_{T\perp\rho}}{2M_h}h_{1T}H_1^{\perp[-]}\\
&\qquad +S_L\frac{2e_t^{\{\mu}\epsilon_{\perp}^{\nu\}\rho}k_{T\perp\rho}}{Q}\left[\frac{M}{M_h}x_Bh_LH_1^{\perp[-]} - \frac{m}{M_h}g_{1L}H_1^{\perp[-]} + g_{1L}\frac{G^{\perp[-]}}{z}\right]\\
&\qquad +S_L\frac{2e_t^{\{\mu}\epsilon_{\perp}^{\nu\}\rho}p_{T\perp\rho}}{Q}\left[\frac{M_h}{M}h_{1L}^{\perp}\frac{H^{[-]}}{z} + \frac{\mathbf{k}_{T\perp}^{\;2}}{MM_h}h_{1L}^{\perp}H_1^{\perp[-]} - x_Bf_L^{\perp}D_1^{[-]}\right]\Bigg\},
\end{aligned}
$$

the hadronic tensor of semi-inclusive DIS

where the approximation-signs indicate that transverse target polarization has only been taken into account at leading order and any polarizations in the final state have been

	result of contraction with $L_{\mu\nu}$
$g_\perp^{\mu\nu}$	$\frac{4Q^2}{y^2}(-1+y-y^2/2)$
$a_\perp^{\{\mu}b_\perp^{\nu\}} - a_\perp \cdot b_\perp g_\perp^{\mu\nu}$	$\frac{4Q^2}{y^2}(1-y)(a\cdot e_x\, b\cdot e_x - a\cdot e_y\, b\cdot e_y)$
$\frac{1}{2}\left[a_\perp^{\{\mu}\epsilon_\perp^{\nu\}\rho}b_{\perp\rho} + b_\perp^{\{\mu}\epsilon_\perp^{\nu\}\rho}a_{\perp\rho}\right]$	$\frac{4Q^2}{y^2}(-1+y)(a\cdot e_x\, b\cdot e_y + a\cdot e_y\, b\cdot e_x)$
$e_t^{\{\mu}a_\perp^{\nu\}}$	$\frac{4Q^2}{y^2}(2-y)\sqrt{1-y}\; a\cdot e_x$
$e_t^{\{\mu}\epsilon_\perp^{\nu\}\rho}a_{\perp\rho}$	$\frac{4Q^2}{y^2}(y-2)\sqrt{1-y}\; a\cdot e_y$
$i\epsilon_\perp^{\mu\nu}$	$\frac{4Q^2}{y^2}\lambda_e(y-y^2/2)$
$ia_\perp^{[\mu}b_\perp^{\nu]}$	$\frac{4Q^2}{y^2}\lambda_e(y-y^2/2)(a\cdot e_x\, b\cdot e_y + a\cdot e_y\, b\cdot e_x)$
$ie_t^{[\mu}b_\perp^{\nu]}$	$\frac{4Q^2}{y^2}\lambda_e y\sqrt{1-y}\; a\cdot e_y$
$e_t^{[\mu}\epsilon_\perp^{\nu]\rho}a_{\perp\rho}$	$\frac{4Q^2}{y^2}\lambda_e y\sqrt{1-y}\; a\cdot e_x$

Table 3.1: Various contractions given frame-independently (see also Ref. [115]).

discarded. The distribution functions depend here on x_B and p_T^2 while the fragmentation functions have the arguments z and $z^2k_T^2$. It should be noted that the hadronic tensor satisfies $q_\mu W^{\mu\nu} = q_\nu W^{\mu\nu} = 0$, expressing electromagnetic gauge invariance.

In the above equation the hadronic tensor is expressed in terms of the various distribution and fragmentation functions. In order to obtain the cross section, Eq. 2.23, the hadronic tensor still needs to be contracted with the leptonic tensor $L_{\mu\nu}$. Those contractions are facilitated by the use of table 3.1. After having made these contractions the result is not yet a simple product between the various distribution and fragmentation functions, but rather a convolution ($\int d^2p_T\, d^2k_T\, \delta^2(p_{T\perp} - P_{h\perp}/z - k_{T\perp})\, f_i(x_B, p_T^2)D_j(z, z^2k_T^2)$). The convolution can be made into a simple product by multiplying the cross sections with some factors $P_{h\perp}$ and subsequently integrate over $d^2P_{h\perp}$. Note that the leptonic tensor is independent of $P_{h\perp}$.

The unpolarized $P_{h\perp}$-integrated cross section is given by ($L_{\mu\nu}^{(U)}$ denotes the unpolarized part of $L_{\mu\nu}$)

$$\begin{aligned}\int d^2P_{h\perp}\, E_{\mathbf{P}_h}E_{\mathbf{l}'}\frac{d^6\sigma}{d^3\mathbf{l}'\, d^3\mathbf{P}_h} &= \frac{1}{4s}\frac{\alpha^2}{Q^4}L_{\mu\nu}^{(U)}\int d^2P_{h\perp}\, 2MW_U^{\mu\nu}\\ &= \frac{2\alpha^2}{sQ^2}\,\frac{1-y+y^2/2}{y^2}\, z\, f_1(x_B)\, D_1(z)\\ &\quad\times\left(1+\mathcal{O}(M/Q)+\mathcal{O}(\alpha_S)\right). \qquad (3.65)\end{aligned}$$

unpolarized cross section for semi-inclusive DIS at leading order

One of the single spin asymmetries we will study here is the beam-spin asymme-

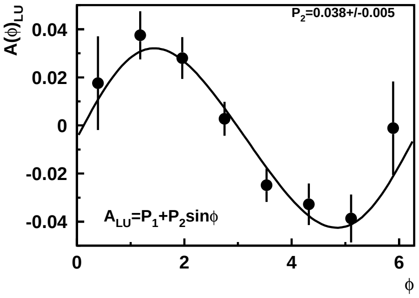

Figure 3.7: Azimuthal beam-spin asymmetry measured by CLAS [121]. The applied cuts are $Q^2 > 1$ GeV^2, $W^2 > 4$ GeV^2, and $0.5 < z < 0.8$.

try. This asymmetry has been measured by CLAS [121] and HERMES [122]. The asymmetry will be defined as

$$A_{LU} = \frac{(L_{\mu\nu}^{\lambda_e=1} - L_{\mu\nu}^{\lambda_e=-1})\, 2MW_{\mathrm{U}}^{\mu\nu}}{\int \mathrm{d}^2P_h^\perp\, (L_{\mu\nu}^{\lambda_e=1} + L_{\mu\nu}^{\lambda_e=-1})\, 2MW_{\mathrm{U}}^{\mu\nu}}, \tag{3.66}$$

where $\lambda_e = 1$ corresponds to a polarization pointing towards the target. For a general weighted azimuthal asymmetry the following definition is introduced

$$A_{(\dots)}^{P_{h\perp}\cdot\hat{a}} \equiv \int \mathrm{d}^2P_{h\perp}\, P_{h\perp}\cdot\hat{a}\, A_{(\dots)}. \tag{3.67}$$

Weighting the beam-spin asymmetry with $P_{h\perp}\cdot e_y$ and integrating over $\mathrm{d}^2P_{h\perp}$ gives [36]

$$\begin{aligned} A_{LU}^{P_{h\perp}\cdot e_y} = \frac{-2y\sqrt{1-y}}{(1-y+y^2/2)\, f_1 D_1}\, \frac{MM_h}{Q}\Big[& \frac{m}{M} z\, f_1 H_1^{\perp[-](1)} - \frac{M_h}{M}\, f_1 G^{\perp[-](1)} - x_B z\, e H_1^{\perp[-](1)} \\ & + \frac{m}{M_h} z\, h_1^{\perp(1)} D_1 - h_1^{\perp(1)} E + \frac{M}{M_h} x_B z\, g^{\perp(1)} D_1 \Big] \\ & \times \left(1 + \mathcal{O}(M/Q) + \mathcal{O}(\alpha_S)\right), \end{aligned} \tag{3.68}$$

azimuthal beam-spin asymmetry for semi-inclusive DIS

where the functions depend on x_B or z.

The asymmetry given above contains besides the contributions given in Mulders, Tangerman [115] and Yuan [117], two additional terms: the term proportional to $h_1^\perp D_1$ and the term proportional to $g^\perp D_1$. Presently, all six contributions are unknown, making this asymmetry unsuited for studying one function in particular. To extract information one should get a handle on some of the contributions, either through phenomenological studies (e.g. see Efremov et al. [123, 124]) or model calculations. For a review on the Collins functions, $H_1^{\perp}$, the reader is referred to Amrath, Bacchetta, and Metz [125] and the references therein. Models of the Boer-Mulders function, $h_1^{\perp}$, have been studied by Gamberg, Goldstein, and Oganessyan [126, 127, 128], Boer, Brodsky, and Hwang [129], and Lu and Ma [130, 131]. Hwang has attempted to construct a model for $g^{\perp}$, but encountered problems with factorization in the model [132].

More easy to interpret is the asymmetry of the produced jet which can be obtained from Eq. 3.68 by summing over all possible final-state hadrons and integrating over their phase space. Neglecting quark mass contributions the azimuthal asymmetry of the jet is directly proportional to $g^{\perp}$,

$$A_{LU,j}^{P_{j\perp}\cdot e_y} = -\frac{M^2}{Q}\,\frac{2y\sqrt{1-y}}{(1-y+y^2/2)}\,\frac{x_B\, g^{\perp(1)}(x_B)}{f_1(x_B)}\,\big(1+O(M/Q)+O(\alpha_S)\big)\,. \qquad (3.69)$$

beam-spin asymmetry for jet production in DIS

As explained in the previous chapter (see subsection 2.5.2), the function $g^{\perp}$ exists owing to the directional dependence of the gauge link which is also connected with the non-validity of the Lorentz invariance relations. This makes the asymmetry of increasing interest for the understanding of the theoretical description (are such functions really non-vanishing?) even though this function does not have a partonic interpretation (like all the other T-odd functions). One way to access the asymmetry for the jet-momentum is to make an extrapolation by first considering the leading hadron, then the sum of the leading and next-to-leading hadron, etc.

Next we consider target-spin asymmetries which have been measured by HERMES [133, 134, 135] and COMPASS [136]. Considering these asymmetries one needs to express the polarization in the lab-frame into the Cartesian basis, Eq. 2.3. In an experimental setup the target is usually polarized along or perpendicular to the electron beam. Both directions are combinations of e_x, e_y and e_z. If the target is longitudinally polarized then it has nonzero S_L and $S_{T\perp}$. The contribution of the latter was suggested by Oganessyan et al. [137, 138] to access transversity via longitudinal target-spin asymmetries (see for related work Diehl, Sapeta [139]).

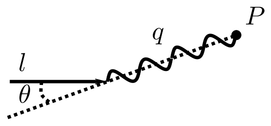

Figure 3.8: Illustration of the lab-frame.

Defining θ to be the angle between $\mathbf{q}$ and $\mathbf{l}$ in the target rest frame (see also Fig. 3.8), the following relation can be obtained

$$\theta = \frac{2Mx_B}{Q}\sqrt{1-y} + O\left(M^2/Q^2\right). \qquad (3.70)$$

Polarizing the target along the beam leads for $S_{T\perp}$ and S_L to

$$S_L = \pm 1 + O\left(M^2/Q^2\right), \tag{3.71}$$

$$|\mathbf{S}_{T\perp}| = \frac{2Mx_B}{Q}\sqrt{1-y} + O\left(M^2/Q^2\right). \tag{3.72}$$

Defining the longitudinal target-spin asymmetry as

$$A_{UL'} = \frac{L^{\mathrm{U}}_{\mu\nu}\,(2MW^{\mu\nu}_{S'_L=1} - 2MW^{\mu\nu}_{S'_L=-1})}{\int \mathrm{d}^2P_{h\perp}\,L^{\mathrm{U}}_{\mu\nu}\,(2MW^{\mu\nu}_{S'_L=1} + 2MW^{\mu\nu}_{S'_L=-1})}, \tag{3.73}$$

where $S'_L = 1$ denotes a polarization against the beam-direction, one obtains [36]

$$\begin{aligned} A^{P_{h\perp}\cdot e_y}_{UL'} = \frac{-2\sqrt{1-y}}{(1-y+y^2/2)\,f_1D_1}\,\frac{MM_h}{Q}\Big[\,(2-y)\Big(\frac{m}{M}z\,g_1H_1^{\perp[-](1)} - \frac{M_h}{M}g_1G^{\perp[-](1)} - x_Bz\,h_LH_1^{\perp[-](1)} \\ + h_{1L}^{\perp(1)}\left[H + 2zH_1^{\perp[-](1)}\right] - \frac{M}{M_h}x_Bz\,f_L^{\perp(1)}D_1\Big) \\ + (1-y)\Big(x_Bzh_1H_1^{\perp[-](1)}\Big) \\ - (1-y+y^2/2)\Big(\frac{M}{M_h}x_Bz\,f_{1T}^{\perp(1)}D_1\Big)\Big] \\ \times(1 + \mathcal{O}(M/Q) + \mathcal{O}(\alpha_S)), \end{aligned} \tag{3.74}$$

longitudinal target-spin azimuthal asymmetry in semi-inclusive DIS

where the functions depend on x_B or z. The functions $f_L^{\perp(1)}$ and $G^{\perp(1)}$, which were neglected in previous analyses, have been included.

Compared to the beam-spin asymmetry there are more terms contributing to the asymmetry. The sizes of the contributions are at present unknown but the asymmetry is certainly not dominated by the contribution from transversity h_1 (see also Hermes [140]). On the other hand, by using the different y-dependence one can in principle extract the contributions from the Sivers function, $f_{1T}^{\perp(1)}$, and transversity. For this extraction different collision energies are required ($y \approx Q^2/(x_Bs)$). Experimental statistics could be improved by integrating over all other external variables.

3.3 The Drell-Yan process

The calculation of the hadronic tensor in Drell-Yan is very similar to the calculations we performed in the previous section. Only the most important steps will be listed.

In the Drell-Yan process the set of light-like vectors ($\{n_-, n_+\}$ with $n_- \sim \overline{n}_+$ and

$n_- \cdot n_+ = 1$) is chosen such that

$$
\begin{aligned}
P_1 &= \frac{x_1 M_1^2}{Q\sqrt{2}} n_- + \frac{Q}{x_1\sqrt{2}} n_+, \\
P_2 &= \frac{Q}{x_2\sqrt{2}} n_- + \frac{x_2 M_2^2}{Q\sqrt{2}} n_+, \\
q &= \frac{Q + \mathcal{O}(M^2/Q)}{\sqrt{2}} n_- + \frac{Q + \mathcal{O}(M^2/Q)}{\sqrt{2}} n_+ + q_T. \qquad (3.75)
\end{aligned}
$$

Sudakov-decomposition for Drell-Yan

In this process one can also resum the contributions of gluons coming from the distribution correlator and connecting with the hard part. The difference with respect to semi-inclusive DIS is that the quark-fragmentation correlator is interchanged with an antiquark-distribution correlator describing an incoming parton. This results in a gauge link running via minus infinity for the distribution correlator. The first order calculation illustrates this difference in direction very clearly. Inserting a longitudinally polarized gluon from the distribution correlator, like Fig. 3.9, gives the following contribution to the hadronic tensor (arguments connected to parent hadrons will be suppressed in this section)

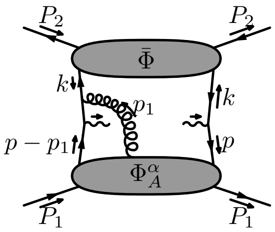

Figure 3.9: A gluon coupling to the incoming antiquark.

$$2MW^{\mu\nu} = \int \mathrm{d}^4p\, \mathrm{d}^4k\, \delta^4(p+k-q) \Big[2Mw^{\mu\nu}_{\text{Fig. (3.9)}} + \text{other diagrams} \Big], \qquad (3.76)$$

$$2Mw^{\mu\nu}_{\text{Fig. (3.9)}} = \int \mathrm{d}^4p_1\, g\, \mathrm{Tr}^{D,C} \Big[\Phi^{+}_{A_l}(p,p_1) \gamma^\mu \overline{\Phi}(k) (i\gamma^- t_l) i \frac{-(\not{k} + \not{p}_1) + m}{(k+p_1)^2 - m^2 + i\epsilon} \gamma^\nu \Big]. \qquad (3.77)$$

In order to perform the integral over p_1^+ the denominator, $(k+p_1)^2 - m^2 + i\epsilon$, is again simplified into $2p_1^+k^- + i\epsilon$ (eikonal approximation). The integral over p_1^+ takes now the form

$$\int \mathrm{d}p_1^+ \, \frac{e^{ip_1^+(\eta-\xi)^-}}{2p_1^+k^- + i\epsilon} A_l^+(\eta) = \frac{-2\pi i}{2k^-} \theta(\xi^- - \eta^-) A_l^+(\eta). \qquad (3.78)$$

This illustrates that there is a contribution when $\eta^- \to -\infty$, but not when $\eta^- \to \infty$. The pole in p_1^+ is now on the other side of the real axis with respect to semi-inclusive DIS, leading to a gauge link via minus infinity. One finds for $2Mw^{\mu\nu}_{\text{Fig. (3.9)}}$

$$\begin{aligned}2Mw^{\mu\nu}_{\text{Fig. (3.9)}} &= \int \frac{\mathrm{d}^4\xi}{(2\pi)^4} e^{ip\xi} \langle P_1, S_1|\bar{\psi}(0)\gamma^\mu \bar{\Phi}(k)\gamma^\nu \\ &\times (-ig)\int_{-\infty}^{\xi^-} \mathrm{d}\eta^-\ A^+(\eta^-, \xi_T)\psi(\xi)|P_1, S_1\rangle_c \,(1 + \mathcal{O}(M/Q)) + \mathcal{O}(\bar{\Phi}_A), \end{aligned} \tag{3.79}$$

which is exactly the first order expansion of a gauge link via minus infinity, and an additional term, $\bar{\Phi}_A$, which gets canceled similarly as in semi-inclusive DIS.

We note here that via the coupling of gluons to an incoming parton we have derived a gauge link via minus infinity. This is similar to the gauge link for the fragmentation correlator which arose from coupling gluons to an incoming quark.

The subleading corrections are also very similar[6]. The complete result reads

$$\begin{aligned}2MW^{\mu\nu} = \frac{1}{3}\int \mathrm{d}^2p_T\ \mathrm{d}^2k_T\ \delta^2(p_T + k_T - q_T)\mathrm{Tr}^D\Bigg[&\Big[\Phi^{[-]}(x_1, p_T)\gamma^\mu\bar{\Phi}^{[-]}(x_2, k_T)\gamma^\nu\Big] \\ &+ \Big[\gamma_\alpha \frac{\not{n}_+}{Q\sqrt{2}}\gamma^\nu \Phi^{[-]\alpha}_{\partial^{-1}G}(x_1, p_T)\gamma^\mu \bar{\Phi}^{[-]}(x_2, k_T) \\ &\quad - \gamma^\alpha \frac{\not{n}_-}{Q\sqrt{2}}\gamma^\mu \bar{\Phi}^{[-]\alpha}_{\partial^{-1}G}(x_2, k_T)\gamma^\nu \Phi^{[-]}(x_1, p_T) + (\mu \leftrightarrow \nu)^*\Big]\Bigg] \\ \times \Big(1 + \mathcal{O}\big(M^2/Q^2\big) + \mathcal{O}(\alpha_S)\Big),&\end{aligned} \tag{3.80}$$

where $\Phi^\alpha_{\partial^{-1}G}$ was defined in Eq. 3.37 and (the contraction over color indices has been made explicit)

$$\begin{aligned}\bar{\Phi}^{[\pm]}_{ij}(x_2, k_T, P_2, S_2) &= \int \frac{\mathrm{d}^2\xi_T\ \mathrm{d}\xi^+}{(2\pi)^3} e^{-ik\xi} \\ &\times \langle P_2, S_2|\psi_{i,a}(\xi)\mathcal{L}^{[\pm]}_{ba}(0, \xi^+)\bar{\psi}_{j,b}(0)|P_2, S_2\rangle_c\Big|_{\substack{\xi^-=0 \\ p^-=x_2P_2^-}}\,, \end{aligned} \tag{3.81}$$

$$\bar{\Phi}^{[\pm]\alpha}_{\partial^{-1}G}(x_2, k_T, P_2, S_2) = \bar{\Phi}^{[\pm]\alpha}_{D,T}(x_2, k_T, P_2, S_2) + k_T^\alpha\ \bar{\Phi}^{[\pm]}(x_2, k_T, P_2, S_2), \tag{3.82}$$

$$\begin{aligned}\bar{\Phi}^{[\pm]\alpha}_{D,ij}(x_2, k_T, P_2, S_2) &= \int \frac{\mathrm{d}^2\xi_T\ \mathrm{d}\xi^+}{(2\pi)^3} e^{-ik\xi} \\ &\times \langle P_2, S_2|\Big[iD^\alpha_\xi \psi_i(\xi)\Big]_a \mathcal{L}^{[\pm]}_{ba}(0, \xi^+)\bar{\psi}_{j,b}(0)|P_2, S_2\rangle_c\Big|_{\substack{\xi^-=0 \\ p^-=x_2P_2^-}}\,. \end{aligned} \tag{3.83}$$

The hadronic tensor in Eq. 3.80 has been derived by employing the diagrammatic approach. Effects from instantons are for instance not included. Such effects could be relevant for the angular distribution of the lepton pair and have recently been studied by Boer, Brandenburg, Nachtmann, and Utermann [141].

---

[6] The two terms at subleading order appear opposite in sign. This sign difference comes from having a quark or antiquark propagator.

In order to make a connection with the Cartesian basis the external momenta are expressed as ($x_1 x_2 s = Q^2 + \mathcal{O}(M^2)$)

$$q = \frac{Q}{\sqrt{2}}\, e_- + \frac{Q}{\sqrt{2}}\, e_+, \tag{3.84}$$

$$P_1 = \frac{x_1 M_1^2 + \mathcal{O}(M_1^4/Q^4)}{Q\sqrt{2}}\, e_- + \frac{Q + \mathcal{O}(M_1^2/Q)}{x_1\sqrt{2}}\, e_+ + P_{1\perp}, \tag{3.85}$$

$$P_2 = \frac{Q + \mathcal{O}(M_2^2/Q)}{x_2\sqrt{2}}\, e_- + \frac{x_2 M_2^2 + \mathcal{O}(M_2^4/Q^4)}{Q\sqrt{2}}\, e_+ + P_{2\perp}. \tag{3.86}$$

Comparing these relations with Eq. 3.75, one can derive that (neglecting M^2/Q^2 corrections)

$$\begin{aligned} n_- &= e_- - \frac{q_{T\perp}}{Q\sqrt{2}}, \\ n_+ &= e_+ - \frac{q_{T\perp}}{Q\sqrt{2}}, \\ q_{T\perp} &= -2x_1 P_{1\perp} = -2x_2 P_{2\perp}. \end{aligned} \tag{3.87}$$

To express the hadronic tensor in the Cartesian basis the following identities can be used

$$\begin{aligned} \Phi^{[-]}_{\text{twist 2}}(x_1, p_T) &= \frac{\not n_+ \not n_-}{2} \Phi^{[-]}_{\text{twist 2}}(x_1, p_T) \frac{\not n_- \not n_+}{2} \\ &= \Bigg[\Phi^{[-]}_{\text{twist 2}}(x_1, p_{T\perp}) - \frac{\not q_{T\perp} \not e_-}{2\sqrt{2}Q} \Phi^{[-]}_{\text{twist 2}}(x_1, p_{T\perp}) \\ &\qquad - \Phi^{[-]}_{\text{twist 2}}(x_1, p_{T\perp}) \frac{\not e_- \not q_{T\perp}}{2\sqrt{2}Q} \Bigg]\Bigg|_{n_\pm \to e_\pm} + \mathcal{O}\left(M^2/Q^2\right), \end{aligned} \tag{3.88}$$

$$\begin{aligned} \bar{\Phi}^{[-]}_{\text{twist 2}}(x_2, k_T) &= \frac{\not n_- \not n_+}{2} \bar{\Phi}^{[-]}_{\text{twist 2}}(x_2, k_T) \frac{\not n_+ \not n_-}{2} \\ &= \Bigg[\bar{\Phi}^{[-]}_{\text{twist 2}}(x_2, k_{T\perp}) - \frac{\not q_{T\perp} \not e_+}{2\sqrt{2}Q} \bar{\Phi}^{[-]}_{\text{twist 2}}(x_2, k_{T\perp}) \\ &\qquad - \bar{\Phi}^{[-]}_{\text{twist 2}}(x_2, k_{T\perp}) \frac{\not e_+ \not q_{T\perp}}{2\sqrt{2}Q} \Bigg]\Bigg|_{n_\pm \to e_\pm} + \mathcal{O}\left(M^2/Q^2\right). \end{aligned} \tag{3.89}$$

This yields for the hadronic tensor [35]

$$
\begin{aligned}
2MW^{\mu\nu} = {} & \frac{1}{3}\int \mathrm{d}^2p_T\;\mathrm{d}^2k_T\;\delta^2(p_{T\perp}+k_{T\perp}-q_{T\perp})\,\mathrm{Tr}^D\bigg[\Big[\Phi^{[-]}(x_1,p_{T\perp})\gamma^\mu\bar{\Phi}^{[-]}(x_2,k_{T\perp})\gamma^\nu\Big] \\
& +\Big[-\frac{\not{p}_{T\perp}\not{e}_-}{2\sqrt{2}Q}\Phi^{[-]}(x_1,p_{T\perp})\gamma^\mu\bar{\Phi}^{[-]}(x_2,k_{T\perp}\gamma^\nu-\frac{\not{k}_{T\perp}\not{e}_-}{2\sqrt{2}Q}\Phi^{[-]}(x_1,p_{T\perp})\gamma^\mu\bar{\Phi}^{[-]}(x_2,k_{T\perp})\gamma^\nu \\
& -\Phi^{[-]}(x_1,p_{T\perp})\gamma^\mu\bar{\Phi}^{[-]}(x_2,k_{T\perp})\frac{\not{e}_+\not{k}_{T\perp}}{2\sqrt{2}Q}\gamma^\nu-\Phi^{[-]}(x_1,p_{T\perp})\gamma^\mu\bar{\Phi}^{[-]}(x_2,k_{T\perp})\frac{\not{e}_+\not{p}_{T\perp}}{2\sqrt{2}Q}\gamma^\nu \\
& +\frac{\gamma_\alpha\not{e}_+}{Q\sqrt{2}}\gamma^\nu\Phi^{[-]\alpha}_{\partial^{-1}G}(x_1,p_{T\perp})\gamma^\mu\bar{\Phi}^{[-]}(x_2,k_{T\perp})-\frac{\gamma_\alpha\not{e}_-}{Q\sqrt{2}}\gamma^\mu\bar{\Phi}^{[-]\alpha}_{\partial^{-1}G}(x_2,k_{T\perp})\gamma^\nu\Phi^{[-]}(x_1,p_{T\perp}) \\
& +(\mu\leftrightarrow\nu)^*\Big]\bigg]\Big(1+\mathcal{O}\big(M^2/Q^2\big)+\mathcal{O}(\alpha_S)\Big)\bigg|_{n_\pm\to e_\pm}\,. \qquad (3.90)
\end{aligned}
$$

the hadronic tensor for Drell-Yan
in the Cartesian basis including M/Q corrections

In the parametrizations of the correlators, which are $n_\pm$-dependent, the $n_\pm$ are replaced by $e_\pm$ (that is where $|_{n_\pm\to e_\pm}$ stands for). The functions in the parametrizations depend on x_1,$p_{T\perp}^2$ or x_2,$k_{T\perp}^2$. Integrated and weighted hadronic tensors are given in appendix 3.A

The above result for the hadronic tensor is similar to the leading order result of Ralston, Soper [44]. The only actual difference is the presence of gauge links in the parton distributions. The Drell-Yan process can be studied experimentally at RHIC [142] and by the proposed PAX-experiment at GSI. This has recently generated several theoretical studies [124, 141, 143, 144, 145].

3.4 Semi-inclusive electron-positron annihilation

For electron-positron annihilation the calculation is also very similar. By including the possible gluon insertions on the outgoing partons one obtains gauge links which are running via plus infinity.

The calculation is set up by choosing the light-like vectors ($\{n_+,n_-\}$ with $n_-\sim\bar{n}_+$ and $n_-\cdot n_+=1$) such that

$$
\begin{aligned}
P_{h_2} &= \frac{M_{h_2}^2}{z_2Q\sqrt{2}}n_-+\frac{z_2Q}{\sqrt{2}}n_+, \\
P_{h_1} &= \frac{z_1Q}{\sqrt{2}}n_-+\frac{M_{h_1}^2}{z_1Q\sqrt{2}}n_+, \\
q &= \frac{Q+\mathcal{O}(M^3/Q)}{\sqrt{2}}n_-+\frac{Q+\mathcal{O}(M^3/Q)}{\sqrt{2}}n_++q_T. \qquad (3.91)
\end{aligned}
$$

Sudakov-decomposition for electron-positron annihilation

The complete result for the hadronic tensor reads (suppressing arguments connected to parent hadrons)

$$\begin{aligned}2MW^{\mu\nu} = 3\int \mathrm{d}^2p_T\ \mathrm{d}^2k_T\ \delta^2(p_T+k_T-q_T)\,\mathrm{Tr}^D \Bigg[&\Big[\Delta^{[-]}(z_1^{-1},p_T)\gamma^\nu\overline{\Delta}^{[-]}(z_2^{-1},k_T)\gamma^\mu\Big]\\ &+\Big[\gamma_\alpha\frac{\not{n}_-}{Q\sqrt{2}}\gamma^\mu\Delta^{[-]\alpha}_{\partial^{-1}G}(z_1^{-1},p_T)\gamma^\nu\overline{\Delta}^{[-]}(z_2^{-1},k_T)\\ &-\gamma^\alpha\frac{\not{n}_+}{Q\sqrt{2}}\gamma^\nu\overline{\Delta}^{[-]\alpha}_{\partial^{-1}G}(z_2^{-1},k_T)\gamma^\mu\Delta^{[-]}(z_1^{-1},p_T)\\ &+(\mu\leftrightarrow\nu)^*\Big]\Bigg]\Big(1+\mathcal{O}\big(M^2/Q^2\big)+\mathcal{O}(\alpha_S)\Big),\end{aligned} \tag{3.92}$$

where $\Delta^{[-]\alpha}_{\partial^{-1}G}$ was defined in Eq. 3.43 and

$$\begin{aligned}&\overline{\Delta}^{[\pm]}_{ij}(z^{-1},k_T,P_h,S_h)\\ &\quad\equiv\frac{1}{3}\sum_X\int\frac{\mathrm{d}^3\mathbf{P}_X}{(2\pi)^3 2E_{\mathbf{P}_X}}\int\frac{\mathrm{d}^2\eta_T\ \mathrm{d}\eta^-}{(2\pi)^3}e^{-ik\eta}\langle\Omega|\overline{\psi}_j(0)\mathcal{L}^{0_T,\,\eta^+}(0^-,\pm\infty^-)|P_X;P_h,S_h\rangle_{\mathrm{out,c}}\\ &\qquad\times{}_{\mathrm{out}}\langle P_X;P_h,S_h|\mathcal{L}^{\pm\infty^-,\,\eta^+}(0_T,\eta_T)\mathcal{L}^{\eta_T,\,\eta^+}(\pm\infty^-,\eta^-)\psi_i(\eta)|\Omega\rangle_{\mathrm{c}}\Big|_{\substack{\eta^+=0\\ k^+=z^{-1}P_h^+}},\end{aligned} \tag{3.93}$$

$$\overline{\Delta}^{[\pm]\alpha}_{\partial^{-1}G}(z^{-1},k_T,P_h,S_h)\equiv\overline{\Delta}^{[\pm]\alpha}_{D,T}(z^{-1},k_T,P_h,S_h)+k_T^\alpha\ \overline{\Delta}^{[\pm]}(z^{-1},k_T,P_h,S_h), \tag{3.94}$$

$$\begin{aligned}&\overline{\Delta}^{[\pm]\alpha}_{D,ij}(z^{-1},k_T,P_h,S_h)\\ &\quad\equiv\frac{1}{3}\sum_X\int\frac{\mathrm{d}^3\mathbf{P}_X}{(2\pi)^3 2E_{\mathbf{P}_X}}\int\frac{\mathrm{d}^2\eta_T\ \mathrm{d}\eta^+}{(2\pi)^3}e^{-ik\eta}\langle\Omega|\overline{\psi}_j(0)\mathcal{L}^{0_T,\,\eta^+}(0^-,\pm\infty^-)|P_h,S_h\rangle_{\mathrm{out,c}}\\ &\qquad\times{}_{\mathrm{out}}\langle P_h,S_h|\mathcal{L}^{\pm\infty^-,\,\eta^+}(0_T,\eta_T)\mathcal{L}^{\eta_T,\,\eta^+}(\pm\infty^-,\eta^-)iD^\alpha_\eta\psi_i(\eta)|\Omega\rangle_{\mathrm{c}}\Big|_{\substack{\eta^+=0\\ k^+=z^{-1}P_h^+}},\end{aligned} \tag{3.95}$$

The external momenta in the Cartesian basis read

$$q=\frac{Q}{\sqrt{2}}e_-+\frac{Q}{\sqrt{2}}e_+, \tag{3.96}$$

$$P_{h_2}=\frac{M_{h_2}^2+\mathcal{O}(M_{h_2}^4/Q^2)}{z_2Q\sqrt{2}}\ e_-+\frac{z_2Q+\mathcal{O}(M_{h_2}^2/Q)}{\sqrt{2}}\ e_+, \tag{3.97}$$

$$P_{h_1}=\frac{z_1Q+\mathcal{O}(M_{h_1}^2/Q)}{\sqrt{2}}\ e_-+\frac{M_{h_1}^2+\mathcal{O}(M_{h_1}^4/Q^2)}{z_1Q\sqrt{2}}\ e_++P_{h_1\perp}, \tag{3.98}$$

giving the relations (neglecting M^2/Q^2 corrections)

$$n_- = e_- - \frac{\sqrt{2}\, q_{T\perp}}{Q}, \qquad n_+ = e_+, \qquad q_{T\perp} = -P_{h_1\perp}/z_1. \tag{3.99}$$

Using the following identities to express the hadronic tensor in the Cartesian basis

$$\begin{aligned}\Delta^{[-]}_{\text{twist }2}(z_1^{-1}, p_T) &= \frac{\not{n}_-\not{n}_+}{2}\Delta^{[-]}_{\text{twist }2}(z_1^{-1}, p_T)\frac{\not{n}_+\not{n}_-}{2}\\ &= \bigg[\Delta^{[-]}_{\text{twist }2}(z_1^{-1}, p_{T\perp}) - \frac{\not{q}_{T\perp}\not{e}_+}{\sqrt{2}Q}\Delta^{[-]}_{\text{twist }2}(z_1^{-1}, p_{T\perp})\\ &\quad - \Delta^{[-]}_{\text{twist }2}(z_1^{-1}, p_{T\perp})\frac{\not{e}_+\not{q}_{T\perp}}{\sqrt{2}Q}\bigg]\bigg|_{n_\pm\to e_\pm} + \mathcal{O}\Big(M^2/Q^2\Big), \end{aligned} \tag{3.100}$$

$$\begin{aligned}\overline{\Delta}^{[-]}_{\text{twist }2}(z_2^{-1}, k_T) &= \frac{\not{n}_+\not{n}_-}{2}\overline{\Delta}^{[-]}_{\text{twist }2}(z_2^{-1}, k_T)\frac{\not{n}_-\not{n}_+}{2}\\ &= \overline{\Delta}^{[-]}_{\text{twist }2}(z_2^{-1}, k_{T\perp})\Big|_{n_\pm\to e_\pm} + \mathcal{O}\Big(M^2/Q^2\Big), \end{aligned} \tag{3.101}$$

one finds [35]

$$\begin{aligned}2MW^{\mu\nu} = 3\int \mathrm{d}^2p_T\, \mathrm{d}^2k_T\, \delta^2(p_{T\perp} + k_{T\perp} + P_{h_1\perp}/z_1)\bigg[\, &\mathrm{Tr}^D\Big[\Delta^{[+]}(z_1^{-1}, p_{T\perp})\gamma^\nu\overline{\Delta}^{[+]}(z_2^{-1}, k_{T\perp})\gamma^\mu\Big]\\ + \bigg[-&\tfrac{\not{p}_{T\perp}\not{e}_+}{Q\sqrt{2}}\Delta^{[+]}(z_1^{-1}, p_{T\perp})\gamma^\nu\overline{\Delta}^{[+]}(z_2^{-1}, k_{T\perp})\gamma^\mu - \tfrac{\not{k}_{T\perp}\not{e}_+}{Q\sqrt{2}}\Delta^{[+]}(z_1^{-1}, p_{T\perp})\gamma^\nu\overline{\Delta}^{[+]}(z_2^{-1}, k_{T\perp})\gamma^\mu\\ + &\tfrac{\gamma_\alpha\not{e}_-}{Q\sqrt{2}}\gamma^\mu\Delta^{[+]\alpha}_{\partial^{-1}G}(z_1^{-1}, p_{T\perp})\gamma^\nu\overline{\Delta}^{[+]}(z_2^{-1}, k_{T\perp}) - \tfrac{\gamma_\alpha\not{e}_+}{Q\sqrt{2}}\gamma^\nu\overline{\Delta}^{[+]\alpha}_{\partial^{-1}G}(z_1^{-1}, k_{T\perp})\gamma^\mu\Delta^{[+]}(z_1^{-1}, p_{T\perp})\\ + &(\mu\leftrightarrow\nu)^*\bigg]\bigg]\Big(1 + \mathcal{O}\Big(M^2/Q^2\Big) + \mathcal{O}(\alpha_S)\Big)\bigg|_{n_\pm\to e_\pm}. \end{aligned} \tag{3.102}$$

hadronic tensor for electron-positron annihilation
including next-to-leading order in M/Q

The integrated and weighted hadronic tensors are given in appendix 3.A.

Subleading order effects in electron-positron annihilation have already been studied by Boer, Jakob, and Mulders in Ref. [103]. The only real difference of the above result with Ref. [103] is that the fragmentation functions contain here a fully closed gauge link.

3.5 Fragmentation and universality

In transverse momentum dependent correlators we encountered gauge links via plus or minus infinity. In subsection 2.6.2 we found that due to the possible interplay between the two mechanisms for T-odd effects (the gauge link and final-state interactions) , it is

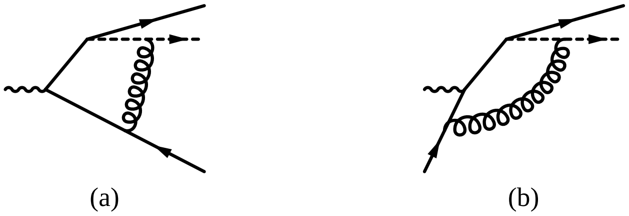

Figure 3.10: Two typical diagrams which appear in model calculations and produce T-odd effects. Diagram (a) appears in electron-positron annihilation and diagram (b) appears in semi-inclusive DIS. The dashed-lines represent some kind of particle (for instance a scalar diquark).

not possible to relate those correlators which have different link structures. However, if one of the mechanisms turns out to be absent or heavily suppressed, then relations between fragmentation functions having different gauge links can be derived.

In 2002, an article written by Metz [100] appeared in which universality of fragmentation was argued. In that paper the effect of the gauge link is modeled through a set of diagrams in semi-inclusive DIS and electron-positron annihilation, see Fig. 3.10. Within the model it is found that the Collins function appears with the same sign in both processes. In order to achieve this result the momentum in the loop in Fig. 3.10 is not integrated over the full integration domain. This restriction is justified to make the model consistent with the parton model but also makes it unclear whether the universality result still holds if this restriction is lifted.

The result of Ref. [100] was formalized in a subsequent paper by Collins and Metz [101] in which it is claimed that the gauge link is taken into account. Having similar diagrams as in Fig. 3.10, the authors *eikonalize* the quark-propagator next to the exchanged gluon, meaning that its transverse momentum is assumed to be small. This procedure is similar to the restriction made in Ref. [100] because it effectively limits the integration domain over the momenta. When comparing the two processes, it was found in Ref. [101] that the pole of the eikonal propagator does not contribute[7] in the cross section and consequently the difference between the processes vanishes[8]. According to the authors this shows that fragmentation functions are universal in QCD.

A first comment on both papers is that restricting the integration domain of the momenta in the loop makes the interesting result less rigorous. It is not clear whether the obtained result finds its origin in the analytical properties of Feynman diagrams or whether it results from the applied restriction. Secondly, it is not clear whether the presence of vertices, through which the production of hadrons from quarks is modeled (like the quark-hadron-diquark vertex), introduce additional analytical structures which might be the origin for the result.

---

[7] Gamberg, Goldstein, and Oganessyan find in Ref. [146] in a slightly different formulation that the eikonal pole does contribute in T-odd effects, giving a sign dependent fragmentation function if only the gauge link is considered (no final-state interactions). This result has been challenged by Amrath, Bacchetta, and Metz in Ref. [125]. However, if the result of Ref. [146] holds then, together with the final-state interactions, this model would illustrate the universality problems with fragmentation.

[8] After a single momentum integration all poles fall on one side of the real axis. This allows one to close the contour on the other side of this axis and one finds that the difference between the processes vanishes.

When comparing the results of Ref. [101] with the analyses in this thesis one observes several differences. For instance, the eikonal pole turns out not to contribute in the analysis of Ref. [101] while we found in subsection 3.2.1 that this pole leads to the gauge link. In addition, the diagrams in Fig 3.10, which should give the effect of the gauge link (although not proven in Ref. [101]), give the same sign for T-odd functions in both processes. This is in contrast with the analysis in subsection 2.6.2 where it was found that there should be a sign-difference if final-state interactions were to be absent. From that point of view the effect of the diagrams in Fig 3.10 should be considered as a final-state interaction and not as an effect of the gauge link.

The idea of not having a gauge link in the fragmentation functions is by itself interesting. Fragmentation functions are defined through matrix elements involving the vacuum which is invariant under translations. It might be possible to use that property to show that fragmentation functions are already gauge invariant without the presence of a gauge link. If a gauge link is not needed to establish gauge invariant fragmentation correlators then the derived gauge link in fragmentation functions for semi-inclusive DIS and electron-positron annihilation might not influence the expectation value of the matrix elements. If this turns out be true then this would make the fragmentation functions sign-independent universal which would also explain the results obtained in Ref. [101]. In addition, in that case the Lorentz-invariance relations for fragmentation functions might be valid as well (see also the discussion in subsection 2.5.2).

Summarizing, the arguments in Ref. [101] lead to an interesting result although several issues need clarification. Another point we discussed was that gauge links might not be relevant for defining gauge invariant fragmentation functions. This could allow for a nonperturbative proof of universality of fragmentation. Experimental and theoretical studies on universality of fragmentation are recommended.

3.6 Deeply virtual Compton scattering

Up to now we derived in this chapter the gauge links in the unintegrated correlators for various high-energy scattering processes. In all these processes interactions between the correlators and the hard diagram were included in the form of gluon-lines. These gluons coupled to external quarks (or fields) on which the equations of motion were applied to derive the gauge links. Studying a different kind of process in which gluons are coupled to internal instead of external partons is therefore interesting. The process studied in this section is deeply virtual Compton scattering (DVCS). Although the gauge link in this process has been derived in several ways and is perfectly known, the method which

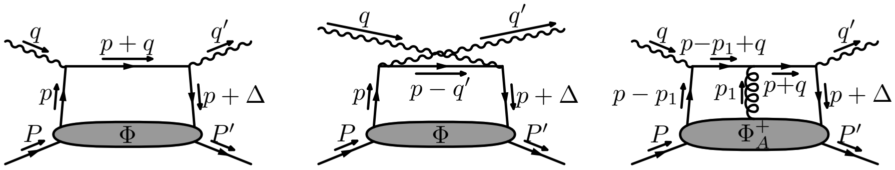

(a) (b) (c)

Figure 3.11: Various contributions in DVCS.

was applied in previous sections seems not to be presented for DVCS in the literature. After some introductory remarks that calculation will be presented here to illustrate the consistency of the applied approach. Note that in this section the considered diagrams are amplitude diagrams.

In the DVCS-process an electron scatters, via the exchange of a virtual photon, off a hadron, giving, besides the production of a physical photon, the hadron a momentum change Δ (with $\Delta^2 \sim -M^2$). This process gained significant popularity after Ji showed its connection with quark angular momentum [147, 148, 149]. Together with the intrinsic spin of the quarks, this provides indirect access to the quark orbital angular momentum as well. Besides the contributions of Ji considerable progress has been made by many others. For an overview and introduction the reader is referred to Goeke, Polyakov, Vanderhaeghen [150], Diehl [151], and Belitsky, Radyushkin [152].

In order to describe the DVCS-process the diagrammatic approach can be employed. We will slightly deviate from the more common notations of DVCS in order to follow the notations of this thesis. Restricting to the lowest order in g, α_S, and $\alpha_{\text{e.m.}}$, there are two contributions to the amplitude which are represented in Fig. 3.11a and Fig. 3.11b. They are given by

$$i\mathcal{M} = \bar{u}(k',\lambda')\gamma_\nu u(k,\lambda)\frac{-i(-ie)(iQ_f e)^2}{q^2}(q')(i)T^{\nu\mu}\epsilon_\mu(q'), \tag{3.103}$$

$$\begin{aligned} T^{\nu\mu} = (i)\int \mathrm{d}^4p\ \mathrm{Tr}^D[\Phi(p,P,P')\gamma^\mu i\frac{\not{p}+\not{q}+m}{(p+q)^2+i\epsilon}\gamma^\nu \\ +\Phi(p,P,P')\gamma^\nu i\frac{\not{p}-\not{q}'+m}{(p-q')^2+i\epsilon}\gamma^\mu] + \mathcal{O}(g), \end{aligned} \tag{3.104}$$

where $\Phi(p,P,P')$ is now an off-forward correlator defined as

$$\Phi_{ij}(p,P,P') \equiv \int \frac{\mathrm{d}^4\xi}{(2\pi)^4} e^{ip\xi}\, {}_{\text{out}}\langle P',S'|\,\bar{\psi}_j(0)\,\psi_i(\xi)\,|P,S\rangle_{\text{in,c}}. \tag{3.105}$$

In the above definition the spin-labels of the hadrons and color indices of the quark-fields have been suppressed.

Introducing a Sudakov-decomposition to facilitate the expansion in M/Q

$$P \equiv \frac{xM^2}{Q\sqrt{2}}n_- + \frac{Q}{x\sqrt{2}}n_+, \qquad q \equiv \frac{Q}{\sqrt{2}}n_- - \frac{Q}{\sqrt{2}}n_+, \tag{3.106}$$

$$g_\perp^{\mu\nu} \equiv g^{\mu\nu} - n_+^\mu n_-^\nu - n_+^\nu n_-^\mu, \qquad \epsilon_\perp^{\mu\nu} \equiv \epsilon^{\rho\sigma\mu\nu} n_{+\rho} n_{-\sigma}, \tag{3.107}$$

where $x = x_B + O\left(M^2/Q^2\right)$, and restricting us to $\Delta^+ \sim Q$ and $\Delta_\perp^2 \sim -M^2$, one obtains in leading order in M/Q (applying also a Fierz-decomposition)

$$T^{\nu\mu} = \left[T^{\nu\mu}_{\text{Fig. (3.11)}a} + T^{\nu\mu}_{\text{Fig. (3.11)}b}\right]\left[1 + O(M/Q)\right] + O(g), \tag{3.108}$$

$$T^{\nu\mu}_{\text{Fig. (3.11)}a} = \int \mathrm{d}p^+ \, \frac{1}{p^+ + q^+ + i\epsilon}\left(g_\perp^{\nu\mu} F(p^+) + (i)\epsilon_\perp^{\nu\mu}\tilde{F}(p^+)\right), \tag{3.109}$$

$$T^{\nu\mu}_{\text{Fig. (3.11)}b} = \int \mathrm{d}p^+ \, \frac{1}{p^+ - q^+ + \Delta^+ - i\epsilon}\left(g_\perp^{\nu\mu} F(p^+) - (i)\epsilon_\perp^{\nu\mu}\tilde{F}(p^+)\right), \tag{3.110}$$

where

$$F(p^+) = \frac{1}{2}\int \frac{\mathrm{d}\xi^-}{2\pi} e^{ip^+\xi^-} {}_{\text{out}}\langle P'|\bar{\psi}(0)\gamma^+\psi(\xi^-)|P\rangle_{\text{in,c}}, \tag{3.111}$$

$$\tilde{F}(p^+) = \frac{1}{2}\int \frac{\mathrm{d}\xi^-}{2\pi} e^{ip^+\xi^-} {}_{\text{out}}\langle P'|\bar{\psi}(0)\gamma^+\gamma_5\psi(\xi^-)|P\rangle_{\text{in,c}}. \tag{3.112}$$

amplitude for DVCS in leading order in M/Q

Since all the correlators are on the light-cone the only other possible leading contributions come from the resummation of A^+-gluons. The above result is therefore complete in the light-cone gauge (to all orders in g) at leading order in M/Q and corresponds to the result obtained by Ji in Ref. [148]. Assuming the expression for the cross section to be gauge invariant leads to a straight gauge link in a covariant gauge between the two quark-fields in the correlators F and $\tilde{F}$ above. These correlators can be parametrized into functions (generalized parton distribution functions) which can be measured in experiments or be predicted by theory.

Instead of assuming the cross section to be gauge invariant we will consider now a covariant gauge and derive the gauge link by including the longitudinally polarized gluons explicitly. The insertion of a single gluon, connecting the correlator and the hard part (see Fig. 3.11c), contributes to the amplitude as

$$T^{\nu\mu} = T^{\nu\mu}_{\text{Fig. (3.11)}c} + \text{other diagrams}, \tag{3.113}$$

$$\begin{aligned} T^{\nu\mu}_{\text{Fig. (3.11)}c} = (i)\int \mathrm{d}^4p \, \mathrm{d}^4p_1 \; \mathrm{Tr}^{D,C}\Big[&\Phi^+_{A_l}(p,p_1,P,P')\gamma^\mu i\frac{\not{p}+\not{q}+m}{(p+q)^2 - m^2 + i\epsilon} \\ &\times (ig\gamma^- t_l) i\frac{\not{p}-\not{p}_1+\not{q}+m}{(p-p_1+q)^2 - m^2 + i\epsilon}\gamma^\nu\Big], \end{aligned} \tag{3.114}$$

where

$$\Phi_{A_l{}^+_{ij}}(p, p_1, P, P') \equiv \int \frac{\mathrm{d}^4\xi\, \mathrm{d}^4\eta}{(2\pi)^8} e^{ip\xi} e^{ip_1(\eta-\xi)} {}_{\mathrm{out}}\langle P'|\, \bar{\psi}_j(0)\, A_l^+(\eta)\, \psi_i(\xi)\, |P\rangle_{\mathrm{in,c}}. \tag{3.115}$$

Analyzing the p_1^+-dependence of Eq. 3.114 and making the parton model assumptions one finds a pole at $p_1^+ \approx p^+ + q^+ \neq 0$. Calculating the integral over p_1^+ by taking the residue one finds

$$\begin{aligned} T^{\nu\mu}_{\mathrm{Fig.\ (3.11)}c} = (i) \int \mathrm{d}p^+\, \frac{\mathrm{d}\xi^-}{2\pi} e^{-iq^+\xi^-} {}_{\mathrm{out}}\langle P'|\bar{\psi}(0)\gamma^\mu(i) \frac{q^-\gamma^+}{2q^-(p^+ + q^+) + i\epsilon} \\ \times (-i) \int_\infty^{\xi^-} \mathrm{d}\eta^-\, A^+(\eta^-) e^{i(p^+ + q^+)\eta^-} \gamma^\nu \psi(\xi^-)|P\rangle_{\mathrm{in,c}} \,(1 + \mathcal{O}(M/Q))\,. \end{aligned} \tag{3.116}$$

We see in the above expression that the first order expansion of the gauge link runs between ∞ and ξ^- instead of between 0 and ξ^-. When evaluating the p^+-integral one obtains the Heaviside function $\theta(-\eta^-)$. From the two conditions, $\infty > \eta^- > \xi^-$ and $0 > \eta^-$, it turns out that of the gauge link only the part between ξ^- and 0 remains. This result can be rewritten as follows

$$\begin{aligned} T^{\nu\mu}_{\mathrm{Fig.\ (3.11)}c} = \int \mathrm{d}p^+\, \frac{1}{p^+ + q^+ + i\epsilon}\, \frac{1}{2} \int \frac{\mathrm{d}\xi^-}{2\pi} e^{ip^+\xi^-} \\ \times \Bigg(g_\perp^{\nu\mu}\, {}_{\mathrm{out}}\langle P'|\bar{\psi}(0)\gamma^+(-i) \int_0^{\xi^-} \mathrm{d}\eta^-\, A^+(\eta^-)\psi(\xi^-)|P\rangle_{\mathrm{in,c}} \\ + (i)\epsilon_\perp^{\nu\mu}\, {}_{\mathrm{out}}\langle P'|\bar{\psi}(0)\gamma^+\gamma_5(-i) \int_0^{\xi^-} \mathrm{d}\eta^-\, A^+(\eta^-)\psi(\xi^-)|P\rangle_{\mathrm{in,c}} \Bigg) \\ \times (1 + \mathcal{O}(M/Q))\,. \end{aligned} \tag{3.117}$$

The equation above is a copy of Eq. 3.109 including the first order gauge link expansion.

Although the momentum of the gluon-line did not vanish (no pole at $p_1^+ = 0$), the procedure of including longitudinally polarized gluons from the correlator as illustrated here still provides the gauge link. The presented calculation can be straightforwardly generalized to all orders in g. In leading order in M/Q one obtains Eq. 3.110 and the matrix elements in Eq. 3.111 and Eq. 3.112 containing the path-ordered exponentials.

3.7 Summary and conclusions

The diagrammatic approach was applied to various scattering processes. Following the ideas of Boer, Mulders, Tangerman [114, 115], and Belitsky, Ji, Yuan [26], we assumed factorization for the correlators and produced the leading order in α_S cross section for semi-inclusive DIS, electron-positron annihilation, and Drell-Yan. In Ref. [115] cross sections were obtained by choosing effectively the $A^+ + A^- = 0$ gauge, leaving only the A_T-fields from the correlators to consider. That result, which includes subleading order corrections in M/Q, was studied in Ref. [114] in more detail by considering the $A^- = 0$ gauge. In that gauge longitudinally polarized gluons between the correlators and the elementary scattering diagram need to be considered as well. In Ref. [114] they were explicitly calculated to order g^2 of which the result was generalized to all orders in g by using Ward identities. Afterwards it was pointed out in Ref. [26] that there is an additional contribution which was not identified before (the transverse gauge link). The theoretical description was here extended by including all leading order α_S corrections and including M/Q corrections. The obtained result is similar to the results of Ref. [115] except that T-odd distribution functions are now also included and the approach is fully color gauge invariant.

The hadronic tensors were expressed in gauge invariant correlators containing gauge links. These gauge links arise from including leading-order-α_S-interactions which consist of gluons interacting between correlators and the elementary scattering diagram. The paths of these gauge links run via plus infinity if the gluons are coupled to an outgoing parton, and via minus infinity if the gluons are coupled to an incoming parton. Following the same approach we also considered the DVCS-process in which gluons couple to internal parton-lines. The path of the obtained gauge link for this process is just a straight line between the two quark-fields as also encountered in DIS.

Using the expressions for the hadronic tensor in semi-inclusive DIS, some explicit asymmetries were derived. One of the more interesting asymmetries is the beam-spin asymmetry for jet-production in DIS, which is proportional to the distribution function $g^\perp$. This function was discussed in chapter 2 and originates from the directional dependence of the gauge link. Whether or not such functions are really non-vanishing is at present an open question. Its measurement would contribute to the understanding of the theoretical description.

In the second part of this chapter, it was pointed out that the interesting arguments for universality of fragmentation as given in Collins, Metz [101] contain some issues which need clarification. Therefore, the difference in paths of the gauge links in the fragmentation functions appearing in semi-inclusive DIS and electron-positron annihilation could lead to different fragmentation functions for the two processes. This might create a problem for extracting transversity via the Collins effect. Alternative ways to access transversity, besides Drell-Yan, are for instance J/ψ production in pp-scattering [153], and via interference fragmentation functions [154, 155, 156, 157] (in which the nonlocality of the operators is light-like).

3.A Hadronic tensors

Based on Ref. [35] some hadronic tensors will be given. Contributions from antiquarks can be included by interchanging q with $-q$ and μ with ν. The following definitions were used (suppressing arguments of parent hadrons):

$$\begin{aligned}
\Phi_{\partial}^{[\pm]\alpha}(x) &= \int \mathrm{d}^2 p_T \;\; p_T^{\alpha}\, \Phi^{[\pm]}(x, p_T), & \bar{\Phi}_{\partial}^{[\pm]\alpha}(x) &= -\int \mathrm{d}^2 p_T \;\; p_T^{\alpha}\, \bar{\Phi}^{[\pm]}(x, p_T),\\
\Delta_{\partial}^{[\pm]\alpha}(z^{-1}) &= \int \mathrm{d}^2 k_T \;\; k_T^{\alpha}\, \Delta^{[\pm]}(z^{-1}, k_T), & \bar{\Delta}_{\partial}^{[\pm]\alpha}(z^{-1}) &= -\int \mathrm{d}^2 k_T \;\; k_T^{\alpha}\, \bar{\Delta}^{[\pm]}(z^{-1}, k_T),\\
\Phi_{D}^{\alpha}(x) &= \int \mathrm{d}^2 p_T \; \Phi_{D}^{[\pm]\alpha}(x, p_T), & \bar{\Phi}_{D}^{\alpha}(x) &= \int \mathrm{d}^2 p_T \; \bar{\Phi}_{D}^{[\pm]\alpha}(x, p_T),\\
\Delta_{D}^{\alpha}(z^{-1}) &= \int \mathrm{d}^2 k_T \; \Delta_{D}^{[\pm]\alpha}(z^{-1}, k_T), & \bar{\Delta}_{D}^{\alpha}(z^{-1}) &= \int \mathrm{d}^2 k_T \; \bar{\Delta}_{D}^{[\pm]\alpha}(z^{-1}, k_T).
\end{aligned} \tag{3.118}$$

Semi-inclusive DIS

The translation of Eq. 3.46 into the Cartesian basis is similar as was done for semi-inclusive electron-positron annihilation or Drell-Yan (see Ref. [35] for details). The unintegrated hadronic tensor reads

$$\begin{aligned}
2MW^{\mu\nu} = \int & \mathrm{d}^2 p_T \, \mathrm{d}^2 k_T \; \delta^2(p_{T\perp} - P_{h\perp}/z - k_{T\perp})\, \mathrm{Tr}^D \Big[\Big(\Phi(x_B, p_{T\perp}) \gamma^{\mu} \Delta(z_1^{-1}, k_{T\perp}) \gamma^{\nu} \Big) \\
& + \Big(\Phi(x_B, p_{T\perp}) \gamma^{\mu} \tfrac{\not{p}_{T\perp} \not{e}_+}{Q\sqrt{2}} \Delta(z_1^{-1}, k_{T\perp}) \gamma^{\nu} - \Phi(x_B, p_{T\perp}) \gamma^{\mu} \tfrac{\not{k}_{T\perp} \not{e}_+}{Q\sqrt{2}} \Delta(z_1^{-1}, k_{T\perp}) \gamma^{\nu} \\
& - \tfrac{\gamma_{\alpha} \not{e}_+}{Q\sqrt{2}} \gamma^{\nu} \Phi_{\partial^{-1}G}^{[+]\alpha}(x_B, p_{T\perp}) \gamma^{\mu} \Delta^{[-]}(z^{-1}, k_{T\perp}) - \Delta_{\partial^{-1}G}^{[+]\alpha}(z^{-1}, k_{T\perp}) \gamma^{\nu} \Phi^{[+]}(x_B, p_{T\perp}) \tfrac{\gamma_{\alpha} \not{e}_-}{Q\sqrt{2}} \gamma^{\mu} \\
& + (\mu \leftrightarrow \nu)^* \Big) \Big] \Big(1 + \mathcal{O}\Big(M^2/Q^2 \Big) + \mathcal{O}(\alpha_S) \Big) \Big|_{n_{\pm} \to e_{\pm}} .
\end{aligned} \tag{3.119}$$

The integrated hadronic tensor reads (employing Eq. 3.38 and Eq. 3.44)

$$\begin{aligned}
\int \mathrm{d}^2 P_{h\perp} \; 2MW^{\mu\nu} = & z^2 \, \mathrm{Tr}^D \Big[\Phi(x_B) \gamma^{\mu} \Delta(z^{-1}) \gamma^{\nu} \\
& + \Big(\frac{\not{e}_+ \gamma_{\alpha}}{Q\sqrt{2}} \gamma^{\nu} \Phi_D^{\alpha}(x_B) \gamma^{\mu} \Delta(z^{-1}) + \frac{\not{e}_- \gamma_{\alpha}}{Q\sqrt{2}} \gamma^{\mu} \Delta_D^{\alpha}(z^{-1}) \gamma^{\nu} \Phi(x_B) \\
& - \frac{\not{e}_- \gamma_{\alpha}}{Q\sqrt{2}} \gamma^{\mu} \Delta_{\partial}^{[-]}(z^{-1}) \gamma^{\nu} \Phi(x_B) - \gamma^{\mu} \frac{\gamma_{\alpha} \not{e}_+}{Q\sqrt{2}} \Delta_{\partial}^{[-]\alpha}(z^{-1}) \gamma^{\nu} \Phi(x_B) \\
& + (\mu \leftrightarrow \nu)^* \Big) \Big] \Big(1 + \mathcal{O}\Big(M^2/Q^2 \Big) + \mathcal{O}(\alpha_S) \Big) \Big|_{n_{\pm} \to e_{\pm}} .
\end{aligned} \tag{3.120}$$

The single weighted hadronic tensor reads

$$\begin{aligned}
\int \mathrm{d}^2 P_{h\perp} \; P_{h\perp}^{\alpha} \; 2MW^{\mu\nu} = & \; z^3 \, \mathrm{Tr}^D \Big[- \Phi_{\partial}^{[+]\alpha}(x_B) \gamma^{\mu} \Delta(z^{-1}) \gamma^{\nu} + \Phi(x_B) \gamma^{\mu} \Delta_{\partial}^{[-]\alpha}(z^{-1}) \gamma^{\nu} \Big] \\
& \times (1 + \mathcal{O}(M/Q) + \mathcal{O}(\alpha_S)) \Big|_{n_{\pm} \to e_{\pm}} .
\end{aligned} \tag{3.121}$$

The Drell-Yan process

The integrated hadronic tensor reads (employing Eq. 3.38 and Eq. 3.82)

$$\begin{aligned}\int \mathrm{d}^2 q_{T\perp}\, 2MW^{\mu\nu} = \frac{1}{3}\,\mathrm{Tr}^D \Big[& \Phi(x_1)\gamma^\mu \bar{\Phi}(x_2)\gamma^\nu \\ & + \Big(-\frac{\not{e}_+\gamma_\alpha}{Q\sqrt{2}}\gamma^\nu \Phi_D^\alpha(x_1)\gamma^\mu \bar{\Phi}(x_2) + \frac{\not{e}_-\gamma_\alpha}{Q\sqrt{2}}\gamma^\mu \bar{\Phi}_D^\alpha(x_2)\gamma^\nu \Phi(x_1) \\ & + \frac{1}{2}\frac{\not{e}_+\gamma_\alpha}{Q\sqrt{2}}\gamma^\nu \Phi_\partial^{[-]\alpha}(x_1)\gamma^\mu \bar{\Phi}(x_2) - \frac{1}{2}\gamma^\nu \frac{\gamma_\alpha \not{e}_-}{Q\sqrt{2}} \Phi_\partial^{[-]\alpha}(x_1)\gamma^\mu \bar{\Phi}(x_2) \\ & - \frac{1}{2}\frac{\not{e}_-\gamma_\alpha}{Q\sqrt{2}}\gamma^\mu \bar{\Phi}_\partial^{[-]\alpha}(x_2)\gamma^\nu \Phi(x_1) + \frac{1}{2}\gamma^\mu \frac{\gamma_\alpha \not{e}_+}{Q\sqrt{2}} \bar{\Phi}_\partial^{[-]\alpha}(x_2)\gamma^\nu \bar{\Phi}(x_1) \\ & + (\mu \leftrightarrow \nu)^* \Big) \Big] \Big(1 + \mathcal{O}\big(M^2/Q^2\big) + \mathcal{O}(\alpha_S)\Big)\Big|_{n_\pm \to e_\pm}. \end{aligned} \tag{3.122}$$

The single weighted hadronic tensor reads

$$\begin{aligned}\int \mathrm{d}^2 q_{T\perp}\, q_{T\perp}^\alpha\, 2MW^{\mu\nu} = & \frac{1}{3}\,\mathrm{Tr}^D \Big[\Phi_\partial^{[-]\alpha}(x_1)\gamma^\mu \bar{\Phi}(x_2)\gamma^\nu - \Phi(x_1)\gamma^\mu \bar{\Phi}_\partial^{[-]\alpha}(x_2)\gamma^\nu \Big] \\ & \times (1 + \mathcal{O}(M/Q) + \mathcal{O}(\alpha_S))\Big|_{n_\pm \to e_\pm}. \end{aligned} \tag{3.123}$$

Semi-inclusive electron-positron annihilation

The integrated hadronic tensor reads (employing Eq. 3.44 and Eq. 3.94)

$$\begin{aligned}\int \mathrm{d}^2 q_{T\perp}\, 2MW^{\mu\nu} = 3\,\mathrm{Tr}^D \Big[& \bar{\Delta}(z_2^{-1})\gamma^\mu \Delta(z_1^{-1})\gamma^\nu \\ & + \Big(\frac{\not{e}_+\gamma_\alpha}{Q\sqrt{2}}\gamma^\nu \bar{\Delta}_D^\alpha(z_2^{-1})\gamma^\mu \Delta(z_1^{-1}) - \frac{\not{e}_-\gamma_\alpha}{Q\sqrt{2}}\gamma^\mu \Delta_D^\alpha(z_1^{-1})\gamma^\nu \bar{\Delta}(z_2^{-1}) \\ & + \frac{\not{e}_-\gamma_\alpha}{Q\sqrt{2}}\gamma^\mu \Delta_\partial^{[+]\alpha}(z_1^{-1})\gamma^\nu \bar{\Delta}(z_1^{-1}) - \gamma^\mu \frac{\gamma_\alpha \not{e}_+}{Q\sqrt{2}} \Delta_\partial^{[+]\alpha}(z_1^{-1})\gamma^\nu \bar{\Delta}(z_2^{-1}) \\ & + (\mu \leftrightarrow \nu)^* \Big) \Big] \Big(1 + \mathcal{O}\big(M^2/Q^2\big) + \mathcal{O}(\alpha_S)\Big)\Big|_{n_\pm \to e_\pm}. \end{aligned} \tag{3.124}$$

The single weighted hadronic tensor reads

$$\begin{aligned}\int \mathrm{d}^2 q_{T\perp}\, q_{T\perp}^\alpha\, 2MW^{\mu\nu} = 3\,\mathrm{Tr}^D \Big[& \bar{\Delta}(z_2^{-1})\gamma^\mu \Delta_\partial^{[+]\alpha}(z_1^{-1})\gamma^\nu - \bar{\Delta}_\partial^{[+]\alpha}(z_2^{-1})\gamma^\mu \Delta(z_1^{-1})\gamma^\nu \Big] \\ & \times (1 + \mathcal{O}(M/Q) + \mathcal{O}(\alpha_S))\Big|_{n_\pm \to e_\pm}. \end{aligned} \tag{3.125}$$

4

Color gauge invariance in hard scattering processes

In the previous chapter several processes were studied at tree-level (leading order α_S). The hard scale was set by an electromagnetic interaction involving two hadrons and, assuming factorization, cross sections were expressed in nonlocal scale-dependent correlators. These correlators contain gauge links of which the path depends on the process. As first noted by Collins [25], this produces a sign-flip for T-odd distribution functions when comparing Drell-Yan with semi-inclusive DIS.

Following the same approach in this chapter, scattering processes will be analyzed in which the hard scale is set by an QCD-interaction (besides the participating hadrons). We will find that the gauge link does not only depend on the process, but even within a process different gauge links appear; the gauge links will depend on the hard part or subprocess. How awkward this at first may seem, the procedure appears to be consistent. A prescription for deducing gauge links will be given together with some results for gluon-gluon correlators.

The fact that the gauge link depends on the diagram and not only on the process immediately raises questions on factorization and universality. This particular topic will be discussed in the last part of this chapter.

4.1 Gauge links in tree-level diagrams

In this section gauge links in QCD-scattering processes will be considered. Having an α_S-interaction in the hard part at lowest order in g, the number of ways in which the gluons can be inserted is richer than for the previously discussed electromagnetic processes. Not only will we find more complex gauge links than in the electromagnetic processes, but we will also observe that the path of the gauge link depends on the elementary scattering diagram within the process.

In the next subsection a simple QCD-scattering process (quark-quark scattering) will be worked out. Using the results of the previous chapter it will be possible to derive the gauge links very quickly. The calculation will elaborate upon the presence of complex link structures in QCD.

In the second and third subsection we will consider processes in which gluons as external partons are present in the form of jets. Although the same approach is followed, the calculation in the second subsection is technically more involved. We will obtain some results for Drell-Yan and semi-inclusive DIS in which an additional gluon-jet is being produced.

The structure of the obtained results suggests a general prescription for deriving gauge links appearing in diagrams. This prescription will be given together with some examples in the last subsection.

As a final remark, most of the calculations will be done at the amplitude level. We will often anticipate by only keeping terms which contribute to the cross section. The intermediate results will be the amplitude diagrams in which path-ordered exponentials appear. However, in order to absorb these path-ordered exponentials into the correlator, one needs to consider the calculation at the cross section level. It is then also essential to sum over the colors of the other external partons.

4.1.1 Gauge links in quark-quark scattering

The quark-quark scattering subprocess is relevant for hadron-hadron collisions and will be studied in this subsection. The gauge links are derived for the correlators which are attached to the elementary scattering subprocess (squared amplitude diagram). All external partons are assumed to be separated by large momentum differences. We shall start by considering gluon insertions from a single distribution correlator and derive the gauge link. Results for the other correlators will be given at the end of this subsection.

Let us begin by considering the subprocess in Fig. 4.1a (the resulting gauge invariant correlator will be given in Eq. 4.6). Including a longitudinally polarized gluon (A^+ with momentum $p_1 \sim n_+$) from a distribution correlator (belonging to the quark entering the graph from the bottom), that gluon can be coupled in four different places: to the incoming quark, to the outgoing quarks, and to the exchanged virtual gluon. The inserted gluon introduces an extra integral over p_1 which needs to be performed. Analyzing the p_1^+-dependence one observes two classes of poles in p_1^+. The first class

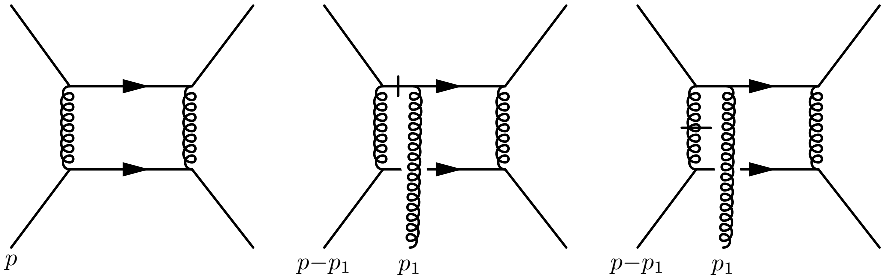

(a) (b) (c)

Figure 4.1: Figure (a) represents a squared Feynman diagram contributing to quark-quark scattering. In figure (b) and figure (c) a gluon is inserted from the correlator into the scattering diagram. In figure (b) the dash indicates a pole at $p_1^+ \approx 0$, while in figure (c) the dash indicates a pole at $p_1^+ \neq 0$.

consists of poles at $p_1^+ \approx 0$ which arise from gluon insertions on external partons in which the introduced propagator (by the inserted gluon) goes on shell (see for instance Fig. 4.1b). The second class contains the poles at $p_1^+ \neq 0$ corresponding to other internal parton-lines going on shell (see for instance Fig. 4.1c).

In the previous chapter we have seen that the poles at $p_1^+ \approx 0$ give a contribution to the gauge link but the meaning of the poles at $p_1^+ \neq 0$ is unclear. Fortunately, in the sum over all possible gluon insertions it turns out that the poles of the second class cancel each other. For instance, in the case of a single gluon insertion one can show the following cancellation by doing the calculation explicitly

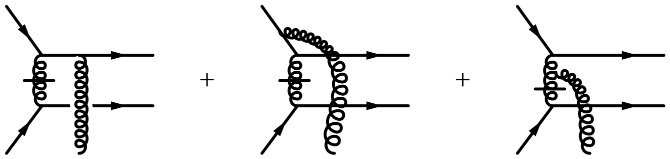

$$= 0, \qquad (4.1)$$

where the dashes indicate the taken residue. This result can be generalized to all order insertions[1] and was noted in Ref. [37].

The cancellation as above is observed in various processes suggesting it to hold for amplitudes in general. Unfortunately, such a proof does not seem to exist (not even for QED) and is not simple to establish. Therefore, two general arguments in favor of this cancellation will be presented, but it should be stressed that via an explicit calculation of the cases considered in this thesis the same results can be obtained.

---

[1] By choosing the momenta in a convenient way (use $\Phi(p, p_1 - p_2, \ldots, p_{n-1} - p_n, p_n)$), the general proof is not much more complicated to show than the equation above.

The first argument is connected with a Ward identity, which states that a longitudinally polarized gluon (on shell) with nonzero momentum does not couple to an amplitude which has only physical external partons. Since the inserted gluon (with $p_i^+ \neq 0$) is coupled to all possible places, except for one particular interaction which is already absorbed in the correlator definition (see for example Fig. 3.1b), such gluons should not be able to contribute in the sum. The second argument in favor is that in the present case (see for instance Fig. 4.1c) the pole at $p_i^+ \neq 0$ corresponds to the internal gluon-line being on shell. However, this configuration is physically not possible, because the coupling between two on shell quarks (with unequal momenta) and an on shell gluon is forbidden by momentum conservation. This is also connected to the fact that all tree-level Feynman amplitudes are finite as long as the external partons are well separated. According to this argument the cancellation in the above equation takes place in a nonphysical area. This argument for a single gluon insertion can be extended to an arbitrary amount of insertions.

Having only the poles at $p_i^+ \approx 0$, the task to perform is to evaluate those poles which arise from inserting gluons on the external parton legs. The calculation of inserting longitudinally polarized gluons to a single external parton leg is similar to the calculations performed in the previous chapter. An explicit example will be shown below. By inserting the gluons on a single quark-line and following the same steps as in the previous chapter, one can derive the gauge link to all orders. There is only one important difference: the color matrices of the inserted vertices (of the inserted gluons) cannot be simply pulled into the considered correlator because of the presence of the virtual gluon inside the graph. Therefore, those color matrices are "standing" on the quark-line on which the gluons were inserted. Taking combinations of insertions on several external legs is relatively straightforward because the manipulations of the inserted gluons on a certain external leg can be performed without using information from the other external legs. As a result, the combination of insertions gives a product of gauge links of which their color matrices remain on the quark-lines on which the gluons were inserted.

As an example, let us reconsider the subprocess given in Fig. 4.1a (also given in Fig. 4.2a). Summing over the colors of the incoming and outgoing partons, its contribution to the cross section is proportional to (where Φ was defined in Eq. 2.37)

$$\begin{aligned}\sigma_{\text{Fig. (4.2)}a} &= K\ \mathrm{Tr}^C\left[t_b t_a \Phi(p)\right]\mathrm{Tr}^C\left[t_b t_a\right]\\ &= \frac{2K}{3}\,\mathrm{Tr}^C\left[\Phi(p)\right] \qquad\qquad \text{(where } K \text{ is some constant).}\end{aligned} \tag{4.2}$$

Using the machinery of the previous chapter[2], the inserted longitudinally polarized gluons from the correlator Φ produce in the amplitude diagram (left-hand-side of the cut) the following gauge links: $\mathcal{L}^{\xi_T,\,\xi^+}(\infty^-,\xi^-)$ on the outgoing quarks and $\mathcal{L}^{\xi_T,\,\xi^+}(\xi^-,-\infty^-)$ on the incoming quarks (the coordinate ξ is related to the field $\psi(\xi)$ in the correlator $\Phi(p)$). Insertions on the right-hand-side of the cut yield similar gauge links. The result of the

---

[2] Issues related to the equations of motion will be discarded in this section.

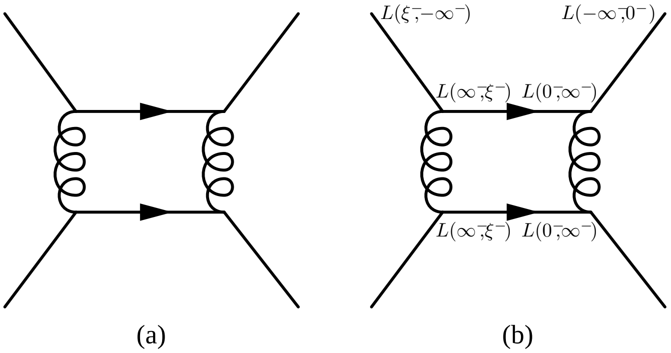

Figure 4.2: Illustration of gauge links in a squared Feynman diagram contributing to quark-quark scattering. Figure (a) represents an ordinary squared Feynman diagram. In figure (b) the result of the gluon insertions is presented. It is shown on which quark-lines the color matrices of the indicated gauge links (L) are acting. The superscripts ξ^+, and ξ_T or 0_T, have been omitted.

all order insertions is graphically illustrated in Fig. 4.2b in which it is shown that the color matrices of the gauge links are at this moment on the external parton-lines. The result of the insertions reads (the notation will be a bit sloppy; the gauge links appear under the ξ integral which is present in the definition of Φ)

$$\begin{aligned}\sigma_{\text{Fig. (4.2)}b} = {} & K\,\mathrm{Tr}^C\left[t_b\mathcal{L}^{0_T,\xi^+}(0^-,\infty^-)\mathcal{L}^{\xi_T,\xi^+}(\infty^-,\xi^-)t_a\Phi(p)\right]\\ & \times\mathrm{Tr}^C\left[t_b\mathcal{L}^{0_T,\xi^+}(0^-,\infty^-)\mathcal{L}^{\xi_T,\xi^+}(\infty^-,\xi^-)t_a\mathcal{L}^{\xi_T,\xi^+}(\xi^-,-\infty^-)\mathcal{L}^{0_T,\xi^+}(-\infty^-,0^-)\right].\end{aligned} \tag{4.3}$$

Using now the identity ($N = 3$)

$$(t^a)_{ij}(t^a)_{kl} = \frac{1}{2}\delta_{il}\delta_{kj} - \frac{1}{2N}\delta_{ij}\delta_{kl}, \tag{4.4}$$

one finds

$$\begin{aligned}\sigma_{\text{Fig. (4.2)}b} = \frac{2K}{3}\bigg(& \frac{-1}{4}\,\mathrm{Tr}^C\left[\Phi(p)\mathcal{L}^{[+]}(0,\xi^-)\mathcal{L}^{[\Box]}(0,\xi^-)\right]\\ & + \frac{5}{12}\,\mathrm{Tr}^C\left[\Phi(p)\mathcal{L}^{[+]}(0,\xi^-)\right]\mathrm{Tr}^C\left[\mathcal{L}^{[\Box]}(0,\xi^-)\right]\bigg),\end{aligned} \tag{4.5}$$

where the transverse gauge links were added for completeness. This addition can be performed uniquely by assuming consistency (gauge invariance). Using Eq. 4.2 for the

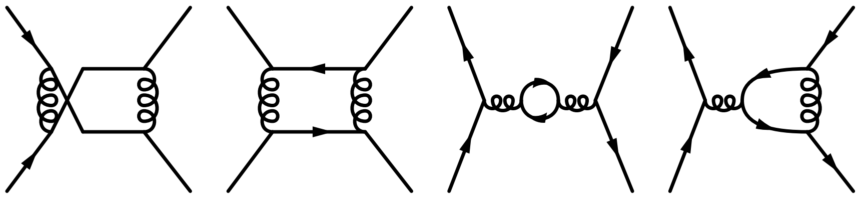

(a) (b) (c) (d)

Figure 4.3: Various quark-(anti)quark scattering subprocesses.

normalization, the gauge invariant quark-quark correlator is obtained [37, 40]

$$\begin{aligned}
&\Phi_{\text{Fig. (4.2)},ij}(x,p_T,P,S)\\
&=\int\frac{d\xi^-\,d^2\xi_T}{(2\pi)^3}e^{ip\xi}\,\langle P,S|\overline{\psi}_j(0)\\
&\quad\times\Big[\tfrac{5}{12}\mathcal{L}^{[+]}(0,\xi^-)\,\mathrm{Tr}^C\,\mathcal{L}^{[\Box]}(0,\xi^-)-\tfrac{1}{4}\mathcal{L}^{[+]}(0,\xi^-)\mathcal{L}^{[\Box]}(0,\xi^-)\Big]\psi_i(\xi)|P,S\rangle\Big|_{\substack{\xi^+=0\\ p^+=xP^+}}. \qquad (4.6)
\end{aligned}$$

In the correlator for this diagram a combination of path-ordered exponentials appear. Such gauge links were not discussed before and although this new result looks rather awkward at first sight, *it is* actually invariant under color gauge transformations. It should also be noted that the appearance of these complex gauge link structures is not just a peculiarity of QCD, but also appears in the QED-version of Fig. 4.2. In that case the gauge link is $\mathcal{L}^{[+]}(0,\xi^-)\mathcal{L}^{[\Box]}(0,\xi^-)$ which was obtained in Ref. [37].

Using the above procedure one can derive the gauge links which appear in other quark-quark and quark-antiquark scattering diagrams, see Fig. 4.3. There is only one issue which still needs to be addressed. When gluons are inserted from several correlators at the same time, interactions *between* the different insertions need to be included. In the previous chapter we discussed processes in which two correlators were present. The interactions between the insertions from the two different correlators were simplified by choosing a suitable gauge. In the present case where four correlators are present, this trick cannot be applied. However, the distribution gauge links as given here are exact when two quark-jet production is considered, giving confidence in the results in which the fragmentation process is included. The results for quark-quark scattering were presented in Ref. [40] and are given in table 4.1. Note that in the limit of $\xi_T \to 0$, all gauge links in table 4.1 reduce to a straight gauge link, $\mathcal{L}^{0_T,\,\xi^+}(0^-,\xi^-)$, between the two quark-fields, see also Fig. 2.11a.

\ correlator diagram	quark distribution	quark fragmentation
Fig. 4.2a	$\frac{5}{12}\mathcal{L}^{[+]}\,\mathrm{Tr}^C\,\mathcal{L}^{[\Box]} - \frac{1}{4}\mathcal{L}^{[+]}\mathcal{L}^{[\Box]}$	$\frac{5}{12}\mathcal{L}^{[-]}\,\mathrm{Tr}^C\,\mathcal{L}^{[\Box]\dagger} - \frac{1}{4}\mathcal{L}^{[-]}\mathcal{L}^{[\Box]\dagger}$
Fig. 4.3a	$\frac{3}{4}\mathcal{L}^{[+]}\,\mathrm{Tr}^C\,\mathcal{L}^{[\Box]} - \frac{5}{4}\mathcal{L}^{[+]}\mathcal{L}^{[\Box]}$	$\frac{3}{4}\mathcal{L}^{[-]}\,\mathrm{Tr}^C\,\mathcal{L}^{[\Box]\dagger} - \frac{5}{4}\mathcal{L}^{[-]}\mathcal{L}^{[\Box]\dagger}$
Fig. 4.3b	$\frac{1}{24}\mathcal{L}^{[+]}\,\mathrm{Tr}^C\,\mathcal{L}^{[\Box]\dagger} + \frac{7}{8}\mathcal{L}^{[-]}$	$\frac{1}{24}\mathcal{L}^{[-]}\,\mathrm{Tr}^C\,\mathcal{L}^{[\Box]} + \frac{7}{8}\mathcal{L}^{[+]}$
Fig. 4.3c	$\frac{3}{8}\mathcal{L}^{[+]}\,\mathrm{Tr}^C\,\mathcal{L}^{[\Box]\dagger} - \frac{1}{8}\mathcal{L}^{[-]}$	$\frac{3}{8}\mathcal{L}^{[-]}\,\mathrm{Tr}^C\,\mathcal{L}^{[\Box]} - \frac{1}{8}\mathcal{L}^{[+]}$
Fig. 4.3d	$\frac{3}{8}\mathcal{L}^{[+]}\,\mathrm{Tr}^C\,\mathcal{L}^{[\Box]\dagger} - \frac{1}{8}\mathcal{L}^{[-]}$	$\frac{3}{8}\mathcal{L}^{[-]}\,\mathrm{Tr}^C\,\mathcal{L}^{[\Box]} - \frac{1}{8}\mathcal{L}^{[+]}$

Table 4.1: The gauge links in the correlators which connect the external parton legs appearing in Fig. 4.2, 4.3. The gauge links in the antiquark correlators in the figures are this case the Hermitean conjugates of the gauge links in the quark correlators.

4.1.2 Gauge links in semi-inclusive DIS and Drell-Yan with an additional gluon in the final state

Introduction

We will consider semi-inclusive DIS and Drell-Yan in which an additional gluon is radiated with some transverse momentum (at least more than the hadronic scale). The additional gluon is assumed to be observed and therefore its momentum is not integrated over. Possible contributions to the processes are given in Fig. 4.4.

In order to obtain the gauge link in the distribution correlator all insertions must be taken. The poles at $p_i^+ \neq 0$ cancel each other for all possible insertions which is compatible with the arguments presented in the previous subsection. Only the poles $p_i^+ \approx 0$, coming from insertions on the external quark and outgoing gluon, will be considered here in detail.

Inserting gluons only on the outgoing quark in semi-inclusive DIS makes the cross section proportional to (see also previous subsection and Fig. 4.4a)

$$\sigma \sim \mathrm{Tr}^C[t_b\,\mathcal{L}^{[+]}(0,\xi^-)\,t_a\,\Phi(p)\,]\,\delta_{ab}, \tag{4.7}$$

where the gauge link appears under the ξ integral in $\Phi(p)$ (sloppy notation). The above expression is by itself not gauge invariant, the possibility of inserting gluons on the radiated gluon simply *has to be* included. From this point of view there can be no reason to neglect such contributions. The interesting point here is that one can simply argue what the gauge link should be. If the procedure is to be consistent then the only possible gauge link which can appear in the correlator is a gauge link via plus infinity. Gauge

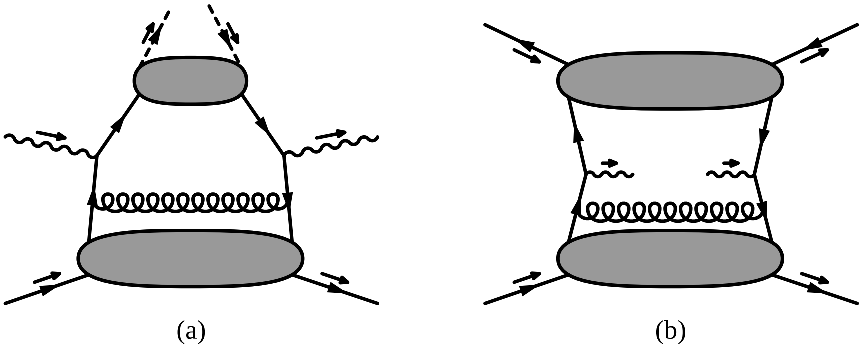
(a) (b)

Figure 4.4: Figure (a) and figure (b) represent contributions to respectively semi-inclusive DIS and Drell-Yan in which an additional jet is being produced.

links via minus infinity or loops, as encountered in the previous subsection, cannot arise because the gluons are inserted on partons which are all outgoing (incoming partons are needed to produce such gauge links). When taking insertions on the radiated gluon into account, there is only one possible way in how those insertions can contribute to obtain the proper gauge link. Inserting gluons on the radiated gluon should lead us to the following replacements

$$\begin{aligned} t_a &\rightarrow \mathcal{L}^{\xi_T,\,\xi^+}(\xi^-,\infty^-)t_a\mathcal{L}^{\xi_T,\,\xi^+}(\infty^-,\xi^-), \\ t_b &\rightarrow \mathcal{L}^{0_T,\,\xi^+}(0^-,\infty^-)t_b\mathcal{L}^{0_T,\,\xi^+}(\infty^-,0^-). \end{aligned} \tag{4.8}$$

Together with the insertions on the outgoing quark this provides us with a gauge link via plus infinity in the quark-quark correlator [37], Eq. 4.7 becomes

$$\begin{aligned} \sigma &\sim \mathrm{Tr}^C[\mathcal{L}^{0_T,\,\xi^+}(0^-,\infty^-)t_b\mathcal{L}^{0_T,\,\xi^+}(\infty^-,0^-)\mathcal{L}^{[+]}(0,\xi^-)\mathcal{L}^{\xi_T,\,\xi^+}(\xi^-,\infty^-)t_a\mathcal{L}^{\xi_T,\,\xi^+}(\infty^-,\xi^-)\Phi]\delta_{ab} \\ &= \frac{4}{3}\mathrm{Tr}^C[\mathcal{L}^{[+]}(0,\xi^-)\Phi]. \end{aligned} \tag{4.9}$$

With simple arguments, the effect of inserting gluons on a radiated gluon in semi-inclusive DIS was derived. Using the same replacement rules, we can now also study the gauge link structure of Drell-Yan plus an additional outgoing gluon (see Fig. 4.4b). Using the same rules, one finds in that case for the gauge link [37]

$$\frac{3}{8}\mathcal{L}^{[+]}(0,\xi^-)\,\mathrm{Tr}^C\left[\mathcal{L}^{[\Box\dagger]}(0,\xi^-)\right] - \frac{1}{8}\mathcal{L}^{[-]}(0,\xi^-). \tag{4.10}$$

The result is here a combination of gauge links via plus and minus infinity. Although the result is not very appealing, it is gauge invariant. The appearance of gauge links via plus and minus infinity appear because insertions were taken on incoming *and* outgoing partons. Based on the previous subsection, such a result was to be expected.

The replacements in Eq. 4.8 were derived by assuming the procedure to be consistent with color gauge invariance. In the following it will be argued that the replacement rules are in fact the proper rules.

The explicit calculation

The derivation of gauge links will be presented which underlies the results of Ref. [37]. The amplitude in semi-inclusive DIS and Drell-Yan in which an additional gluon is produced will be considered at order α_S, and the gauge link will be derived by including gluon insertions. Before we begin with the technical derivation we note that if the polarization vector of the outgoing gluon is replaced by its momentum, then the amplitude vanishes which is a result of a Ward identity (at this order in α_S there are no ghost contributions).

For the coupling of an inserted gluon on the external gluon-line some work needs to be performed. Consider the outgoing gluon with momentum l for a given diagram in a particular amplitude (for instance the left-hand-side of the cut in Fig. 4.4b). In order to indicate the presence of the outgoing gluon, the polarization vector $\epsilon^{(c)\dagger}_{a\beta}(l)$ will be introduced, where c is the "color charge" of the gluon ($c \in 1,\ldots,8$), a is the color index ($a \in 1,\ldots,8$), and β is the usual Lorentz-index. Although $\epsilon^{(c)\dagger}_{a\beta}(l)$ is proportional to δ_{ac} (as $e^{\alpha}_{1} \sim \delta^{\alpha}_{1}$), this property will not be used because it is preferred here to show explicitly the presence of this external outgoing gluon. Using these definitions, the considered diagram can be expressed as ($i, j, k, l \in 1, 2, 3$, and the Dirac indices are not explicitly shown)

$$t^{a}_{ij}\, g_{\alpha'}{}^{\beta}\, \epsilon^{(c)\dagger}_{a\beta}(l)\, M^{\alpha'}_{ijkl}(p,l)\, \Phi_{kl}(p), \tag{4.11}$$

in which M denotes the remainder of the expression for the diagram and t^a is a 3×3 color matrix. Although the calculation will be performed at the amplitude level, the full correlator Φ is present in the above expression for economics of notation. We will not rely on the part of Φ which is in the conjugate amplitude.

Inserting a gluon with momentum $p_1 \sim n_+$ and polarization n_+ on the radiated gluon replaces Φ by Φ_A and changes the above expression into (in the Feynman gauge)

$$\begin{aligned}
&\int \mathrm{d}^4 p_1\, t^{b}_{ij} \frac{(-i)g_{\alpha'\alpha}}{(l-p_1)^2 + i\epsilon} f^{bsa} \\
&\times \Big(g^{\alpha -}(l-2p_1)^{\beta} + g^{-\beta}(p_1+l)^{\alpha} - 2l^{-} g^{\alpha\beta} \Big)\, \epsilon^{(c)\dagger}_{a\beta}(l)\, M^{\alpha'}_{ijkl}(p{-}p_1, l)\, \Phi^{+}_{A_s,kl}(p,p_1) \\
&\quad = \int \mathrm{d}^4 p_1\, t^{b}_{ij} \frac{(-i)g_{\alpha'\alpha}}{(l-p_1)^2 + i\epsilon} f^{bsa} \\
&\qquad \times \Big(-2l^{-} g^{\alpha\beta} + (l-p_1)^{\alpha} n_{+}^{\beta} + n_{+}^{\alpha} l^{\beta} \Big)\, \epsilon^{(c)\dagger}_{a\beta}(l)\, M^{\alpha'}_{ijkl}(p{-}p_1, l)\, \Phi^{+}_{A_s,kl}(p,p_1).
\end{aligned} \tag{4.12}$$

When referring to this equation, we will refer to the right-hand-side. The first term of Eq. 4.12 does not change the original Lorentz structure of the diagram and will yield the first order expansion of the gauge link. The second and third term have a less clear meaning. In the processes studied in this subsection the second term vanishes in the sum over all diagrams in the amplitude, and the third term does not couple to the Hermitean conjugate amplitude and vanishes therefore in the cross section. Both terms do therefore not contribute which is a result of a Ward identity which can be applied since $l - p_1 \neq 0$.

In other processes like two-gluon production the second and third term do not vanish. As will be shown later, it turns out that these terms together with the ghost contributions exactly cancel the nonphysical polarizations of the radiated gluon in the Feynman gauge. This cancellation is far from being trivial and it should be considered as a firm consistency check.

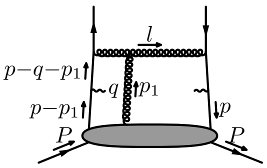

Figure 4.5: Example

When continuing with the above expression, Eq. 4.12, one should realize that there could be an additional p_1^+-dependence in the rest of the diagram (in M), see for instance Fig. 4.5. Before closing the contours and evaluating the integrals by taking their residues, the powers of p_1^+ in the denominator and in the numerator should be counted. Using that $\Phi \sim \not{p}$ it is possible to show that the denominator is one order higher than the numerator which justifies the closing of the contour at infinity. Using this result the p_1^+-dependence in the possible present internal quark propagator (in M) can be analyzed more closely. The p_1^+ in the numerator can be discarded because that term removes the pole at $p_1^+ = 0$ leaving the pole at $p_1^+ \neq 0$ behind. Such poles do not contribute which can be checked explicitly. The p_1^+-dependence in the denominator can be discarded as well because only the poles at $p_1^+ = 0$ will be considered.

Continuing with the non-vanishing terms of Eq. 4.12 and performing the integrations leads to (using that $i f^{bsa} t_b = [t_s, t_a]$)

$$
\begin{aligned}
&\text{first term of Eq. (4.12)}\\
&\quad = g_{\alpha'}{}^{\beta}\, \epsilon^{(c)\dagger}_{\alpha\beta}(l)\, (t_s\, t_a)_{ij}\, M^{\alpha'}_{ijkl}(p,l)\\
&\qquad \times \int \frac{\mathrm{d}^4\xi}{(2\pi)^4} e^{ip\xi} \langle P,S|\overline{\psi}_l(0)(-ig) \int_{\xi^-}^{\infty} \mathrm{d}\eta^- A_s^+(\eta^-,0,\xi_T)\psi_k(\xi)|P,S\rangle\\
&\quad + g_{\alpha'}{}^{\beta}\, \epsilon^{(c)\dagger}_{\alpha\beta}(l)\, (t_a\, t_s)_{ij}\, M^{\alpha'}_{ijkl}(p,l)\\
&\qquad \times \int \frac{\mathrm{d}^4\xi}{(2\pi)^4} e^{ip\xi} \langle P,S|\overline{\psi}_l(0)(-ig) \int_{\infty}^{\xi^-} \mathrm{d}\eta^- A_s^+(\eta^-,0,\xi_T)\psi_k(\xi)|P,S\rangle,
\end{aligned}
\tag{4.13}
$$

which is exactly the first order expansion of replacement stated in Eq. 4.8. The above equation expresses that two link operators are produced for insertions on outgoing gluons. In the following we will generalize this result to all possible insertions.

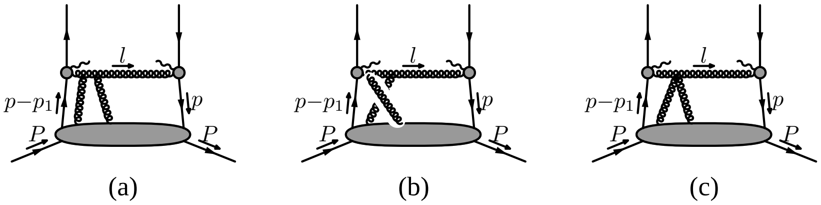

Figure 4.6: Various insertions in the squared amplitude. The discussed interference terms in figure (a) and figure (b) cancel the contribution of figure (c). For the sum of these three diagrams one remains with the non-interference contributions (the part of the inserted vertices consisting of metric tensors) of figure (a) and figure (b).

When attaching more than a single gluon we have to consider the Lorentz structure of the inserted vertices a bit more closely (see the three terms in Eq. 4.12). The inserted vertex which is the closest to the electromagnetic interaction will be called the first vertex (see for instance the left triple-gluon vertex in Fig. 4.6a), and so on. When inserting a number of gluons the second term of the first inserted vertex still vanishes by a Ward identity in the sum over all amplitude diagrams. The combination of the first term of the first vertex with the second term of the second vertex also vanishes because of a Ward identity, and so on. The same holds for the third term of the last vertex which does not couple to the conjugate amplitude. The conclusion is that the only non-vanishing contributions come from the part of the inserted vertices which are products of metric tensors and interference terms. These interference terms consist of contractions between terms like the second and third in Eq. 4.12 belonging to different insertions.

Consider two adjacent insertions with momenta $p_1 - p_2$ and p_2 on a gluon-line with momentum $l - p_1$, giving the additional gluon propagators: $(l - p_1)^2$ and $(l - p_2)^2$ (see Fig. 4.6a). The interference term between those two insertions produce a term in the numerator proportional to $(l - p_2)^2$ canceling one of the gluon propagators. This interference term is canceled if one includes the contributions from the insertion in which the considered vertices interchanged (see Fig. 4.6b) and the insertion in which the two gluons couple into a four-gluon vertex[3] (see Fig. 4.6c). When an interference term does not come from adjacent insertions, then this cancellation occurs in a slightly more complicated manner. It will be assumed that similar cancellations also appear when more than two of those terms interfere.

Attaching N gluons to the outgoing gluon and considering now only the metric tensors of the insertions (like the first term of Eq. 4.12) modifies in the Feynman gauge

---

[3] Up to now we have not considered insertions in which the gluons from the correlator cross. When allowing for N such insertions one should actually add for all diagrams a symmetry factor $1/N$. The diagram which has the four-gluon vertex counts in that case double and should be multiplied by two.

Eq. 4.11 into

$$\int \left(\prod_i \mathrm{d}^4 p_i \right) t^b_{ij} \frac{(-2l^-)(-i)}{(l-p_1)^2 + i\epsilon} f^{bl_1c_2} \times \frac{(-2l^-)(-i)}{(l-p_2)^2 + i\epsilon} f^{c_2l_2c_3} \dots \frac{(-2l^-)(-i)}{(l-p_N)^2 + i\epsilon} f^{c_Nl_Na}$$
$$\times\ g_{\alpha'}{}^{\beta}\ \epsilon^{(c)\dagger}_{\alpha\beta}(l)\ M^{\alpha'}_{ijkl}(p{-}p_1, l)\ \Phi^{+\dots+}_{A_{l1}\dots A_{lN},kl}(p, p_1{-}p_2, \dots, p_{N-1}{-}p_N, p_N), \quad (4.14)$$

where we already anticipated on leaving out terms which do not contribute to the cross section. Considering the color structure explicitly, Eq. 4.14 reads (see Eq. 4.16 for clarification)

$$\text{Eq. (4.14)} = \int \mathrm{d}^4 p_1\ \dots \mathrm{d}^4 p_N\ \frac{1}{-p_1^+ + i\epsilon} \cdots \frac{1}{-p_N^+ + i\epsilon} g_{\alpha'}{}^{\beta}$$
$$\times \left[\begin{array}{l} \text{A sum over all possible combinations of } t_a \text{ and } N \text{ color matrices } t_{l_i} \text{ with the} \\ \text{index } i \text{ on the right of } t_a \text{ going down (from left to right) and on the left of } t_a \\ \text{going up. The sign of each combination is } (-1)^{\text{number of terms right of } t_a} \end{array} \right]_{ij}$$
$$\times\, \epsilon^{(c)\dagger}_{\alpha\beta}(l)\ M^{\alpha'}_{ijkl}\ \Phi^{+\dots+}_{A_{l1}\dots A_{lN},kl}(p_1, \dots, p_N). \quad (4.15)$$

The factor in the middle contains the following terms in the case of four gluon insertions,

$$t_{l_1} t_{l_2} t_a t_{l_4} t_{l_3} - t_{l_2} t_a t_{l_4} t_{l_3} t_{l_1} + t_{l_1} t_{l_4} t_a t_{l_3} t_{l_2} + \dots \quad (4.16)$$

Performing the integrations over p_i leads to a path-ordered product. Using the following identity for non-commuting a's and b's[4] which can be proven by using induction

$$\int_{\xi}^{C} \mathrm{d}\eta_1 \int_{\eta_1}^{C} \mathrm{d}\eta_2 \dots \int_{\eta_N}^{C} \mathrm{d}\eta_N \Big[b(\eta_1) \dots b(\eta_m) a(\eta_N) \dots a(\eta_{m+1})$$
$$+ \text{ all possible coordinate permutations such that the } b\text{'s are}$$
$$\text{path-ordered and the } a\text{'s are anti-path-ordered} \Big]$$
$$= \int_{\xi}^{C} \mathrm{d}\eta_1 \int_{\eta_1}^{C} \mathrm{d}\eta_2 \dots \int_{\eta_{m-1}}^{C} \mathrm{d}\eta_m\ b(\eta_1) \dots b(\eta_m)$$
$$\times \int_{\xi}^{C} \mathrm{d}\eta_{m+1} \int_{\eta_{m+1}}^{C} \mathrm{d}\eta_{m+2} \dots \int_{\eta_{N-1}}^{C} \mathrm{d}\eta_N\ a(\eta_N) \dots a(\eta_{m+1}), \quad (4.17)$$

identity to obtain a product of ordered exponentials one obtains for the part of Eq. 4.15, which consists of m t-matrices left of t_a and n t-matrices right of t_a (with $n + m = N$), the following expression

---

[4] So $[a(x_1), a(x_2)] \neq 0$ and $[a(x_1), b(x_2)] \neq 0$.

$$\begin{aligned}
&[t_{l_1} \dots t_{l_m} t_a t_{l_N} \dots t_{l_{m+1}}]_{ij}\, g_{\alpha'}{}^{\beta}\, \epsilon^{(c)\dagger}_{a\beta}(l)\, M^{\alpha'}_{ijkl}(p,l) \\
&\times \int \frac{\mathrm{d}^4\xi}{(2\pi)^4} e^{ip\xi} \langle P,S\,|\overline{\psi}_l(0)(-i)^{m+n} \int_{\xi^-}^{\infty} \mathrm{d}\eta_1^- \int_{\eta_1^-}^{\infty} \mathrm{d}\eta_2^- \,\dots \int_{\eta_{m-1}^-}^{\infty} \mathrm{d}\eta_m^-\, A^+_{l_1}(\eta_1^-) \dots A^+_{l_m}(\eta_m) \\
&\times \int_{\infty}^{\xi^-} \mathrm{d}\eta_N^-\, A^+_{l_N}(\eta_N) \int_{\eta_N^-}^{\xi^-} \mathrm{d}\eta_{N-1}^-\, A^+_{l_{N-1}}(\eta_{N-1}) \dots \int_{\eta_{m+2}^-}^{\xi^-} \mathrm{d}\eta_{m+1}^-\, A^+_{l_{m+1}}(\eta_{m+1}) \psi_k(\xi) |P,S\,\rangle .
\end{aligned} \tag{4.18}$$

This expression represents the m^{th} order expansion of $\mathcal{L}^{\xi_T,\xi^+}(\xi^-,\infty^-)$ multiplied with the n^{th} order expansion of $\mathcal{L}^{\xi_T,\xi^+}(\infty^-,\xi^-)$.

Including now all terms of Eq. 4.15 by summing the above expression over all possible values of n and m, and summing over all N, one obtains

$$\begin{aligned}
&\epsilon^{(c)\dagger}_{a\beta}(l)\, g_{\alpha'}{}^{\beta}\, M^{\alpha'}_{ijkl}(p,l) \\
&\qquad \times \int \frac{\mathrm{d}^4\xi}{(2\pi)^4} e^{ip\xi} \langle P,S\,|\overline{\psi}_l(0) \left[\mathcal{L}^{\xi_T,\,\xi^+}(\xi^-,\infty^-) t_a \mathcal{L}^{\xi_T,\,\xi^+}(\infty^-,\xi^-)\right]_{ij} \psi_k(\xi)|P,S\,\rangle,
\end{aligned} \tag{4.19}$$

which is exactly the replacement rule as stated in Eq. 4.8.

By taking all possible insertions on a radiated gluon the derivation of the gauge link was shown in considerable detail in the Feynman gauge. The color matrices of these gauge links are convoluted with the rest of the diagram and are not directly acting on the fields in the considered correlator (see the next subsection for how this expression gets handled further). The calculation for an incoming gluon is very similar and its result will be stated in the next subsection.

4.1.3 Prescription for deducing gauge links in tree-level diagrams

The previous subsections suggest a general procedure for evaluating gauge links appearing in tree-level squared amplitude diagrams. Although not rigorously proven[5], a prescription will be given together with some examples. We note that the derived gauge links appear under the ξ integral of the considered correlator (the notation is a bit sloppy).

In order to determine the gauge link for a correlator (its parent hadron is moving mainly in the n_+-direction), which is connected to a specific elementary tree-level squared amplitude diagram having physical external partons, the following set of rules can be applied:

---

[5] In all considered cases the prescription yielded the correct result. The structure of the calculations in the previous subsections indicates that a general proof by induction should be feasible.

1. Write down the contribution of this diagram to the cross section keeping only the color factors. Rewrite this expression into a product of the amplitude diagram (left-hand-side of the squared diagram) and the conjugate amplitude diagram (right-hand-side of the squared diagram). Color charges of external partons must be made explicit. For the considered correlator we simply use Φ_{ab}, for the other incoming and outgoing quarks we apply the vectors ($u_j^{(i)}$ and $u_j^{(i)\dagger}$) indicating their color charge i and component j and similarly for antiquarks ($v_j^{(i)\dagger}$ and $v_j^{(i)}$). For the gluons we introduce $\epsilon_b^{(a),\text{in/out}}$ where a is the color charge and b is the color component. Any structure constant, f^{abc} has to be expressed in terms of the basic color matrices, $t_{jk}^{(i)}$ via the relation $f^{abc} = (-2i)\,\text{Tr}^C[t_c[t_a, t_b]]$.

2. Taking all the insertions from a quark distribution or antiquark fragmentation correlator on the external partons in the amplitude diagram (except for the parton connected to the considered correlator), can be translated into the following replacements (outgoing refers to crossing the cut):

   - an outgoing quark: $u_i^{(k)\dagger} \to u_j^{(k)\dagger}\,\mathcal{L}_{ji}^{\xi_T,\,\xi^+}(\infty^-, \xi^-)$
   - an outgoing antiquark: $v_i^{(k)} \to \mathcal{L}_{ij}^{\xi_T,\,\xi^+}(\xi^-, \infty^-)\,v_j^{(k)}$
   - an outgoing gluon: $\epsilon_a^{(c),\text{out}\dagger} t_{ij}^{(a)} \to \mathcal{L}_{ik}^{\xi_T,\,\xi^+}(\xi^-, \infty^-)\,\epsilon_a^{(c),\text{out}\dagger} t_{kl}^{(a)}\,\mathcal{L}_{lj}^{\xi_T,\,\xi^+}(\infty^-, \xi^-)$
   - an incoming quark: $u_i^{(k)} \to \mathcal{L}_{ij}^{\xi_T,\,\xi^+}(\xi^-, -\infty^-)\,u_j^{(k)}$
   - an incoming antiquark: $v_i^{(a)\dagger} \to v_j^{(a)\dagger}\,\mathcal{L}_{ji}^{\xi_T,\,\xi^+}(-\infty^-, \xi^-)$
   - an incoming gluon: $\epsilon_b^{(a),\text{in}} t_{ij}^{(b)} \to \mathcal{L}_{ik}^{\xi_T,\,\xi^+}(\xi^-, -\infty^-)\,\epsilon_b^{(a),\text{in}} t_{kl}^{(b)}\,\mathcal{L}_{lj}^{\xi_T,\,\xi^+}(-\infty^-, \xi^-)$

   The coordinate ξ is the argument of the parton-field in the quark distribution or antiquark fragmentation correlator. If the considered correlator is quark fragmentation or antiquark distribution correlator, the same rules apply but with ξ replaced by 0. See also the correlators given in section 3.3 and section 3.4 for further clarification.

3. For the insertions in the conjugate amplitude diagram one makes the following replacements when considering a quark distribution or antiquark fragmentation correlator (outgoing refers to crossing the cut):

   - an outgoing quark: $u_i^{(k)} \to \mathcal{L}_{ij}^{0_T,\,\xi^+}(0^-, \infty^-)\,u_j^{(k)}$
   - an outgoing antiquark: $v_i^{(k)\dagger} \to v_j^{(k)\dagger}\mathcal{L}_{ji}^{0_T,\,\xi^+}(\infty^-, 0^-)$
   - an outgoing gluon: $\epsilon_a^{(c),\text{out}} t_{ij}^{(a)} \to \mathcal{L}_{ik}^{0_T,\,\xi^+}(0^-, \infty^-)\,\epsilon_a^{(c),\text{out}} t_{kl}^{(a)}\,\mathcal{L}_{lj}^{0_T,\,\xi^+}(\infty^-, 0^-)$
   - an incoming quark: $u_i^{(k)\dagger} \to u_j^{(k)\dagger}\mathcal{L}_{ji}^{0_T,\,\xi^+}(-\infty^-, 0)$
   - an incoming antiquark: $v_i^{(a)} \to \mathcal{L}_{ij}^{0_T,\,\xi^+}(0^-, -\infty^-)v_j^{(a)}$

- an incoming gluon: $\epsilon_b^{(a)\mathrm{in}\dagger} t_{ij}^{(b)} \to \mathcal{L}_{ik}^{0_T,\,\xi^+}(0^-,-\infty^-)\epsilon_b^{(a)\mathrm{in}\dagger} t_{kl}^{(b)} \mathcal{L}_{lj}^{0_T,\,\xi^+}(-\infty^-,0^-)$

   and replaces 0 by ξ when considering a quark fragmentation or antiquark distribution correlator.

4. Using that $u_b^{(r)} = \delta_{rb}$, $\epsilon_b^{(r)} = \delta_{rb}$, etc., simplify the obtained expression. At this point it is essential to sum over the colors of the other external partons. In the final expression the transverse gauge link pieces are included which can be done uniquely.

5. Divide the expression by the normalization which can be obtained by replacing all $\mathcal{L}$'s by 1 and Φ by $1/3$.

6. The result is the gauge link of the considered correlator.

To illuminate this set of rules three examples with explicit results will be given.

Example: Drell-Yan

We will reconsider the gauge link in the distribution correlator in Drell-Yan. The parent hadron is assumed to be moving mainly in the n_+-direction. The result of each step of the prescription is as follows:

1 : $\sigma = K\,\mathrm{Tr}^C\,[\Phi[v^{(r)}(k)v^{(r)\dagger}(k)]]$, where K is some constant. In analogy with Dirac spinors one has in this trace $[v^{(r)}(k)v^{(r)\dagger}(k)]_{ij} \equiv v_i^{(r)}(k)v_j^{(r)\dagger}(k)$.

2 : $\sigma = K\,\mathrm{Tr}^C\,[\Phi[v^{(r)}(k)v^{(r)\dagger}(k)]\mathcal{L}^{\xi_T,\,\xi^+}(-\infty^-,\xi^-)]$.

3 : $\sigma = K\,\mathrm{Tr}^C\,[\Phi\mathcal{L}^{0_T,\,\xi^+}(0^-,-\infty^-)[v^{(r)}(k)v^{(r)\dagger}(k)]\mathcal{L}^{\xi_T,\,\xi^+}(-\infty^-,\xi^-)]$.

4 : $\sigma = K\,\mathrm{Tr}^C[\Phi\mathcal{L}^{0_T,\,\xi^+}(0^-,-\infty^-)\mathcal{L}^{\xi_T,\,\xi^+}(-\infty^-,\xi^-)] = K\,\mathrm{Tr}^C[\Phi\mathcal{L}^{[-]}(0,\xi^-)]$,

where in the last step the transverse gauge link was included.

5 : normalization is K.

6 : the gauge link is $\mathcal{L}^{[-]}(0,\xi^-)$.

Example: Drell-Yan and gluon-jet

In this example the gauge link is calculated for a distribution correlator (with parent hadron along n_+) in Drell-Yan with an extra gluon-jet in the final state, see for instance

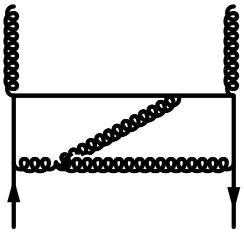

Figure 4.7: A tree-level diagram contributing to three jet-production.

Fig. 4.4b. The results read:

$$
\begin{aligned}
1 &: \sigma = K\,\mathrm{Tr}^C\,[\Phi t_b[v^{(r)}(k)v^{(r)\dagger}(k)]t_a]\epsilon_b^{(s)\mathrm{out}}\epsilon_a^{(s)\mathrm{out}\dagger}.\\
2 &: \sigma = K\,\mathrm{Tr}^C\,[\Phi t_b[v^{(r)}(k)v^{(r)\dagger}(k)]\mathcal{L}^{\xi_T,\,\xi^+}(-\infty^-,\xi^-)\\
&\qquad \times\mathcal{L}^{\xi_T,\,\xi^+}(\xi^-,\infty^-)t_a\mathcal{L}^{\xi_T,\,\xi^+}(\infty^-,\xi^-)]\epsilon_b^{(s)\mathrm{out}}\epsilon_a^{(s)\mathrm{out}\dagger}.\\
3 &: \sigma = K\,\mathrm{Tr}^C\,[\Phi\mathcal{L}^{0_T,\,\xi^+}(0^-,\infty^-)t_b\mathcal{L}^{0_T,\,\xi^+}(\infty^-,0^-)\mathcal{L}^{0_T,\,\xi^+}(0^-,-\infty^-)\\
&\qquad \times[v^{(r)}(k)v^{(r)\dagger}(k)]\mathcal{L}^{\xi_T,\,\xi^+}(-\infty^-,\xi^-)\mathcal{L}^{\xi_T,\,\xi^+}(\xi^-,\infty^-)t_a\mathcal{L}^{\xi_T,\,\xi^+}(\infty^-,\xi^-)]\epsilon_b^{(s)\mathrm{out}}\epsilon_a^{(s)\mathrm{out}\dagger}.\\
4 &: \sigma = (K/2)\,\mathrm{Tr}^C[\Phi\mathcal{L}^{[+]}(0,\xi^-)]\,\mathrm{Tr}^C[\mathcal{L}^{[\Box]\dagger}(0,\xi^-)] - \frac{K}{6}\,\mathrm{Tr}^C[\Phi\mathcal{L}^{[-]}(0,\xi^-)].\\
5 &: \text{normalization is } \frac{4}{3}\,K.\\
6 &: \text{the gauge link is } \frac{3}{8}\mathcal{L}^{[+]}(0,\xi^-)\,\mathrm{Tr}^C[\mathcal{L}^{[\Box]\dagger}(0,\xi^-)] - \frac{1}{8}\mathcal{L}^{[-]}(0,\xi^-).
\end{aligned}
$$

Example: Three jet-production in hadron-hadron collisions

In this example we consider the gauge link for the distribution correlator, with parent hadron along n_+, attached to the lower quark-lines in the diagram in Fig. 4.7. This diagram contributes to three jet-production in hadron-hadron collisions. The results read:

$$
\begin{aligned}
1 : \sigma &= iK\,\mathrm{Tr}^C[\Phi t_a t_b t_c u^\dagger u t_d t_e]\,f^{efg}\epsilon_f^{(h)\mathrm{out}\dagger}\epsilon_g^{(i)\mathrm{out}\dagger}\epsilon_d^{(j)\mathrm{in}}\epsilon_a^{(h)\mathrm{out}}\epsilon_c^{(i)\mathrm{out}}\epsilon_b^{(j)\mathrm{in}\dagger}\\
&= K\,\mathrm{Tr}^C\,[\Phi t_a t_b t_c[u^\dagger u]t_d[t_f,t_g]]\epsilon_f^{(h)\mathrm{out}\dagger}\epsilon_g^{(i)\mathrm{out}\dagger}\epsilon_d^{(j)\mathrm{in}}\epsilon_a^{(h)\mathrm{out}}\epsilon_c^{(i)\mathrm{out}}\epsilon_b^{(j)\mathrm{in}\dagger}.
\end{aligned}
$$

$$2:\sigma = K\,\mathrm{Tr}^C[\Phi t_a t_b t_c[u^\dagger u]\mathcal{L}^{\xi_T,\,\xi^+}(\infty^-,-\infty^-)t_d\mathcal{L}^{\xi_T,\,\xi^+}(-\infty^-,\infty^-)[t_f,t_g]\mathcal{L}^{\xi_T,\,\xi^+}(\infty^-,\xi^-)]$$

$$\times\,\epsilon_f^{(h)\mathrm{out}\dagger}\epsilon_g^{(i)\mathrm{out}\dagger}\epsilon_d^{(j)\mathrm{in}}\epsilon_a^{(h)\mathrm{out}}\epsilon_c^{(i)\mathrm{out}}\epsilon_b^{(j)\mathrm{in}\dagger},$$

$$3:\sigma = K\,\mathrm{Tr}^C[\Phi\mathcal{L}^{0_T,\,\xi^+}(0^-,\infty^-)t_a\mathcal{L}^{0_T,\,\xi^+}(\infty^-,-\infty^-)t_b\mathcal{L}^{0_T,\,\xi^+}(-\infty^-,\infty^-)t_c[u^\dagger u]$$

$$\times\,\mathcal{L}^{\xi_T,\,\xi^+}(\infty^-,-\infty^-)t_d\mathcal{L}^{\xi_T,\,\xi^+}(-\infty^-,\infty^-)[t_f,t_g]\mathcal{L}^{\xi_T,\,\xi^+}(\infty^-,\xi^-)]$$

$$\times\,\epsilon_f^{(h)\mathrm{out}\dagger}\epsilon_g^{(i)\mathrm{out}\dagger}\epsilon_d^{(j)\mathrm{in}}\epsilon_a^{(h)\mathrm{out}}\epsilon_c^{(i)\mathrm{out}}\epsilon_b^{(j)\mathrm{in}\dagger}.$$

$$4:\sigma = \frac{-K}{24}\,\mathrm{Tr}^C\left[\Phi\mathcal{L}^{[+]}(0,\xi^-)\right] + \frac{K}{8}\,\mathrm{Tr}^C\left[\Phi\mathcal{L}^{[+]}(0,\xi^-)\mathcal{L}^{[\Box]}(0,\xi^-)\right]\mathrm{Tr}^C\left[\mathcal{L}^{[\Box]\dagger}(0,\xi^-)\right].$$

5 : normalization is $K/3$.

6 : gauge link is $\dfrac{-1}{8}\mathcal{L}^{[+]}(0,\xi^-) + \dfrac{3}{8}\mathcal{L}^{[+]}(0,\xi^-)\mathcal{L}^{[\Box]}(0,\xi^-)\,\mathrm{Tr}^C\left[\mathcal{L}^{[\Box]\dagger}(0,\xi^-)\right]$.

4.2 Relating correlators with different gauge links

The gauge invariant correlators, appearing in the diagrams, will here be related to the correlators introduced in chapter 2. We will find that the T-odd functions, appearing in different diagrams, can in general differ by more than just a sign.

The gauge link structure consists in general of several terms of which each term consists of a link ($\mathcal{L}^{[+]}$ or $\mathcal{L}^{[-]}$) multiplied by some traces of gauge loops. After an integration over the transverse momentum of a correlator these gauge links collapse on the light-cone, one remains with a simple straight gauge link. The transverse momentum integrated distribution and fragmentation functions are therefore universal[6].

To treat the first transverse moment of T-even distribution functions, one can use time-reversal to project out the T-even structure of the unintegrated correlator. This enables one to write the T-even part of the correlator as the average of itself and the correlator having the time-reversed gauge link ($\infty \leftrightarrow -\infty$, as done in Eq. 2.62). Using the identities in Eq. 2.70, which also gives the relation (based on $\mathrm{Tr}^C\, t_a = 0$)

$$\partial^\alpha_{\xi_T}\,\mathrm{Tr}^C\left[\mathcal{L}^{[\Box]}(0,\xi^-)\right]\Big|_{\xi_T=0} = 0, \tag{4.20}$$

one can show that the first transverse moment of the unintegrated correlator is link-independent. The first transverse moment of T-even distribution functions is therefore universal.

The first transverse moment of T-odd distribution functions having some gauge link is treated analogously. The T-odd part of the correlator is projected out by taking the difference of itself and the time-reversed one (see for example Eq. 2.63). Using the identities in Eq. 2.70 and Eq. 4.20 one can show that the first transverse moment of a T-odd distribution correlator equals the T-odd correlator as defined in Eq. 2.63 up to a constant. Therefore one can relate the first transverse moment of T-odd distribution functions to the ones appearing in semi-inclusive DIS.

---

[6] In a fragmentation correlator the gauge links appear in two different matrix elements. To show the universality of integrated fragmentation correlators with an arbitrary gauge link, one can choose the light-cone gauge.

For example, let us consider the first transverse moment of the T-odd part of a distribution correlator containing the gauge link: $\mathcal{L}' = \frac{3}{8}\mathcal{L}^{[+]}(0,\xi^-)\,\mathrm{Tr}^C[\mathcal{L}^{[\square]\dagger}(0,\xi^-)] - \frac{1}{8}\mathcal{L}^{[-]}(0,\xi^-)$. Using time reversal the first transverse moment reads as follows [37]

$$\begin{aligned}
\Phi_{\partial}^{[\text{T-odd}]\mathcal{L}'\alpha} &= \frac{1}{2}\int \mathrm{d}^2p_T\; p_T^\alpha \int \frac{\mathrm{d}\xi^-\,\mathrm{d}^2\xi_T}{(2\pi)^3}e^{ip\xi} \\
&\times\Big(\langle P,S\,|\overline{\psi}(0)[\tfrac{3}{8}\mathcal{L}^{[+]}(0,\xi^-)\,\mathrm{Tr}^C[\mathcal{L}^{[\square]\dagger}(0,\xi^-)] - \tfrac{1}{8}\mathcal{L}^{[-]}(0,\xi^-)]\psi(\xi)|P,S\,\rangle_{\mathrm{c}} \\
&\quad - \langle P,S\,|\overline{\psi}(0)[\tfrac{3}{8}\mathcal{L}^{[-]}(0,\xi^-)\,\mathrm{Tr}^C[\mathcal{L}^{[\square]}(0,\xi^-)] - \tfrac{1}{8}\mathcal{L}^{[+]}(0,\xi^-)]\psi(\xi)|P,S\,\rangle_{\mathrm{c}}\Big)\Big|_{\substack{\xi^+=0\\ p^+=xP^+}} \\
&= \frac{5}{4}\Phi_{\partial}^{[\text{T-odd}]\alpha}
\end{aligned} \qquad (4.21)$$

The above expression is equivalent to $\frac{5}{4}$ times the first transverse moment of the T-odd correlator as defined in Eq. 2.63. The first transverse moment of the T-odd functions (like the Sivers function $f_{1T}^{\perp(1)}$) is therefore $\frac{5}{4}$-times the T-odd function which is measured in semi-inclusive DIS.

For fragmentation functions the interplay of the two possible mechanisms for T-odd effects created the problem for comparing the fragmentation functions in semi-inclusive DIS with the functions in electron-positron annihilation. The first transverse moment of those fragmentation functions read

$$\begin{aligned}
\Delta_{\partial}^{[\pm]\alpha}(z^{-1}) &= \frac{1}{3}\sum_X\int\frac{\mathrm{d}^3\mathbf{P}_X}{(2\pi)^3 2E_{\mathbf{P}_X}}\int\frac{\mathrm{d}\xi^+}{2\pi}e^{iP_h^-\xi^+/z}\,{}_{\text{out}}\langle P_h,P_X|\overline{\psi}(0)\mathcal{L}^{0_T,\xi^-}(0^+,\pm\infty^+)|\Omega\rangle_{\mathrm{c}} \\
&\times\langle\Omega|\Bigg[(-g)\int_{\pm\infty}^{\xi^+}\mathrm{d}\eta^+\;\mathcal{L}^{0_T,\,\xi^-}(\pm\infty^+,\eta^+)G_T^{-\alpha}(\eta)\mathcal{L}^{0_T,\,\xi^+}(\eta^+,\xi^+) \\
&\qquad + \mathcal{L}^{0_T,\,\xi^-}(\pm\infty^+,\xi^+)iD_T^\alpha\Bigg]\psi(\xi)|P_h,P_X\rangle_{\text{out,c}}\Big|_{\substack{\eta^-=\xi^-=0\\ \eta_T=\xi_T=0}}.
\end{aligned} \qquad (4.22)$$

By making comparisons in the light-cone gauge, the first transverse moment of a fragmentation correlator with some gauge link can be expressed in the transverse moments of the fragmentation functions appearing in semi-inclusive DIS and electron-positron annihilation.

As an example, let us consider the correlator with the gauge link structure $\mathcal{L}' =$

a:

Fig. 4.2a	Fig. 4.3a	Fig. 4.3b	Fig. 4.3c	Fig. 4.3d
1/2	−3/2	−3/4	5/4	5/4

b:

Fig. 4.2a	Fig. 4.3a	Fig. 4.3b	Fig. 4.3c	Fig. 4.3d
−1/2	3/2	3/4	−5/4	−5/4

Table 4.2: The comparison of functions having complex gauge links with the functions measured in semi-inclusive DIS and electron-positron annihilation. The factors in the table are obtained by joggling with color matrices. The factors are thus effectively a function of N_c.
a: The factors for T-odd distribution functions. The first moment of a T-odd function appearing Fig. 4.2 and Fig. 4.3 is the T-odd function of semi-inclusive DIS multiplied by the given factor. So $\Phi^{[\text{T-odd}]\alpha}_{\text{Fig.}(\ldots)\partial} = \text{factor} \times \Phi^{[\text{T-odd}]\alpha}_{\partial}$.
b: The factors for T-even and T-odd fragmentation functions, the first transverse moment of the functions in Fig. 4.2, and Fig. 4.3 can be written as a linear combination of the functions appearing in electron-positron annihilation and semi-inclusive DIS. So $\Delta_{\text{Fig.}(\ldots)}{}^{\alpha}_{\partial} = (\Delta^{[+]}{}^{\alpha}_{\partial} + \Delta^{[-]}{}^{\alpha}_{\partial})/2 + \text{factor} \times (\Delta^{[+]}{}^{\alpha}_{\partial} - \Delta^{[-]}{}^{\alpha}_{\partial})/2$.

$\mathcal{L}^{[\Box]}(0,\xi^+)\mathcal{L}^{[+]}(0,\xi^+)$. When taking its first transverse moment one obtains

$$\begin{aligned}
\Delta^{\mathcal{L}'\alpha}_{\partial}(z^{-1}) = {}& \frac{1}{3}\sum_X \int \frac{d^3\mathbf{P}_X}{(2\pi)^3 2E_{\mathbf{P}_X}} \int \frac{d\xi^+}{2\pi} e^{iP_h^-\xi^+/z} \\
&\times {}_{\text{out}}\langle P_h, P_X|\overline{\psi}_a(0)\mathcal{L}^{0_T,\,\xi^-}_{ab}(0^+,\infty^+)\mathcal{L}^{0_T,\,\xi^-}_{ef}(-\infty^+,\infty^+)|\Omega\rangle_{\text{c}} \\
&\times \langle\Omega|\Bigg[(-g)\int_{\infty}^{-\infty} d\eta^+\, \mathcal{L}^{0_T,\,\xi^-}_{bc}(\infty^+,\eta^+)G^{-\alpha}_{cd}(\eta)\mathcal{L}^{0_T,\,\xi^-}_{de}(\eta^+,-\infty^+)\mathcal{L}^{0_T,\,\xi^-}_{fg}(\infty^+,\xi^+) \\
&+ \mathcal{L}^{0_T,\,\xi^-}_{be}(\infty^+,-\infty^+)(-g)\int_{\infty}^{\xi^+} d\eta^+\, \mathcal{L}^{0_T,\,\xi^-}_{fc}(\infty^+,\eta^+)G^{-\alpha}_{cd}(\eta)\mathcal{L}^{0_T,\,\xi^-}_{dg}(\eta^+,\xi^+) \\
&+ \mathcal{L}^{0_T,\,\xi^-}_{be}(\infty^+,-\infty^+)\mathcal{L}^{0_T,\,\xi^-}_{fg}(\infty^+,\xi^+)iD^{\alpha}\Bigg]\psi_g(\xi)|P_h, P_X\rangle_{\text{out,c}}\Big|_{\substack{\eta^-=\xi^-=0 \\ \eta_T=\xi_T=0}}.
\end{aligned} \tag{4.23}$$

By comparing this expression to $\Delta^{[\pm]}_{\partial}$ in the light-cone gauge one finds

$$\Delta^{\mathcal{L}'\alpha}_{\partial}(z^{-1}) = 2\Delta^{[+]\alpha}_{\partial}(z^{-1}) - \Delta^{[-]\alpha}_{\partial}(z^{-1}). \tag{4.24}$$

The above expression states that the functions with this particular gauge link are equivalent to twice the functions measured in electron-positron annihilation minus the functions which are measured in semi-inclusive DIS. That relation holds for T-even and T-odd fragmentation functions.

Using the method as given above, the functions appearing in quark-quark scattering can be compared with the functions appearing in semi-inclusive DIS and electron-positron annihilation. The results are given in table 4.2.

In this section it was shown how the integrated functions and the first transverse moments can be compared with the functions in semi-inclusive DIS and electron-positron annihilation. For the higher transverse moments this comparison is not always possible. In those higher moments new matrix elements are encountered which do not appear in semi-inclusive DIS or electron-positron annihilation.

4.3 Unitarity in two-gluon production

The gauge link does not only depend on the process but also depends on the diagram, forming a potential danger for unitarity. If a theory is unitary then the cross section for the production of nonphysical boson polarizations is canceled by the cross section for the production of ghosts and antighosts. The fact that QCD is an unitary theory is not trivially to see. In Ref. [17, 158] 't Hooft and Veltman showed that in the sum over all diagrams unitarity is maintained to all orders in QCD. Having different gauge links (and thus different functions) for each squared amplitude diagram, it is not clear whether the approach still obeys unitarity. In this section it will be argued at lowest order in α_S that including a gauge link in the correlators does not produce nonphysical polarizations in two-gluon production in quark-antiquark scattering. This may be considered as a firm consistency check. Before starting the gauge link calculation let us review, without the gauge link, the unitarity proof for this process to some extent.

Consider the gluon-production amplitude of the process

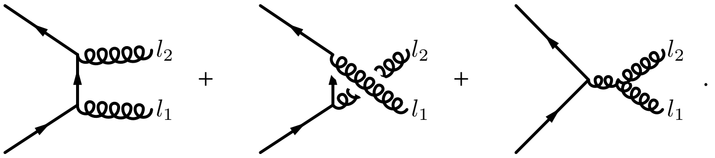

(4.25)

When squaring this amplitude there are nonphysical polarizations contributing in the Feynman gauge. In the complete square those polarizations have either $\epsilon(l_1)$ being forwardly polarized ($\epsilon^\alpha(l) \sim l^\alpha$) and $\epsilon(l_2)$ being backwardly polarized ($\epsilon^\alpha(l) \sim \bar{l}^\alpha$, the bar denotes reversal of spatial components), or vice versa. Together they contribute to the cross section as

$$\left|\text{Eq. (4.25)}\right|^2 = 2\bar{v}(k)\not{l}_2 t_d u(p) \frac{f^{dab}}{(l_1+l_2)^2} \left[\bar{v}(k)\not{l}_1 t_{d'} u(p) \frac{f^{d'ba}}{(l_1+l_2)^2}\right]^\dagger . \tag{4.26}$$

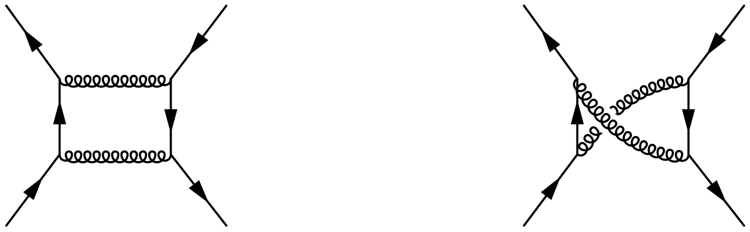

$$\frac{1}{64}\mathcal{L}^{[-]}(0,\xi^-) + \frac{21}{64}\mathcal{L}^{[+]}(0,\xi^-)\,\mathrm{Tr}^C\,\mathcal{L}^{[\Box]\dagger}(0,\xi^-)$$

$$-\frac{5}{4}\mathcal{L}^{[-]}(0,\xi^-) + \frac{3}{4}\mathcal{L}^{[+]}(0,\xi^-)\,\mathrm{Tr}^C\,\mathcal{L}^{[\Box]\dagger}(0,\xi^-)$$

Figure 4.8: Two elementary scattering squared amplitude diagrams and the gauge links corresponding to the correlators attached to the quarks below (parent hadron is assumed to be moving along the n_+-direction). The gauge links are derived by applying the prescription of the previous section. As shown in this section, the prescription gives the correct result when the gluons crossing the cut have a physical polarization.

The ghost-production amplitude is

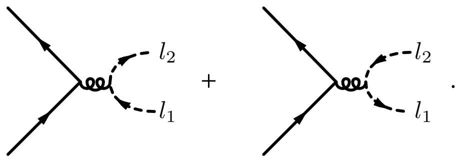

(4.27)

Taking the square of this amplitude exactly yields Eq. 4.26 with an opposite sign[7]. The cross section for the production of nonphysical polarizations is therefore canceled by the ghost and antighost contributions. One remains with purely transversely polarized outgoing gluons. This explicitly shows unitarity at this order in α_S.

Including the gluon insertions for the gauge link one finds in general different gauge links for different diagrams (see for instance Fig. 4.8). Having different gauge links for the diagrams and thereby also having different functions, it is a priory not clear whether such a cancellation between ghosts and nonphysical gluon polarizations still occurs. In the remainder of this section the rather technical argument will be briefly outlined that this is still the case. Important intermediate results are illustrated in Fig. 4.9 and Fig. 4.10. The reader who is not interested in the derivation of these results can skip the next paragraphs and can read the last paragraph of this section.

When inserting a gluon with momentum p_i on an outgoing gluon-line with momentum l and carrying the vector index α, the inserted vertex has the following form

---

[7] The opposite sign comes from the cut fermion loop.

$$-2l^- g^{\alpha'\alpha} + (l-p_i)^{\alpha'} n_+^{\alpha} + n_+^{\alpha'} l^{\alpha}, \tag{4.28}$$

where α' is contracted with the internal part of the amplitude. When considering multiple insertions, the terms of the inserted vertices, which are like the first term of Eq. 4.28, give back the same elementary amplitude diagram with gauge links according to the replacement rule as given in subsection 4.1.3 step 2 (this has been shown in subsection 4.1.2). Arising from multiple insertions, we also discussed in subsection 4.1.2 interference contributions between terms like the second and third term of Eq. 4.28. These interference terms are expected to cancel against insertions containing four-gluon vertices. Of all the insertions, this leaves us to discuss the vertices in which combinations between terms like the first term with the second or third term appear. Those combinations were canceled in semi-inclusive DIS and Drell-Yan in which an additional gluon was radiated, but they do not cancel in the present case.

Consider N gluon insertions in which the vertices contain $N-1$ terms are like the first term in Eq. 4.28 and one term like the third term in Eq. 4.28. This particular combination contributes as having the outgoing gluon being backwardly polarized (it becomes proportional to $l_1 \cdot \epsilon(l_1)$). Coupling this term to the conjugate amplitude leads to a forwardly polarized gluon on l_2 in the amplitude (see the discussion at the beginning of this section). In the sum over the amplitude diagrams only one non-vanishing contribution remains. This contribution comes from the diagram with the two triple-gluon vertices (like the third term of Eq. 4.25) and is proportional to $l_1^{\alpha'}$. It gets contracted with the inserted vertex $(n_+^{\alpha'} l_1^{\alpha})$, making this particular contribution proportional to $(-i)l^-/(-2l^- p_1^+ + i\epsilon)$ when the inserted gluon propagator (corresponding to this vertex) is included. When comparing this with the first term of Eq. 4.12 one finds that the contribution here is opposite in sign and is divided by a factor of 2. Being opposite in sign this contribution is as if we would have coupled the gluon to an antighost (with a ghost on l_2) giving $1/2$ times the N^{th} order expansion of the gauge link.

When considering N gluon insertions with $N-2$ terms like the first term of Eq. 4.28 and 2 terms like the third term of Eq. 4.28, one finds that this contribution can also be interpreted as coupling to an antighost multiplied with $-(1/2)^2$ times the N^{th} order expansion of the gauge link. Considering now N insertions and summing over all possible third terms (number m) and first terms (total number of combinations is $N!/(N!-m!)/m!$), one finds that this contributes as if we would have inserted gluons on an antighost but with the following factor in front of the N^{th} order expansion of the gauge link

$$\sum_{m=1}^{N} \frac{(-1)^{m+1}}{2^m}\, \frac{N!}{(N-m)!m!} = 1 - \left(\frac{1}{2}\right)^N . \tag{4.29}$$

Summarizing, when inserting gluons on the external gluon-line carrying momentum l_1 one encounters besides the discussed replacement rule several other terms. Some of these cancel when insertions with the four-gluon vertices are included. The others can be interpreted as insertions on an antighost-line (in the amplitude) with $1-2^{-N}$ times

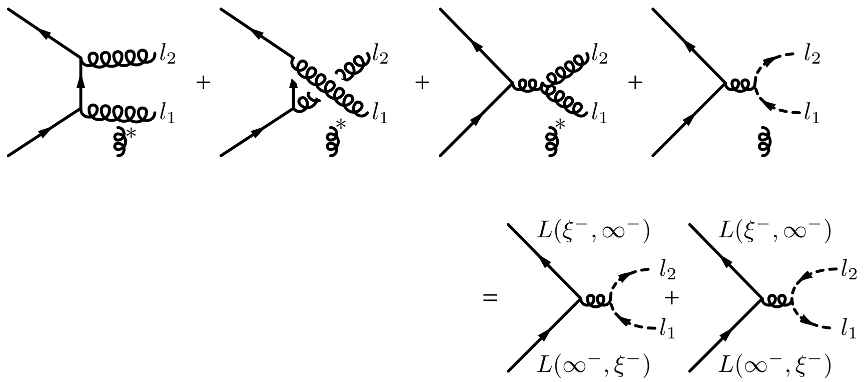

Figure 4.9: Illustration of the calculation. The $*$ indicates that of all the insertions on l_1 and l_2 only certain parts are included. Each of those parts consists of several (zero or more) terms like the first term of Eq. 4.28, and several terms (one or more) like the second *or* third term of Eq. 4.28.

the N^{th} order expansion of the gauge link. The replacement rule is similar as for the gluons.

Inserting N gluons on external ghost-lines and antighost-lines is relatively simple. One obtains the original amplitude diagram times the N^{th}-order expansion of the gauge link multiplied by $(1/2)^N$. The replacement rule is similar to the replacement rule as for insertions on external gluon-lines, but the factor $(1/2)^N$ at each order of the expansion prevents one forming a gauge link which would make the correlator gauge invariant. However, the insertions on an antighost-line together with the contributions of insertions on an external gluon-line, in which terms appear like the third of Eq. 4.28, can be recast into a ghost-antighost production diagram with a full gauge link ($(1/2)^N$+ Eq. 4.29 = 1).

The contributions, arising from insertions with terms like the second term of Eq. 4.28, work out in very similar way. Those terms can be interpreted as coupling to a ghost-line. Together with the insertions on a ghost-line the result can be written as the production of ghost-antighost multiplied with a full gauge link. The result of the above calculation has been represented in Fig. 4.9.

Summarizing, when inserting gluons in the two-gluon production amplitude, one obtains the gauge link for each amplitude diagram plus some additional terms. Part of these additional terms (interferences between the second and the third term of Eq. 4.28) should be canceled by four-gluon vertices as explained in subsection 4.1.2. The other terms together with the insertions on ghost-lines combine into full gauge links with an elementary ghost-antighost production-diagram. We remain now with the same set of elementary scattering diagrams in which gauge links according to the replacement rules appear. Those gauge links are at this moment not absorbed in the correlator. The result

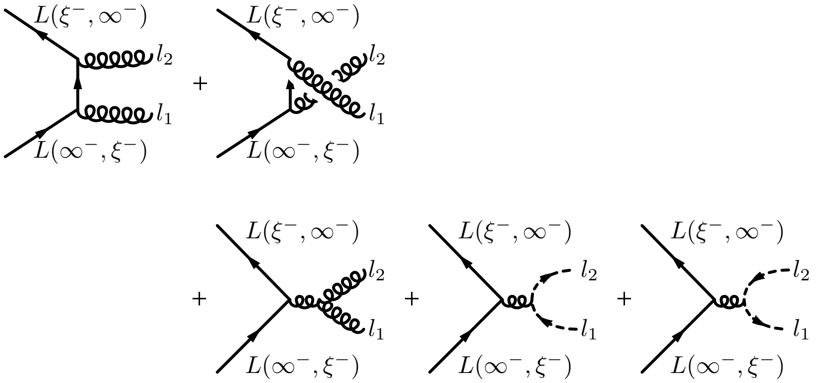

Figure 4.10: The result of the insertions on l_1 and l_2 on the amplitude level. In obtaining this result properties of the conjugate amplitude were used. In the diagrams it is indicated on which quark-lines the color matrices of the gauge links are standing.

is illustrated in Fig. 4.10.

Insertions in the conjugate part of the diagram yield the same result. Since the insertions do not modify the property that if one external gluon is forwardly polarized the other has to be backwardly polarized, one can even take combinations of insertions on the left-hand-side and on the right-hand-side of the cut and obtain the same result.

To show unitarity is now relatively straightforward. On the amplitude level, one can show that if one gluon has a nonphysical polarization, then the other gluon must have a nonphysical polarization as well in order to have a non-vanishing amplitude. This contribution, which comes from the diagram with the triple-gluon vertex, is canceled in the cross section by the ghost-antighost contributions, because the gauge link for ghost-antighost production is similar to the gauge link of that contribution. This shows for this example that the procedure of obtaining gauge links is consistent.

4.4 Gauge links in gluon-gluon correlators

In the description of evolution and in the treatment of hadron-hadron collisions, one encounters quark-quark correlators and gluon-gluon correlators. In this section the gauge links in gluon-gluon correlators will be studied. Defining transverse momentum dependent gluon distribution and fragmentation functions is a difficult task. In several articles this topic has been studied (see for instance Collins, Soper [111, 112], Rodrigues, Mulders [159], Burkardt [90], and Ji, Ma, Yuan [160]), but a definition, including hard-part-dependent gauge links as obtained for quark distribution functions, has not yet been derived on the basis of the diagrammatic expansion. Using the same techniques as for the quark distribution correlator and assuming the theory to be consistent, it is possible to “derive” gluon distribution correlators. Although one would rather like to show the consistency of the theory, the approach to be followed here provides at least some insight.

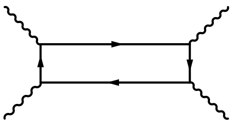

Figure 4.11: A contribution to photon photon-distribution scattering. The correlator is connected to the photons entering from the bottom of the graph.

Similarly as for the quark-quark correlator the photon-photon correlator can be derived using the LSZ-reduction formalism[8]. In the Coulomb gauge a photon-photon correlator without gauge link (appearing for instance in photon photon-distribution scattering, see Fig. 4.11) reads

$$\Phi^{\alpha\beta}_{AA}(x, p_T, P, S) = \int \frac{\mathrm{d}\xi^- \mathrm{d}^2\xi_T}{(2\pi)^3} e^{ip\xi} \times \langle P, S|A^\alpha(0)A^\beta(\xi)|P, S\rangle \Big|_{\substack{\xi^+=0\\ p^+=xP^+}} . \qquad (4.30)$$

Although this correlator is not gauge invariant, the expression for the cross section is actually already gauge invariant which can be seen as follows. Making a gauge transformation modifies Eq. 4.30 into

$$\Phi^{\alpha\beta}_{AA}(p, P, S) = \int \frac{\mathrm{d}\xi^- \mathrm{d}^2\xi_T}{(2\pi)^3} e^{ip\xi} \langle P, S|\Big(A^\alpha(0) + \partial^\alpha \Xi(0)\Big)\Big(A^\beta(\xi) + \partial^\beta \Xi(\xi)\Big)|P, S\rangle \Big|_{\substack{\xi^+=0\\ p^+=xP^+}} . \qquad (4.31)$$

When performing a partial integration the derivatives become proportional to the momentum p. These terms, however, do not show up in the cross section because they do not couple in the sum over all diagrams (Ward identity). The expression for the cross section is thus shown to be gauge invariant.

Being gauge invariant, the expression for the cross section can be compared to any other gauge invariant object. If they are the same in a certain gauge (for instance $\bar{n}(p) \cdot A = 0$), then they are the same in any gauge. This justifies the use of the correlator

$$\text{Eq. (4.30)} \rightarrow \int \frac{\mathrm{d}\xi^-\ \mathrm{d}^2\xi_T}{(2\pi)^3} e^{ip\xi} \bar{n}_\delta(p) \bar{n}_\gamma(p) \langle P, S|F^{\delta\alpha}(0) F^{\gamma\beta}(\xi)|P, S\rangle \Big|_{\substack{\xi^+=0\\ p^+=xP^+}} , \qquad (4.32)$$

with $n(p)^2 = 0$, $n(p) \sim p$, $\bar{n}(p) \cdot p = 1$. So by starting with a certain correlator connected to the cross section we were able to derive its gauge invariant form.

In general processes other kind of correlators appear, also containing gauge links. In principle these gauge links can be obtained by following the same procedure as outlined in the subsection 4.1.3 for the insertions. The result one obtains is the A-fields together with the presence of gauge links. Now to show to which gauge invariant expressions the obtained correlators correspond is more difficult than the previously considered case. The main problem is that one picks up a contribution of the gauge link when doing a partial integration as performed in Eq. 4.31. Such contributions are similar to the gluonic pole matrix elements which we also encountered for the quark-quark correlators. Since there is no reason to neglect those terms, this forms at present the main obstacle for obtaining gauge invariant gluon-gluon correlators.

---

[8] Identifying A-fields with partons is a complicated procedure in the LSZ-formalism in an arbitrary gauge (see for instance Itzykson, Zuber [161]). However, in the Coulomb gauge it is relatively simple, motivating the choice for this gauge.

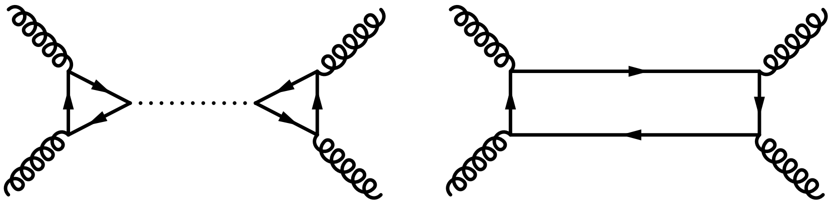

Figure 4.12: Two processes with gluon distribution functions attached to the gluons entering the graphs from the bottom. Figure (a) contributes to Higgs-production and figure (b) contributes to two jet-production in hadron-hadron scattering.

So how can one proceed? Well, one could argue that although it is not completely clear how to obtain the correlator in terms of the F-fields, the longitudinal gauge link as obtained by the presented rules should still be correct. If the approach is consistent then these longitudinal links should be closed at infinity by adding transverse gauge links, which can be done uniquely. In addition, if the cross section is gauge invariant (as it should be), then one can compare this expression in the light-cone gauge with any other gauge invariant expression. Comparing with the same expression, but with the A-fields replaced with the F-fields provides then a gauge invariant definition. It provides a solution for the moment, but more research is definitely needed here.

Using this approach one is able to obtain gauge invariant correlators. As an example, results will be given here for the two subprocesses illustrated in Fig. 4.12. Using the prescription of subsection 4.1.3 and factorizing the color matrices with which the gluons couple into the hard part, the gauge link for the diagram contributing to Higgs-production can be found to be[9] (Fig. 4.12a)

$$\begin{aligned}\Phi^{\alpha\beta}_{\text{Fig. (4.12)}a} = & 2\int \frac{\mathrm{d}\xi^-\,\mathrm{d}^2\xi_T}{(2\pi)^3}\,e^{ip\xi} \\ & \times \langle P,S\,|\,\mathrm{Tr}^C\Big[F^{+\beta}(0)\mathcal{L}^{[-]}(0,\xi^-)F^{+\alpha}(\xi)\left[\mathcal{L}^{[-]}(0,\xi^-)\right]^\dagger\Big]\,|P,S\,\rangle_{\mathrm{c}}\Big|_{\substack{\xi^+=0\\ p^+=xP^+}}\,. \end{aligned} \tag{4.33}$$

All matrices in the above expression are 3×3 matrices. This expression is equivalent to the result of Ji, Ma, and Yuan who study in Ref. [160] this particular process as a first step to factorization of effects from intrinsic transverse momentum in hadron-hadron collisions. The equivalence can be seen by the following relation $2\,\mathrm{Tr}^C[t_a\mathcal{L}^{[-]}(0,\xi^-)t_b\mathcal{L}^{[-]\dagger}(0,\xi^-)] = \mathcal{L}^{[-]}_{ab}(0,\xi^-)$ in which the A_l-fields on right-hand-side are contracted with the structure constants (if^{alb}) instead of the color matrices. In a sense this relation was obtained in subsection 4.1.2.

---

[9] In this diagram there is a virtual loop present which we have not considered before. In the next section we will study gauge links and loop corrections and we will argue that poles in the loop from insertions can be discarded.

Another example is the gauge link of a subprocess which contributes to two jet-production in hadron-hadron scattering (see Fig. 4.12b). The gauge invariant gluon-gluon correlator is found to be

$$\begin{aligned}\Phi^{\alpha\beta}_{\text{Fig. (4.12)}b} = 2\int \frac{\mathrm{d}\xi^-\,\mathrm{d}^2\xi_T}{(2\pi)^3}e^{ip\xi} \\ \times \langle P,S|\Bigg[\frac{3}{8}\,\mathrm{Tr}^C\Big[F^{+\alpha}(\xi)[\mathcal{L}^{[+]}(0,\xi^-)]^\dagger F^{+\beta}(0)\mathcal{L}^{[-]}(0,\xi^-)\Big]\,\mathrm{Tr}^C\Big[\mathcal{L}^{[\Box]}(0,\xi^-)\Big] \\ -\frac{1}{8}\,\mathrm{Tr}^C\Big[F^{+\alpha}(\xi)\mathcal{L}^{[+]\dagger}(0,\xi^-)F^{+\beta}(0)\mathcal{L}^{[+]}(0,\xi^-)\Big]\Bigg]|P,S\rangle_c\Big|_{\substack{\xi^+=0\\ p^+=xP^+}}.\end{aligned} \tag{4.34}$$

In this new result various gauge links via plus and minus infinity appear. It is not possible to rewrite this result in terms of gauge links in which only structure constants are used (as in the previous example).

In Ref. [90] Burkardt studied gluon distribution functions and suggested a sum rule for the Sivers quark and gluon distribution functions. It may be good to point out that those gluon distribution functions, containing gauge links via plus infinity, appear in semi-inclusive lepton-hadron scattering, like two-jet production. A contribution to that cross section would be Fig. 4.12b in which the incoming gluons from the top of the graph are replaced by incoming virtual photons.

In this section a method for obtaining gauge invariant gluon-gluon correlators has been suggested although a significant amount of work remains to be done. Note that one still needs to look for observables sensitive to the path of the gauge link. Those observables should be sensitive to the intrinsic transverse momenta of the gluons. One particular observable will be discussed for hadron-hadron scattering in the next chapter.

4.5 Factorization and universality

Up to now processes have been described by using the diagrammatic approach in which correlators were attached to an infinite number of hard scattering diagrams. These correlators, like Φ, Φ_A, and Δ_{AA}'s as defined in section 2.4, contained a certain renormalization scale and it has been assumed that these correlators could be factorized, enabling one to calculate in principle its scale dependence process-independently. We found at leading order in α_S that in several semi-inclusive processes, this infinite set of hard scattering diagrams and correlators combined into a finite set of diagrams convoluted with a finite set of gauge invariant correlators (containing a gauge link). Although the starting point was purely process-independent, it turned out that the hard scattering part determined the path of the gauge links in the final result. In this section the validity of the applied factorized approach will be discussed.

Whether processes allow for a factorized description has been studied for several decades. Ellis, Georgi, Machacek, Politzer, and Ross studied the issue of factorization for semi-inclusive DIS and Drell-Yan [162, 163]. By applying methods of Libby and Sterman [164, 165], Collins and Sterman were able to show in Ref. [166] to all orders in α_S that semi-inclusive electron-positron annihilation is free of infra-red divergences (divergences appearing in separate diagrams when momenta of virtual or radiated partons vanish, $l \to 0$). Subsequently, Collins and Soper introduced in Ref. [111, 112] infra-red free factorization formulas for electron-positron annihilation with two almost back-to-back hadrons being observed. Those factorization formulas were constructed at high q_T (order $-q_T^2 \sim q^2 = Q^2 \gg M^2$) and for fully integrated over q_T, where q_T is the transverse momentum of the virtual photon with respect to the observed hadrons. A factorization theorem for low q_T ($q_T^2 \sim -M^2$) was also proposed. In that theorem the infra-red part, coming from the vertex correction in which all momenta become soft, was factorized from the jets into a soft factor. In the same paper also an attempt was made to describe Drell-Yan, but a factorization theorem could not be obtained due to the interplay of final-state and initial-state interactions. Possible problems due to this interplay were also noticed by Doria, Frenkel, and Taylor [167].

The study on Drell-Yan was continued in several papers among which papers of Collins, Qiu, Soper, and Sterman [56, 104, 168, 169, 170, 171, 172], and Bodwin [173]. In the end it was believed that the problems of initial and final-state interactions were under control, because the interactions between spectators were expected to be on a longer time scale and should therefore vanish by unitarity[10]. This yielded fairly well established factorization theorems for q_T-integrated Drell-Yan and small q_T-unintegrated Drell-Yan [113]. In 1992 Collins included straightforwardly polarizations of participating hadrons into the factorization theorems [174] and suggested in Ref. [23] a factorization theorem for semi-inclusive DIS at small q_T.

In 2002, Brodsky, Hwang, and Schmidt showed that final-state interactions between spectators lead to single spin asymmetries in semi-inclusive DIS [24]. Based on this surprising result, Collins concluded that the studied interactions are actually on a shorter time-scale than it at first sight seems. He pointed out in Ref. [25] that such interactions could give problems for transverse momentum dependent factorization theorems (at small q_T) in Drell-Yan in which both initial and final-state interactions are present.

The discussion on factorization and universality for transverse momentum dependent cross sections was recently continued in several papers. In 2004, Ji, Ma, and Yuan argued and claimed in Ref. [175, 176] to have shown all order factorization theorems at small q_T for Drell-Yan and semi-inclusive DIS. A one loop calculation illustrated the factorization theorems, which was generalized to all orders by using power counting. Complications from combining final and initial-state interactions, which appear at two loops or higher (see for instance Fig. 4.13), were not explicitly addressed. Further, it was not discussed whether or not the fragmentation functions are process-independent.

By showing explicit results, it was subsequently pointed out in Ref. [37, 38, 39] that there could be a problem for the transverse momentum dependent factorization theorems at small q_T for semi-inclusive DIS and Drell-Yan. The problem appears due to the presence of the gauge link which has a non-expected behavior in processes in which there are initial and final QCD-states present (in the language of Ref. [101, 175, 176] this issue appears at two loops and higher). This will be elaborated upon in the next subsections.

---

[10] Being on a longer time scale it was not expected that those interactions could influence the short time scale production of the virtual photon.

The study on universality and factorization was continued by Collins and Metz [101]. Inspired by earlier work of Metz [100], the conclusion was drawn that the fragmentation process is universal for which an additional argument was provided (which was discussed in section 3.5). Universality of transverse momentum dependent distribution and fragmentation functions was consequently claimed for semi-inclusive DIS, electron-positron annihilation, and Drell-Yan, but the issue of final and initial-state interactions in Drell-Yan was not further illuminated.

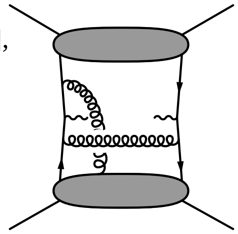

Figure 4.13: A combined initial and final-state interaction in Drell-Yan

The mentioned references use various starting points for the discussion of factorization, which prevents straightforward comparisons of their results. However, one important point, namely the coupling of almost collinear and longitudinally polarized gluons to various places in elementary diagrams yielding the gauge link, is obtained in essentially the same manner in all the approaches. Being similar, the results on this point should be equivalent. Another point in the discussion of factorization are the virtual corrections which have not been studied so far in this thesis. Therefore, we shall consider the vertex and self energy corrections in the next subsection. Together with the results on gauge links appearing in tree-level diagrams, the validity of factorization theorems for various processes will be discussed in the second subsection.

4.5.1 Virtual corrections

In this subsection gauge links will be discussed for diagrams in which virtual corrections appear. Intuitively one can already guess the outcome. Since virtual corrections do not modify the nature of the external particles (incoming or outgoing), one does not expect to find different gauge links for diagrams in which virtual corrections are included. In this subsection technical arguments for some specific cases in semi-inclusive DIS will be given to show that this idea indeed holds. It will be argued in the Feynman gauge that the first order expansion of the gauge link is the same as for the diagram in which the virtual correction is absent [38]. The conclusion drawn for semi-inclusive DIS also holds for Drell-Yan and semi-inclusive electron-positron annihilation. The first order expansion of the gauge link is sufficient to illustrate the complications related to factorization.

Vertex correction

We will begin by studying the problem in QED and then extend the result to QCD. There are three possible ways to insert a single photon with momentum p_1 to the vertex correction diagram (showing the integral over p_1 explicitly),

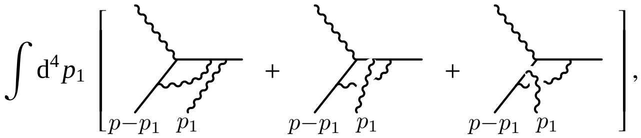

(4.35)

where the lines at the bottom of the graph are connected to the relevant part of the correlator $\Phi_A^+(p, p_1)$.

The momentum dependence p_1 can be routed back to the correlator via the photon propagator or via the electron propagators. We will choose here the latter. Having this p_1-dependence, the propagators contain poles in p_1^+ which can be evaluated by taking their residues. By introducing dashes for the taken residues, this pole calculation is made more explicit

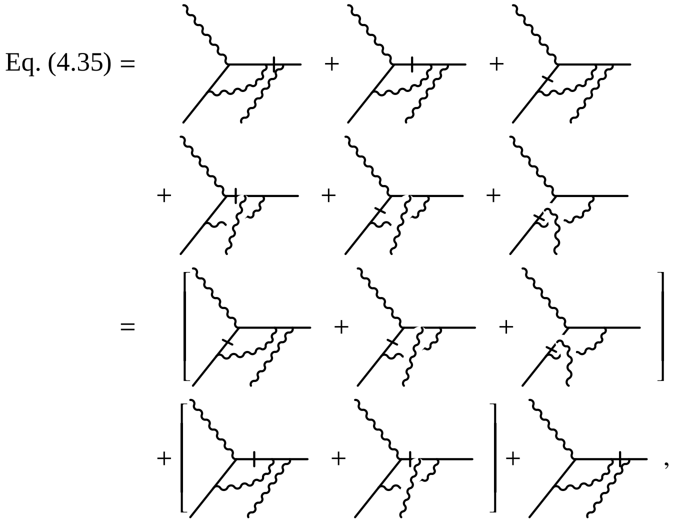

(4.36)

where the possibility that two propagators going simultaneously on shell has been discarded. It is fairly straightforward to show that the bracketed terms vanish by doing the calculation explicitly. The last diagram contains the pole on the external parton and yields the first order expansion of the gauge link.

This result will now be extended to QCD. The virtual photon and the inserted photon are replaced by gluons, and the electrons are replaced by quarks. The calculation is in QCD slightly different, because in the QCD-version of Eq. 4.36 the order of the color matrices in the bracketed terms is different. This can be solved by using the freedom on how to route the p_1-momentum through the loop, giving us the following identity

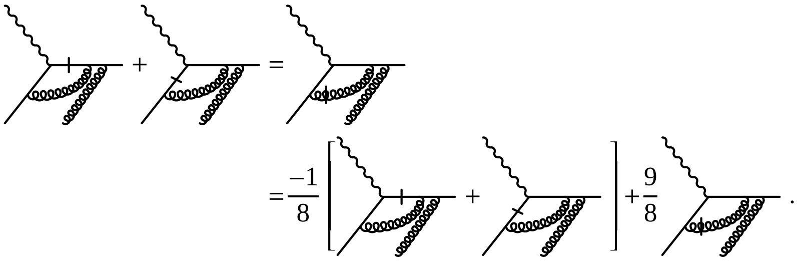

(4.37)

Substituting this identity in the QCD-version of Eq. 4.36 all bracketed terms (present in Eq. 4.36, 4.37) are canceled. We remain with the last diagram of the QCD-version of Eq. 4.36 (giving the first order of the gauge link), the last diagram of Eq. 4.37, and the diagram in which the gluon is inserted on the virtual gluon. The latter diagram contains the inserted vertex consisting of three terms: $-2l^- g^{\alpha'\alpha} + n_+^{\alpha'} l^\alpha + (l-p_1)^{\alpha'} n_+^\alpha$ (similarly to Eq. 4.28). The first term cancels the last diagram of Eq. 4.37, while the second and third terms are canceled by terms appearing in a similar way when treating the self energy corrections (see further below). The conclusion is that the first order of the gauge link for the vertex corrected diagram is similar to the uncorrected diagram.

Self energy correction

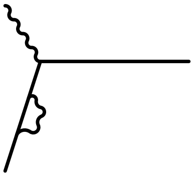

Figure 4.14: Self energy correction on the parton belonging to the correlator.

The calculation of the gauge link in a diagram in which the parton connected to the considered correlator has a self energy correction (see Fig. 4.14) is similar to the calculation of the vertex correction. It can be straightforwardly shown that the gauge link is the same as for the uncorrected diagram. The calculation for the diagram, in which the self energy correction is on the other external parton, is conceptually more difficult. That calculation will be presented here in more detail. We will begin with QED and then extend the result to QCD.

When taking a self energy diagram which is not directly connected to the considered correlator there are three possible places to insert a photon for the gauge link. This gives the following in terms of their residues

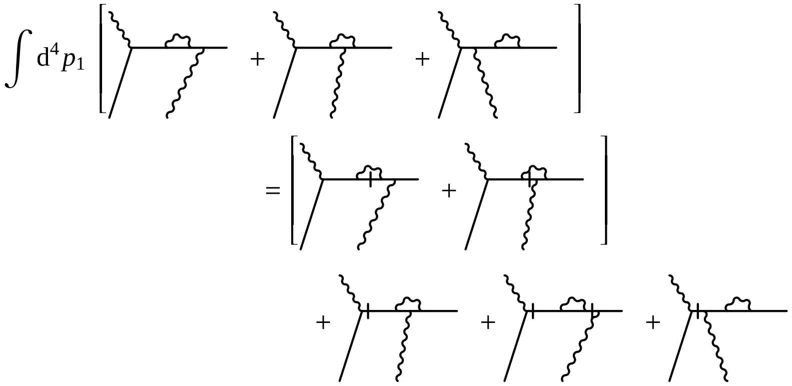

(4.38)

The term between brackets on the right-hand-side again cancels. The first of the three remaining terms can be calculated explicitly and yields the first order gauge link multiplied with $(-)\delta Z_2$ (δZ_2 is of order g^2). The second term is more difficult to calculate, because it contains a double pole. To circumvent this double pole problem we will exponentiate this diagram together with the last diagram.

Consider N (including $N = 0$) consecutive self energy loops on an electron-line. Inserting a single photon either before or after each loop and summing over N, the result can be written as product between two geometrical series of which one depends on p_1 and yields the first order gauge link expansion multiplied by Z_2, and the other just gives Z_2. Together, this gives the first order gauge link expansion multiplied with $Z_2^2 \approx 1 + 2\delta Z_2$. Note that in this sum also the first order link diagram without self energy correction is included. The total result of all insertions to order g^3 is the first order link expansion (order g) times δZ_2 (order g^2).

In QCD one has to route the momentum partly through the virtual gluon as done when treating the vertex correction. Similarly as for the vertex correction, one obtains the first order gauge link expansion for the sum over the insertions, but some terms remain which come from the insertion on the virtual gluon of the self energy correction. Similar results are achieved when the self energy correction is on the other parton leg (see Fig. 4.14). Together, the remaining terms of the self energy corrections cancel the remaining term produced by the vertex correction.

The conclusion is that the first order of the gauge link remains unchanged when including virtual corrections in semi-inclusive DIS. The same conclusions can be reached for semi-inclusive electron-positron annihilation and Drell-Yan.

4.5.2 Evolution, factorization, and universality

Scaling violations arise in a natural way when including higher order corrections in α_S. In this subsection α_S corrections in combination with gauge links will be discussed.

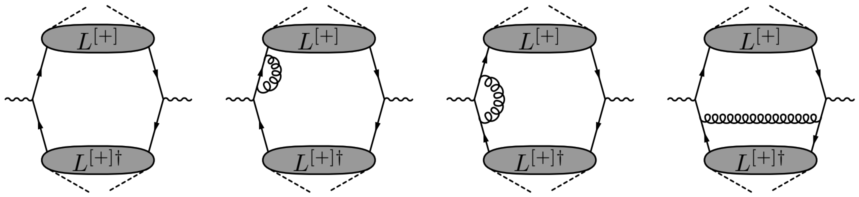

Figure 4.15: Various elementary scattering diagrams convoluted with gauge invariant correlators contributing to electron-positron annihilation. All corrections have correlators with gauge links via plus infinity. The derivation of those gauge links in similar to semi-inclusive DIS and Drell-Yan.

One of the corrections, which was not discussed, is the self energy correction of the inserted gluons (or gauge link). Since virtual corrections are not expected to modify the gauge link structure of the graph, it will be assumed that its result can be rewritten as a charge renormalization (α_S, see for related work Collins, Soper, Sterman [105]).

Semi-inclusive electron-positron annihilation

To compare the process at two different scales Q^2, corrections in α_S should be included. At order α_S there are various contributions of which some typical examples are given in Fig. 4.15. In the figures the gauge links are indicated which result from all gluon insertions in the elementary scattering diagram. The gauge links are in this case all the same. When constructing the correlators, gluon radiation was absorbed up to some scale we will call $\mu^2 \sim M^2$. When increasing the scale of the process, additional gluons will be radiated having a transverse momentum of at least μ^2. Since we are considering small q_T their transverse momenta cannot be to high (they should still be in the order of the hadronic scale). Although the gauge link was determined in subsection 4.1.2 for gluons having a large transverse momentum, the technical derivation for the gauge link is expected to be the same in the limit of $-l_T^2 \rightarrow \mu^2$. That conclusion can also be reached by following the general arguments as given in subsection 4.1.2.

When integrating over q_T and over the unobserved gluon (with momentum l) one finds at this order that the infra-red divergences[11] are canceled in the cross section, which is consistent with the result of Collins and Soper [111, 112]. When considering finite small q_T and integrating the unobserved gluon over a restricted region $\mathbf{l}_T^2 < \Lambda^2$, where Λ^2 is of some hadronic scale, the cancellation of infra-red divergences can also be found. It may be good to point out that if the radiated gluon is integrated over a restricted part of its full phase-space, the bilocal operators in the correlators are still off the light-cone and transverse momentum dependent effects (like T-odd effects) are still included. The factorized approach appears to be consistent. When constructing factorized correlators appearing in cross sections for small q_T, no problems are encountered in perturbation theory at this order in α_S. Since soft gluon radiation does not modify the original gauge links, ladder diagrams (like the last diagram in Fig. 4.15) can be included when constructing the correlators, giving them a scale-dependence.

---

[11] The infra-red divergences appear when $l \rightarrow 0$ in separate (hard) scattering diagrams which are convoluted with correlators. Following the general arguments of subsection 4.1.2, the gauge links depend on the nature of the external particles, giving every correlator a gauge link via plus infinity.

Drell-Yan

The situation is quite different for Drell-Yan. Considering α_S corrections in a similar way (see Fig. 4.16), one encounters various gauge links in the correlators for the corrections. Gluon insertions on the radiated gluon were included to obtain gauge invariant correlators. If the approach is to be consistent (gauge invariant) then those contributions *cannot* be neglected or circumvented unless there are additional analytical properties of the correlator[12]. Note that when the transverse momentum of the radiated gluon is of a hadronic size, the interactions appear at a similar time-scale as the insertions on the incoming antiquark in Drell-Yan or as the insertions on the outgoing quark in ordinary DIS.

The above results point to difficulties when calculating the scale-dependence of the overall process. When considering α_S corrections to compare different scales, the behavior of the correlators is different. Since brehmsstralung diagrams have different correlators then the tree-level diagram, the effect of this kind of radiation cannot be absorbed in a correlator or other constructed objects (like for instance a soft factor) in the approach followed here. The scale-dependence is thus significantly more difficult to calculate than in electron-positron annihilation. It should be noted that when simplifying this process to QED, the problem of the gauge links in combination with radiation does not appear. Since the photon does not carry any charge, the gauge links do not change when photon radiation is included. QCD has a different behavior here.

In the previous chapter, section 3.2, the equations of motion were applied in the calculation of gauge links. Considering the diagrams, it seems that when increasing the scale of the process, which produces more gluon radiation, the gauge links in the correlators get modified. If radiation effects can be absorbed into the correlators appearing in the factorized form $\Phi \otimes \overline{\Phi} \otimes H$, then it seems as if the equations of motion were applied in the wrong way, or that the equations of motion are not invariant under scale transformations[13]. Note that this problem does not appear when discussing electron-positron annihilation. In the following it will be indicated how this problem can be circumvented.

---

[12] For instance if T-odd distribution functions are zero or if gauge links are not an intrinsic property of the nucleon, but a vacuum effect instead.

[13] The same problem also appears in semi-inclusive DIS (see Fig. 3.2). When applying the equations of motion we assumed analytical properties of the gluon connecting the fragmentation correlator (it was assumed to be outgoing). This assumption could be invalid and may need improvement.

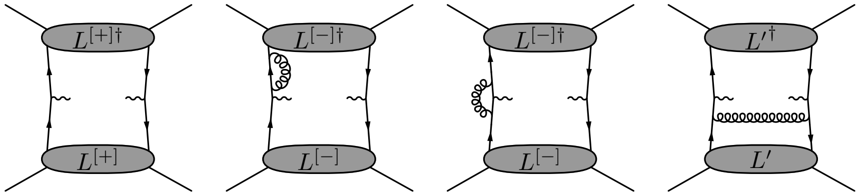

Figure 4.16: Various elementary scattering diagrams convoluted with gauge invariant correlators contributing in Drell-Yan. At this order in α_S, all virtual corrections have correlators with gauge links via minus infinity, while all real corrections have correlators with the gauge link $\mathcal{L}' = \frac{3}{8}\mathcal{L}^{[+]}\,\mathrm{Tr}^C\,\mathcal{L}^{[\square]\dagger} - \frac{1}{8}\mathcal{L}^{[-]}$.

We will try to construct the factorized correlator connected to the external partons which enter the process from above in perturbation theory, although this is strictly speaking not allowed. Constructing the correlator, the incoming hadron and its remnant is expanded in free parton states. Note that only the connected part of the diagrams needs to be considered. Since those partons are then essentially free, the gauge link in the lower correlator can be determined by using the results of the previous sections. For the subprocess in Drell-Yan in which partons, which cannot be absorbed in the lower correlator, do not cross the cut, one finds the gauge link for the lower correlator to run via minus infinity. However, if one of the partons, connected to the upper hadron, radiates a gluon to the final state (note that its energy depends of the process), then the gauge link in the lower correlator gets modified. So for each component of the Fock-state expansion of the upper correlator, one can calculate the gauge link for the lower correlator. However, each Fock-state component will have in general different gauge links, making the procedure unsuitable for constructing the upper correlator factorized from the rest of the process. This problem only appears for cross sections which are sensitive to intrinsic transverse momentum. After an integration over q_T, one finds at leading order in M/Q that all gauge links in the correlators are on the light-cone and run along straight paths between the two quark-fields (see Fig. 2.11a). In that case the problems with gauge links and factorization disappear.

The above arguments illustrate that even when applying perturbation theory and a simple Fock-state expansion one encounters difficulties with factorization theorems sensitive to the intrinsic transverse momentum. This problem originates from gluons which are inserted on both initial and final-state partons. Since this issue has not been explicitly discussed in Ref. [101, 175, 176], factorization for azimuthal asymmetries at small q_T remains an open question for Drell-Yan. These problems are not encountered when considering fully q_T-integrated factorization theorems at leading twist. In that case one finds that the infra-red divergences are canceled at this order in α_S. At subleading twist, the q_T-integrated factorization theorem contains correlators off the light-cone (see the previous chapter, appendix 3.A) and therefore it suffers from the

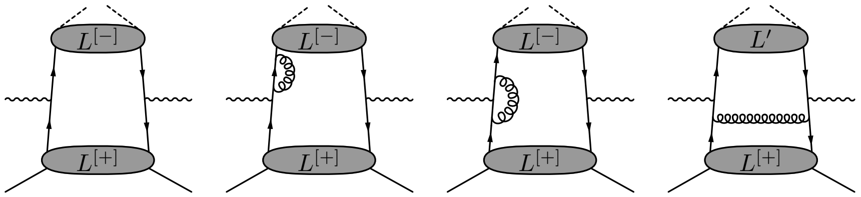

Figure 4.17: Various elementary scattering diagrams convoluted with gauge invariant correlators contributing in semi-inclusive DIS. At this order in α_S, the distribution correlator contains a gauge link via plus infinity. The virtual corrections have a fragmentation correlator with a gauge link via minus infinity, while all real corrections have a fragmentation correlator with the gauge link $\mathcal{L}' = \frac{3}{8}\mathcal{L}^{[+]}\mathcal{L}^{[\Box]\dagger} - \frac{1}{8}\mathcal{L}^{[-]}$.

same problems as for the transverse momentum dependent factorization theorem.

Semi-inclusive DIS

The situation of semi-inclusive DIS is similar to Drell-Yan (see also Fig. 4.17). The real α_S corrections modify the original link structure of the fragmentation correlator. This forms a problem for factorization theorems which include effects from intrinsic transverse momentum. The integrated cross section is still infra-red free at leading twist, but at subleading twist problems with factorization occur.

Concerning the construction of factorized correlators via a Fock-state expansion, when expanding the fragmentation correlator in free parton states one finds for each component the same gauge link in the distribution correlator. This points out that for (multiple) jet-production in DIS factorization theorems sensitive to intrinsic transverse momentum effects might be feasible. When expanding the distribution correlator in parton states, several partons will cross the cut which cannot be absorbed in the fragmentation correlator. These partons influence the gauge link structure which forms a problem for constructing the distribution correlator in semi-inclusive DIS.

It may be good to point out that if gluonic-pole matrix elements for fragmentation vanish, then the fragmentation process is universal (universality of fragmentation functions has been advocated by Collins and Metz [100, 101]). In that case the problem with gauge links in the fragmentation correlator does not exist and factorization theorems could be feasible.

As a final remark, in Ref. [175, 176] factorization has been discussed including M/Q effects. However, since contributions from gluons at M/Q have been discarded (the $\Phi_{\partial^{-1}G}$ and $\Delta_{\partial^{-1}G}$ terms of chapter 3), it is not clear whether the factorization theorems are complete as they stand.

4.6 Summary and conclusions

In this chapter gauge links appearing in more complicated diagrams were considered. When deriving those gauge links by considering gluon interactions between the correlators and the hard part, two classes of poles were encountered. The first class contains the poles $p_i^+ \approx 0$ which correspond to the limit in which the gluon momenta vanish. This class yields contributions to the gauge link. The second class contains the other poles and in the examples shown, those poles canceled. Supplementing general arguments in favor of this cancellation have been given and a set of rules has been conjectured that allows one to deduce gauge links for arbitrary diagrams. Applying these rules for gluon-gluon correlators, gauge invariant transverse momentum dependent gluon distribution functions were obtained. In a sense, these rules factorize interactions between a correlator and the elementary scattering part.

It was found that gauge links do in general not only depend on the overall process but also depend on the elementary scattering diagram. The encountered gauge links also had more complicated paths than the ones appearing in semi-inclusive DIS or Drell-Yan. To compare the correlators with these different gauge links, we considered the first transverse moments of distribution and fragmentation functions. It was found that these transverse moments can be related to the transverse moments appearing in semi-inclusive DIS and electron-positron annihilation. For the higher transverse moments no relations were obtained.

The fact that the gauge link in the correlator depends on the subprocess instead of the overall process could form a potential danger for the unitarity of the approach. However, in an explicit nontrivial example (two-gluon production) it was found that the factorized description in terms of gauge invariant correlators still respects unitarity.

We also discussed the subject of factorization and universality for semi-inclusive DIS, electron-positron annihilation, and Drell-Yan. In semi-inclusive electron-positron annihilation we did not encounter any inconsistencies because QCD-states appeared only in the final state. For semi-inclusive DIS and Drell-Yan there was in Ref. [101, 175, 176] recently important progress reported on small q_T-unintegrated[14] factorization theorems, but one particular issue of dealing with both final and initial-state interactions has not satisfactory been treated. This issue is related to the observation that gauge links in transverse momentum dependent correlators can get modified when considering radiation effects. This could create a problem for factorizing effects from intrinsic transverse momentum appearing in cross sections for semi-inclusive DIS and Drell-Yan. Since fully q_T-integrated factorization theorems contain at subleading twist effects from intrinsic transverse momentum (see appendix 3.A), it forms at that order a potential problem as well. Factorization of intrinsic transverse momentum dependent effects in Drell-Yan and semi-inclusive DIS remains therefore at present an open issue [39]. Similar problems also appear for semi-inclusive hadron-hadron scattering.

The non-Abelian character plays an essential role in the discussion of final and initial-state interactions. For instance, in QED where photons do not carry charge, photon radiation does not modify the gauge link structure. Although more complicated gauge links than the ones appearing in semi-inclusive DIS and Drell-Yan are still encountered, factorization of effects from intrinsic transverse momentum in hard QED scattering processes should be feasible.

---

[14] q is the momentum of the virtual photon and $-q_T^2 \sim M^2$

It may be good to point out that in QCD the problems for semi-inclusive DIS originate from the gauge link in the fragmentation correlator in combination with gluon radiation. If this gauge link turns out to be irrelevant (which means that gluonic-pole matrix elements for fragmentation functions would be suppressed), then the problems with factorizing effects from intrinsic transverse momentum disappear. In that scenario, which is favored by the in section 3.5 differently given interpretation of the results obtained by Collins and Metz [101], factorization theorems including effects from intrinsic transverse momentum might be obtainable. Such factorization theorems can also be expected to hold for (multiple) jet-production in DIS, because in those cases the problem with fragmentation functions is not present.

As a last remark, in the diagrammatic approach used in this thesis, no assumptions were made for the correlators other than the assumptions similar to the parton model (see chapter 2). Many issues might be unknown for that reason, one of them being the evolution equations for transverse momentum dependent functions (for a detailed study of this problem see Henneman [66]). It is possible that additional assumptions, which should be physically justified, might solve some of the issues. One possibility could be that gauge links in general do not influence the expectation values of matrix elements. In that case T-odd distribution functions would be zero and proofs on factorization and universality would be simplified significantly. Another possibility could be that gauge links correspond to certain interactions in the hard part in a particular kinematical limit (for instance the vertex correction in the limit that the gluon is collinear with one of the external quarks). In that case the gauge link is not an intrinsic property of the nucleon, allowing (part of) its contribution to be possibly absorbed in other matrix elements or factors.

5

Results for single spin asymmetries in hadronic scattering

In the previous chapter the necessary tools were developed to determine the Wilson lines which appear in correlators in hard scattering processes. As discussed, it is not clear whether effects from intrinsic transverse momentum allow for a factorized description in hadron-hadron scattering. We will assume it does and obtain results for single spin asymmetries. In these asymmetries the effect of the gauge link appears to be more than just a sign; it also determines the sizes of the asymmetries. It will be shown how the intrinsic transverse momenta of quarks can be accessed by observing unpolarized hadrons in opposite jets. For the ease of the calculation, only contributions from quark distribution and fragmentation functions will be considered. Gluon distribution and fragmentation functions are neglected, but can be straightforwardly incorporated by following the same procedure.

5.1 Introduction

We will study the transverse momentum dependent distribution and fragmentation functions via single spin asymmetries in hadron-hadron scattering. Within the applied diagrammatic approach, an odd number of T-odd functions is needed to produce cross sections for single spin asymmetries at leading order in α_S. At leading twist, T-odd functions are transverse momentum dependent. Integrated T-odd distribution functions are assumed to be zero and unpolarized integrated T-odd fragmentation functions appear only at subleading twist [99]. Single spin asymmetries at leading order in inverse powers of the hard scale must therefore arise from intrinsic transverse momenta.

The validity of the applied theoretical description depends on two issues. The first issue is connected to factorization. This was discussed in the previous chapter and in the present study it will be assumed to hold. The second issue is related to asymptotic freedom. It is expected that only those processes can be described perturbatively in which observed external hadrons are well separated in momentum space. The observed outgoing hadrons must have a large perpendicular momentum with respect to the beam-axis. For observed hadrons close to the beam-axis, one does not only have a problem with perturbation theory, but one will also encounter interference effects between the hard scattering process and the remnant of the incoming hadrons. In that case fracture functions need to be included.

One of the most studied semi-inclusive cross section in hadron-hadron collisions is single hadron production. It is also this process in which the first single spin asymmetries in inelastic collisions were observed [20]. Since then, single spin asymmetries have been measured in several processes (see for instance Ref. [177, 178, 179, 180, 181, 182, 183, 184]), and extensive theoretical studies have been made (see for instance Ref. [57, 72, 185, 186, 187, 188, 189, 190, 191]). The main theoretical challenge with single hadron production at large transverse momentum is that there is no observable which is directly connected to the intrinsic transverse momenta of the partons. This makes the extraction of the transverse momentum dependent functions complex. It could be that the only possible manner of extracting information is to consider a specific form for the transverse momentum dependence of distribution or fragmentation functions (for example $\exp[-k_T^2/M^2]$). Such a form can lead to problems with the gauge link because it generally contains higher order transverse moments. At present only the first transverse moment of functions can be easily related to the transverse moment of functions appearing in semi-inclusive DIS and electron-positron annihilation. In the higher transverse moments new matrix elements are involved which are more difficult to relate (see also section 4.2). Besides, for the higher transverse moments convergence becomes an issue as well.

The two hadron production process, in which the two hadrons belong to different jets and are approximately back-to-back in the perpendicular plane, does offer an observable directly sensitive to the intrinsic transverse momenta. The fact that the two hadrons are not completely back-to-back can at leading order in α_S be interpreted as an effect from intrinsic transverse momentum. This process will be studied in this chapter. Having obtained transverse target-spin asymmetries, a simple extension will be made to jet-jet production by just summing over the observed hadrons and observing the jet instead. This latter process has been studied by Boer and Vogelsang in Ref. [192] (see also Vogelsang, Yuan [193] for related work). The study here should be considered as an extension of Ref. [192] to hadron-hadron production including a full treatment of gauge links.

To find out what observables are present, let us reconsider the Drell-Yan process. The extraction of the intrinsic transverse momenta is connected with momentum conservation in the hard scattering cross section, which in the case of Drell-Yan is expressed by a four dimensional delta-function in Eq. 3.76. The presence of a hard scale, originating from the electromagnetic interaction involving two hadrons, allows for a Sudakov-decomposition. This enables one to eliminate two delta-functions, leading to the fixed light-cone momentum fractions x_1 and x_2. The remaining two-dimensional delta-function, $\delta^2(p_T{+}k_T{-}q_T)$ in Eq. 3.80, is directly connected to the intrinsic transverse momenta of quarks. Note that the momenta p_T and k_T are transverse with respect to their parent hadron. These momenta can be accessed by considering azimuthal asymmetries (see Drell-Yan in appendix 3.A).

In the hadron-hadron production process, there are four correlators and two hard scales present. If we use the large momentum difference of the initial hadrons to fix the perpendicular plane ($\perp$) and the light-cone momentum fractions of the initial quarks, then the remaining two dimensional delta-function reads $\delta^2(p_{1\perp}{+}p_{2\perp}{-}k_{1\perp}{-}k_{2\perp})$. The momentum $p_{i\perp}$ is already transverse with respect to its parent hadron, so $p_{1\perp}{=}p_{1T\perp}$. This is not the case for $k_{i\perp}$ because the momenta of the outgoing hadrons, K_i, have large perpendicular components. It is convenient to make the decomposition $k_i{=}K_i/z_i{+}k_{iT}$, where k_{iT} is defined to be transverse with respect to K_i and is of a hadronic scale. The large momentum difference between $K_{1\perp}$ and $K_{2\perp}$, which is still present in the two-dimensional delta-function, can then be used to fix one of the remaining light-cone momentum fractions, z_i. This leaves one delta-function behind which contains the non-back-to-backness and forms a natural observable as we will see. In the case of two-jet production there is no other light-cone momenta to fix. In that case the sum of the two jet momenta in the perpendicular plane is already proportional to the intrinsic transverse momenta of the partons, providing one a two-dimensional vector variable.

5.2 Calculating cross sections for hadronic scattering

The calculation for the cross sections will be outlined. After considering kinematics, observables will be defined which are sensitive to transverse momentum dependent functions. The cross sections will be expressed in an elementary hard scattering cross section, fragmentation functions, and distribution functions. Those functions are defined through bilocal matrix elements and contain a gauge link which depends on the squared amplitude diagram (which we also call subprocess). A simplification of the cross section will be achieved by introducing *gluonic-pole cross sections*. This enables one to express the cross section in simple hard scattering cross sections convoluted with the in chapter 2 defined distribution and fragmentation functions.

Kinematics

For the ease of the calculation we will work in the center of mass frame of the incoming hadrons. The incoming hadron with momentum P_1 fixes the direction of the z-axis and the spatial momenta which are perpendicular to this axis will carry the subscript $\perp$. The hadron with momentum P_2 enters the process from the opposite direction. A hard scale is set by $s \equiv (P_1 + P_2)^2$. The pseudo-rapidity is defined as $\eta_i \equiv -\ln(\tan(\theta_i/2))$, where θ_i is the polar angle of an outgoing hadron with respect to the beam-axis. We introduce a scaling variable $x_{i\perp}$ defined as $x_{i\perp} \equiv 2|\mathbf{K}_{i\perp}|/\sqrt{s}$, where K_i is the momentum of an observed outgoing hadron. These definitions yield the following relations

$$\begin{aligned} P_1 \cdot K_1 &= \tfrac{1}{4} s x_{1\perp} e^{-\eta_1} + \mathcal{O}(M^2), \qquad & P_2 \cdot K_1 &= \tfrac{1}{4} s x_{1\perp} e^{\eta_1} + \mathcal{O}(M^2), \\ P_1 \cdot K_2 &= \tfrac{1}{4} s x_{2\perp} e^{-\eta_2} + \mathcal{O}(M^2), \qquad & P_2 \cdot K_2 &= \tfrac{1}{4} s x_{2\perp} e^{\eta_2} + \mathcal{O}(M^2). \end{aligned} \tag{5.1}$$

The Mandelstam variables for the partons are defined as

$$\hat{s} \equiv (p_1 + p_2)^2, \qquad \hat{t} \equiv (p_1 - k_1)^2, \qquad \hat{u} \equiv (p_1 - k_2)^2, \tag{5.2}$$

and fulfill $\hat{s} + \hat{t} + \hat{u} = p_1^2 + p_2^2 + k_1^2 + k_2^2$. The variable y, which is observable and the analogue of the y variable used in semi-inclusive DIS, is defined to be

$$y \equiv \frac{-\hat{t}}{\hat{s}} = \frac{1}{\exp(\eta_1 - \eta_2) + 1} \left(1 + \mathcal{O}(M^2/s)\right). \tag{5.3}$$

Defining observables

Using the diagrammatic expansion (see also chapter 2) the cross section for two hadron production reads (ϕ_i's are the azimuthal angles of the observed hadrons)

$$\begin{aligned} \mathrm{d}\sigma =& \frac{1}{2s} \, \frac{d^3K_1}{(2\pi)^3\, 2E_{\mathbf{K}_1}} \, \frac{d^3K_2}{(2\pi)^3\, 2E_{\mathbf{K}_2}} \, \mathcal{A}^2 \\ =& \frac{x_{1\perp} x_{2\perp} s}{128(2\pi)^4} \mathrm{d}x_{1\perp}\, \mathrm{d}x_{2\perp}\, \mathrm{d}\eta_1\, \mathrm{d}\eta_2\, \frac{\mathrm{d}\phi_1}{2\pi} \, \frac{\mathrm{d}\phi_2}{2\pi} \, \mathcal{A}^2 \, \left(1 + O\left(\frac{M^2}{s}\right)\right), \end{aligned} \tag{5.4}$$

where $\mathcal{A}^2 = \sum_X \int \frac{d^3\mathbf{P}_X}{(2\pi)^3 2E_{\mathbf{P}_X}} (2\pi)^4 \delta(P_1{+}P_2{-}K_1{-}K_2{-}P_X)\ |\mathcal{M}|^2$ which is generically expressed as

$$\begin{aligned}\mathcal{A}^2 = \int \mathrm{d}^4p_1\ \mathrm{d}^4p_2\ \mathrm{d}^4k_1\ \mathrm{d}^4k_2\ \ (2\pi)^4\ \delta^4(p_1{+}p_2{-}k_1{-}k_2) \\ \times \mathrm{Tr}^{D,C}\left\{\Phi(p_1)\otimes\Phi(p_2)\otimes\Delta(k_1)\otimes\Delta(k_2)\right. \\ \left.\otimes H(p_1,p_2,k_1,k_2)\otimes H^*(p_1,p_2,k_1,k_2)\right\},\end{aligned} \quad (5.5)$$

suppressing the momenta and spins of parent hadrons. The symbol ⊗ represent a convolution in color and Dirac indices, and the hard elementary scattering amplitudes are denoted by H. The gauge links of the correlators can be derived by applying techniques developed in the previous chapter. Those gauge links depend in general on the subprocess.

Each of the external partons and its parent hadron have both a nearly light-like momentum in a more or less common direction (parton model assumption). The introduction of the light-like vectors, n_{P_i}, with $n_{P_i}\cdot\bar{n}_{P_i} = 1$ (bar denotes reversal of spatial components) such that n_{P_i} is proportional to P_i in the asymptotic limit, allows us to classify at which order components appear. The components $p_i\cdot\bar{n}_{P_i}$ appear at order $\sqrt{s}$ (and similarly for fragmentation), the spatial transverse components appear all at a hadronic scale. The light-like components which are left, $p_i\cdot n_{P_i}$, appear at order $M^2/\sqrt{s}$. Parton momentum fractions are defined as usual

$$x_i \equiv \frac{p_i\cdot\bar{n}_{P_i}}{P_i\cdot\bar{n}_{P_i}}, \qquad\qquad z_i \equiv \frac{K_i\cdot\bar{n}_{K_i}}{k_i\cdot\bar{n}_{K_i}}. \quad (5.6)$$

The light-cone momentum components $p_i{\cdot}n_{P_i}$ can be simply integrated because they are suppressed in the hard parts. The hard scale s can be used to fix the incoming light-cone momentum fractions, x_1 and x_2, in terms of z_1 and z_2. This gives

$$\begin{aligned}&\int \mathrm{d}^4p_1\ \mathrm{d}^4p_2\ \mathrm{d}^4k_1\ \mathrm{d}^4k_2\ \ \delta^4(p_1+p_2-k_1-k_2) \\ &=\frac{2}{s}\int \mathrm{d}(p_1\cdot\bar{n}_{P_1})\ \mathrm{d}(p_2\cdot\bar{n}_{P_2})\ \mathrm{d}(k_1\cdot\bar{n}_{K_1})\ \mathrm{d}(k_2\cdot\bar{n}_{K_2})\ \ \delta(x_1-\tfrac{2}{s}r\cdot P_2)\,\delta(x_2-\tfrac{2}{s}r\cdot P_1) \\ &\quad\times\int \mathrm{d}^2p_{1T}\ \mathrm{d}^2p_{2T}\ \mathrm{d}^2k_{1T}\ \mathrm{d}^2k_{2T}\ \delta^2(q_{T\perp}-r_\perp) \\ &\quad\times\int \mathrm{d}(p_1\cdot n_{P_1})\ \mathrm{d}(p_2\cdot n_{P_2})\ \mathrm{d}(k_1\cdot n_{K_1})\ \mathrm{d}(k_2\cdot n_{K_2})\ \Big(1+\mathcal{O}(M^2/s)\Big),\end{aligned} \quad (5.7)$$

$$\text{with} \qquad q_T \equiv p_{1T}+p_{2T}-k_{1T}-k_{2T}, \qquad\qquad r \equiv \frac{K_1}{z_1}+\frac{K_2}{z_2}. \quad (5.8)$$

The transverse parton momenta ($\{p_{1T},\ p_{2T},\ k_{1T},\ k_{2T}\}$) are four-vectors and defined to be transverse with respect to their parent hadron while the symbol ⊥ means perpendicular with respect to P_1 and P_2. The vector q_T is thus of a hadronic scale and all its components are in general nonzero. In the case of jet-jet production the integrals over k_1 and k_2 do not appear in the expression above, $q_T = p_{1T} + p_{2T}$, and K_i/z_i is replaced by k_i^{jet}. In that case the vector $r_\perp$ gives access to the intrinsic transverse momenta of the initial partons (q_T) which is similar to Drell-Yan.

Another hard scale is formed by the scalar product of K_1 and K_2. This scale, which is present in $\delta^2(q_{T\perp} - r_\perp)$, can be used to express one of the light-cone momentum fractions in terms of the others, so $z_1(x_1, x_2, z_2)$ or $z_2(x_1, x_2, z_1)$. One remains with an integral over one momentum fraction. Since the choice for this fraction is arbitrary, a more symmetrical expression can be obtained by introducing an additional integral over $x_\perp$, giving (for details see Ref. [40])

$$\begin{aligned}
&\int \mathrm{d}^4 p_1\, \mathrm{d}^4 p_2\, \mathrm{d}^4 k_1\, \mathrm{d}^4 k_2\;\; \delta^4(p_1 + p_2 - k_1 - k_2)\\
&\quad = \frac{4}{s^2 x_{1\perp} x_{2\perp}} \int \mathrm{d}x_\perp\, \mathrm{d}(p_1 \cdot \bar{n}_{P_1})\, \mathrm{d}(p_2 \cdot \bar{n}_{P_2})\, \mathrm{d}(k_1 \cdot \bar{n}_{K_1})\, \mathrm{d}(k_2 \cdot \bar{n}_{K_2})\\
&\quad\quad \times \delta\left(x_1 - \tfrac{1}{2} x_\perp \left(e^{\eta_1} + e^{\eta_2}\right)\right)\, \delta\left(x_2 - \tfrac{1}{2} x_\perp \left(e^{-\eta_1} + e^{-\eta_2}\right)\right)\\
&\quad\quad \times \delta\left(z_1^{-1} - \frac{x_\perp}{x_{1\perp}}\right)\, \delta\left(z_2^{-1} - \frac{x_\perp}{x_{2\perp}}\right)\\
&\quad\quad \times \int \mathrm{d}^2 p_{1T}\, \mathrm{d}^2 p_{2T}\, \mathrm{d}^2 k_{1T}\, \mathrm{d}^2 k_{2T}\, \delta\left(\frac{q_{T\perp} \cdot e_{1N}}{\sqrt{s}} - \tfrac{1}{2} x_\perp \sin\delta\phi\right)\\
&\quad\quad \times \int \mathrm{d}(p_1 \cdot n_{P_1})\, \mathrm{d}(p_2 \cdot n_{P_2})\, \mathrm{d}(k_1 \cdot n_{K_1})\, \mathrm{d}(k_2 \cdot n_{K_2})\, \left(1 + \mathcal{O}(M/\sqrt{s})\right),
\end{aligned} \tag{5.9}$$

where $e_{1\perp} \equiv K_{1\perp}/|\mathbf{K}_{1\perp}|$, $e_{1N}^{\sigma} \equiv (-2/s)\epsilon^{\mu\nu\rho\sigma} P_{1\mu} \times P_{2\nu} e_{1\perp\rho}$ and $\delta\phi$ is defined in Fig. 5.1 and is of order $\mathcal{O}(M/\sqrt{s})$. The above expression illustrates that the non-back-to-backness, $\delta\phi$, provides access to the transverse momenta of the quarks (via $q_{T\perp}$). Weighting the cross section with $\sin\delta\phi$ produces a projection of q_T which leads to the first transverse moments of distribution and fragmentation functions.

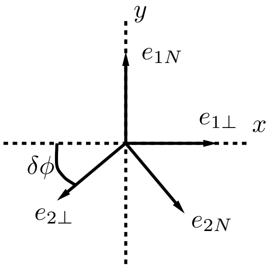

Figure 5.1: Plane perpendicular to the incoming hadron momenta.

The following cross sections are now defined

$$\begin{aligned}
\langle\, \mathrm{d}\sigma\, \rangle &\equiv \int \mathrm{d}\phi_2\, \frac{\mathrm{d}\sigma}{\mathrm{d}\phi_2}\\
&= \frac{\mathrm{d}x_{1\perp}\, \mathrm{d}x_{2\perp}\, \mathrm{d}\eta_1\, \mathrm{d}\eta_2}{32\pi s}\, \frac{\mathrm{d}\phi_1}{2\pi} \int \frac{\mathrm{d}x_\perp}{x_\perp} \Sigma(x_\perp),
\end{aligned} \tag{5.10}$$

$$\begin{aligned}\langle\, \tfrac{1}{2}\sin(\delta\phi)\,\mathrm{d}\sigma\,\rangle &\equiv \int \mathrm{d}\phi_2\;\; \tfrac{1}{2}\sin(\delta\phi)\frac{\mathrm{d}\sigma}{\mathrm{d}\phi_2}\\ &= \frac{\mathrm{d}x_{1\perp}\;\mathrm{d}x_{2\perp}\;\mathrm{d}\eta_1\;\mathrm{d}\eta_2}{32\pi s^{3/2}}\,\frac{\mathrm{d}\phi_1}{2\pi}\int\frac{\mathrm{d}x_\perp}{x_\perp^2}e_{1N}\cdot\Sigma_\partial(x_\perp),\end{aligned} \tag{5.11}$$

where

$$\begin{aligned}\Sigma(x_\perp) \equiv{}& (P_1\cdot\bar{n}_{P_1})(P_2\cdot\bar{n}_{P_2})(K_1\cdot\bar{n}_{K_1})(K_2\cdot\bar{n}_{K_2})\\ &\times\int \mathrm{d}^2p_{1T}\;\mathrm{d}^2p_{2T}\;\mathrm{d}^2k_{1T}\;\mathrm{d}^2k_{2T}\;\Phi(x_1,p_{1T})\otimes\Phi(x_2,p_{2T})\otimes\Delta(z_1^{-1},k_{1T})\\ &\qquad\otimes\Delta(z_2^{-1},k_{2T})\otimes H(p_1,p_2,k_1,k_2)\otimes H^*(p_1,p_2,k_1,k_2),\end{aligned} \tag{5.12}$$

$$\begin{aligned}\Sigma_\partial^\alpha(x_\perp) \equiv{}& (P_1\cdot\bar{n}_{P_1})(P_2\cdot\bar{n}_{P_2})(K_1\cdot\bar{n}_{K_1})(K_2\cdot\bar{n}_{K_2})\\ &\times\int \mathrm{d}^2p_{1T}\;\mathrm{d}^2p_{2T}\;\mathrm{d}^2k_{1T}\;\mathrm{d}^2k_{2T}\;\;[q_T^\alpha]\;\;\Phi(x_1,p_{1T})\otimes\Phi(x_2,p_{2T})\otimes\Delta(z_1^{-1},k_{1T})\\ &\qquad\otimes\Delta(z_2^{-1},k_{2T})\otimes H(p_1,p_2,k_1,k_2)\otimes H^*(p_1,p_2,k_1,k_2).\end{aligned} \tag{5.13}$$

In the expressions the momentum fractions, $x_1,\; x_2,\; z_1,$ and z_2, are a function of $x_\perp$ via the arguments of the first four delta-functions in Eq. 5.9.

Calculating cross sections

In the case studied here, gluon distribution and fragmentation functions are neglected. Taking only the quark and antiquark correlators into account, the forms of the expressions for $\mathscr{A}^2$, Σ and Σ_∂ will be presented. These were obtained in Ref. [40] by using FORM [120].

The following sum of diagrams contribute to $\mathscr{A}^2$, Σ and Σ_∂

$$D_{qq}^{[tt]} + D_{qq}^{[tu]} + D_{q\bar{q}}^{[tt]} + D_{q\bar{q}}^{[ts]} + D_{q\bar{q}}^{[st]} + D_{q\bar{q}}^{[ss]} + (K_1 \leftrightarrow K_2) + (q \leftrightarrow \bar{q}), \tag{5.14}$$

where the D stands for the diagrams as displayed in Fig. 5.2. For $\mathscr{A}^2$ the following convolution can be obtained

$$\begin{aligned}\mathscr{A}^2 \sim{}& \int \mathrm{d}x_\perp\;\mathrm{d}^2p_{1T}\;\mathrm{d}^2p_{2T}\;\mathrm{d}^2k_{1T}\;\mathrm{d}^2k_{2T}\;\delta\!\left(\frac{q_{T\perp}\cdot e_{1N}}{\sqrt{s}} - \tfrac{1}{2}x_\perp\sin\delta\phi\right)\\ &\times\sum_D\sum_{i,j,k,l} f_i^{[D]}(x_1,p_{1T}^2)\;f_j^{[D]}(x_2,p_{2T}^2)\frac{\mathrm{d}\sigma_{ijkl}^{[D]}}{\mathrm{d}\hat{t}}D_k^{[D]}(z_1,z_1^2k_{1T}^2)\;D_l^{[D]}(z_2,z_2^2k_{2T}^2),\end{aligned} \tag{5.15}$$

where the $f_i^{[D]}$ and $D_k^{[D]}$ represent some distribution and fragmentation functions having a diagram-dependent gauge link, the light-cone momentum fractions are fixed by the first four delta-functions in Eq. 5.9, and $\mathrm{d}\sigma_{ijkl}^{[D]}/\mathrm{d}\hat{t}$ is an elementary parton scattering subprocess (or diagram) convoluting the functions.

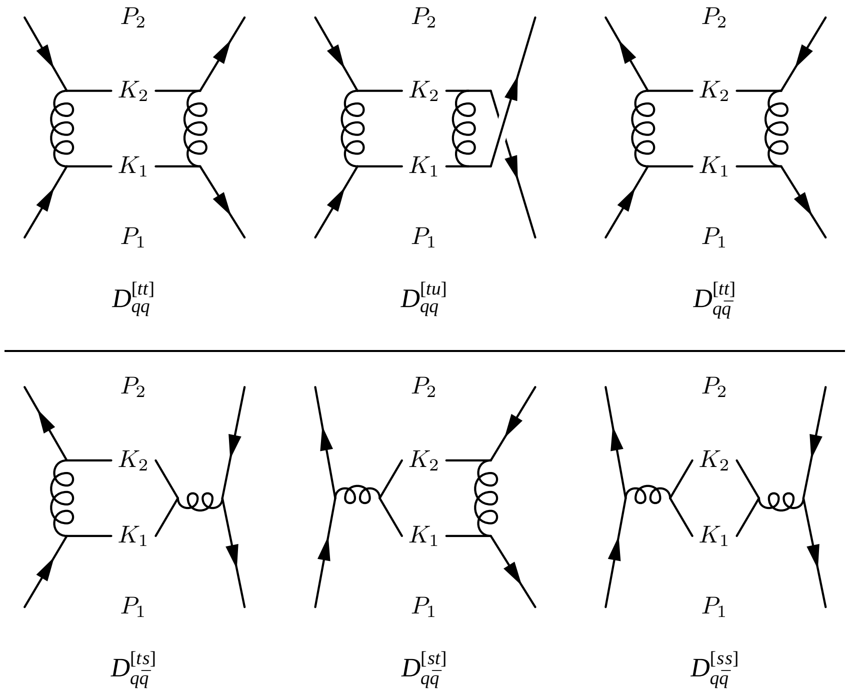

Figure 5.2: Contributions in hadron-hadron production. In the figures only the hard part is shown, omitting the correlators and parent hadrons.

In the unweighted cross section, $\langle\, d\sigma\, \rangle$, the intrinsic transverse momenta can be neglected at leading order in $M/\sqrt{s}$. In that case all the gauge links in the correlators are the same and on the light-cone, see Fig. 2.11a. The sum over diagrams can be performed, yielding a simple parton scattering cross section in Σ

$$\Sigma \sim \int \frac{dx_\perp}{x_\perp} \sum_{i,j,k,l} f_i(x_1)\, f_j(x_2)\, \frac{d\sigma_{ijkl}}{d\hat{t}} D_k(z_1)\, D_l(z_2). \qquad (5.16)$$

Also here the light-cone momentum fractions are a function of $x_\perp$ and $d\sigma_{ijkl}\,/d\hat{t}$ is the elementary parton scattering cross section.

In a weighted single spin asymmetry each contribution consists of three integrated correlators (T-even) containing gauge links on the light-cone and one correlator (T-odd) of which a transverse moment is taken (as discussed in the introduction). The first transverse moment of a function can be related to the functions defined in chapter 2 (see also the previous chapter, section 4.2). The first transverse moment of a fragmentation function is in general a combination of the ones appearing in semi-inclusive DIS and electron positron annihilation. Containing an arbitrary gauge link, a fragmentation function can be written as

$$D_i^{[\mathcal{L}'](1)} = C(\mathcal{L}')\,\tilde{D}_i^{(1)} + D_i^{(1)}, \tag{5.17}$$

where C is some calculable constant and where definitions of Ref. [35] were applied

$$D_i^{(1)}(z) \equiv \frac{1}{2}\Big(D_i^{[+](1)}(z) + D_i^{[-](1)}(z)\Big), \qquad \tilde{D}_i^{(1)}(z) \equiv \frac{1}{2}\Big(D_i^{[+](1)}(z) - D_i^{[-](1)}(z)\Big). \tag{5.18}$$

The functions $D_i^{(1)}(z)$ are independent of the gauge link direction, while the functions $\tilde{D}_i^{(1)}(z)$ exist by the presence of the gauge link. The tilde functions therefore vanish if the transverse momentum dependent fragmentation functions appearing in electron-positron annihilation are the same as in semi-inclusive DIS (for a discussion on universality, see subsection 3.5). For single spin asymmetries this leads for Σ_∂^α to

$$\begin{aligned}
\Sigma_\partial &\sim \int \frac{\mathrm{d}x_\perp}{x_\perp^2} \sum_D \sum_{i,j,k,l} f_i^{[D](1)}(x_1)\; f_j^{[D]}(x_2) \frac{\mathrm{d}\sigma_{ijkl}^{[D]}}{\mathrm{d}\hat{t}} D_k^{[D]}(z_1)\; D_l^{[D]}(z_2) + \ldots \\
&= \int \frac{\mathrm{d}x_\perp}{x_\perp^2} \sum_{i,j,k,l} f_i^{(1)}(x_1)\; f_j(x_2)\; \underbrace{\sum_D C_{G,f(1)}^{[D]} \frac{\mathrm{d}\sigma_{ijkl}^{[D]}}{\mathrm{d}\hat{t}}}_{\text{gluonic-pole cross section}} D_k(z_1)\, D_l(z_2) + \ldots,
\end{aligned} \tag{5.19}$$

where terms related to the first transverse moment of the T-odd function $f_i^{[D](1)}(x_1)$ have been explicitly shown. The combination $\sum_D C_{G,f(1)}^{[D]} \mathrm{d}\sigma_{ijkl}^{[D]}/\mathrm{d}\hat{t}$ is given the name gluonic-pole scattering. The color factors, $C_G^{[D]}$, are obtained by comparing the diagram dependent functions, $f_i^{[D](1)}$, with the in chapter 2 defined functions $f_i^{(1)}$. For the fragmentation functions $\tilde{D}_i^{(1)}$, which are similarly defined as T-odd distribution functions (compare Eq. 5.18 with Eq. 2.63), one also finds color factors. For the functions $D_i^{(1)}$ all the color factors are simply 1 because those functions are independent of the link direction. The functions $D_i^{(1)}$ are therefore convoluted with ordinary parton scattering cross sections.

It may be good to point out that since the first transverse moment of a T-odd distribution function is of order g and higher, the calculation of a single gluon insertion in the diagrammatic approach (for the gauge link) is already sufficient to obtain the color factors $C_G^{[D]}$. The fact that the all order insertions provide fully gauge invariant correlators can be seen as a consistency check.

5.3 Results for cross sections and asymmetries

In this section an explicit cross section and several single transverse target-spin asymmetries will be given. The unpolarized observed hadrons, or jets, are assumed to be approximately opposite in the perpendicular plane. The results are based on Ref. [40] in which explicit expressions as a function of y can also be found. The quark-quark subprocesses together with the gluonic-pole subprocesses are given appendix 5.A.

Unpolarized cross section for hadron-hadron production

The unpolarized unweighted cross section for hadron-hadron production is found to be a simple convolution between the integrated functions and an elementary parton scattering cross section, reading

$$\begin{aligned}\langle\, \mathrm{d}\sigma \,\rangle = \mathrm{d}x_{1\perp}\, \mathrm{d}x_{2\perp}\, \mathrm{d}\eta_1\, \mathrm{d}\eta_2\, \frac{\mathrm{d}\phi_1}{2\pi} \int \frac{\mathrm{d}x_\perp}{x_\perp} \\ \times \sum_{q_1q_2q_3q_4} f_1^{q_1}(x_1) f_1^{q_2}(x_2)\, \frac{\hat{s}}{2}\, \frac{\mathrm{d}\hat{\sigma}_{q_1q_2\to q_3q_4}}{\mathrm{d}\hat{t}}\, D_1^{q_3}(z_1) D_1^{q_4}(z_2) \\ \times \left(1 + \mathcal{O}\left(\frac{M}{\sqrt{s}}\right) + \mathcal{O}(\alpha_S)\right), \quad (5.20)\end{aligned}$$

integrated cross section for hadron-hadron production

where the summation is over all quark and antiquark flavors. The arguments of the functions are defined through $x_1 = x_\perp(\exp(\eta_1)+\exp(\eta_2))$, $x_2 = x_\perp(\exp(-\eta_1)+\exp(-\eta_2))$, and $z_i = x_{i\perp}/x_\perp$. Furthermore, the variable $\hat{s}$ depends on $x_\perp$ and y through the relation $\hat{s} = x_\perp^2 s/(4y(1-y))$.

Single transverse target-spin asymmetries

In the $\sin\delta\phi$ weighted asymmetry for hadron-hadron production, gluonic-pole scattering subprocesses are encountered. The asymmetry reads

$$
\begin{aligned}
&\left\langle\, \tfrac{1}{2}\sin(\delta\phi)\mathrm{d}\sigma \,\right\rangle \\
&= \mathrm{d}x_{1\perp}\, \mathrm{d}x_{2\perp}\, \mathrm{d}\eta_1\, \mathrm{d}\eta_2\, \frac{\mathrm{d}\phi_1}{2\pi}\, \cos(\phi_1-\phi_S) \int \frac{\mathrm{d}x_\perp}{x_\perp} \\
&\quad\times\Bigg\{ \frac{M_1}{x_\perp\sqrt{s}} \sum_{q_1q_2q_3q_4} f^{q_1}{}_{1T}^{\perp(1)}(x_1)\, f_1^{q_2}(x_2) \frac{\hat{s}}{2} \frac{\mathrm{d}\hat{\sigma}_{\widehat{gq}_1 q_2\to q_3q_4}}{\mathrm{d}\hat{t}} D_1^{q_3}(z_1) D_1^{q_4}(z_2) \\
&\qquad + \frac{M_2}{x_\perp\ \sqrt{s}} \sum_{q_1q_2q_3q_4} h_1^{q_1}(x_1) h^{q_2}{}_1^{\perp(1)}(x_2)\, \frac{\hat{s}}{2}\, \frac{\mathrm{d}\Delta\hat{\sigma}_{q_1^\uparrow \widehat{gq}_2^\uparrow\to q_3q_4}}{\mathrm{d}\hat{t}}\, D_1^{q_3}(z_1) D_1^{q_4}(z_2) \\
&\qquad - \frac{M_{h_1}}{x_\perp\ \sqrt{s}} \sum_{q_1q_2q_3q_4} h_1^{q_1}(x_1)\, f_1^{q_2}(x_2) \frac{\hat{s}}{2} \frac{\mathrm{d}\Delta\hat{\sigma}_{q_1^\uparrow q_2\to q_3^\uparrow q_4}}{\mathrm{d}\hat{t}} H^{q_3}{}_1^{\perp(1)}(z_1) D_1^{q_4}(z_2) + (K_1\leftrightarrow K_2) \\
&\qquad - \frac{M_{h_1}}{x_\perp\ \sqrt{s}} \sum_{q_1q_2q_3q_4} h_1^{q_1}(x_1)\, f_1^{q_2}(x_2)\, \frac{\hat{s}}{2}\, \frac{\mathrm{d}\Delta\hat{\sigma}_{q_1^\uparrow q_2\to \widehat{gq}_3^\uparrow q_4}}{\mathrm{d}\hat{t}} \widetilde{H}^{q_3}{}_1^{\perp(1)}(z_1) D_1^{q_4}(z_2) + (K_1\leftrightarrow K_2) \Bigg\} \\
&\quad\times\left(1 + \mathcal{O}\left(\frac{M}{\sqrt{s}}\right) + \mathcal{O}(\alpha_S)\right), \qquad (5.21)
\end{aligned}
$$

weighted asymmetry for hadron-hadron production

where the summation is over all quark and antiquark flavors. The arguments of the functions are defined through $x_1 = x_\perp(\exp\eta_1 + \exp\eta_2)$, $x_2 = x_\perp(\exp-\eta_1 + \exp-\eta_2)$, and $z_i = x_{i\perp}/x_\perp$. Further, $\hat{s}$ depends on $x_\perp$ and y through $\hat{s} = x_\perp^2 s/(4y(1-y))$.

The asymmetry for hadron-jet production where the hadron belongs to a different jet is obtained by replacing $D_1(z_2)$ by $\delta(1-z_2)\delta_{j_2q}$ which fixes $x_\perp$ to be $x_{2\perp}$ (the subscript 2 refers to the measured jet), and setting all other functions to zero. This yields

$$
\begin{aligned}
\langle\, \tfrac{1}{2}\sin(\delta\phi)\mathrm{d}\sigma\, \rangle = \mathrm{d}x_{1\perp}\ \mathrm{d}x_{2\perp}\ \mathrm{d}\eta_1\ \mathrm{d}\eta_2\ \frac{\mathrm{d}\phi_1}{2\pi}\ \cos(\phi_1-\phi_S)&\\
\times\Bigg\{\ \frac{M_1}{x_{2\perp}\sqrt{s}}\sum_{q_1q_2q_3q_4} f^{q_1}{}_{1T}^{\perp(1)}(x_1)\, f_1^{q_2}(x_2)\frac{\hat{s}}{2}\frac{\mathrm{d}\hat{\sigma}_{\widehat{gq}_1q_2\to q_3q_4}}{\mathrm{d}\hat{t}} D_1^{q_3}(z_1)&\\
+\ \frac{M_2}{x_{2\perp}\ \sqrt{s}}\sum_{q_1q_2q_3q_4} h_1^{q_1}(x_1)h^{q_2}{}_1^{\perp(1)}(x_2)\frac{\hat{s}}{2}\frac{\mathrm{d}\Delta\hat{\sigma}_{q_1^\uparrow\widehat{gq}_2^\uparrow\to q_3q_4}}{\mathrm{d}\hat{t}} D_1^{q_3}(z_1)&\\
-\ \frac{M_{h_1}}{x_{2\perp}\sqrt{s}}\sum_{q_1q_2q_3q_4} h_1^{q_1}(x_1)\, f_1^{q_2}(x_2)\frac{\hat{s}}{2}\frac{\mathrm{d}\Delta\hat{\sigma}_{q_1^\uparrow q_2\to q_3^\uparrow q_4}}{\mathrm{d}\hat{t}} H^{q_3}{}_1^{\perp(1)}(z_1)&\\
-\ \frac{M_{h_1}}{x_{2\perp}\sqrt{s}}\sum_{q_1q_2q_3q_4} h_1^{q_1}(x_1)\, f_1^{q_2}(x_2)\frac{\hat{s}}{2}\frac{\mathrm{d}\Delta\hat{\sigma}_{q_1^\uparrow q_2\to \widehat{gq}_3^\uparrow q_4}}{\mathrm{d}\hat{t}}\ \widetilde{H}^{q_3}{}_1^{\perp(1)}(z_1)\ \Bigg\}&\\
\times\left(1+\mathcal{O}\left(\frac{M}{\sqrt{s}}\right)+\mathcal{O}(\alpha_S)\right).& \qquad (5.22)
\end{aligned}
$$

weighted asymmetry for hadron-jet production

The $\sin\delta\phi$ weighted asymmetry for jet-jet production, where the jets are approximately back-to-back in the perpendicular plane, reads

$$
\begin{aligned}
\langle\, \tfrac{1}{2}\sin(\delta\phi)\mathrm{d}\sigma\, \rangle = \mathrm{d}x_{1\perp}\ \mathrm{d}x_{2\perp}\ \mathrm{d}\eta_1\ \mathrm{d}\eta_2\ \frac{\mathrm{d}\phi_1}{2\pi}\ \cos(\phi_1-\phi_S)\ \delta(x_{1\perp}{-}x_{2\perp})&\\
\times\Bigg\{\ \frac{M_1}{\sqrt{s}}\sum_{q_1q_2q_3q_4}\ f^{q_1}{}_{1T}^{\perp(1)}(x_1)\, f_1^{q_2}(x_2)\ \frac{\hat{s}}{2}\ \frac{\mathrm{d}\hat{\sigma}_{\widehat{gq}_1q_2\to q_3q_4}}{\mathrm{d}\hat{t}}&\\
+\ \frac{M_2}{\sqrt{s}}\sum_{q_1q_2q_3q_4}\ h_1^{q_1}(x_1)h^{q_2}{}_1^{\perp(1)}(x_2)\ \frac{\hat{s}}{2}\ \frac{\mathrm{d}\Delta\hat{\sigma}_{q_1^\uparrow\widehat{gq}_2^\uparrow\to q_3q_4}}{\mathrm{d}\hat{t}}\ \Bigg\}&\\
\times\left(1+\mathcal{O}\left(\frac{M}{\sqrt{s}}\right)+\mathcal{O}(\alpha_S)\right).& \qquad (5.23)
\end{aligned}
$$

weighted asymmetry for jet-jet production

As discussed in the previous section, in jet-jet production effects from intrinsic transverse momentum can also be studied through the vector $r_\perp^\alpha$. The asymmetry given here is just one projection of this vector. An $r_\perp$-weighted asymmetry could give a better separation between the two contributions.

5.4 Summary and conclusions

Effects from intrinsic transverse momentum were studied through single spin asymmetries in hadron-hadron collisions. Assuming factorization, the diagrammatic expansion was applied to derive the tree-level expressions and to illustrate effects of the gauge link. That this effect can be more than just a sign was pointed out in chapter 4 and is a generalization of the earlier work in chapter 3. Contributions to the cross sections were considered from quark and antiquark distribution and fragmentation functions. For the contributions from gluons a similar procedure can be followed.

A challenge was how to extract the transverse momentum dependent functions from the cross section. It was found that by weighting with a specific angle (the non-back-to-backness), the asymmetry becomes proportional to three integrated distribution and fragmentation functions and one distribution or fragmentation function of which the first transverse moment is taken. This method has the advantage that no momentum dependence of functions needs to be assumed, offering a model-independent way of studying effects from intrinsic transverse momentum. Whether such a method can also be applied in the case of single hadron production remains to be seen.

The distribution and fragmentation functions contain gauge links which were calculated by using the prescription of the previous chapter. Those gauge links become relevant when considering transverse moments of the transverse momentum dependent functions. The first transverse moments of the correlators in hadron-hadron scattering also appear (with factors) in semi-inclusive DIS and electron-positron annihilation. For the higher moments such relations have not been achieved (see chapter 4).

The single spin asymmetries were obtained in terms of functions containing a subprocess-dependent (diagram-dependent) gauge link. Consequently, the asymmetries were rewritten as a folding of the functions defined in chapter 2 with newly defined gluonic-pole cross sections. Those gluonic-pole cross sections are just partonic scattering diagrams where each diagram is weighted with an additional factor (compare for instance Eq. 5.24 with Eq. 5.25). This factor comes from taking the first transverse moment of the T-odd functions. Except for the fragmentation functions $D_i^{(1)}$ where such factors do not appear, the T-odd functions are of order g and higher (see for instance Eq. 2.71). Therefore, these factors can already be calculated by doing a single gluon insertion. The all order insertions, as performed in the previous chapter to obtain gauge invariant results, are not necessary to produce these factors but of course provide confidence on the approach we have followed. Since single gluon insertions are sufficient to produce these factors, comparisons with the results of Qiu and Sterman [57] are possible.

5.A Partonic cross sections

In this appendix the elementary and gluonic-pole scattering subprocesses will be listed. The elementary expressions are taken from Bacchetta, Radici [156] in which minus signs from interchanging fermions are made explicit. Interchanging k_1 with k_2 is equivalent to interchanging $\hat{u}$ with $\hat{t}$ or $y \leftrightarrow (1-y)$. For constructing the cross sections a useful relation is $4x_1x_2y(1-y) = x_\perp^2[1+\mathcal{O}(M^2/s)]$ which can be employed underneath the $x_\perp$ integral.

Quark-quark scattering

The unpolarized quark-quark scattering subprocesses are given by

$$\frac{\mathrm{d}\hat{\sigma}^{[tt]}_{qq'\to qq'}}{\mathrm{d}\hat{t}} = \frac{4\pi\alpha_S^2}{9\,\hat{s}^2}\,\frac{\hat{s}^2+\hat{u}^2}{\hat{t}^2}, \qquad \frac{\mathrm{d}\hat{\sigma}^{[uu]}_{qq'\to q'q}}{\mathrm{d}\hat{t}} = \frac{4\pi\alpha_S^2}{9\,\hat{s}^2}\,\frac{\hat{s}^2+\hat{t}^2}{\hat{u}^2},$$
$$\frac{\mathrm{d}\hat{\sigma}^{[tu]}_{qq\to qq}}{\mathrm{d}\hat{t}} = \frac{4\pi\alpha_S^2}{27\hat{s}^2}\,\frac{\hat{s}^2}{\hat{t}\hat{u}},$$

giving for the total cross section

$$\frac{\mathrm{d}\hat{\sigma}_{qq\to qq}}{\mathrm{d}\hat{t}} = \frac{\mathrm{d}\hat{\sigma}^{[tt]}_{qq'\to qq'}}{\mathrm{d}\hat{t}} + \frac{\mathrm{d}\hat{\sigma}^{[uu]}_{qq'\to q'q}}{\mathrm{d}\hat{t}} - 2\,\frac{\mathrm{d}\hat{\sigma}^{[tu]}_{qq\to qq}}{\mathrm{d}\hat{t}}. \tag{5.24}$$

For unpolarized gluonic-pole-quark scattering (gluonic pole is associated with first quark) the above expression is modified into

$$\frac{\mathrm{d}\hat{\sigma}_{\widehat{g}qq\to qq}}{\mathrm{d}\hat{t}} = C^{[tt,qq]}_{G,f(1)}\,\frac{\mathrm{d}\hat{\sigma}^{[tt]}_{qq'\to qq'}}{\mathrm{d}\hat{t}} + C^{[uu,qq]}_{G,f(1)}\,\frac{\mathrm{d}\hat{\sigma}^{[uu]}_{qq'\to q'q}}{\mathrm{d}\hat{t}} - 2C^{[tu,qq]}_{G,f(1)}\,\frac{\mathrm{d}\hat{\sigma}^{[tu]}_{qq\to qq}}{\mathrm{d}\hat{t}}. \tag{5.25}$$

Consulting table 4.2 one has the following factors: $C^{[tt,qq]}_{G,f(1)} = 1/2$, $C^{[uu,qq]}_{G,f(1)} = 1/2$, and $C^{[tu,qq]}_{G,f(1)} = -3/2$.

The relevant polarized quark-quark subprocesses are

$$\frac{\mathrm{d}\Delta\hat{\sigma}^{[tt]}_{q^\uparrow q'\to q^\uparrow q'}}{\mathrm{d}\hat{t}} = -\frac{8\pi\alpha_S^2}{9\,\hat{s}^2}\,\frac{\hat{u}\hat{s}}{\hat{t}^2}, \qquad \frac{\mathrm{d}\Delta\hat{\sigma}^{[tu]}_{q^\uparrow q\to q^\uparrow q}}{\mathrm{d}\hat{t}} = -\frac{8\pi\alpha_S^2}{27\,\hat{s}^2}\,\frac{\hat{s}}{\hat{t}},$$

giving for the cross sections

$$\frac{\mathrm{d}\Delta\hat{\sigma}_{q^\uparrow q\to q^\uparrow q}}{\mathrm{d}\hat{t}} = \frac{\mathrm{d}\Delta\hat{\sigma}^{[tt]}_{q^\uparrow q'\to q^\uparrow q'}}{\mathrm{d}\hat{t}} - \frac{\mathrm{d}\Delta\hat{\sigma}^{[tu]}_{q^\uparrow q\to q^\uparrow q}}{\mathrm{d}\hat{t}}, \tag{5.26}$$

$$\frac{\mathrm{d}\Delta\hat{\sigma}_{q^\uparrow q^\uparrow\to qq}}{\mathrm{d}\hat{t}} = \frac{\mathrm{d}\Delta\hat{\sigma}^{[tu]}_{q^\uparrow q^\uparrow\to qq}}{\mathrm{d}\hat{t}} = -\frac{8\pi\alpha_S^2}{27\,\hat{s}^2}, \tag{5.27}$$

For the polarized gluonic-pole scattering cross sections, the above expressions are modified into

$$\frac{d\Delta\hat{\sigma}_{q^\uparrow q\to\widehat{g}\bar{q}^\uparrow q}}{d\hat{t}} = C^{[tt,qq]}_{G,D(1)}\frac{d\Delta\hat{\sigma}^{[tt]}_{q^\uparrow q'\to q^\uparrow q'}}{d\hat{t}} - C^{[tu,qq]}_{G,D(1)}\frac{d\Delta\hat{\sigma}^{[tu]}_{q^\uparrow q\to q^\uparrow q}}{d\hat{t}}, \tag{5.28}$$

$$\frac{d\Delta\hat{\sigma}_{q^\uparrow\widehat{g}\bar{q}^\uparrow\to qq}}{d\hat{t}} = C^{[tu,qq]}_{G,f(2)}\frac{d\Delta\hat{\sigma}^{[tu]}_{q^\uparrow q^\uparrow\to qq}}{d\hat{t}}. \tag{5.29}$$

Table 4.2 gives the relations: $C^{[tt,qq]}_{G,D(1)} = -1/2, C^{[tu,qq]}_{G,D(1)} = 3/2, C^{[tu,qq]}_{G,f(2)} = -3/2$.

Quark-antiquark scattering

The unpolarized quark-antiquark subprocesses are given by

$$\frac{d\hat{\sigma}^{[tt]}_{q\bar{q}'\to q\bar{q}'}}{d\hat{t}} = \frac{4\pi\alpha_S^2}{9\,\hat{s}^2}\frac{\hat{s}^2+\hat{u}^2}{\hat{t}^2}, \qquad \frac{d\hat{\sigma}^{[ss]}_{q\bar{q}\to q'\bar{q}'}}{d\hat{t}} = \frac{4\pi\alpha_S^2}{9\,\hat{s}^2}\frac{\hat{t}^2+\hat{u}^2}{\hat{s}^2},$$

$$\frac{d\hat{\sigma}^{[ts]}_{q\bar{q}\to q\bar{q}}}{d\hat{t}} = \frac{4\pi\alpha_S^2}{27\,\hat{s}^2}\frac{\hat{u}^2}{\hat{t}\hat{s}},$$

giving for the cross section

$$\frac{d\hat{\sigma}_{q\bar{q}\to q\bar{q}}}{d\hat{t}} = \frac{d\hat{\sigma}^{[tt]}_{q\bar{q}'\to q\bar{q}'}}{d\hat{t}} + \frac{d\hat{\sigma}^{[ss]}_{q\bar{q}\to q'\bar{q}'}}{d\hat{t}} - 2\frac{d\hat{\sigma}^{[ts]}_{q\bar{q}\to q\bar{q}}}{d\hat{t}}. \tag{5.30}$$

For the unpolarized gluonic-pole scattering cross section, the above expression is modified into

$$\frac{d\hat{\sigma}_{\widehat{g}q\bar{q}\to q\bar{q}}}{d\hat{t}} = C^{[tt,q\bar{q}]}_{G,f(1)}\frac{d\hat{\sigma}^{[tt]}_{q\bar{q}'\to q\bar{q}'}}{d\hat{t}} + C^{[ss,q\bar{q}]}_{G,f(1)}\frac{d\hat{\sigma}^{[ss]}_{q\bar{q}\to q'\bar{q}'}}{d\hat{t}} - 2C^{[ts,q\bar{q}]}_{G,f(1)}\frac{d\hat{\sigma}^{[ts]}_{q\bar{q}\to q\bar{q}}}{d\hat{t}}, \tag{5.31}$$

where $C^{[tt,q\bar{q}]}_{G,f(1)} = -3/4, C^{[ss,q\bar{q}]}_{G,f(1)} = 5/4, C^{[ts,q\bar{q}]}_{G,f(1)} = 5/4$ (using table 4.2).

The polarized quark-antiquark scattering subprocesses are

$$\frac{d\Delta\hat{\sigma}^{[ss]}_{q^\uparrow\bar{q}^\uparrow\to q'\bar{q}'}}{d\hat{t}} = -\frac{8\pi\alpha_S^2}{9\,\hat{s}^2}\frac{\hat{t}\hat{u}}{\hat{s}^2}, \qquad \frac{d\Delta\hat{\sigma}^{[st]}_{q^\uparrow\bar{q}^\uparrow\to q\bar{q}}}{d\hat{t}} = -\frac{8\pi\alpha_S^2}{27\,\hat{s}^2}\frac{\hat{u}}{\hat{s}},$$

$$\frac{d\Delta\hat{\sigma}^{[tt]}_{q^\uparrow\bar{q}'\to q^\uparrow\bar{q}'}}{d\hat{t}} = -\frac{8\pi\alpha_S^2}{9\,\hat{s}^2}\frac{\hat{u}\hat{s}}{\hat{t}^2}, \qquad \frac{d\Delta\hat{\sigma}^{[ts]}_{q^\uparrow\bar{q}\to q^\uparrow\bar{q}}}{d\hat{t}} = -\frac{8\pi\alpha_S^2}{27\hat{s}^2}\frac{\hat{u}}{\hat{t}},$$

giving for the cross sections

$$\frac{\mathrm{d}\Delta\hat{\sigma}_{q^{\uparrow}\bar{q}^{\uparrow}\to q\bar{q}}}{\mathrm{d}\hat{t}} = \frac{\mathrm{d}\Delta\hat{\sigma}^{[ss]}_{q^{\uparrow}\bar{q}^{\uparrow}\to q'\bar{q}'}}{\mathrm{d}\hat{t}} - \frac{\mathrm{d}\Delta\hat{\sigma}^{[st]}_{q^{\uparrow}\bar{q}^{\uparrow}\to q\bar{q}}}{\mathrm{d}\hat{t}}, \tag{5.32}$$

$$\frac{\mathrm{d}\Delta\hat{\sigma}_{q^{\uparrow}\bar{q}\to q^{\uparrow}\bar{q}}}{\mathrm{d}\hat{t}} = \frac{\mathrm{d}\Delta\hat{\sigma}^{[tt]}_{q^{\uparrow}\bar{q}'\to q^{\uparrow}\bar{q}'}}{\mathrm{d}\hat{t}} - \frac{\mathrm{d}\Delta\hat{\sigma}^{[ts]}_{q^{\uparrow}\bar{q}\to q^{\uparrow}\bar{q}}}{\mathrm{d}\hat{t}}, \tag{5.33}$$

$$\frac{\mathrm{d}\Delta\hat{\sigma}_{q^{\uparrow}\bar{q}\to\bar{q}^{\uparrow}q}}{\mathrm{d}\hat{t}} = \frac{\mathrm{d}\Delta\hat{\sigma}^{[ts]}_{q^{\uparrow}\bar{q}\to\bar{q}^{\uparrow}q}}{\mathrm{d}\hat{t}} = -\frac{8\pi\alpha_S^2}{27\hat{s}^2}. \tag{5.34}$$

For the gluonic-pole scattering cross sections the above expression is modified into

$$\frac{\mathrm{d}\Delta\hat{\sigma}_{q^{\uparrow}\widehat{g\bar{q}}^{\uparrow}\to q\bar{q}}}{\mathrm{d}\hat{t}} = C^{[ss,q\bar{q}]}_{G,\bar{f}(2)}\frac{\mathrm{d}\Delta\hat{\sigma}^{[ss]}_{q^{\uparrow}\bar{q}^{\uparrow}\to q'\bar{q}'}}{\mathrm{d}\hat{t}} - C^{[st,q\bar{q}]}_{G,\bar{f}(2)}\frac{\mathrm{d}\Delta\hat{\sigma}^{[st]}_{q^{\uparrow}\bar{q}^{\uparrow}\to q\bar{q}}}{\mathrm{d}\hat{t}}, \tag{5.35}$$

$$\frac{\mathrm{d}\Delta\hat{\sigma}_{q^{\uparrow}\bar{q}\to\widehat{g q}^{\uparrow}\bar{q}}}{\mathrm{d}\hat{t}} = C^{[tt,q\bar{q}]}_{G,D(1)}\frac{\mathrm{d}\Delta\hat{\sigma}^{[tt]}_{q^{\uparrow}\bar{q}'\to q^{\uparrow}\bar{q}'}}{\mathrm{d}\hat{t}} - C^{[ts,q\bar{q}]}_{G,D(1)}\frac{\mathrm{d}\Delta\hat{\sigma}^{[ts]}_{q^{\uparrow}\bar{q}\to q^{\uparrow}\bar{q}}}{\mathrm{d}\hat{t}}, \tag{5.36}$$

$$\frac{\mathrm{d}\Delta\hat{\sigma}_{q^{\uparrow}\bar{q}\to\widehat{g\bar{q}}^{\uparrow}q}}{\mathrm{d}\hat{t}} = C^{[ts,q\bar{q}]}_{G,D(1)}\frac{\mathrm{d}\Delta\hat{\sigma}^{[ts]}_{q^{\uparrow}\bar{q}\to\bar{q}^{\uparrow}q}}{\mathrm{d}\hat{t}}, \tag{5.37}$$

where $C^{[ss,q\bar{q}]}_{G,\bar{f}(2)} = 5/4$, $C^{[st,q\bar{q}]}_{G,\bar{f}(2)} = 5/4$, $C^{[tt,q\bar{q}]}_{G,D(1)} = 3/4$, $C^{[ts,q\bar{q}]}_{G,D(1)} = -5/4$, $C^{[ts,q\bar{q}]}_{G,\bar{D}(1)} = -5/4$ (using table 4.2).

6

Summary and conclusions

Effects from intrinsic transverse momentum of partons were studied in several hard scattering processes with an emphasis on color gauge invariance. In order to describe the processes, the diagrammatic expansion was employed which is a field-theoretical approach. Extending the work of Boer, Mulders [114] and Belitsky, Ji, Yuan [26], factorization of effects from intrinsic transverse momentum was assumed, and by considering an infinite number of diagrams the tree-level expressions including M/Q corrections were evaluated in chapter 3 for semi-inclusive DIS, Drell-Yan, and electron-positron annihilation. In those processes transverse momentum dependent distribution and fragmentation functions were encountered which are defined through matrix elements in which bilocal operators are folded with a gauge link. From a theoretical point of view, the presence of this gauge link (also called Wilson line) is pleasant because it makes the bilocal operator invariant under color gauge transformations. These gauge links are of increasing interest because by several papers, among which Brodsky, Hwang, Schmidt [24], Collins [25], and Belitsky, Ji, Yuan [26], it has been shown that the gauge links are not the same in every process and could lead to observable effects.

Distribution and fragmentation functions containing a gauge link were discussed in chapter 2. These functions describe the way in which quarks are distributed in a nucleon or how a quark decays into a jet and a particular hadron. They form a bridge between theoretical predictions and experimental observations, and are vital for our understanding of the nucleon's substructure. In the diagrammatic approach these functions naturally appear when studying hard scattering processes. The exact form of these functions, including the path of the gauge link, is thus not a starting point but rather derived.

In the transverse momentum integrated distribution functions the presence of the gauge link did not produce new effects in contrast to the transverse momentum dependent functions. In the latter the gauge link does not run along a straight path between the two quark-fields and therefore allows for the existence of T-odd distribution functions. The existence of such functions was conjectured by Sivers [21, 22] in order to explain the observation of single spin asymmetries. As pointed out by Collins [25], those functions have the interesting property that they appear with different signs when comparing Drell-Yan with semi-inclusive DIS. This interesting prediction should of course be experimentally verified.

Another possible source for T-odd effects was uncovered by Qiu and Sterman [84, 85]. They suggested that the presence of gluonic pole matrix elements could produce single spin asymmetries in hadron-hadron collisions. It was shown in chapter 2 that those matrix elements have the same form as matrix elements from which the T-odd distribution functions are defined. The presence of the gauge link and the gluonic pole matrix elements are therefore in essence the same mechanism.

The path of the gauge link in the transverse momentum dependent functions runs in a particular direction via the light-cone boundary (see Fig. 2.11). In chapter 2 it was discussed that this direction is a potential source for new effects or functions (see for related work Goeke, Metz, Schlegel [79]). While calculating the longitudinal target-spin and beam-spin asymmetries for semi-inclusive DIS in chapter 3, it was found that one of these new functions, $g^{\perp}$, could produce a nonzero azimuthal single spin asymmetry for jet-production in lepton-hadron scattering. Given the reason for the existence of this function, this prediction deserves experimental verification.

The presence of gauge links in transverse momentum dependent fragmentation functions confronted us in chapter 2 with issues related to universality. It was found that transverse momentum dependent fragmentation functions could appear to be different when comparing semi-inclusive DIS with electron-positron annihilation. The reason for this difference is that for fragmentation functions there are two possible sources for T-odd effects: the gauge link and final-state interactions. If one of the two mechanisms is suppressed, relations between the two processes can be drawn. It should be pointed out that Collins and Metz obtained in Ref. [100, 101] in a quite general treatment fragmentation functions which appear with the same sign in the two different processes. This interesting result was discussed in chapter 3 and deserves further attention. Also from the experimental side this universality issue can be addressed. For instance, by comparing properties, like the z-dependence, of transverse momentum dependent fragmentation functions between different processes.

In chapter 4 it was discovered that gauge links can arise which are much more complex than the gauge links in the discussed electromagnetic processes. Besides being more complex, the path of the gauge link turned out to not only depend on the process, but also on the subprocess (or squared amplitude diagram). These complex structures predict that T-odd distribution functions can in general differ by more than just a sign when comparing different processes. In fact only their first transverse moment can be straightforwardly compared between different processes. A prescription was given in order to deduce the gauge link in squared amplitude diagrams, and it was shown in a two gluon-production process that nonphysical polarizations of the gluons are canceled among diagrams although separate diagrams are convoluted with functions having diagram-dependent gauge links. This is a firm consistency test of the applied approach.

An illustration of these more complex gauge links was given in hadron-hadron production in hadron-hadron scattering. In hadron-hadron scattering the challenge is to extract the transverse momentum dependent functions. In chapter 5 such an observable was presented. This observable has the advantage that it does not require input on the explicit form for the momentum dependence of the functions. By using this observable, it was shown that effects from the gauge link yield more than just a sign in single spin asymmetries. The expression for the single spin asymmetry was found to be a set of elementary scattering subprocesses convoluted with universal integrated functions and a function of which a transverse moment was taken. In this latter function the gauge link depends on the subprocess. Since the first transverse moment of functions can be related to a set of “standard” functions, which also appear in semi-inclusive DIS and electron-positron annihilation (just a factor), the asymmetries were rewritten in terms of these “standard” functions folded with the newly defined gluonic-pole cross sections. Gluonic-pole cross sections are just elementary parton scattering cross sections in which the various subprocesses (squared amplitude diagrams) are weighted with a particular factor. Contributions from gluon distribution and fragmentation functions were discarded for the ease of the calculation, but should be included in future studies to make realistic estimates of single spin asymmetries. The definition of transverse momentum dependent gluon distribution functions was addressed in chapter 4, but needs further improvement. Just like experiments could verify in the Drell-Yan process the sign change of T-odd distribution functions, experiments should also be able to check the more involved appearance of T-odd distribution functions in hadron-hadron production. Other processes which also contain such more complicated effects are photon-jet production, and two jet-production.

Besides leading to new effects, the gauge link also poses theoretical challenges among which the issue of factorization of intrinsic transverse momentum dependent effects. This issue underlies most treatments and results in this field including this thesis. Recently, significant progress was made by Ji, Ma, and Yuan in Ref. [175, 176] and by Collins and Metz in Ref. [101]. They considered semi-inclusive DIS and Drell-Yan at small measured q_T (q is the momentum of the virtual photon and $q_T^2 \sim -M^2$).

One particular issue which was not explicitly addressed is the path of the gauge link in distribution and fragmentation functions connected to higher order diagrams (two loops or higher). At those orders it was argued in chapter 4 that the effect of gauge links might endanger factorization of intrinsic transverse momentum dependent effects in semi-inclusive DIS and Drell-Yan. This could form a problem for azimuthal asymmetries at small q_T at leading order in M/Q and at subleading order for fully q_T-integrated cross sections. This issue awaits further clarification. Model calculations could be very useful here. Just like a model calculation uncovered the possible existence of T-odd distribution functions, a two loop model calculation could illustrate some of the important aspects related to factorization.

In this thesis effects from intrinsic transverse momentum were studied in hard scattering processes. The existing theoretical formalism was further developed and several issues have been clarified. Various cross sections and asymmetries were obtained. Their measurement can contribute to our understanding of the nucleon's substructure within the framework of QCD and very likely will guide physicists in answering several remaining questions.

Acknowledgements

Several persons are acknowledged for the support they have given me in the last four years. First I would like to acknowledge my supervisor Piet Mulders. Piet, in het begin vond ik het moeilijk om m’n eigen weg te zoeken, maar achteraf ben ik je dankbaar voor de zelfstandigheid die je mij hebt gegeven. Verder heb je mij erg gemotiveerd door mij vanaf het begin als een zelfstandig natuurkundige te behandelen en door mij de mogelijkheid te geven om naar workshops en conferenties te gaan. Naast onze samenwerking aan artikelen waardeer ik ook zeer dat je er altijd was op de momenten dat ik je echt nodig had.

The second person who I would like to thank is Daniel Boer. Daniel, de inspiratie die je kunt geven tijdens het discussieren, je snelle manier van begrijpen, en je talent van meedenken zijn uitzonderlijk. Ik wil je bedanken voor de samenwerking van de afgelopen jaren en voor het nauwkeurig lezen van het proefschrift. Mede dankzij jou kan ik nu met tevredenheid terugkijken op de resultaten van dit proefschrift.

I also would like to acknowledge Alessandro Bacchetta and Cedran Bomhof. I appreciate the collaboration we had and the results we obtained. In addition, it was also a pleasure to share an office with you. Acknowledged are also my collaborators Ben Bakker and Miranda van Iersel. Ook hier kijk ik met plezier terug naar de resultaten die we hebben bereikt. En Ben, ik dank je voor de vele uiteenlopende discussies die we gehad hebben en voor je altijd beschikbare wijze adviezen.

I also would like to thank the reading comittee, Mauro Anselmino, Daniel Boer, Markus Diehl, Eric Laenen, and Gerard van der Steenhoven for the time they have spent on reading my thesis and for the suggestions they have made. Acknowledged is also Bob van Eijk for leading the useful evaluation meetings in the last four years. Ik keek altijd naar dit soort gesprekken uit. I also would like to thank Philipp Hägler, John McNamara, and Paul van der Nat for reading and correcting parts of the thesis.

Besides the people alread mentioned, I met in the last years several others at conferences and workshops with whom I had nice discussions: Umberto D’Alesio, Elke

Aschenauer, Harut Avakian, Elena Boglione, John Collins, Delia Hasch, Leonard Gamberg, Dae Sung Hwang, Elliot Leader, Andreas Metz, Gunar Schnell, Dennis Sivers, and Werner Vogelsang. I also would like to thank the members of the theory group (including secretaries) for a stimulating and friendly atmosphere. Especially I acknowledge Paul Becherer, Henk Blok, Hartmut Erzgräber, David Fokkema, Hugo Schouten, Harmen Warringa, and Erik Wessels for their endless discussions.

Acknowledged are also my friends for their support in the last years. I also thank my parents, sister, and their families. Ik dank jullie voor de gegeven mogelijkheid om te kunnen studeren en voor de gegeven ondersteuning.

The last person I would like to thank is Călina Ciuhu. Călina, înţelegerea şi sprijinul tău mi-au fost de mare ajutor. Dar mai ales îţi mulţumesc pentru dragostea şi motivaţia oferită de-a lungul acestor ani.

Bibliography

[1] A. Einstein, *Annalen Phys.* **17**: 891–921 (1905).

[2] P. A. M. Dirac, *Proc. Roy. Soc. Lond.* **A133**: 60–72 (1931).

[3] C. D. Anderson, *Phys. Rev.* **43**: 491–494 (1933).

[4] O. Chamberlain, E. Segre, C. Wiegand, and T. Ypsilantis, *Phys. Rev.* **100**: 947–950 (1955).

[5] F. Reines and C. L. Cowan, *Phys. Rev.* **92**: 830–831 (1953).

[6] M. Gell-Mann, *Phys. Lett.* **8**: 214–215 (1964).

[7] G. Zweig, *An su(3) model for strong interaction symmetry and its breaking. 2* (1964), CERN-TH-412.

[8] F. Abe et al. (CDF), *Phys. Rev. Lett.* **74**: 2626–2631 (1995), `hep-ex/9503002`.

[9] S. Abachi et al. (D0), *Phys. Rev. Lett.* **74**: 2632–2637 (1995), `hep-ex/9503003`.

[10] J. D. Jackson and L. B. Okun, *Rev. Mod. Phys.* **73**: 663–680 (2001), `hep-ph/0012061`.

[11] W. Ehrenberg and R. E. Siday, *Proc. Phys. Soc.* **B62**: 8 (1949).

[12] Y. Aharonov and D. Bohm, *Phys. Rev.* **123**: 1511–1524 (1961).

[13] Y. Aharonov and D. Bohm, *Phys. Rev.* **115**: 485–491 (1959).

[14] R. G. Chambers, *Phys. Rev. Lett.* **5**: 3–5 (1960).

[15] A. Airapetian et al. (HERMES), *Phys. Rev. Lett.* **94**: 012002 (2005), `hep-ex/0408013`.

[16] G. ’t Hooft and M. J. G. Veltman, *Nucl. Phys.* **B44**: 189–213 (1972).

[17] G. ’t Hooft and M. J. G. Veltman, *Nucl. Phys.* **B50**: 318–353 (1972).

[18] D. J. Gross and F. Wilczek, *Phys. Rev. Lett.* **30**: 1343–1346 (1973).

[19] H. D. Politzer, *Phys. Rev. Lett.* **30**: 1346–1349 (1973).

[20] G. Bunce et al., *Phys. Rev. Lett.* **36**: 1113–1116 (1976).

[21] D. W. Sivers, *Phys. Rev.* **D41**: 83 (1990).

[22] D. W. Sivers, *Phys. Rev.* **D43**: 261–263 (1991).

[23] J. C. Collins, *Nucl. Phys.* **B396**: 161–182 (1993), `hep-ph/9208213`.

[24] S. J. Brodsky, D. S. Hwang, and I. Schmidt, *Phys. Lett.* **B530**: 99–107 (2002), `hep-ph/0201296`.

[25] J. C. Collins, *Phys. Lett.* **B536**: 43–48 (2002), `hep-ph/0204004`.

[26] A. V. Belitsky, X. Ji, and F. Yuan, *Nucl. Phys.* **B656**: 165–198 (2003), `hep-ph/0208038`.

[27] M. Anselmino, A. Efremov, and E. Leader, *Phys. Rept.* **261**: 1–124 (1995), `hep-ph/9501369`.

[28] V. Barone and P. Ratcliffe, *Transverse spin physics* (World scientific publishing co., River Edge, USA, 2003).

[29] F. Halzen and A. D. Martin, *Quarks and leptons: An introductory course in modern particle physics* (Wiley, New York, USA, 1984).

[30] E. Leader, *Spin in particle physics* (Cambridge University Press, Cambridge, UK, 2001).

[31] M. E. Peskin and D. V. Schroeder, *An Introduction to quantum field theory* (Addison-Wesley, Cambridge, USA, 1995).

[32] L. H. Ryder, *Quantum field theory* (Cambridge University Press, Cambridge, UK, 1985).

[33] S. Weinberg, *The Quantum theory of fields: Foundations*, volume 1 (Cambridge University Press, Cambridge, UK, 1995).

[34] S. Weinberg, *The Quantum theory of fields: Modern applications*, volume 2 (Cambridge University Press, Cambridge, UK, 1996).

[35] D. Boer, P. J. Mulders, and F. Pijlman, *Nucl. Phys.* **B667**: 201–241 (2003), `hep-ph/0303034`.

[36] A. Bacchetta, P. J. Mulders, and F. Pijlman, *Phys. Lett.* **B595**: 309–317 (2004), `hep-ph/0405154`.

[37] C. J. Bomhof, P. J. Mulders, and F. Pijlman, *Phys. Lett.* **B596**: 277–286 (2004), `hep-ph/0406099`.

[38] F. Pijlman, *Few Body Syst.* **36**: 209–213 (2005), `hep-ph/0409332`.

[39] F. Pijlman (2004), `hep-ph/0411307`.

[40] A. Bacchetta, C. J. Bomhof, P. J. Mulders, and F. Pijlman, *Phys. Rev.* **D72**: 034030 (2005), `hep-ph/0505268`.

[41] D. E. Soper, *Phys. Rev.* **D15**: 1141 (1977).

[42] J. C. Collins and D. E. Soper, *Phys. Rev.* **D16**: 2219 (1977).

[43] D. E. Soper, *Phys. Rev. Lett.* **43**: 1847 (1979).

[44] J. P. Ralston and D. E. Soper, *Nucl. Phys.* **B152**: 109 (1979).

[45] P. J. Mulders, *Transverse momentum dependence in structure functions in hard scattering processes* (2001), Vrije universiteit Amsterdam, unpublished notes.

[46] A. Bacchetta, U. D'Alesio, M. Diehl, and C. A. Miller, *Phys. Rev.* **D70**: 117504 (2004), `hep-ph/0410050`.

[47] C. S. Lam and W.-K. Tung, *Phys. Rev.* **D18**: 2447 (1978).

[48] R.-b. Meng, F. I. Olness, and D. E. Soper, *Nucl. Phys.* **B371**: 79–110 (1992).

[49] J. D. Bjorken and S. D. Drell, *Relativistic quantum fields* (McGraw-Hill Book Company, 1965).

[50] K. G. Wilson, *Phys. Rev.* **179**: 1499–1512 (1969).

[51] H. D. Politzer, *Nucl. Phys.* **B172**: 349 (1980).

[52] G. Altarelli and G. Parisi, *Nucl. Phys.* **B126**: 298 (1977).

[53] R. K. Ellis, W. Furmanski, and R. Petronzio, *Nucl. Phys.* **B207**: 1 (1982).

[54] R. K. Ellis, W. Furmanski, and R. Petronzio, *Nucl. Phys.* **B212**: 29 (1983).

[55] J.-w. Qiu and G. Sterman, *Nucl. Phys.* **B353**: 105–136 (1991).

[56] J.-w. Qiu and G. Sterman, *Nucl. Phys.* **B353**: 137–164 (1991).

[57] J.-w. Qiu and G. Sterman, *Phys. Rev.* **D59**: 014004 (1999), `hep-ph/9806356`.

[58] R. L. Jaffe, *Nucl. Phys.* **B229**: 205 (1983).

[59] R. L. Jaffe Lectures presented at the Los Alamos School on Quark Nuclear Physics, Los Alamos, N.Mex., Jun 10-14, 1985.

[60] M. Diehl and T. Gousset, *Phys. Lett.* **B428**: 359–370 (1998), `hep-ph/9801233`.

[61] A. Bacchetta and P. J. Mulders, *Phys. Rev.* **D62**: 114004 (2000), `hep-ph/0007120`.

[62] R. L. Jaffe and X.-D. Ji, *Nucl. Phys.* **B375**: 527–560 (1992).

[63] P. J. Mulders and R. D. Tangerman, *Nucl. Phys.* **B461**: 197–237 (1996), Hep-ph/9510301.

[64] D. Boer, *Azimuthal asymmetries in hard scattering processes*, Ph.D. thesis, Vrije universiteit Amsterdam (1998).

[65] R. Brock et al. (CTEQ), *Rev. Mod. Phys.* **67**: 157–248 (1995).

[66] A. A. Henneman, *Scale dependence of correlations on the light-front*, Ph.D. thesis, Vrije universiteit Amsterdam (2005).

[67] R. L. Jaffe (1996), Lectures on QCD, `hep-ph/9602236`.

[68] B. L. G. Bakker, E. Leader, and T. L. Trueman, *Phys. Rev.* **D70**: 114001 (2004), `hep-ph/0406139`.

[69] A. Bacchetta, *Probing the transverse spin of quarks in deep inelastic scattering*, Ph.D. thesis, Vrije Universiteit Amsterdam (2002), `hep-ph/0212025`.

[70] M. Anselmino, M. Boglione, and F. Murgia, *Phys. Lett.* **B362**: 164–172 (1995), `hep-ph/9503290`.

[71] M. Anselmino and F. Murgia, *Phys. Lett.* **B442**: 470–478 (1998), `hep-ph/9808426`.

[72] M. Anselmino, U. D'Alesio, and F. Murgia, *Phys. Rev.* **D67**: 074010 (2003), `hep-ph/0210371`.

[73] D. Boer and P. J. Mulders, *Phys. Rev.* **D57**: 5780–5786 (1998), `hep-ph/9711485`.

[74] M. Anselmino, V. Barone, A. Drago, and F. Murgia (2002), `hep-ph/0209073`.

[75] S. J. Brodsky, D. S. Hwang, and I. Schmidt, *Nucl. Phys.* **B642**: 344–356 (2002), `hep-ph/0206259`.

[76] J. Levelt and P. J. Mulders, *Phys. Rev.* **D49**: 96–113 (1994), `hep-ph/9304232`.

[77] R. D. Tangerman and P. J. Mulders, *Phys. Rev.* **D51**: 3357–3372 (1995), `hep-ph/9403227`.

[78] D. Boer and P. J. Mulders, *Phys. Rev.* **D57**: 5780–5786 (1998), `hep-ph/9711485`.

[79] K. Goeke, A. Metz, and M. Schlegel, *Phys. Lett.* **B618**: 90–96 (2005), `hep-ph/0504130`.

[80] D. Boer (2003), `hep-ph/0312149`.

[81] A. Bacchetta, M. Boglione, A. Henneman, and P. J. Mulders, *Phys. Rev. Lett.* **85**: 712–715 (2000), `hep-ph/9912490`.

[82] S. J. Brodsky, P. Hoyer, N. Marchal, S. Peigne, and F. Sannino, *Phys. Rev.* **D65**: 114025 (2002), `hep-ph/0104291`.

[83] J. Soffer, *Phys. Rev. Lett.* **74**: 1292–1294 (1995), `hep-ph/9409254`.

[84] J.-w. Qiu and G. Sterman, *Phys. Rev. Lett.* **67**: 2264–2267 (1991).

[85] J.-w. Qiu and G. Sterman, *Nucl. Phys.* **B378**: 52–78 (1992).

[86] N. Hammon, O. Teryaev, and A. Schafer, *Phys. Lett.* **B390**: 409–412 (1997), `hep-ph/9611359`.

[87] D. Boer, P. J. Mulders, and O. V. Teryaev, *Phys. Rev.* **D57**: 3057–3064 (1998), `hep-ph/9710223`.

[88] Y. Kanazawa and Y. Koike, *Phys. Rev.* **D64**: 034019 (2001), `hep-ph/0012225`.

[89] D. Boer and J.-w. Qiu, *Phys. Rev.* **D65**: 034008 (2002), `hep-ph/0108179`.

[90] M. Burkardt, *Phys. Rev.* **D69**: 091501 (2004), `hep-ph/0402014`.

[91] A. P. Bukhvostov, E. A. Kuraev, and L. N. Lipatov, *Yad. Fiz.* **39**: 194–207 (1983).

[92] A. P. Bukhvostov, E. A. Kuraev, and L. N. Lipatov, *Yad. Fiz.* **38**: 439–453 (1983).

[93] A. P. Bukhvostov, E. A. Kuraev, and L. N. Lipatov, *Zh. Eksp. Teor. Fiz.* **87**: 37–55 (1984).

[94] R. Jakob, P. J. Mulders, and J. Rodrigues, *Nucl. Phys.* **A626**: 937–965 (1997),

`hep-ph/9704335`.

[95] A. A. Henneman, D. Boer, and P. J. Mulders, *Nucl. Phys.* **B620**: 331–350 (2002), `hep-ph/0104271`.

[96] K. Goeke, A. Metz, P. V. Pobylitsa, and M. V. Polyakov, *Phys. Lett.* **B567**: 27–30 (2003), `hep-ph/0302028`.

[97] A. Bacchetta, R. Kundu, A. Metz, and P. J. Mulders, *Phys. Lett.* **B506**: 155–160 (2001), `hep-ph/0102278`.

[98] A. Bacchetta, R. Kundu, A. Metz, and P. J. Mulders, *Phys. Rev.* **D65**: 094021 (2002), `hep-ph/0201091`.

[99] A. Bacchetta and P. J. Mulders, *Phys. Lett.* **B518**: 85–93 (2001), `hep-ph/0104176`.

[100] A. Metz, *Phys. Lett.* **B549**: 139–145 (2002), `hep-ph/0209054`.

[101] J. C. Collins and A. Metz, *Phys. Rev. Lett.* **93**: 252001 (2004), `hep-ph/0408249`.

[102] J. Levelt and P. J. Mulders, *Phys. Lett.* **B338**: 357–362 (1994), `hep-ph/9408257`.

[103] D. Boer, R. Jakob, and P. J. Mulders, *Nucl. Phys.* **B504**: 345–380 (1997), `hep-ph/9702281`.

[104] J. C. Collins, D. E. Soper, and G. Sterman, *Phys. Lett.* **B109**: 388 (1982).

[105] J. C. Collins, D. E. Soper, and G. Sterman, *Nucl. Phys.* **B223**: 381 (1983).

[106] K. Hagiwara, K.-i. Hikasa, and N. Kai, *Phys. Rev.* **D27**: 84 (1983).

[107] M. Ahmed and T. Gehrmann, *Phys. Lett.* **B465**: 297–302 (1999), `hep-ph/9906503`.

[108] D. Boer, *Nucl. Phys.* **B603**: 195–217 (2001), `hep-ph/0102071`.

[109] J. D. Bjorken, J. B. Kogut, and D. E. Soper, *Phys. Rev.* **D3**: 1382 (1971).

[110] A. V. Efremov and A. V. Radyushkin, *Theor. Math. Phys.* **44**: 774 (1981).

[111] J. C. Collins and D. E. Soper, *Nucl. Phys.* **B193**: 381 (1981).

[112] J. C. Collins and D. E. Soper, *Nucl. Phys.* **B194**: 445 (1982).

[113] J. C. Collins, D. E. Soper, and G. Sterman, *Adv. Ser. Direct. High Energy Phys.* **5**: 1–91 (1988), `hep-ph/0409313`.

[114] D. Boer and P. J. Mulders, *Nucl. Phys.* **B569**: 505–526 (2000), `hep-ph/9906223`.

[115] P. J. Mulders and R. D. Tangerman, *Nucl. Phys.* **B461**: 197–237 (1996), `hep-ph/9510301`.

[116] A. Afanasev and C. E. Carlson (2003), `hep-ph/0308163`.

[117] F. Yuan, *Phys. Lett.* **B589**: 28–34 (2004), `hep-ph/0310279`.

[118] A. Metz and M. Schlegel, *Eur. Phys. J.* **A22**: 489–494 (2004), `hep-ph/0403182`.

[119] J.-W. Qiu, *Phys. Rev.* **D42**: 30–44 (1990).

[120] J. A. M. Vermaseren (2000), `math-ph/0010025`.

[121] H. Avakian et al. (CLAS), *Phys. Rev.* **D69**: 112004 (2004), `hep-ex/0301005`.

[122] E. Avetisyan, A. Rostomyan, and A. Ivanilov (HERMES) (2004), `hep-ex/0408002`.

[123] A. V. Efremov, K. Goeke, and P. V. Pobylitsa, *Phys. Lett.* **B488**: 182–186 (2000), `hep-ph/0004196`.

[124] A. V. Efremov, K. Goeke, S. Menzel, A. Metz, and P. Schweitzer, *Phys. Lett.* **B612**: 233–244 (2005), `hep-ph/0412353`.

[125] D. Amrath, A. Bacchetta, and A. Metz, *Phys. Rev.* **D71**: 114018 (2005), `hep-ph/0504124`.

[126] G. R. Goldstein and L. Gamberg (2002), `hep-ph/0209085`.

[127] L. Gamberg, G. R. Goldstein, and K. A. Oganessyan, *AIP Conf. Proc.* **675**: 489–493 (2003), `hep-ph/0211155`.

[128] L. P. Gamberg, G. R. Goldstein, and K. A. Oganessyan, *Phys. Rev.* **D67**: 071504 (2003), `hep-ph/0301018`.

[129] D. Boer, S. J. Brodsky, and D. S. Hwang, *Phys. Rev.* **D67**: 054003 (2003), `hep-ph/0211110`.

[130] Z. Lu and B.-Q. Ma, *Phys. Rev.* **D70**: 094044 (2004), `hep-ph/0411043`.

[131] Z. Lu and B.-Q. Ma, *Phys. Lett.* **B615**: 200–206 (2005), `hep-ph/0504184`.

[132] D. Hwang, *T-odd effects in sidis*, Presented at SIR-2005, JLAB, Newport News (2005).

[133] A. Airapetian et al. (HERMES), *Phys. Rev. Lett.* **84**: 4047–4051 (2000), `hep-ex/9910062`.

[134] A. Airapetian et al. (HERMES), *Phys. Rev.* **D64**: 097101 (2001), `hep-ex/0104005`.

[135] A. Airapetian et al. (HERMES), *Phys. Lett.* **B562**: 182–192 (2003), `hep-ex/0212039`.

[136] P. Pagano (COMPASS) (2005), `hep-ex/0501035`.

[137] K. A. Oganessian, H. R. Avakian, N. Bianchi, and A. M. Kotzinian (1998), `hep-ph/9808368`.

[138] K. A. Oganessyan, P. J. Mulders, and E. De Sanctis, *Phys. Lett.* **B532**: 87–92 (2002), `hep-ph/0201061`.

[139] M. Diehl and S. Sapeta, *Eur. Phys. J.* **C41**: 515–533 (2005), `hep-ph/0503023`.

[140] A. Airapetian et al. (HERMES), *Phys. Lett.* **B622**: 14–22 (2005), `hep-ex/0505042`.

[141] D. Boer, A. Brandenburg, O. Nachtmann, and A. Utermann, *Eur. Phys. J.* **C40**: 55–61 (2005), `hep-ph/0411068`.

[142] M. Grosse Perdekamp and A. Ogawa, *Nucl. Phys.* **A711**: 69–75 (2002).

[143] A. V. Efremov, K. Goeke, and P. Schweitzer, *Eur. Phys. J.* **C35**: 207–210 (2004), `hep-ph/0403124`.

[144] A. Bianconi and M. Radici, *J. Phys.* **G31**: 645–658 (2005), `hep-ph/0501055`.

[145] L. P. Gamberg and G. R. Goldstein (2005), `hep-ph/0506127`.

[146] L. P. Gamberg, G. R. Goldstein, and K. A. Oganessyan, *Phys. Rev.* **D68**: 051501 (2003), `hep-ph/0307139`.

[147] X.-D. Ji, *Phys. Rev. Lett.* **78**: 610–613 (1997), `hep-ph/9603249`.

[148] X.-D. Ji, *Phys. Rev.* **D55**: 7114–7125 (1997), `hep-ph/9609381`.

[149] X.-D. Ji, *Phys. Rev.* **D58**: 056003 (1998), `hep-ph/9710290`.

[150] K. Goeke, M. V. Polyakov, and M. Vanderhaeghen, *Prog. Part. Nucl. Phys.* **47**: 401–515 (2001), `hep-ph/0106012`.

[151] M. Diehl, *Phys. Rept.* **388**: 41–277 (2003), `hep-ph/0307382`.

[152] A. V. Belitsky and A. V. Radyushkin, *Phys. Rept.* **418**: 1–387 (2005), `hep-ph/0504030`.

[153] M. Anselmino, V. Barone, A. Drago, and N. N. Nikolaev, *Phys. Lett.* **B594**: 97–104 (2004), `hep-ph/0403114`.

[154] R. L. Jaffe, X.-m. Jin, and J. Tang, *Phys. Rev. Lett.* **80**: 1166–1169 (1998), `hep-ph/9709322`.

[155] A. Bacchetta and M. Radici, *Phys. Rev.* **D69**: 074026 (2004), `hep-ph/0311173`.

[156] A. Bacchetta and M. Radici, *Phys. Rev.* **D70**: 094032 (2004), `hep-ph/0409174`.

[157] P. B. van der Nat and K. Griffioen (HERMES) (2005), `hep-ex/0501009`.

[158] G. ’t Hooft, *Nucl. Phys.* **B33**: 173–199 (1971).

[159] P. J. Mulders and J. Rodrigues, *Phys. Rev.* **D63**: 094021 (2001), `hep-ph/0009343`.

[160] X.-d. Ji, J.-P. Ma, and F. Yuan, *JHEP* **07**: 020 (2005), `hep-ph/0503015`.

[161] C. Itzykson and J. B. Zuber, *Quantum field theory* (Mcgraw-hill, New York, USA, 1980).

[162] R. K. Ellis, H. Georgi, M. Machacek, H. D. Politzer, and G. G. Ross, *Phys. Lett.* **B78**: 281 (1978).

[163] R. K. Ellis, H. Georgi, M. Machacek, H. D. Politzer, and G. G. Ross, *Nucl. Phys.* **B152**: 285 (1979).

[164] G. Sterman, *Phys. Rev.* **D17**: 2773 (1978).

[165] S. B. Libby and G. Sterman, *Phys. Rev.* **D18**: 3252 (1978).

[166] J. C. Collins and G. Sterman, *Nucl. Phys.* **B185**: 172 (1981).

[167] R. Doria, J. Frenkel, and J. C. Taylor, *Nucl. Phys.* **B168**: 93 (1980).

[168] J. C. Collins, D. E. Soper, and G. Sterman, *Phys. Lett.* **B126**: 275 (1983).

[169] J. C. Collins, D. E. Soper, and G. Sterman, *Phys. Lett.* **B134**: 263 (1984).

[170] J. C. Collins, D. E. Soper, and G. Sterman, *Nucl. Phys.* **B250**: 199 (1985).

[171] J. C. Collins, D. E. Soper, and G. Sterman, *Nucl. Phys.* **B261**: 104 (1985).

[172] J. C. Collins, D. E. Soper, and G. Sterman, *Nucl. Phys.* **B308**: 833 (1988).

[173] G. T. Bodwin, *Phys. Rev.* **D31**: 2616 (1985).

[174] J. C. Collins, *Nucl. Phys.* **B394**: 169–199 (1993), `hep-ph/9207265`.

[175] X.-d. Ji, J.-p. Ma, and F. Yuan, *Phys. Rev.* **D71**: 034005 (2005), `hep-ph/0404183`.

[176] X.-d. Ji, J.-P. Ma, and F. Yuan, *Phys. Lett.* **B597**: 299–308 (2004), `hep-ph/0405085`.

[177] D. L. Adams et al. (E581), *Phys. Lett.* **B261**: 201–206 (1991).

[178] D. L. Adams et al. (FNAL-E704), *Phys. Lett.* **B264**: 462–466 (1991).

[179] A. Bravar et al. (Fermilab E704), *Phys. Rev. Lett.* **77**: 2626–2629 (1996).

[180] L. Apanasevich et al. (Fermilab E706), *Phys. Rev. Lett.* **81**: 2642–2645 (1998), `hep-ex/9711017`.

[181] K. Krueger et al., *Phys. Lett.* **B459**: 412–416 (1999).

[182] S. S. Adler et al. (PHENIX), *Phys. Rev. Lett.* **91**: 241803 (2003), `hep-ex/0304038`.

[183] J. Adams et al. (STAR), *Phys. Rev. Lett.* **92**: 171801 (2004), `hep-ex/0310058`.

[184] S. S. Adler (PHENIX) (2005), `hep-ex/0507073`.

[185] R. L. Jaffe and N. Saito, *Phys. Lett.* **B382**: 165–172 (1996), `hep-ph/9604220`.

[186] M. Anselmino, M. Boglione, and F. Murgia, *Phys. Rev.* **D60**: 054027 (1999), `hep-ph/9901442`.

[187] M. Anselmino, M. Boglione, U. D'Alesio, E. Leader, and F. Murgia, *Phys. Rev.* **D70**: 074025 (2004), `hep-ph/0407100`.

[188] B. Jager, M. Stratmann, and W. Vogelsang, *Phys. Rev.* **D70**: 034010 (2004), `hep-ph/0404057`.

[189] U. D'Alesio and F. Murgia, *Phys. Rev.* **D70**: 074009 (2004), `hep-ph/0408092`.

[190] M. Anselmino, M. Boglione, U. D'Alesio, E. Leader, and F. Murgia, *Phys. Rev.* **D71**: 014002 (2005), `hep-ph/0408356`.

[191] W. Vogelsang (2005), `hep-ph/0503036`.

[192] D. Boer and W. Vogelsang, *Phys. Rev.* **D69**: 094025 (2004), `hep-ph/0312320`.

[193] W. Vogelsang and F. Yuan, *Phys. Rev.* **D72**: 054028 (2005), `hep-ph/0507266`.

Samenvatting

Enkelvoudige spin asymmetrieën en ijkinvariantie in harde verstrooiingsprocessen

De materie om ons heen is opgebouwd uit kleinere bouwsteentjes. De kleinste bouwsteentjes die wij kennen, worden de *elementaire deeltjes* genoemd en zijn op dit moment dus niet op te delen in nog kleinere deeltjes. Voorbeelden van deze elementaire deeltjes zijn het elektron en het foton. Op dit moment is de grootte van deze deeltjes niet bekend, ze worden beschouwd oneindig klein te zijn oftewel puntachtig klein. In de studie van elementaire deeltjes speelt een bepaalde familie van deeltjes, genaamd *hadronen*, een belangrijke rol. In tegenstelling tot de elementaire deeltjes hebben hadronen wel degelijk een zekere grootte. Een voorbeeld van een hadron is bijvoorbeeld het proton met een afmeting van ongeveer $0,0000000000001$ cm. Hadronen zijn echter geen elementaire deeltjes, ze zijn opgebouwd uit kleinere puntdeeltjes die *quarks* en *gluonen* heten. Op dit moment weten we al aardig wat over de opbouw van hadronen uit deze quarks en gluonen, en daar zouden we graag nog veel meer over willen weten. Niet alleen vanwege de structuur, maar ook omdat de daaraan gerelateerde natuurkunde uitdagend en verrassend is. In dit proefschrift zullen dan ook de drie pijlers van de moderne natuurkunde: de *relativiteitstheorie*, de *quantumtheorie* en het concept symmetrie (in het bijzonder *ijkinvariantie*), worden aangewend om een beschrijving te realiseren.

De natuurkunde die nodig is voor de beschrijving van elementaire deeltjes is in veel opzichten totaal anders dan waar wij in ons dagelijks leven aan gewend zijn. Zo spelen op die hele kleine schaal quantumeffecten een belangrijke rol. Intuititief zijn we gewend dat objecten *gelokaliseerd* zijn, betekenende dat objecten altijd op een bepaalde lokatie zijn (de Dom staat bijvoorbeeld ergens in Utrecht). In een quantumtheorie is dit anders. De positie van een bepaald deeltje is wel meetbaar, maar indien er geen meting wordt uitgevoerd, dan is het deeltje in zekere zin overal (in dat geval is de Dom overal in Utrecht). Dat lijkt misschien absurd (in het geval van de Dom), maar voor hele kleine deeltjes is dit wel degelijk het geval en experimenteel geverifieerd.

Het feit dat deeltjes niet meer gelokaliseerd zijn, leidt tot effecten die in de klassieke theorie (zonder quantumeffecten) niet bestaan. Een voorbeeld is het twee-spleten-experiment met elektronen, zie figuur 6.1. Wanneer een elektronenbron één elektron per tijdseenheid produceert, dan blijkt er een interferentiepatroon te ontstaan op het scherm achter de twee spleten. Dit interferentiepatroon is te verklaren door aan te nemen dat het enkele elektron in plaats van door één spleet, door beide spleten *tegelijk* is gegaan. Het niet lokaal zijn van de deeltjes is dus de oorzaak van het effect.

Doordat deeltjes niet gelokaliseerd zijn, is de beschrijving van de krachten op deeltjes anders dan in een klassieke theorie. In hetzelfde twee-spleten-experiment verandert het interferentiepartoon bijvoorbeeld als er een lange staafmagneet wordt geplaatst tussen de twee spleten (in M). Ondanks dat het elektron klassiek gezien deze magneet niet voelt, verandert het interferentiepatroon toch. Dit quantumeffect is simpelweg on-

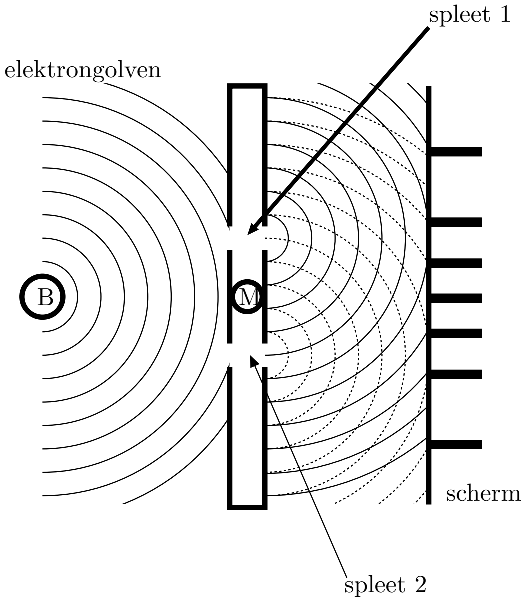

Figure 6.1: Een voorstelling van een elektron uit *B* dat een beeld produceert op het scherm. Doordat het elektron in een quantumtheorie niet lokaal is, golft het elektron als het ware door de ruimte naar het scherm toe (het scherm is bijvoorbeeld een fotografische plaat). Deze golven zijn aangegeven met halve cirkels en zijn vergelijkbaar met watergolven. Doordat deze golven door twee spleten reizen, ontstaan er effectief twee golfbronnen aan de rechterkant van de twee spleten. Aan de rechterkant van de twee spleten lopen de golven daarom door elkaar heen en ontstaat er op het scherm een patroon. Dit patroon wordt gevormd door de snijpunten van twee golflijnen en wordt het interferentiepatroon genoemd. Het interferentiepatroon verandert wanneer er in *M* een lange staafmagneet wordt geplaatst die het vlak in- of uitwijst. Ondanks dat deze magneet geen elektrische of magnetische velden produceert die voelbaar zijn voor de elektrongolven, verandert het interferentiepatroon toch. Deze verandering is onder andere afhankelijk van de richting in welke de magneet wijst: het vlak in of uit.

denkbaar in de klassieke natuurkunde en heet het *Aharonov-Bohm effect*. Volgens de klassieke natuurkunde produceert de magneet een magnetisch veld maar in deze specifieke situatie kunnen de elektrongolven het magnetisch veld echter niet voelen. Om het effect te kunnen verklaren moet er dus nog iets anders zijn wat de elektrongolven wel beïnvloedt. Dit andere veld wordt het *ijkveld* of *fotonveld* genoemd en dit veld blijkt inderdaad op het quantumniveau met de elektrongolven te kunnen wisselwerken. Het effect hangt samen met een theoretisch begrip genaamd *ijkinvariantie*.

Wanneer we de allerkleinste deeltjes bestuderen moeten we onder andere deze effecten in kaart brengen. Een probleem bij de studie van de structuur van hadronen is dat de bouwelementen, de quarks en gluonen, alleen lijken te bestaan in de hadronen zelf. In tegenstelling tot alle andere deeltjes die wij kennen (en dat zijn er heel wat), zijn quarks en gluonen nog nooit vrij geobserveerd. Het zijn dus een soort legoblokjes die afzonderlijk niet lijken te bestaan. Dit roept natuurlijk vragen op die op dit moment nog niet volledig zijn begrepen, en dit maakt de verdeling van quarks en gluonen in een hadron natuurlijk des te interessanter.

De structuur van hadronen wordt bestudeerd in experimenten. Eén van die experimenten is *elektron-hadron verstrooiing*. In dat experiment botst een elektron met hoge snelheid op een hadron. Door deze botsing breekt het hadron op in stukken en dat levert een scala aan andere deeltjes en andere soorten hadronen op, allemaal met bepaalde snelheden en richtingen. Het theoretische model wat wordt toegepast is eenvoudig in oorsprong. Het idee is dat in bepaalde situaties de kans dat een bepaald deeltje of hadron na een botsing wordt gemeten evenredig is met de kans dat een quark in een hadron wordt geraakt, vermenigvuldigt met de kans dat ditzelfde quark vervalt in het gemeten hadron. Er wordt dus verondersteld dat het vervalproces van een quark onafhankelijk is van de structuur van het geraakte hadron. Deze aanname, genaamd *factorizatie*, kan gedeeltelijk worden onderbouwd en heeft in veel experimenten ook een goede beschrijving gegeven.

Een observatie die tot voor kort nog onbegrepen was, is het optreden van *enkelvoudige spin asymmetrieën* in elektron-hadron verstrooiing en *hadron-hadron verstrooiing*. In het laatste experiment worden in plaats van een elektron op een hadron te schieten twee hadronen keihard op elkaar geschoten en wordt er een ander soort hadron na de botsing gemeten. Hadronen kunnen in het algemeen een spin hebben. Dat betekent dat ze als het ware tollen om hun eigen as. Als in het experiment blijkt dat waneer de spin van het ingaande hadron wordt omgedraaid ook de snelheid of richting van het gemeten deeltje verandert, spreekt men van een enkelvoudige spin asymmetrie. Deze asymmetrieën treden ook op in de eerder besproken elektron-hadron verstrooiing. In figuur 1.3 op bladzijde 10 is voor dit proces de gemeten asymmetrie (langs de verticale as) weergegeven.

In dit proefschrift wordt de oorzaak van deze enkelvoudige spin asymmetrieën onderzocht. In hoofdstuk 2 wordt een aantal hoge energie verstrooiingsprocessen geïntroduceerd. De basis van de theorie wordt uitgelegd en de *distributie en fragmentatie functies* worden gedefinieerd die later blijken op te duiken in experimentele grootheden. Deze functies beschrijven de structuur van het hadron en bevatten de informatie die we willen weten. In hoofstuk 2 is een nieuwe klasse van functies ontdekt die ons begrip van de structuur kunnen vergroten. Een voorbeeld van deze nieuwe functies is $g^{\perp}$, aangegeven in vergelijking 2.65 (op bladzijde 34).

In hoofdstuk 3 wordt getracht een aantal verstrooiingsprocessen te beschrijven. In deze beschrijving blijkt dat ijkinvariantie een grote rol speelt. Ijkinvariantie is een wiskundige symmetrie die aanwezig zou moeten zijn in de theoretische beschrijving. Tot voor kort was dit niet helemaal netjes meegenomen, maar men wist ook niet of het missen van de symmetrie werkelijk een probleem zou kunnen zijn. Door in dit proefschrift de theorie nauwkeurig uit te werken, wordt er een bijdrage geleverd aan het herstellen van ijkinvariantie. Behalve dat dit een verbeterde theoretische beschrijving oplevert, blijkt er een subtiel effect te zijn wat een natuurlijke verklaring voor het optreden van enkelvoudige spin asymmetrieën geeft. Een verklaring in elektron-hadron verstrooiing is de wisselwerking tussen de geraakte quark en het *ijkveld* (*gluonveld*) van het hadron (de gluonen zijn geïllustreerd in figuur 1.2 door gekrulde lijnen). Het effect is daardoor in een aantal opzichten vergelijkbaar met het Aharonov-Bohm effect. In beide gevallen wordt het effect veroorzaakt doordat een deeltje (hetzij elektron of quark) wisselwerkt met een ijkveld in gebieden waar de elektrische en magnetische velden geen effect hebben.

Deze effecten in kaart brengend, zien we in hoofdstuk 3 dat de functies van hoofdstuk 2 kunnen worden gemeten in elektron-hadron verstrooiing. Vergelijking 3.64 is bijvoorbeeld belangrijk om de verscheidene functies te kunnen meten. In hoofdstuk 4 wordt de theorie verder ontwikkeld om ook hadron-hadron verstrooiing te kunnen beschrijven. Eén van de belangrijkste resultaten, maar technisch van aard, wordt geïllustreerd in de figuren 4.9 en 4.10. In dit hoofdstuk wordt verder ook de consistentie van de gefactorizeerde aanpak besproken: Is het vervalproces van quarks in hadronen wel onafhankelijk van de structuur van het geraakte hadron? Het antwoord op deze vraag blijkt niet eenvoudig. In hoofdstuk 5 worden de ontwikkelde technieken van hoofdstuk 4 gebruikt om voorspellingen te doen voor asymmetrieën in hadron-hadron verstrooiingsprocessen. Experimenten kunnen deze voorspellingen verifiëren en daarmee de geldigheid van de ontwikkelde ideeën toetsen.